TYCHO:
conceptual design of a satellite demonstrator mission to Earth-Moon-libration point EML-4 as preparation for a communication relay service

TYCHO:
Entwurf einer Satellitendemonstrationsmisson
zum Erde-Mond-Librationspunkt EML-4
als Vorbereitung für einen Kommunikationsrelayservice

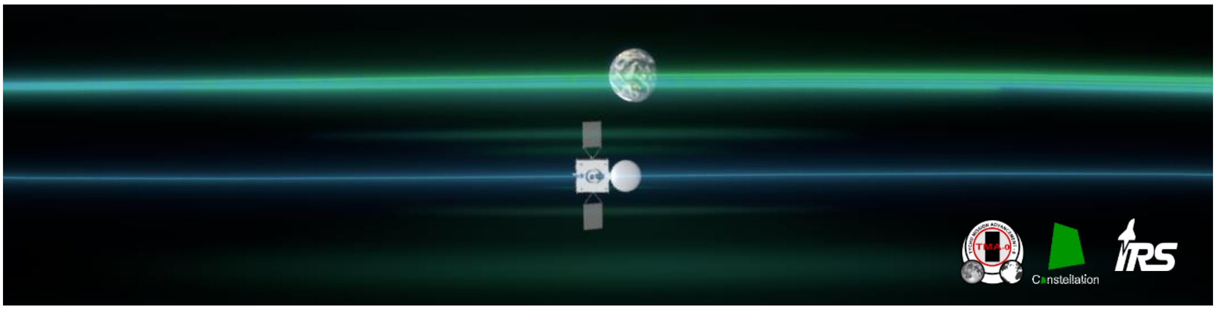

Diploma thesis by
Dipl.-Ing. (FH) **Andreas HORNIG**
IRS-13-S60

Supervisor:
Prof. Dr. rer. nat. Hans-Peter Röser (IRS, University of Stuttgart)

Thesis committee members:
Dr. Rolf Janovsky (OHB-System)
Dipl.-Ing. Maren Homeister (OHB-System)
Dipl.-Ing. Kai-Sören Klemich (IRS, University of Stuttgart)

Institute of Space Systems (IRS)
University of Stuttgart

May 2013

Prologue

"The only way of discovering the limits of the possible is to venture a little way past them into the impossible"

Sir Arthur C. Clarke [1]

"And all I ask is a tall ship and a star to steer her by"

John Edward Masefield, OM [2]

For my parents Dieter and Marita Hornig and my sister Ina-Christin Hornig!

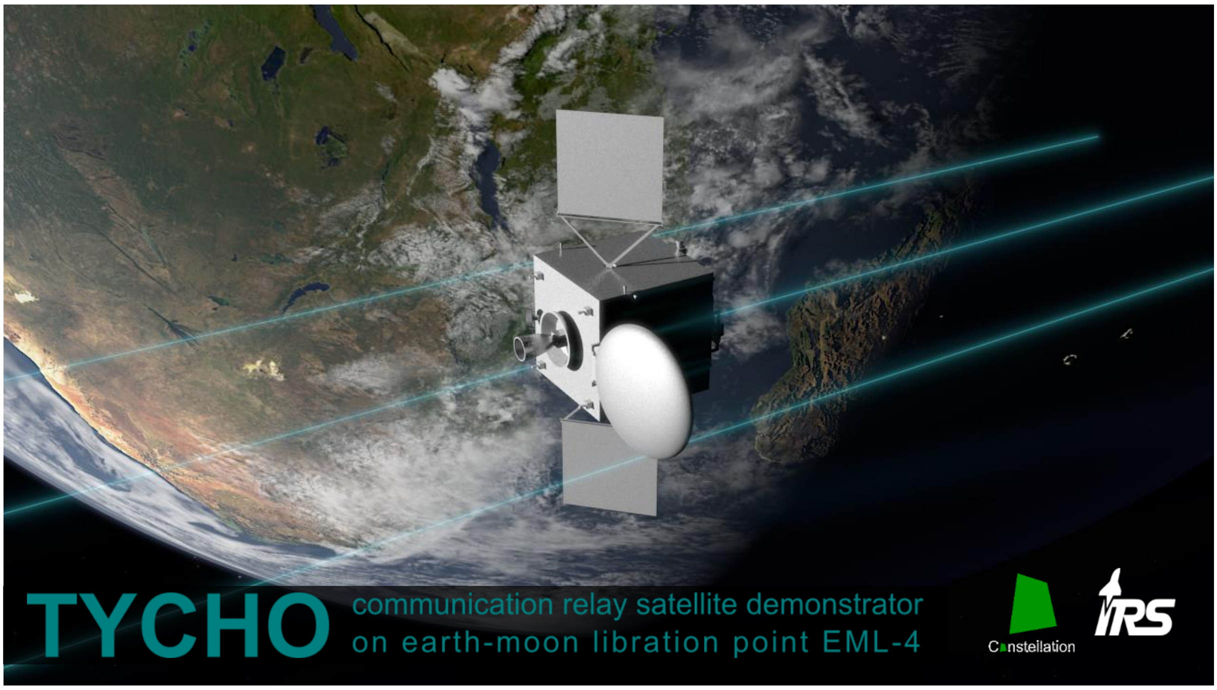

Scope of Work

Scope of diploma thesis for Mr. Dipl.-Ing. (FH) Andreas Hornig

TYCHO-L4/L5 - conceptual design of a satellite demonstrator mission to Earth-Moon-libration point L4/L5 as preparation for a communication relay service

In 2011 a mission concept for a communication relay satellite for the Earth-Moon Lagrange point L4 or L5 was proposed as a technology demonstrator and science mission for a SGAC- and OHB scholarship. The mission named TYCHO-L4/L5 is outlined in a demonstration part for the communication relay service and in a science part supporting the demonstration as well as for environmental sensing in the L4 or L5 orbit. The communication service shall serve as a long-term infrastructure for different Moon missions on lunar surface, lunar orbit and to the L1 and L2 points. The scientific mission part shall enable environmental research of dust and solar intensity and identify possible effects on the TYCHO and other missions caused by the environment in L4 or L5.

The TYCHO concept is divided in two independent missions, the demonstrator mission with a mission duration of one to two years demonstrating the operational mission, and the operational service mission with a mission duration of 10 to 15 years. This mission duration is aimed for to be comparable with state of the art geosynchronous communication satellites and to be able to use standard communication busses. Furthermore this duration also allows measuring one solar intensity cycle.

In this thesis the mission concept shall be analyzed as a feasibility study and a preliminary design concept for the demonstrator mission shall be conducted. This requires an elaboration of the mission, satellite system, subsystems and the scale of service. The main focus shall be on the service characteristics of the communication relay in order to serve as a long-term infrastructure for partner missions to the Moon.

Within the scope of this thesis the following points are to be analyzed:

- market analysis to determine service users and applications
- characterization & description of the Lagrangian points in the Earth-Moon system and their possible applications
- definition of mission objectives and requirements
- selection of applicable payloads for the scientific mission for Lagrangian point environment sensing, as well as relevant demonstrations of conventional and new communication technologies
- identification of system defining design parameters (design drivers) and the resulting system sensitivities due to these parameters
- mission analysis and modeling of the trajectory from the Earth to the L4 or L5 orbit (transfer, check for injection, orbit perturbations, orbit keeping, graveyard-option)
- preliminary design of the system and subsystems (communication, electrical power system, attitude and orbital control, propulsion, thermal control)
- selection of applicable space transportation services (launcher, launch sites, start orbit, etc.)
- identification of communication targets on lunar surface, in lunar orbit and L1/L2 orbits and applicable ground terminals on Earth, designing the communication link budgets
- evaluation of the options and alternatives on the basis of different criteria (mass, ISP, communication parameters, service time, etc.) and comparison with similar missions and communication satellites.

UNIVERSITÄT STUTTGART
INSTITUT FÜR RAUMFAHRTSYSTEME
im Raumfahrtzentrum Baden-Württemberg (RZBW)

IRS

Pfaffenwaldring 29 · 70569 Stuttgart · Tel.: (0711) 685-62375 · Fax: (0711) 685-63596 · www.irs.uni-stuttgart.de

Aufgabenstellung für die Diplomarbeit von Herrn Dipl.-Ing. (FH) Andreas Hornig

TYCHO-L4/L5 – Entwurf einer Satellitendemonstrationsmission zum Erde-Mond-Librationspunkt L4/L5 als Vorbereitung für einen Kommunikationsrelayservice

In 2011 wurde im Rahmen eines SGAC- und OHB-Stipendiums ein Missionskonzept für einen Kommunikationsrelaysatelliten für den Erde-Mond-Lagrangepunkt L4 oder L5 als technischer Demonstrator und als Wissenschaftsmission erstellt. Die TYCHO-L4/L5 genannte Mission gliedert sich in den Demonstrationsanteil für den Kommunikationsservice und in den Wissenschaftsanteil zur Unterstützung der Demonstration als auch für eine Umgebungsuntersuchung im L4- oder L5-Orbit. Der Kommunikationsservice soll dabei als längerfristige Infrastruktur für verschiedene Mondmissionen auf der Mondoberfläche, im Mondorbit und zu den L1- und L2-Punkten dienen. Der Wissenschaftsanteil soll Umgebungsuntersuchungen im L4 oder L5 zu Staub und Sonnenaktivität ermöglichen und mögliche Auswirkungen auf die eigene und andere Missionen aufzeigen.

Das TYCHO Konzept gliedert sich in zwei separate Missionen, der Demonstrationsmission mit einer Zeitdauer von ein bis zwei Jahren, um die operationelle Mission zu demonstrieren, und der operationellen Servicemission mit einer Missionsdauer zwischen 10 und 15 Jahren. Diese Missionsdauer wird angestrebt, um mit dem aktuellen Stand geostationärer Kommunikationssatelliten vergleichbar zu sein und um Standardkommunikationsbusse verwenden zu können. Diese Zeitdauer ermöglicht auch einen Sonnenintensitätszyklus zu durchlaufen.

In der Arbeit soll dieses Missionskonzept in eine Machbarkeitsstudie untersucht und einen Vorentwurf für die Demonstrationsmission durchgeführt werden. Dazu ist es notwendig die Mission, die Systeme, Subsysteme und den Serviceumfang auszuarbeiten. Das Hauptaugenmerk der Untersuchung soll auf den Servicecharakter des Kommunikationsrelay gelegt werden, um langfristig eine Infrastruktur für Partnermissionen zum Mond zu bedienen.

Im Rahmen dieser Arbeit sind folgende Punkte zu bearbeiten:

- Marktanalyse zur Servicenutzerbestimmung und Anwendungen.
- Charakterisierung & Beschreibung der Lagrangepunkte im Erde-Mond-System und ihrer möglichen Anwendungen
- Definition der Missionsziele und Anforderungen
- Auswahl geeigneter Nutzlasten für den Wissenschaftsmissionsanteil zur Lagrangepunktsumgebungsuntersuchung, sowie relevanter Demonstrationen für konventionelle und neuere Kommunikationstechnologien
- Identifizierung der Systembestimmenden Entwurfsparameter (Designtreiber) und der Systemsensitivität zu diesen Parametern
- Missionsanalyse und Modellierung der Trajektorien von der Erde in den L4- oder L5-Orbit (Transfer, Überprüfung auf Injektion, Bahnstörungen, Orbiterhalt, Graveyard-Option)
- Vorauslegung der Systeme und Subsysteme (Kommunikation, Electrical Power System, Lage- und Bahnregelung, Antrieb, Thermalhaushalt)
- Auswahl geeigneter Space Transportation Services (Launcher, Startorte, Startorbit, etc.)
- Bestimmung von Kommunikationszielen auf der Mondoberfläche, Mondorbit und L1/L2-Orbits und geeignete Bodenterminals auf der Erde, Auslegung des Kommunikationslinks
- Evaluierung der Varianten anhand verschiedener Kriterien (Masse, Isp, Kommunikationsparameter, Servicezeit, etc.) und Vergleich zu ähnlichen Missionen und Kommunikationssatelliten

Stuttgart, den 12.07.2012	Stuttgart, den 12.07.2012	Bremen, den 13.8.2012
Hans-Peter Röser	Kai-S. K	
Prof. Dr. Hans-Peter Röser (IRS)	Dipl.-Ing. Kai-Sören Klemich (IRS)	Dr. Rolf Janovsky (OHB)

Author

Andreas HORNIG

Address: König-Karl-Straße 27
D-70372 Stuttgart

Mobile: 0049 (0)160/ 9795 8 432
Email: hornig@aerospaceresearch.net
Web: www.aerospaceresearch.net

Affidavit

I hereby declare that I wrote this thesis on my own and without the use of any other than the cited sources and tools.

Stuttgart, May 2013

Andreas HORNIG ________________________________

Acknowledgement

"If I have seen further it is by standing on the shoulders of giants."
Sir Isaac Newton [3]

This concept started as a simple idea of a roughly sketched mission for a competition in 2011 but its significance as an infrastructure for future lunar missions kept me fascinated. Since then it culminated in this conceptual study that became my thesis work. I would like to express my gratitude to those who supported me during this longer period of time.

First I would like to thank my supervisor Prof. Dr. H.-P. Röser, Director of the Institute of Space Systems for his academic and personal support during my course of studies, for this thesis and beyond my extra-curricular activities at the University of Stuttgart. I also express my deep gratitude to him and to Dr.-Ing. R. Janovsky, Head of Space Systems Studies at OHB System, for giving me the opportunity to advance my mission idea into a concept study.

I would like to particularly thank my mentors M. Homeister (OHB) and K-S. Klemich (IRS) for their exceptional support, comments, suggestions and insights. Mrs. Homeister really demonstrated on a high level the daily aspects I like and admire about systems engineering. I also appreciate the comments and colleagueship of the fellow employees of the Space Systems Studies Department at OHB.

Special thanks go to professors and staff of the Institute of Space Systems (IRS): Dr. C. Nöldeke and U. Beyermann (IRS and Tesat Spacecom) for their lectures and extraordinaire suggestions for the satellite communication payload, to Dr.-Ing. Srama (IRS and Max Planck Institute for Nuclear Physics) for his lectures and expertise in space dust and to Dr.-Ing. R. Laufer (IRS, Baylor Univ., ISU) for mission details of the LUNAR MISSION BW1. Thanks also to R. Gabrielli and B. Olberts for personal advise and support.

I am really thankful for all the support of all 10000 users of our distributed computing platform Constellation, who donated their idle PC time at home for solving a small but important part of the trajectory from the Earth to the EML-4 target orbit. This platform would not be possible without the long-time help and contribution of L. Bausch.

Many thanks go also to my friends and fellow students for motivation and constructive criticism. I thank A. Frey for pointing me to a severe logic bug in my trajectory simulation code and for motivating me by co-organizing the SpaceUp Stuttgart unconference with me during my thesis time. I really appreciated the hospitality of my friends A. Pilibosyan, J. Krzikawski and T. Zillmann during my time in Bremen. I would like to thank my friends at SGAC for giving me positive feedback after the presentation of the TYCHO idea at SGC 2011.

Finally, my sincere thanks go to my family. This work only exists due to their support and motivation. I dedicate this work to my parents Dieter and Marita Hornig and to my sister Ina Christin Hornig for their encouragement as long as I remember. I am really grateful for their faith in my path of life.

Andreas HORNIG

Stuttgart, 2013

Abstract

Most high-priority landing sites on the lunar surface do not have direct and permanent communication with the Earth. In this thesis the TYCHO mission concept is presented that utilizes the Earth-Moon libration point EML-4 for a long-term and open relay service for permanent communication between the Earth and lunar missions. TYCHO is a dual satellite mission with the TMA-0 demonstrator qualifying the mission and subsystem components and with the following operational mission TMA-1 satellite that provides the communication relay service. Furthermore it surveys the EML-4 environment to detect the disputed Kordylewski cloud dust and other harmful effects on the satellite.

The thesis outlines a complete phase 0/A for TMA-0 architecture and system design on basis of the user and mission requirements for the operational TMA-1 mission. The weak stability boundary transfer and target orbits are analyzed. The orbit design includes a disposal transfer to lunar surface to minimize the risk of space debris. The communication payload includes K-band links and an optical free-space laser link for high data-rates. The perspectives and applications of the mission are discussed and the preliminary cost budget and mission phase plans are set.

The results show that a fast deliverable, low cost demonstrator TMA-0 satellite for the TYCHO mission is feasible with current state of the art technology and methods. Certain technology developments for flexible and variable communication as well as a special orbit keeping strategy on the EML-4 target orbit are identified. TYCHO could be the first EML-4 relay communication satellite with a positive effect in the communication market.

Kurzfassung

Die meisten Landestellen mit höchster Priorität auf der Mondoberfläche haben keine direkte und permanente Kommunikationsverbindung mit der Erde. In dieser Diplomarbeit wird das TYCHO Missionskonzept präsentiert, das den Erde-Mond-Librationspunkt EML-4 für eine offene und Langzeitkommunikationsinfrastruktur zwischen Erde und Mondmissionen anwendet. TYCHO ist duale Satellitenmission mit dem TMA-0 Demonstratorsatelliten, der die Mission und Subsystemkomponenten qualifiziert, und mit dem nachfolgenden operationellen TMA-1 Satelliten, der den Kommunikationsrelaisservice bereitstellt. Weiterhin wird die EML-4-Umgebung untersucht, um Staub der kontroversen Kordylewski-Wolke oder andere, für den Satelliten schädliche Effekte zu detektieren.

Die Arbeit behandelt eine vollständige Phase 0/A Konzeptstudie für die TMA-0 Architektur und das Systemdesign, die auf die Anforderungsanalyse für die operationelle TMA-1 Mission basiert. Der Weak-Stability-Transferorbit und der Zielorbit werden analysiert. Die Bahnanalyse enthält ebenfalls ein End-of-Life-Transfer auf die Mondoberfläche, um das Weltraumschrottrisiko zu minimieren. Die Kommunikationsnutzlast besteht aus K-Band-Links und einem optischen, Laser-Link für hohe Datenraten. Die Perspektiven und die Anwendungen dieser Mission werden diskutier und die vorläufigen Kostenbudget- und Missionsphasenpläne werden aufgestellt.

Das Ergebnis zeigt, dass ein schnell umsetzbarer, kosteneffizienter TMA-0 Demonstratorsatellit bestehend aus hauptsächlich aktueller Technik und Methoden realisierbar ist. Sowohl bestimmte Technologien für adaptive Kommunikation als auch besondere Bahnregelungsstrategien für den EML-4-Orbit werden identifiziert. TYCHO könnte der erste EML-4-Kommunikationsrelaissatellit werden und einen positiven Effekt im Kommunikationsmarkt haben.

1 Table of Contents

1.1 List of Figures

1.2 List of Tables

1.3 List of Abbreviations and Acronyms

***A**DN*	ammonium dinitramide (NH4N(NO2)2)
AHP	analytic hierarchy process
AKM	apogee kick-motor
Al	aluminum
AND	ammonium dinitramide
AOC, -S	attitude and orbital control system
***B**ER*	bit error rate
BOL	begin of life
***C**CSDS*	consultative committee for space data systems
CDMA	code division multiple access
CEA	NASA Chemical Equilibrium with Application
CMOS	Complementary Metal Oxide Semiconductor
CNES	Centre National d'Études Spatiales
CNSA	China National Space Administration
COTS	commercial off-the-shelf
CSM	Command / Service Module (Apollo)
***D**elta-V*	velocity increment
DC	direct current
DLR	German Aerospace Centre
DoD	depth of Discharge
DRS	data relay satellite
DSN	deep space network
***E**ADS*	European Aeronautic Defence and Space Company
EAM	European apogee motor
Eb/NO	energy per bit to noise power spectral density ratio
ECS	étage supérieur cryotechnique
ECSS	European Cooperation for Space Standardization
EDRS	European Data Relay Satellite Service
EIRP	equivalent isotropically radiated power
ELS	Ensemble de Lancement Soyuz
EML	Earth-Moon-libration (see L)
EOCV	end of charge voltage
EODC	end of discharge voltage
EOL	end-of-life
EPC	electric power conditioner
EPS	electric power subsystem
EQFLUX	equivalent fluences
ESA	European Space Agency
ESAS	Exploration Systems Architecture Study
ESMO	European Student Moon Orbiter
***F**CC*	Federal Communications Commission
FDI	fault detection isolation
FeO	iron(II) oxide
FHT	Feldspathic Highland Terrane
FO	flow control orifice
FOV	field-of-view
***G**aAs*	gallium arsenide
GAP	polyglycidylazide
GEO	geostationary orbit
GLXP	Google Lunar X-Prize
GMAT	NASA General Mission Analysis Tool
GNSS	global navigation satellite system
GPS	Global Positioning System
GSD	ground sample distance
GSO	geosynchronous orbit
GTO	geostationary transfer orbit
***H**AN*	hydroxyl ammonium nitrate
HEO	highly elliptical orbit
HPBW	half-power beamwidth
HPGP	high performance green propulsion
***I**AU*	International Astronomical Union
ILN	International Lunar Network
iMPD	see PPT
IMU	inertial measurement unit
IOD	in-orbit demonstration
IP	internet protocol
IPDV	internet packet delay variation
IR	infrared
IRS	Institute of Space Systems, University of Stuttgart
ISO	isolator and terminator
ISRO	Indian Space Research Organisation
ISP	specific impulse
ISS	international space station
ITAR	international traffic in arms regulations
ITU	International Telecommunication Union
***J**AXA*	Japan Aerospace Exploration Agency
***K**REEP*	K (potassium), REE (rare earth elements), P (phosphorus)

L	libration or Lagrangian point
LADEE	Lunar Atmosphere and Dust Environment Explorer
Laser	light amplification by stimulated emission of radiation
LCROSS	Lunar Crater Observation and Sensing Satellite
LCT	laser communication terminal
LCT	lunar communication terminal
LEO	low Earth orbit
LiOn	lithium-ion
LL	lunar lander
LLO	low lunar orbit
LM	landing module
LNSS	lunar navigation satellite system
LO	lunar orbiter
LR	lunar rover
LRO	Lunar Reconnaissance Orbiter
LUPOS	Lunar Positioning System
***M**CO*	Mars Climate Orbiter
MEJI	Mars Exploration Joint Initiative
MEOP	maximum operational pressure
MIBIT	minimum impulse bit
MIPS	million instructions per second
MLI	multi-layer insulation
MMH	Monomethylhydrazine (CH6N2)
MMU	mass memory unit
MOM	manned orbiting module
MON	mixed oxides of nitrogen (N2O4)
MR	mission requirement
***N**ASA*	National Aeronautics and Space Administration
NEO	near Earth object
NIST	National Institute of Standards and Technology
N2H4	hydrazine
***O**BDH*	onboard data handling
OHB	Orbitale Hochtechnologie Bremen
OGS	optical ground station
***P**CDU*	power conditioning and distribution unit
PDHT	payload data handling and transmission
PFD	power flux density
PLM	payload mass
PPT	pulsed plasma thrusters
PR	pressure regulator
PT	pressure transducer
PV	pyro valve – nominal open
PV-c	pyro valve – nominal close
P2P	peer to peer
***R**CS*	reaction control system
REACH	Registration, Evaluation, Authorisation and Restriction of Chemicals
RF	radio frequency
RFDU	radio frequency distribution unit
RFSA	Russian Federal Space Agency
RPM	revolutions per minute
RX	signal reception
R3BP	restricted three-body problem
***S**ADM*	solar array drive mechanism
S/C	spacecraft
SDRN	satellite data relay network (Luch)
SDTS	small deep space transponder
SEL	Sun-Earth-libration (see L)
SGEO	Small GEO
SILEX	semiconductor-laser inter-satellite link experiment
SJL	Sun-Jupiter-libration (see L)
SLEO	Small Leopard
SODA	Solar Orbiter Dust Analyzer
SOI	sphere of influence
SPA	South Pole Aitken Terrane
SPENVIS	Space Environment Information System
SR	system requirement
SRS	space research satellite
SSPA	solid state power amplifier
STK	AGI Satellite Tool Kit
STS	Space Transportation System
SV	service valve
SVHC	substances of very high concern
***T**BC*	to be confirmed
TCS	thermal control subsystem
TDRS	Tracking and Data Relay Satellite
TMA	TYCHO Mission Advancement
TMA-0	demonstrator communication satellite
TMA-1	operational communication satellite
TRL	technology readiness level
TT&C	telemetry, tracking and control
TWT,-A	travelling wave tube amplifier
TX	signal transmission
***U**N*	United Nation
UR	user requirement
***V**DM*	vehicle dry mass
***W**SB*	weak stability boundary
WGS	wave guide switch

1.4 List of Symbols

$\boldsymbol{a}$	acceleration
a	semi-major axis
A	surface area
A_e/A_T	exit-to-thrust-area ratio
$\boldsymbol{BER}$	bit error rate
$\boldsymbol{c}$	speed of light
C	Jacobi constant
C	I_z
C/N_0	carrier-to-noise density ratio
C_e	battery energy storage capacity
$\boldsymbol{d}$	distance
d_a	diameter of aperture
D_r	receiver antenna diameter
D_t	transmit antenna diameter
DoD	depth of discharge
$\boldsymbol{e}$	eccentricity
e_r	receiver antenna pointing error
e_t	transmit antenna pointing offset
$E_{\boldsymbol{ph}}$	energy per photon
E_b/N_0	received energy-per-bit to noise-density
EIRP	equivalent isotropically radiated power
$\boldsymbol{f}$	frequency
F	force
F_{view}	view factor
FOV	field-of-view
$\boldsymbol{g_0}$	standard gravity
G	gravitational constant
G_{pr}	receiver antenna gain (net)
G_{pt}	peak transmitter antenna gain
G_r	receiver antenna gain
G_t	transmit antenna gain
GSD	ground sample distance
$\boldsymbol{h}$	Planck constant
$H_{thruster}$	angular momentum by thrusters
$HPBW$	half-power beamwidth
$\boldsymbol{i}$	imaginary number
i	orbit inclination
$\hat{\imath}, \hat{\jmath}, \hat{k}$	unit vectors as axes representation
I_x, I_y, I_z	moments of inertia
ISP	specific impulse
$\boldsymbol{k}$	Boltzmann constant
$\boldsymbol{L}$	slant length of cone from the apex
L_a	atmospheric losses
L_d	distribution unit losses
L_{imp}	implementation losses
L_l	line losses
L_{pt}	transmit antenna pointing loss
L_s	space losses
$\boldsymbol{m}, \boldsymbol{M}$	mass
$\dot{m}$	mass flow rate
M_T	wheel motor torque
$MIBIT$	minimum impulse bit
$\boldsymbol{N_{ph}}$	photons-per-bit
n_{pixel}	number of sensor pixels (row., col.)
$\boldsymbol{P_c}$	chamber pressure
P_d	power level during daylight
P_e	power level during eclipse
P_r	received power
P_s	operation power level
P_{sa}	generate power by solar array
P_{sm}	system power level
P_t	transmitted power
$\boldsymbol{Q}$	heat power
$\boldsymbol{r}, \boldsymbol{R}$	radius
R_r	radius vector ratio
R	data-rate
R_{cor}	corrected data-rate
$req.\ E_b/N_0$	required received energy-per-bit to noise-density
$\boldsymbol{S}$	radiation intensity
S_p	signal path length
S_0	solar constant
$\boldsymbol{t}$	time
t_{burn}	burn time
T_d	daylight time
T_e	eclipse time
T_p	orbit period time
T	temperature
T_c	charging time
$\boldsymbol{U}$	effective potential
U_Ω	generalized potential
$\boldsymbol{v}$	velocity
v_{exit}	exhaust gas velocity

$\mathbf{x}, \mathbf{y}, \mathbf{z}$	position coordinates
X_e & X_d	efficiency terms of power paths
$\boldsymbol{\alpha}$	absorptance
α_p	panel misalignment
α_{sat}	satellite absorptivity
$\Delta \boldsymbol{m}$	mass decrement
Δv	velocity increment, delta-v
$\boldsymbol{\delta}$	solar cell degradation
δv	small velocity change
$\delta x, \delta y, \delta z$	small displacements
δt	Small time difference
$\boldsymbol{\epsilon}$	emissivity
ϵ_{sat}	satellite emittance
ϵ_e	ecliptic angle
$\boldsymbol{\eta}$	solar cell efficiency
η_r	antenna efficiency
η_{or}	optical efficiency of the receiver
η_{ot}	optical efficiency of the transmitter
$\boldsymbol{\theta}$	gimbal angle of reaction wheels
θ_r	receiver antenna beamwidth
θ_t	transmit antenna beamwidth
θ_x, θ_y	half-power beamwidth along the major axis
$\boldsymbol{\kappa}$	dimensionless mass ratio
$\boldsymbol{\lambda}$	wave length
$\lambda_{1,2}$	eigenvalues of linearized evolution matrix
$\boldsymbol{\mu}$	standard gravitational parameter
$\boldsymbol{\pi}$	Pi
π	dimensionless mass ratio
$\boldsymbol{\sigma}$	Stefan-Boltzmann constant
$\boldsymbol{\tau}$	e-fold time
$\boldsymbol{\Phi}$	radiation flux
$\boldsymbol{\omega_z}$	angular velocity around z-axis
Ω	angular velocity
Ω_a	solid angle

2 TYCHO Conceptual Mission Design

2.1 Introduction

In the current wake of mission plans to the Moon and to the Earth-Moon libration points (EML) by several agencies and organizations (LADEE by NASA, Change-e by CNSA, Chandrayaan by ISRO) TYCHO identifies the key role of telecommunication provision for the future path of lunar exploration. It demonstrates an interesting extension to existing communication methods to the Moon and beyond by combining innovative technology with a next frontier location and the commercial space communication sector.

Most high-priority landing sites on the lunar surface do not have direct and permanent communication with the Earth because they are on the shielded zone on the far side of the Moon. Furthermore lunar missions on lunar surface or in lunar orbit only have periodic connections to their accompanying orbiters or to their allocated Earth ground stations. The TYCHO mission shall provide this permanent communication service to different lunar mission as a universal and open service.

The TYCHO mission represents a valuable asset for the lunar architecture, making use of new technologies. To minimize the risks the mission involves two satellites, the demonstration mission TMA-0 (TYCHO Mission Advancement) satellite qualifying the mission and subsystem components in a fast and cost efficient way and the following operational mission TMA-1satellite that provides the communication relay service to partnering lunar missions.

The innovation is the EML-4 orbit destination and the provision of communication service to the Moon for different and not just one organization's endeavor in a cost effective way.

The operational TMA-1 satellite is a stand-alone mission integrated in existing space communication networks to provide open communication service to external lunar missions. Therefore the long-time stable libration points EML-4 and -5 are selected to guarantee an operation time of up to 10 years. It also enables utilization of the libration point environment for space weather observation. This includes sensors for space dust, solar and cosmic radiation activity for satellite lifetime estimation and lunar crew protection by means of early-warning system. An early-warning system for solar radiation and high energetic particles will provide additional response time for manned lunar missions.

The TMA-0 satellite is TYCHO's first phase and a proposed in orbit demonstrator (IOD) mission to the Earth-Moon libration point EML-4. It demonstrates major critical aspects of the relay services needed for automated exploratory and manned missions (Moon bases) on the rim and far side surface, to lunar orbits and even to EML-2 halo orbits (satellites and space stations). The mission's main advantage is the cost efficient demonstration and qualification of the mission and system architecture that shall be the basis for the following operational TMA-1 satellite. The communication subsystem is a platform for conventional radio frequency communication but also a test-bed for optical communication with high a data-rate laser link to serve the expected future requirements of manned and autonomous lunar missions (observatories, lunar pole missions). Besides technology demonstration, the TMA-0 mission includes scientific payloads for space dust detection and solar radiation intensity measurement. This shall provide new knowledge about the EML-4 environment and the effects on satellites and may influence the design of the TMA-1 satellite. In this way the space weather and early warning concept can be demonstrated on TMA-0 and utilized on TMA-1.

The thesis describes the mission concept and the pre-design of the demonstrator TMA-0 satellite according to the operational TMA-1 mission requirements as well as the advantages and benefits of a permanent communication service between the Earth and the Moon.

2.2 Thesis and Concept Combined Structure

This thesis encompasses a phase 0-A conceptual design study of the demonstrator mission for the TYCHO relay satellite and combines it with the requirements of a thesis. The study describes the objectives of the mission and focuses on critical points determining the mission feasibility. Therefore the requirement elicitation and analysis on user, mission and system level are described and components for the satellite mission architecture are analyzed. The thesis includes aspects of a technical report and scientific explanations for the decisions taken leading to the proposed mission architecture.

2.3 Mission Concept Origin and Name Sake

This study is the continuation of a mission concept proposed by the author that won the Space Generation Advisory Council and OHB Scholarship Opportunity in 2011. The competition called for a description of *an innovative mission to the Moon; "innovative" may describe a technical aspect of the mission (such as the propulsion system or scientific purpose) or a non-technical aspect (such as multi-lateral, international partnerships or funding methods)*. The thesis is based on the competition concept and defines a demonstrator mission to qualify certain mission critical points, to lay out the mission objectives and whether or not such a mission is feasible.

The mission name TYCHO is inspired by the science-fiction novel “2001: A Space Odyssey” by Arthur C. Clarke [4] where a signal is sent by an alien made monolith buried in Moon's Tycho crater to another monolith orbiting Jupiter as the main plot device. The mission was named as a tribute to Arthur C. Clarke as an author and one of the contributors to the popularity of the idea that geostationary satellites would be ideal telecommunications relays as well as a reference to the Tycho crater as one of the possible communication targets.

2.4 Brief History of Lunar Relay Satellite Proposals

Lunar relay satellites and relay satellites in general have been used for various missions since the beginning of the space era in the 1950s. One of the earliest communication relay concepts is that of an Earth to Earth relay via a satellite on geo stationary or geo synchronous orbit (GEO) around the Earth proposed by Arthur C. Clarke and realized with Telstar 1 in 1962 [5] [6] [7].

In 1962 before the Apollo mission, Steg and Shoemaker proposed a satellite mission to EML-4 and -5 with several scientific applications and also highlighting these unique positions as “[…] a communication base for lunar and inter planetary missions” [8].

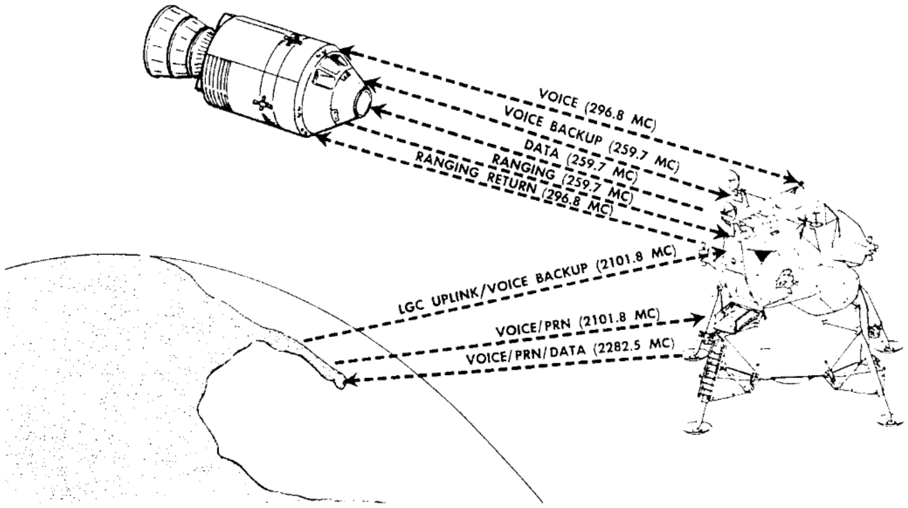

Figure 1: Apollo in flight communication [9]

For the Apollo lunar missions, conducted between 1969 and 1972, the Command / Service Module (CSM) in lunar orbit could be used to re-route communication between the Landing Module (LM) and Earth thus serving as a relay satellite for redundancy reasons and while in sight [9].

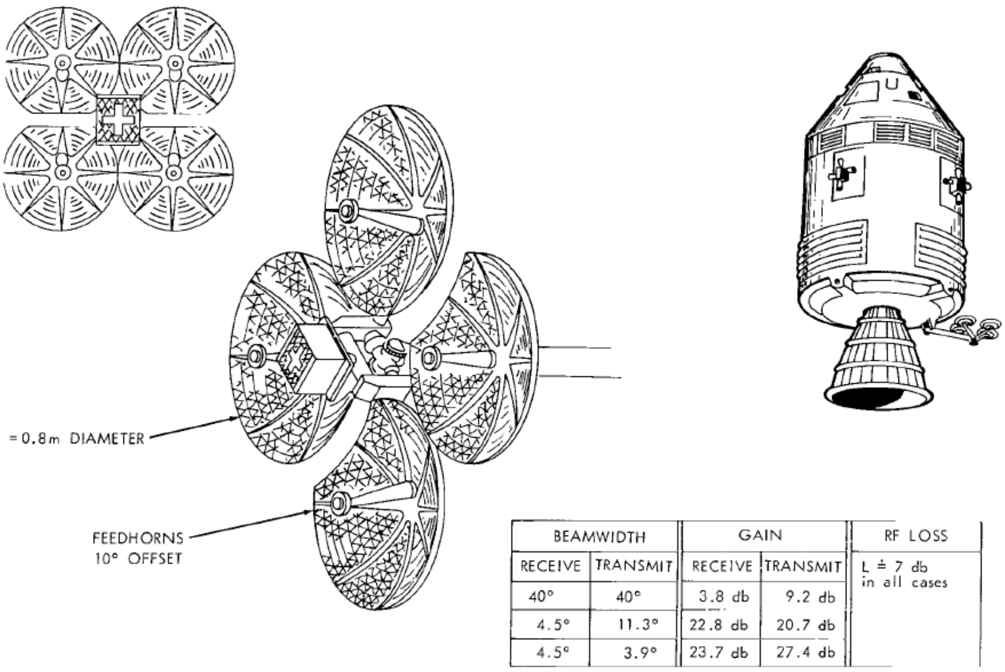

BEAMWIDTH		GAIN		RF LOSS
RECEIVE	TRANSMIT	RECEIVE	TRANSMIT	L ≐ 7 db in all cases
40°	40°	3.8 db	9.2 db	
4.5°	11.3°	22.8 db	20.7 db	
4.5°	3.9°	23.7 db	27.4 db	

Figure 2: Hummingbird satellite proposed for EML-2 by P.E. Schmid

To provide lunar far side communication and decrease black-out times of the CSM, two Hummingbird satellites around EML-2 were proposed by P. E. Schmid in 1968 but not realized for the Apollo missions [10]. However, these relay satellites were planned to be placed on the Earth-Moon plane with an offset of 3000 km in order to allow a wider coverage of Earth’s surface. As an alternative, an orbit with a periodic, three-dimensional orbit near the EML-2 point was proposed by W.E. Farquhar, who was the first to name it halo orbit [11]. Halo orbits are not in the Earth-Moon plane and the result of gravitational forces of the two celestial bodies and the centrifugal forces on the space craft. Farquhar found solutions for halo orbits by the aid of numerical simulations on the emerging computer systems at that time.

After the Apollo programs, only unmanned orbiters and landers were sent to the Moon with either direct-to-Earth communication or dual satellite missions where one satellite served as the relay for the other satellite (LRO & LCROSS) [12].

Further relay satellites were installed in Earth's GEO like the Tracking and Data Relay Satellites (TDRS) to support the space transport system STS Space Shuttle and International Space Station (ISS) missions or in orbit around Mars like Mars Reconnaissance Orbiter (MRO) in 2006 to relay surface exploration missions [13]. None of them utilizes libration points and none of them is usable as relay from their specific moons. However for Mars, a long-term relay communication infrastructure is set up in Mars orbit. The orbiters of Mars Climate Orbiter (MCO), 2001 Mars Odyssey and MRO by NASA as well as Mars Express by ESA provide communication relay links between Earth and their own mission landers and rovers and also for the landers and rovers of the other missions. The cooperation for Mars exploration will be further increased by the Mars Exploration Joint Initiative (MEJI) to join the resources and infrastructure for future missions of both agencies [14].

The TYCHO mission concept will re-focus on EML-4 and -5 as a point for communication satellites again. It follows the innovative idea of a long-term communication infrastructure for servicing lunar missions so that they can use the TYCHO relay satellite instead of their own accompanying relay satellites and are not limited as with applying direct-to-Earth communication. Both aspects have not been realized before and the TYCHO architecture can be included in a joint initiative for the exploration of the Moon.

2.5 Universal Lunar Communication Relay Service

In 2008 NASA and ESA engaged a study for a similar approach for the exploration of the Moon as they do with the Mars Exploration Joint Initiative. The Comparative Exploration Architecture Study identified the degree to which collaboration could complement, augment or enhance the lunar exploration plans of one another. This endeavor shall lead to an open architecture for international and commercial participation that was not applied to past lunar mission of both agencies [15].

International collaboration initiatives already let to universal or standardized communication infrastructures like Earth ground segments (Deep Space Network, ESTRACK, etc.) and communication satellites as well as relay satellite networks for space research vessels in Earth orbit (TDRS, EDRS). Furthermore there are efforts to establish a universal communication lunar ground network (ILN) connecting different exploratory and manned missions and provide communication gateways to Earth [16].

A universal lunar communication relay service can bridge communication gaps between both infrastructures on Earth and Moon. It shall reduce development time and costs for lunar missions due to the standardized access to the service. The Mars communication relay infrastructure partly serves as a model for a possible infrastructure in the Earth-Moon system. For these reasons TYCHO found its market niche in the universal communication relay service segment fulfilling the international commitment of a joint exploration of the Moon.

3 TYCHO Communication Relay Satellite Mission Objective Statement

The TYCHO mission is one option to provide such a universal communication relay satellite service for a specific region of the Moon. It could support a diverse range of lunar missions. This chapter presents the requirements of future lunar missions for such a relay satellite. It describes the effects, space applications and benefits of the triangle Earth-Moon libration points. Lastly it explains the need for a demonstrator mission TMA-0 as a precursor for the operational TYCHO mission TMA-1.

3.1 Mission Statement

The purpose of the TYCHO mission is outlined in the following mission statement:

The TYCHO mission provides communication relay services between the Earth and the Moon via the Earth-Moon libration point EML-4.

It serves as a long-term infrastructure for different Moon missions on the lunar surface, lunar orbits and to the EML-1 and EML-2 points.

*The mission is divided in a demonstrator satellite TMA-0 proving that it is possible with the use of today's technology and the operational satellite TMA-1, which provides the long-term communication service (*Figure 3*).*

The mission will opening up new scientific knowledge and market opportunities.

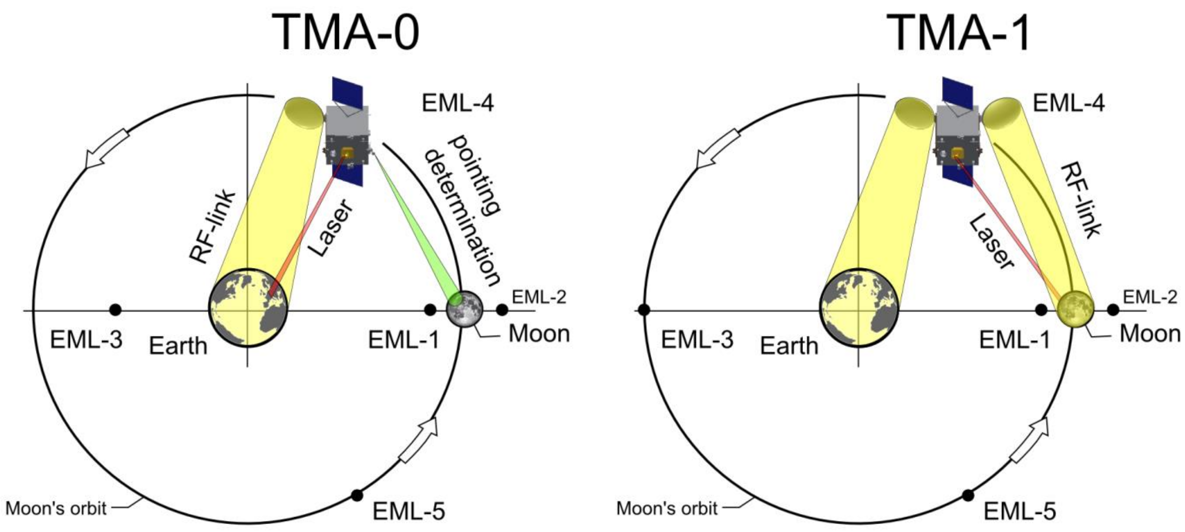

Figure 3: Demonstrator TMA-0 and operational TMA-1 satellites

3.2 Libration Points

The TYCHO mission shall provide telecommunication from Earth to the Moon and beyond from the triangular Earth-Moon libration point EML-4. This chapter characterizes the libration points in the Earth-Moon system, the importance for the TYCHO mission and their possible applications for future missions.

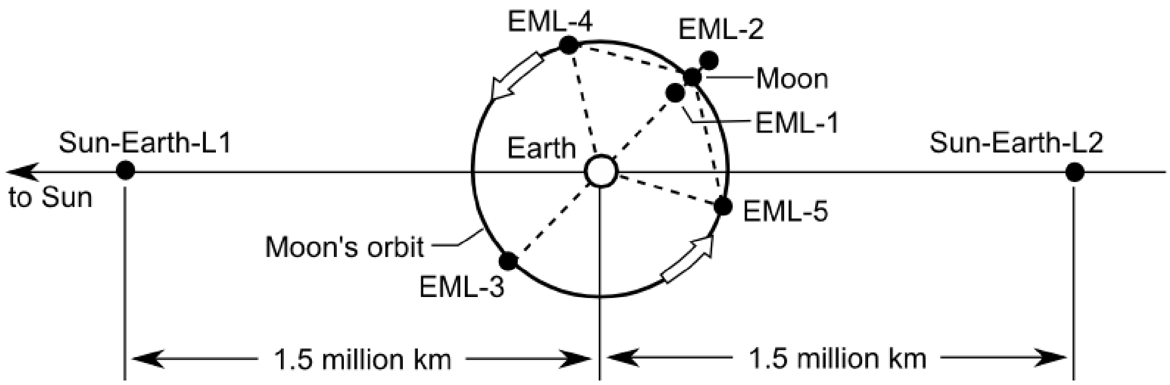

Figure 4: Libration points for Earth-Moon system and for Sun-Earth system

Libration points, also named Lagrange points (named after the Italian mathematician and astronomer Joseph-Louis Lagrange) are the five equilibrium points in space in the vicinity of two orbiting primary masses where a small secondary mass m has zero velocity and zero acceleration and where m appears to be at rest in relation to the primary masses m_1 and m_2 (Figure 4). For an inertial observer these libration points move on a circular orbit with the same angular velocity as the two primaries.

In case when the two primary masses are much larger than the secondary mass the system is referred as “restricted”. Our solar system contains many examples where this description of the restricted three-body problem can be accurate, for example the Sun-Earth (SEL), Sun-Jupiter (SJL) or Earth-Moon (EML) system configuration.

This chapter presents an abbreviated mathematical derivation of the five libration points by means of the Earth-Moon libration points, their characteristics and several relevant space applications on these special points.

3.2.1 Earth-Moon Libration Point 4 Orbit

The mathematical description of the libration points in this chapter is based on “Orbital Mechanics for Engineering Students” by H. Curtis [17].

The Earth-Moon system is a co-moving frame with its two celestial bodies orbiting around each other at a certain distance. The origin of the reference frame xyz lies in the center of their combined mass with the x-axis direction towards the smaller mass m_2. The absolute acceleration of m can be found with the five term relative acceleration formula,

$$\ddot{\vec{r}} = \vec{a}_G + \dot{\vec{\Omega}} \times \vec{r} + \vec{\Omega}\left(\vec{\Omega} \times \vec{r}\right) + 2\,\vec{\Omega} \times \vec{v}_{rel} + \vec{a}_{rel} \qquad 3.1$$

where $\ddot{\vec{r}}$ is the acceleration of a particle, $\vec{a}_G$ the acceleration of the origin of the moving frame, $\vec{a}_{rel}$ the acceleration of the particle relative to the moving frame. The results of the translational and rotational acceleration of the moving frame are respect in the first and second term. The third term $\vec{\Omega}(\vec{\Omega} \times \vec{r})$ is due to the rotation of the moving frame and the centripetal acceleration. The coriolis acceleration is due to the motion of the particle within the moving frame and the fourth term $2\,\vec{\Omega} \times \vec{v}_{rel}$. Lastly the acceleration of the particle within the moving frame is the fifth term.

The inertial velocity of the center $\vec{v}_G$ of mass (the origin of the xyz frame) and the angular velocity of the circular orbit of the two primaries are (almost) constant, thus leading to $\vec{a}_G = 0$ and $\dot{\Omega} = 0$ reducing the equation to:

$$\ddot{\vec{r}} = \vec{\Omega} \times \left(\vec{\Omega} \times \vec{r}\right) + 2\,\vec{\Omega} \times \vec{v}_{rel} + \vec{a}_{rel} \tag{3.2}$$

Solving this equation according to their components and collecting terms yields

$$\ddot{\vec{r}} = (\ddot{x} - 2\Omega\dot{y} - \Omega^2 x)\hat{\boldsymbol{\imath}} + (\ddot{y} - 2\Omega\dot{x} - \Omega^2 y)\hat{\boldsymbol{\jmath}} + \dot{z}\hat{\boldsymbol{k}} \tag{3.3}$$

This expression describes the inertial acceleration in terms of quantities with respect to the rotating frame. The movement of the secondary mass in this system is due to gravity forces described by Newton's second law by

$$m\ddot{\vec{r}} = \vec{F}_1 + \vec{F}_2 \tag{3.4}$$

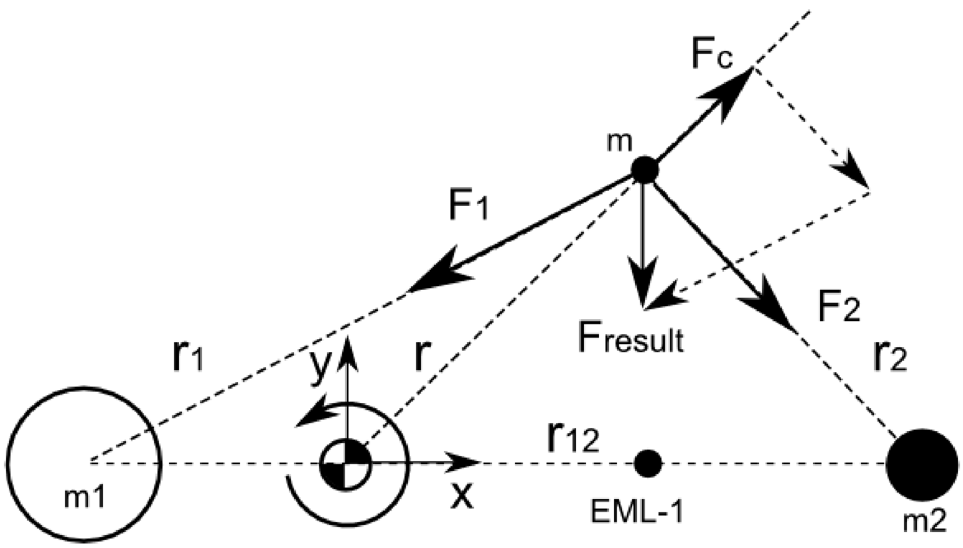

Figure 5: Restoring force acting on a particle near to EML-1.
The gravitational forces F_1 and F_2, the centrifugal force F_c and the restoring force F_{result}

And the single forces (Figure 5) of the primaries on the secondary mass *m* are

$$\vec{F}_1 = -\frac{Gm_1 m}{r_1^3}\vec{r}_1 = -\frac{\mu_1 m}{r_1^3}\vec{r}_1 \tag{3.5}$$

$$\vec{F}_2 = -\frac{Gm_2 m}{r_2^3}\vec{r}_2 = -\frac{\mu_2 m}{r_2^2}\vec{r}_2 \tag{3.6}$$

with

$$\mu_1 = Gm_1 \; and \; \mu_2 = Gm_2 \qquad 3.7$$

Combining the equations and eliminating m yields

$$\ddot{\vec{r}} = -\frac{\mu_1}{r_1^3}\vec{r}_1 - \frac{\mu_2}{r_2^3}\vec{r}_2 \qquad 3.8$$

the accelerations $\ddot{\vec{r}}$ of the small mass due to the forces both primaries. Using this equation with the mass relative radius of Earth and Moon towards the origin of the reference frame

$$\pi_1 = \frac{m_1}{m_1+m_2} \; and \; \pi_2 = \frac{m_2}{m_1+m_2} \qquad 3.9$$

the inertial acceleration in the rotating system is described by

$$\ddot{x} - 2\Omega\dot{y} - \Omega^2 x = -\frac{\mu_1}{r_1^3}(x+\pi_2 r_{12}) - \frac{\mu_2}{r_2^3}(x-\pi_1 r_{12}) \qquad 3.10$$

$$\ddot{y} + 2\Omega\dot{x} - \Omega^2 y = -\frac{\mu_1}{r_1^3}y - \frac{\mu_2}{r_2^3}y \qquad 3.11$$

$$\ddot{z} = -\frac{\mu_1}{r_1^3}z - \frac{\mu_2}{r_2^3}z \qquad 3.12$$

The three scalar equations of the motions for the restricted three-body problem (R3BP) are obtained. The influences of the two primaries' rotation are only acting on the x and y components and not on the z component of the secondary particle within the reference frame. For each position in the co-rotating frame and with the initial velocity of the particle the acceleration can be obtained.

3.2.1.1 Lagrange Points

The set of inertial acceleration equations has no closed analytical solution. However they can be used to determine the locations of the five equilibrium points where the velocity and acceleration states for all three directions of each point in the rotational frame are known.

$$\dot{x} = \dot{y} = \dot{z} = 0 \; and \; \ddot{x} = \ddot{y} = \ddot{z} = 0 \qquad 3.13$$

Substituting these conditions in the inertial acceleration we obtain

$$-\Omega^2 x = -\frac{\mu_1}{r_1^3}(x+\pi_2 r_{12}) - \frac{\mu_2}{r_2^3}(x-\pi_1 r_{12}) \qquad 3.14$$

$$-\Omega^2 y = -\frac{\mu_1}{r_1^3}y - \frac{\mu_2}{r_2^3}y \qquad 3.15$$

$$0 = -\frac{\mu_1}{r_1^3}z - \frac{\mu_2}{r_2^3}z \qquad 3.16$$

and since both, $-\mu_1/r_1^3 > 0$ and $-\mu_2/r_2^3 > 0$, the equilibrium points lie in the orbital plane.

From Equation 3.9, the distance to the center is a fraction of the one primary's mass in relation to the combined mass with respect to the distance between the two bodies. Then it is obvious

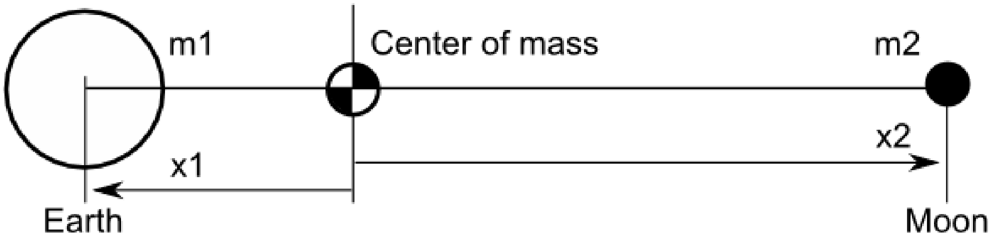

Figure 6: Center of mass of two masses orbiting each other

$$\pi_1 = 1 - \pi_2 \quad 3.17$$

using this relation in the previous equation and defining $y \neq 0$ we obtain

$$(1-\pi_2)(x+\pi_2 r_{12})\frac{1}{r_1^3} + \pi_2(x+\pi_2 r_{12} - r_{12})\frac{1}{r_2^3} = \frac{x}{r_{12}^3} \quad 3.18$$

$$(1-\pi_2)\frac{1}{r_1^3} + \pi_2\frac{1}{r_2^3} = \frac{1}{r_{12}^3} \quad 3.19$$

In $1/r_1^3$ and $1/r_2^3$ of Equation 3.18 can be treated as two linear equations and can be simultaneously solved to obtain

$$\frac{1}{r_1^3} = \frac{1}{r_2^3} = \frac{1}{r_{12}^3} \;\; or \;\; r_1 = r_2 = r_{12} \quad 3.20$$

With z = 0 and Equation 4.17 it yields

$$r_1 = (x+\pi_2 r_{12})\,\hat{\imath} + y\,\hat{\jmath} + z\,\hat{k} \quad 3.21$$

$$r_2 = (x-\pi_1 r_{12})\,\hat{\imath} + y\,\hat{\jmath} + z\,\hat{k} \quad 3.22$$

$$r_{12}^2 = (x+\pi_2 r_{12})^2 + y^2 \quad 3.23$$

$$r_{12}^2 = (x+\pi_2 r_{12} - r_{12})^2 + y^2 \quad 3.24$$

Solving the right-hand sides of the two equations yields

$$x = \frac{r_{12}}{2} - \pi_2\, r_{12} \quad 3.25$$

Substituting this back into Equations 3.21 and 3.22 and solving for y results in

$$y = \pm\frac{\sqrt{3}}{2} r_{12} \quad 3.26$$

Both equations describe the coordinate of the libration points L4 and L5 and they are the same distances $r_{12}$from the primaries m_1 and m_2 that both primaries have between each other.

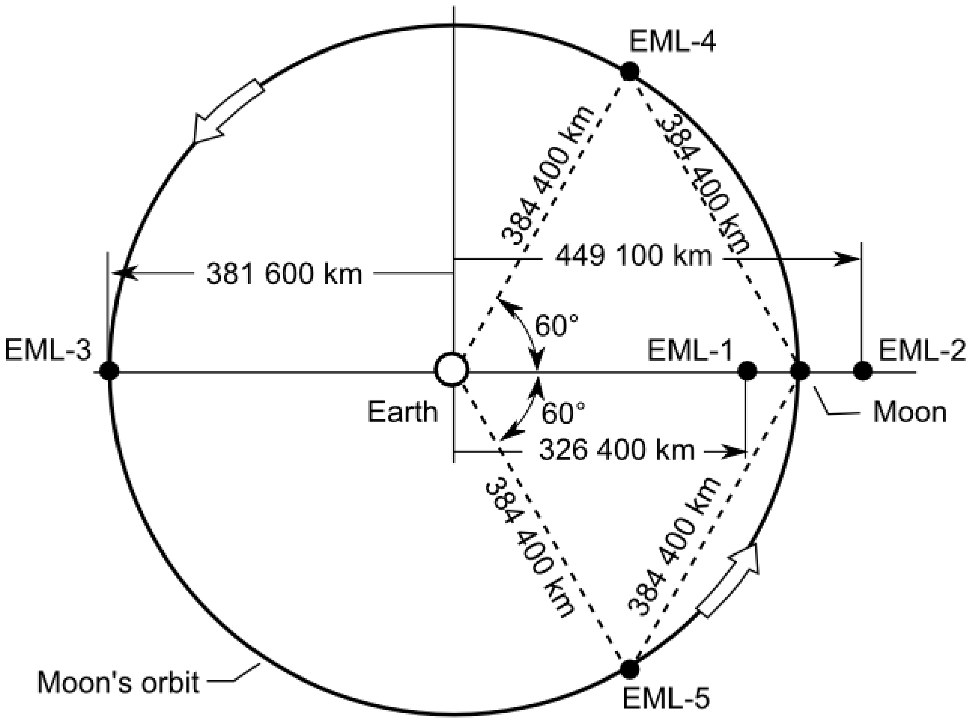

Figure 7: Libration points in the Earth-Moon system

The coordinates of the triangular libration points L4 and L5 (Figure 7) are

$$\text{L4: } \left(\frac{r_{12}}{2} - \pi 2\, r_{12}, +\frac{\sqrt{3}}{2} r_{12}, 0\right) \quad 3.27$$

$$\text{L5: } \left(\frac{r_{12}}{2} - \pi 2\, r_{12}, -\frac{\sqrt{3}}{2} r_{12}, 0\right) \quad 3.28$$

The collinear libration points L1-3 are determined by setting y=0 as well as z=0.

$$\text{L1: } \left(r_{12}\left[1 - \left(\frac{\pi_2}{3}\right)^{\frac{1}{3}}\right], 0{,}0\right) \quad 3.29$$

$$\text{L2: } \left(r_{12}\left[1 + \left(\frac{\pi_2}{3}\right)^{\frac{1}{3}}\right], 0{,}0\right) \quad 3.30$$

$$\text{L3: } \left(-r_{12}\left[1 + \frac{5}{12}\pi_2\right], 0{,}0\right) \quad 3.31$$

In this system the energy and angular momentum of the relative motion are constant in the two-body problem, but also the total energy of the secondary relative to the rotating frame is constant. The so called Jacobi Constant C that was named by German mathematician Carl Jacobi, who discovered it 1836, is used to describe the energy conservation.

$$\frac{1}{2}v^2 - \frac{1}{2}\Omega(x^2 + y^2) - \frac{\mu_1}{r_1} - \frac{\mu_2}{r_2} = C \quad 3.32$$

The equation includes the kinetic energy per unit mass relative to the rotating frame $v^2/2$ the gravitational potential energies $-\mu_1/r_1$ and $-\mu_2/r_2$ of the two primary masses and the centrifugal force per mass unit induced by the rotational frame $\Omega(x^2+y^2)/2$.

$$v^2 = \Omega(x^2+y^2) + \frac{2\mu_1}{r_1} + \frac{2\mu_2}{r_2} + 2C \qquad 3.33$$

The Jacobi constant describes regions in this rotational frame which the secondary mass can reach and when it increases the secondary's body velocity also increases.

3.2.1.2 Stability

The stability of the libration points is one of the main advantages for space applications utilizing these regions in space. The presented mathematical description is based on "Astronautics" by Prof. U. Walter and "The Lagrange Points - Document Created for WMAP Education and Outreach" by N.J. Cornish [18] [19].

A linear stability check can now be performed about each libration point. For small departure displacements allows linearization of the equation of motion

$$x = x_i + \delta x,\ v_x = \delta v_x \qquad 3.34$$

$$y = y_i + \delta y,\ v_y = \delta v_y \qquad 3.35$$

with (x_i, y_i) as position of each position of the libration points. The equation of motion is then

$$\frac{d}{dt}\begin{pmatrix}\delta x\\ \delta y\\ \delta v_x\\ \delta v_y\end{pmatrix} = \begin{pmatrix} 0 & 0 & 1 & 0\\ 0 & 0 & 0 & 1\\ \frac{d^2U_\Omega}{dx^2} & \frac{d^2U_\Omega}{dxdy} & 0 & 2\Omega\\ \frac{d^2U_\Omega}{dydx} & \frac{d^2U_\Omega}{dy^2} & -2\Omega & 0\end{pmatrix}\begin{pmatrix}\delta x\\ \delta y\\ \delta v_x\\ \delta v_y\end{pmatrix} \qquad 3.36$$

The second derivatives of the generalized potential U_Ω

$$U_\Omega = U - \vec{v}\,(\vec{\Omega}\times\vec{r}) + \frac{1}{2}(\vec{\Omega}\times\vec{r})(\vec{\Omega}\times\vec{r}) \quad at \quad r = (x_i, y_i) \qquad 3.37$$

are evaluated.

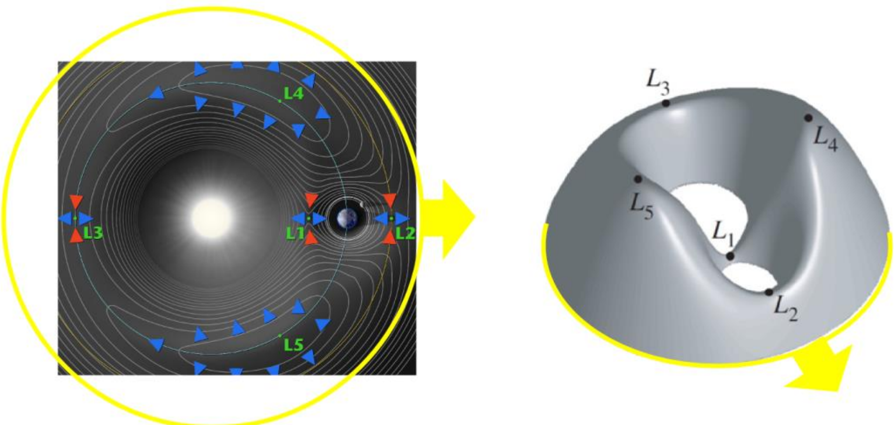

Figure 8: Effective potential U in the R3BP (two views) [19]

For L1 and L2 the second derivatives are given as saddle points on the curvature on the effective potential

$$\frac{d^2U_\Omega}{dx^2} = \pm 9\Omega^2,\ \frac{d^2U_\Omega}{dy^2} = \pm 3\Omega^2, \quad \frac{d^2U_\Omega}{dxdy} = \frac{d^2U_\Omega}{dydx} = 0 \tag{3.38}$$

and are used to solve the eigenvalues of the linearized evolution matrix. The matrix yields

$$\lambda_{1,2} = \pm\Omega\sqrt{1+2\sqrt{7}}\ and\ \sigma_{1,2} = \pm i\Omega\sqrt{2\sqrt{7}-1} \tag{3.39}$$

and the second derivatives for L3 are

$$\frac{d^2U_\Omega}{dx^2} = -3\Omega^2,\ \frac{d^2U_\Omega}{dy^2} = \frac{7m_2}{8m_1}\Omega^2, \quad \frac{d^2U_\Omega}{dxdy} = \frac{d^2U_\Omega}{dydx} = 0 \tag{3.40}$$

and are used to solve the eigenvalues of the linearized evolution matrix. The matrix yields

$$\lambda_{1,2} = \pm\Omega\sqrt{\frac{3m_1}{8m_2}}\ and\ \sigma_{1,2} = \pm i\Omega\sqrt{7} \tag{3.41}$$

L1 and L2 are unstable due to the positive, real root and displacements from the equilibrium points grow exponentially on the configuration line.

$$\Delta x = \Delta x_0 \exp\left(\frac{t}{\tau}\right) \tag{3.42}$$

In this equation τ is the e-fold time and is the ratio of orbiting time to the positive, real Eigenvalue. The e-fold times for L1, L2 and L3 then are

$$\tau_{L1} = \tau_{L2} = \frac{T_p}{2\pi\sqrt{1+2\sqrt{7}}} \tag{3.43}$$

$$\tau_{L3} = \frac{T_p}{\pi}\sqrt{\frac{3m_1}{8m_2}} \tag{3.44}$$

In the Earth-Moon system the e-fold times are $\tau_{L1} = \tau_{L2} \approx 1.8\ days$ and $\tau_{L3} \approx 47\ days$. So a satellite parked in EML-1 or EML-2 would wander off after a few days unless course corrections are made.

The libration points L4 and L5 are stable due to the coriolis force. A mass initially placed near these libration points accelerates down the potential and is coriolis force sends it back into an orbit around the libration point. The second derivatives is given by

$$\frac{d^2U_\Omega}{dx^2} = -\frac{3}{4}\Omega^2,\ \frac{d^2U_\Omega}{dy^2} = \frac{9}{4}\Omega^2, \quad \frac{d^2U_\Omega}{dxdy} = \frac{d^2U_\Omega}{dydx} = \frac{3\sqrt{3}}{4}\kappa\Omega^2 \tag{3.45}$$

$$\kappa = \frac{m_1-m_2}{m_1+m_2} \tag{3.46}$$

The Eigenvalues of the matrix are determined analogously

$$\lambda_{1,2} = \pm\frac{i\Omega}{2}\sqrt{2-\sqrt{27\kappa^2-23}}\ and\ \sigma_{1,2} = \pm\frac{i\Omega}{2}\sqrt{2+\sqrt{27\kappa^2-23}} \tag{3.47}$$

And when the Eigenvalues are purely imaginary L4 and L5 are stable, thus finding

$$\kappa^2 \geq \frac{23}{27} \quad and \quad \sqrt{27\kappa^2 - 23} \leq 2 \tag{3.48}$$

To satisfy these conditions the first equation requires

$$m_1 \geq 24 m_2 \left(\frac{1+\sqrt{1-4/625}}{2}\right) \tag{3.49}$$

and this leads to $m_1 \geq 1.76 \times 10^{24} kg$ with the mass of Earth $m_1 = 5.974 \times 10^{24} kg$ with Moon $m_2 = 7.349 \times 10^{22} kg$, and the second condition is always satisfied. This means that the libration points in our Earth-Moon system are longtime stable for this mathematically approach when the mass of the secondary object is negligibly small in relation to the primaries. However external perturbations induced by other sources like the gravity of Jupiter or solar radiation pressure on the secondary object affect the stability of the orbit.

Asteroids in the Sun-Jupiter SJL-4 and -5 points were observed since 1096 and named Trojan asteroids after the mythological Trojan War with the naming convention of the Greek camp in the leading SJL-4 and the Trojan camp in the following SJL-5 points. More than 5000 Trojan asteroids have been found to date and distributed on inclination up to 40° [20]. Since then Trojan asteroids are found in other libration points and even with $2010\, TK_7$ the first Trojan was found in the Sun-Earth SEL-4 point.

3.2.2 Applications in Earth-Moon Libration Point 4

The EML-4 and EML-5 libration points are very interesting for space applications, taking advantages of one or all their main advantageous features, like long-time orbit stability or the fixed position in the reference tow body system. This subchapter will present possible space applications in the Earth-Moon libration points.

3.2.2.1 Relay Satellite Communication

Communication satellites take advantage of the fixed position and the long-time stability in the libration point region. The fixed position allows a fixed communication link towards the Moon and its surface because the Moon has a bounded rotation with Earth. In that way the same surface area is visible not only to Earth but also to the libration points except EML-3 that is blocked by Earth. But in contrast to EML-1 and -2, the triangular libration points EML-4 and -5 allows longer mission times with less AOCS maneuvers due to less delta-v for station keeping.

Relay links are not only possible between Earth and the Moon. The neighboring EML-2 is an attractive position for radio astronomy satellites and even future space stations, where a direct communication towards Earth is not possible. Their data have to be transmitted via a relay satellite and such a satellite in EML-4 offers advantages compared to one in an EML-2 halo orbit. The data of lunar surface missions can also be relayed with a set of lunar orbiters. But it is a similar case as with a relay in EML-2 with the difference that the amount of delta-v for the attitude and orbital control subsystem (AOCS) is higher. Mainly because the mass distribution of the Moon is not equally distributed and the not spherical shape result in a center of gravity that does not lie in the geometric center. This leads to ascending orbits and a limited in-orbit time because of propellant needs. The lunar synchronous orbit lies beyond the lunar sphere of influence and cannot be used as an alternative. There are efforts to find frozen lunar orbits where all the gravity perturbation during the orbits counteracts and does not lead to descending orbits. So far the lunar orbiters orbit time ranged from a few years in lower lunar orbits like Luna 22 and several years in high elliptic orbits like Explorer 35 (shut off after 6 years) and ending in crash landing on Moon. Hence for a lunar satellite relay, several satellites are needed in the configurations (like Walker-configuration). [21]

A satellite on an orbit of the Moon can also be used for signal conversion and amplification of missions to Earth's weak stability boundary (WSB).

For a future exploration of space relay satellites are an important building block in the backbone of the space exploration infrastructure supporting a wide range of missions.

3.2.2.2 Science

Scientific research in the EML-4 and -5 is essential for the TYCHO mission as well as for human kind. The triangular libration points are not yet explored besides short passages of the Japanese space probe Hiten and remote sensing from Earth with low resolution radar and telescopes. In-situ observation and measurements can be preceded with higher resolutions. Furthermore the orbit can be used for observations of the universe with less Earth disturbances and within a longer time scale.

3.2.2.2.1 Gravity Trap for Space-Dust

The triangular libration points are "mass traps" for negligible masses compared to the masses of the primaries Earth and Moon. However the existence of the Kordylewski clouds is still under dispute. A concentration of space dust is assumed to exist in these points and firstly proposed by Kazimierz Kordylewski in the 1960. He visually observed and took photographs of lunar libration clouds. [22] Observing the clouds are difficult to achieve from the Earth and not all scientists were able to reproduce the observation and to investigate the clouds. It is assumed that the clouds consist of captured micro particles and that the clouds extend up to a radius of 5000 km around the EML-4 and -5 points. [23] This range into the operational zone of TYCHO and the particles could interfere with the satellite and possess a potential threat to the solar-arrays and further components leading to an increased degradation. This investigation is of interest for evaluating the mission time of the operational TYCHO satellite TMA-1 and shall be explored with the demonstration mission beforehand. Additionally the features of the Kordylewski cloud like concentration, particle sizes, relative velocity and composition is of great interest for the science community to determine the existence of the clouds and to conclude the origin of these particles.

Moreover the position is of use for particle research because the magnetic field of Earth is hardly influencing the partly charged particles. This makes it more suitable for space dust research in general like lunar ejecta (10 nm to 1 mm particle diameters), other solar system planets ($0.2\ to\ 20\ \mu m$ and $10^{-13}\ to\ 10^{-4}\ g$) or even cosmic space dust. Of course it is also of interest for micro meteorite detection [24].

3.2.2.2.2 Space Weather

Space weather is a collective term for environmental conditions in near-Earth space and describes magnetic fields and radiation. TYCHO can be a platform for measuring these physical parameters during the transfer between Earth and up to the WSB zone and during the mission on EML-4 over a longer period.

During the transfer time from Earth outwards, the satellite will pass the van-Allen belt and the magnetic field of Earth in general. The van-Allen belt is one of three layers held within Earth’s magnetic field and containing energetic charged particles, plasma. It ranges between 1000 km and 60000 km. The charged particles influence the satellite systems and can even pose a threat to circuitry and material. This is not only of interest for science, but also influences the transfer orbit design. The design trades off the number of passages through the belt with the aim of a low number of repetitions, and the dry system mass wants to be maximized and this is sometimes achieved by several ignitions in periapsis to raise the apoapsis. This is of importance for orbits with periapsis in LEO near to the gravity well. Plasma measurement of the belts can be done during transfer times. When within the target orbit only the sources of the van-Allen belt, solar wind and other cosmic rays interfering with the magnetic field, can be measured and the effects of Earth’s magneto-tail reaches into the libration point region.

Another field of research is cosmic and solar radiation and intensity. The solar magnetic intensity cycles have an average period of 11 years and influences the atmospheric weather on Earth and influences satellites in Earth orbit. In addition, solar flares, coronal mass ejections, are streams of highly energetic particles even present radiation hazards for satellites and manned space flight [25]. Observation of the solar intensity during a long mission time of 10 years may help our understanding about earth atmosphere and solar flare particles can be researched with less magnetic influences before they are affected within the van-Allen belt. Additionally for manned spaceflight in Earth’s and lunar orbit a satellite may serve as a sensor in an early warning system providing additional reaction time for astronauts to take response actions. Due to velocities of 800 km/s of the fast solar wind and 400 km/s of the slow solar wind is slow enough to have a response time of 8 to 16 minutes to protect against the particle impacts and radiation doses [26]. For dangers like x-ray and gamma-ray bursts with speed of light velocities it serves as an immediate warning system. This is true for the assumption of a direct propagation path of the threads via the EML point to the protective area.

3.2.2.2.3 Observation and Astronomy

The triangular libration point orbits are also of interest for observation of the Moon and astronomy.

Moon observation takes advantage of the same footprint area that can be scanned over a longer period of time and on a region that cannot be observed from an Earth based point of view. This allows detection of topographic changes like new craters by meteorite strikes, plasma conducts or dust and particle movement above lunar surface.

Instead of pointing with the satellite to the Moon, astronomy is the other main sensing application in several ways. The obvious application is an astronomy satellite in EML-4 due to the stable equilibrium point with restoring effects. This allows again less intensive delta-v maneuvers for station keeping for a single satellite but also for formation flying for an array of satellites working together to increase the aperture of the astronomy satellite [27]. But the EML-4 also supports radio astronomy in EML-2 behind the Moon. Such astronomy missions could take advantage of the blocked position in the radio shadow and thus increasing the signal to noise ratio for their measurements. However, the returning way for sending back the acquired data is also blocked and a relay satellite is needed either in an EML-2 halo orbit with y- and z-axis amplitudes that allow to relay signals received from the astronomy mission below in EML-2 point to be transmitted to Earth or by using the triangular libration points EML-4 or -5.

3.2.2.3 Infrastructure

For future exploration missions infrastructure is needed and some of them are proposed for libration points. This sub-chapter presents a selection of applications on the EML-4 and -5 points where TYCHO can be used directly as a communication satellite platform or as a design basis.

3.2.2.3.1 Space Station and Gateway Infrastructure

Space stations and human space flight in general is an important aspect of space exploration to allow research that is not possible with remote sensing and remote controlled and autonomous vessels. There are proposals for a gateway station in EML-4 for deep space destination or to catch a near Earth asteroid (NEO) and move it to the libration point for further research or even asteroid mining. Other parked masses in orbit would be propellants for refill purposes.

The operation of space stations and the scientific research require high data-rate links to Earth. The additional voice communication is an important point for crewed mission including medical and safety monitoring and telecommunication of the personal with ground mission personal and their families [28] [29]. For a space station in EML-1, a link via EML-4 can be used for redundancy purposes and for a space station in EML-2, either a large halo or an additional relay satellite has to be chosen.

3.2.2.3.2 Interplanetary Transport Network

The configurations of the gravitation sources that are responsible for the libration points also offer the so called Interplanetary Transport Network. This is a collection of path ways for objects through the Earth-Moon and even through the solar system where little energy is needed. Starting on the libration points small delta-v maneuvers will move the spacecraft nearer to the gravity and pulled towards it. This effect was used also by Hiten to rescue the mission after failed transfer orbit injection with a delta-v deficit of 50 m/s [30]. It is even possible to use these gravitational manifold tubes between libration points for interplanetary transfer even connecting these path ways to planets into the solar system. Transfers with this methods take long-times and are hardly suitable for manned space flight, but for probes.

3.2.2.3.3 Lunar Navigation Satellite System

Transfers to the Moon and within the Earth-Moon system are navigated with position data provided by the internal inertial measurement system, by active ranging or transmitted as data from Earth, where it has been determined with radar or ranging methods. There are proposals to use the side beam of the Earth targeting GNS-Satellites that are propagated besides the

Earth and into space [31] [32]. These side beams possess less power density, can be scattered by Earth's atmosphere and are not permanently accessible in Earth orbits. With GNSS satellites on the libration points, an autonomous transfer between Earth and Moon may be possible. Distributing GNSS time signals from the libration points extended with signals from the Earth or the Moon, it can be used for positioning of automated transfer vessels and increasing their navigation accuracy. Further concepts (LUPOS) [33] propose a lunar positioning for surface navigation of rovers and vessels. Such lunar positioning and navigation systems are set up in Walker-configuration in lunar orbit and are also influenced by the gravitational effects with descending orbits. Such satellites placed in the libration points may offer support for a lunar navigation system.

3.2.3 Effects on Space Mission Design and Operation

The special features of the EML-4 orbit causes several conditions that affect the space mission design and the operation of the satellite. This chapter lays out detailed analyses of parameters that are used to specify the mission requirements of the operational mission TMA-1 that will then be used for re-evaluations for the requirement derivations for the demonstrator mission TMA-0.

3.2.3.1 Coverage Area on Moon

The TMA-0 demonstrator is placed in a libration point around EML-4 and this defines the line-of-sight towards the Earth and the Moon. According to the propagation cones of both signal links originating from EML-4, both coverage areas are forming a distinguished footprint on the celestial body. The footprint area almost covers the same lunar positions due to the bounded rotation of the Moon. The only changing effect is the lunar libration tumbling around its axis. For the Moon footprint it is important to find hotspots of scientific or other missions' interest inside the footprint area. This gives a scope of possible future missions that can be supported and serviced.

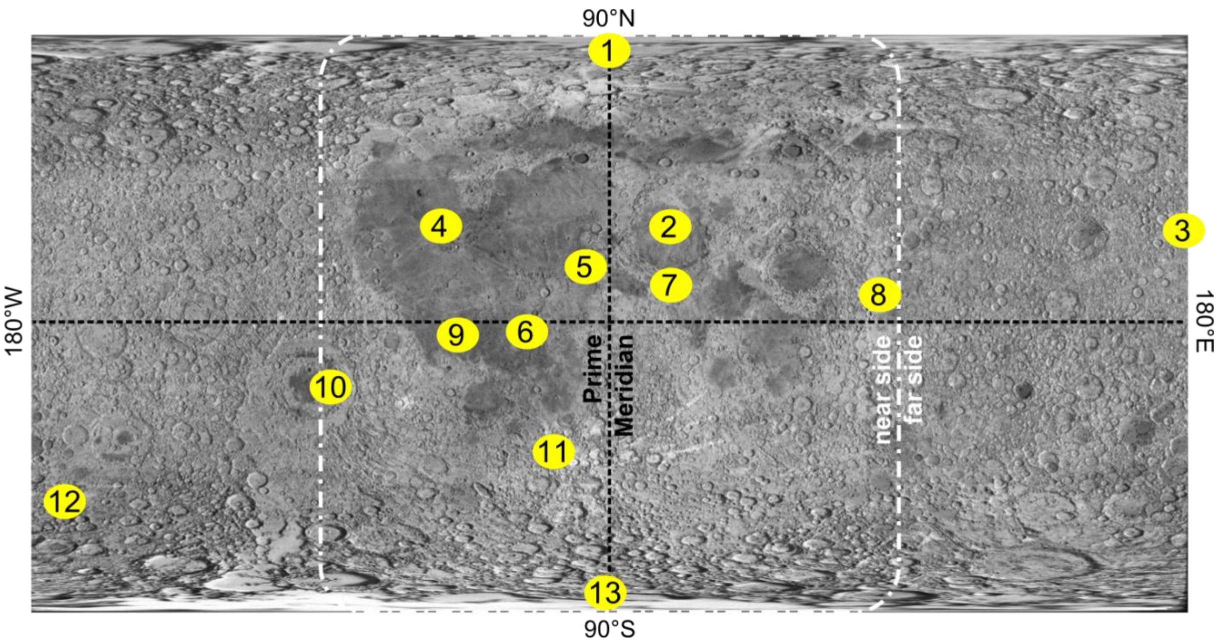

Figure 9: Lunar map including top 10 sites of NASA ESAS and Apollo 18 – 20 landing sites [34]

Table 1: High priority landing sites

Lunar Areas of Scientific Interest				
#	Location	Selection	Longitude*	Latitude*
1	North Pole	ESAS Top 10	89.5 N	91.0 E
2	Hadley Rille	Apollo 19	26.5 N	4.7 E
3	Central Highlands	ESAS Top 10	26.0 N	178.0 E
4	Aristarchus Plateau	ESAS Top 10	26.0 N	49.0 W
5	Rima Bode	ESAS Top 10	13.0 N	3.9 W
6	Copernicus Crater	Apollo 18	9.7 N	20.0 W
7	Mare Tranquilitatis	ESAS Top 10	8.0 N	21.0 E
8	Mare Smythii	ESAS Top 10	2.5 N	86.5 E
9	Oceanus Procellarum	ESAS Top 10	3.0 S	43.0 W
10	Oriantale Basin Floor	ESAS Top 10	19.0 S	88.0 W
11	Tycho Crater	Apollo 20	43.3 S	11.4 W
12	South Pole Aitken Basin	ESAS Top 10	54.0 S	162.0 W
13	South Pole	ESAS Top 10	89.9 S	180.0 W

This table includes a list of lunar locations of special scientific and mission interest. It is ordered according to longitude coordinate and does not reflect an order of importance.
*(*Selenographic Coordinates)*

The selected lunar areas are among the top 10 Exploration Systems Architecture Study (ESAS) [35] [36] conducted by NASA in November 2005 with a focus in manned missions. The list is expanded by the landing sites of the cancelled Apollo missions 18 – 20 for a possible reboot of Apollo scientific goals.

The coverage area is analyzed with AGI’s Satellite Tool Kit (STK) [37]. The model includes grid points with a precision of 2° on surface altitude provided by the Kaguya topographic terrain map (JAXA). This reflects the altitude contours of lunar surface to allow signal shadow zones in valley areas and the grid covers the complete surface that allows a combined analysis of several signal origins from the Earth, EML-4 and EML-5.

The Earth signal is sent from the position representing the ground station position of the Deep Space Network (DSN) facility in Madrid and is assumed for this analysis as the only signal source out of three DSN facilities. This reflects the minimum configuration of ground stations needed for the TMA-1 mission with a limited access time to the Moon or to TMA-1 due to earth’s rotation. With three positions like the DSN constellation, a full access is still possible and also presented below.

The EML-4 signal propagates from the exact, in-plane position in EML-4. This is modeled for STK with an ephemeris file for the references frame on the libration point itself in the rotation Earth-Moon frame.

The EML-2 signal propagates from a halo orbit with z-axis and y-axis amplitudes of 8000 km. The minimum halo orbit amplitudes for communication are 1737 km that corresponds to the radius of the Moon and would bring the satellite out of the Moon shielded zone. The ephemeris file includes positions for an orbit period with half of that of the primaries of 13.65 days. This modeling is adequate with respect to the grid precision and for a detailed orbit model STK shall be used in a further study.

All three signal cones from Madrid, EML-4 and EML-2 of this analysis are set to capture the lunar center of mass and the cones encompass the complete volume of the Moon. This allows for the maximum footprint to be projected on the surface. A further constraint is set for each grid point to register only signals with an entering elevation of minimum 5°. This is included to model the reception antenna. Signals received under flat elevation angles are often disturbed by reflections of the same signals and also of the environmental noise reflected by the lunar surface material acting as a reflector. This modeling reduces the footprint area. The simulation time is set to one Moon orbit of 27.3 days to include Earth rotation and the frequent access of once per day from the Earth ground station and the comparison relay satellite on the EML-2 halo orbit with a period 13.65 days. While the footprint area from Earth and EML-4 are almost fixed due to the orbital constellation, the footprint for the EML-2 halo relay is moving and alternately covering also north and south poles due to its orbit.

The results of the coverage analysis are shown in Figure 10 to Figure 12, the corresponding Table 2 to Table 5 provide the access times as fraction of one Moon orbit period to the defined sites of interest.

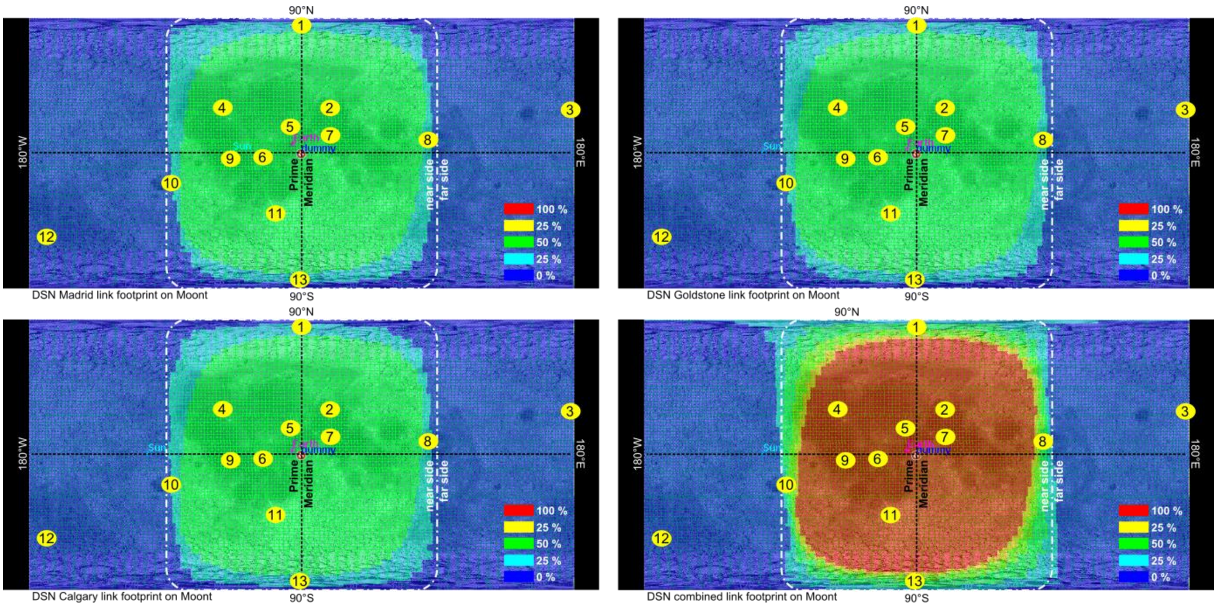

Figure 10: Coverage time on the Moon from Deep Space Network (DSN).
Madrid, Goldstone (top left & right) and DSN Calgary, all three DSN locations combined (bottom left & right)

Table 2: Coverage access on selected locations during the simulation time (1/2)

Coverage Time at Different Lunar Locations in Percent [%] (1/2)					
#	Target Location	Communication Link from…			
		DSN			
		Madrid	Calgary	Goldstone	Combined
1	North Pole	13.3	8.3	14.0	24.8
2	Hadley Rille	49.9	48.9	49.6	100
3	Central Highlands	0.0	0.0	0.0	0.0
4	Aristarchus Plateau	49.9	48.9	49.6	100
5	Rima Bode	49.9	48.9	49.6	100
6	Copernicus Crater	49.9	48.9	49.6	100
7	Mare Tranquilitatis	49.9	48.9	49.6	100
8	Mare Smythii	19.3	19.2	19.5	30.4
9	Oceanus Procellarum	49.9	48.9	49.6	100
10	Orientale Basin Floor	12.3	15.5	12.4	29.5
11	Tycho Crater	49.9	48.9	49.6	100
12	South Pole Aitken Basin	0.0	0.0	0.0	0.0
13	South Pole	6.3	10.8	6.6	17.8

Coverage access in percent by grid points on selected locations during the simulation time

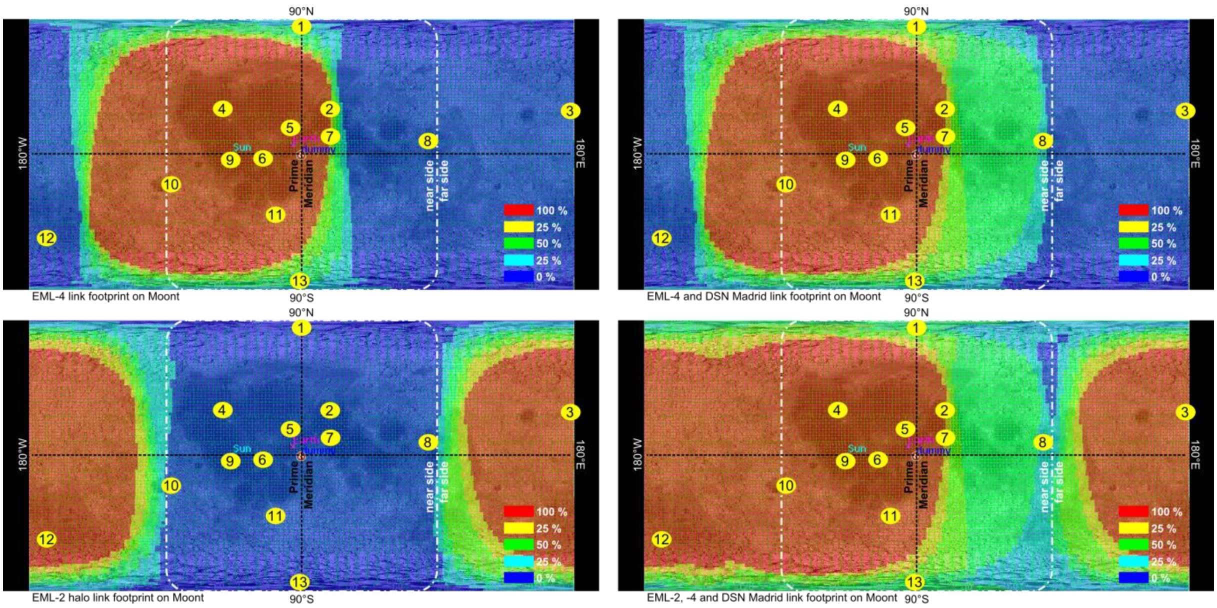

Figure 11: Coverage time on the Moon from EML-4, EML-2 and DSN.
EML-4, EML-4 and DSN Madrid (top left & right) and EML-2 halo, EML-2, -4 and DSN Madrid combined (bottom left & right)

Table 3: Coverage access on selected locations during the simulation time (2/2)

Coverage Time at Different Lunar Locations in Percent [%] (2/2)					
#	Target Location	Communication Link from…			
		EML-4	EML-2 halo	EML-4	EML-2 & -4
				DSN combined	DSN Madrid
1	North Pole	20.2	19.2	38.5	49.3
2	Hadley Rille	100	0.0	100	100
3	Central Highlands	0.0	100	0.0	100
4	Aristarchus Plateau	100	0.0	100	100
5	Rima Bode	100	0.0	100	100
6	Copernicus Crater	100	0.0	100	100
7	Mare Tranquilitatis	71.7	0.0	100	86.1
8	Mare Smythii	0.0	10.7	30.4	30.4
9	Oceanus Procellarum	100	0.0	100	100
10	Orientale Basin Floor	100	11.4	100	100
11	Tycho Crater	100	0.0	100	100
12	South Pole Aitken Basin	0.0	100	0.0	100
13	South Pole	22.4	18.6	36.6	46.3

Coverage access by grid points on selected locations during the simulation time

Except the Central Highlands, Mare Smythii and the South Pole Aitken Basin, all other locations can be reached by the EML-4 position, even the lunar poles, for a certain time.

A satellite in EML-2 halo orbit can access fewer locations but offers an exclusive access to locations on the far side like the Central Highlands and the South Pole Aitken Basin. Access times to the poles are in a similar range for the EML-4 and EML-2 satellites but the EML-2 satellite is able to send signals with a higher elevation and even reaching deeper into craters because of the z-axis amplitude of the orbit and the closer distance. Whereas the EML-4 satellite is placed on the Moon’s orbit plane and only benefits of the natural lunar libration, a tumbling of the lunar rotation axis giving access to lunar poles. Implementing an inclined orbit around EML-4 could improve this. This is discussed in more detail in Chapter 4.2.3.1.

Table 4: Coverage of the Moon from Deep Space Network (DSN)

Coverage of the Moon	DSN Madrid	DSN Calgary	DSN Goldstone	DSN Combined
% Satisfied	51.17	51.41	51.26	51.58
Area Covered (km²)	19405237.05	19496944.91	19437820.83	19560535.19

The DSN coverage of the lunar surface only satisfies the near side and some small parts of the far side due to lunar libration of the rotation axis. Even though it covers this area, the regions near to the transition to the far side shows less coverage time and the communication link falls below 5° elevation angle. With three ground stations located on Earth with a difference of 120° longitude, a permanent coverage time is possible in most of lunar near side regions. Hence in this area TMA-1 can serve for redundancy communication or to provide additional bandwidth.

Table 5: Coverage of the Moon from EML points and EML point in combination with DSN

Coverage of the Moon	EML-4	EML-2	EML-4 & DSN Combined	EML-2,4 & DSN Madrid
% Satisfied	51.01	54.60	68.01	99.98
Area Covered (km²)	19344770.76	20705562.45	25792246.9	37912429.37

A full lunar surface coverage requires a satellite in EML-4 (or EML-5) position, a satellite in EML-2 halo orbit and three ground stations on Earth. This provides coverage of 99.98 % of the surface and is a benefit for a lunar communication network and permanent observation.

3.2.3.1.1 Discussion of EML-4 Coverage

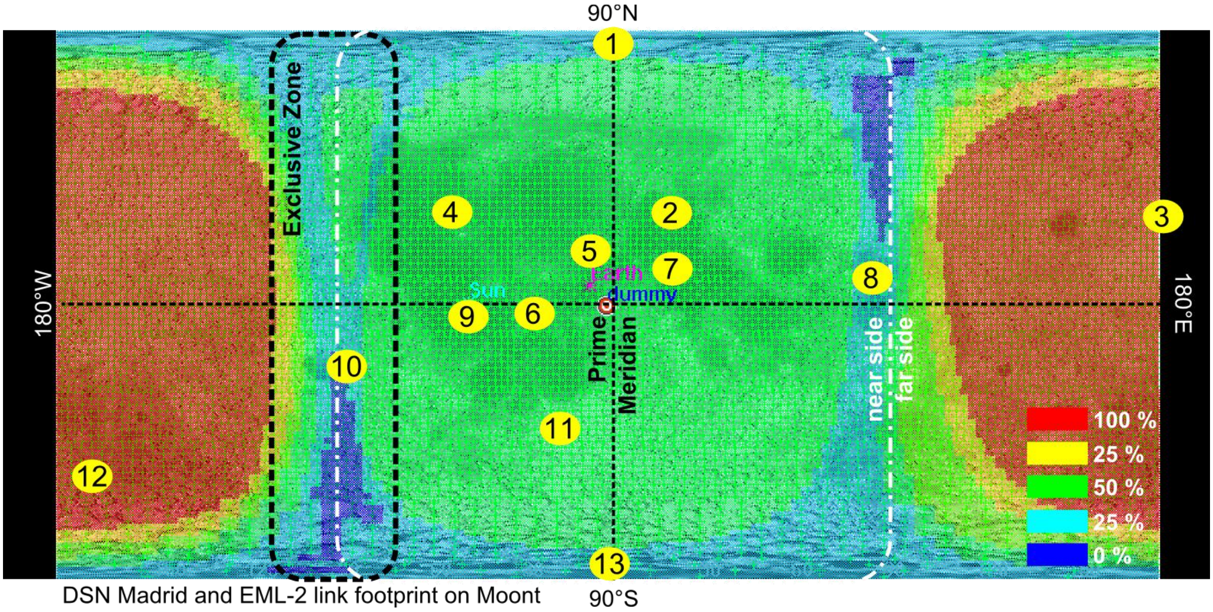

Figure 12: Lunar coverage map with EML-4 exclusive zone.
Showing the coverage gap between the DSN Madrid and the EML-2 halo orbit relay satellite coverage zones. This is the exclusive zone only accessible from EML-4

The overall EML-4 coverage zone ranges from 20°E - 140°W, 85°N - 85°S, as shown in Figure 11.

An overlay of the EML-2 and DSN coverage areas (Figure 12) shows that the zone marked as exclusive zone is only accessible from an EML-4 satellite. The Orientale Basin Floor high priority landing site is in this EML-4 exclusive footprint zone between 80°W-100°W and 85°N-85°S. In there, it has a full signal coverage from EML-4 and only a part access from Earth during 12.3 % of the Moon’s orbit period with one DSN ground station. With all three DSN station in increases access time during 36.9% of one Moon orbit period.

The EML-2 relay satellite only provides access time to the Orientale Basin Floor during 11.4% of one Moon orbit period. The exclusive zone region lies on the edge of the near side and far side of the Moon and is of special interest for radio astronomy that needs to be placed on Moon with a blocked line-of-sight towards the Earth. This shielded zone provides a special and needed environment for astronomical research. So the exclusive zone coverage marks a unique selling proposition for lunar mission who requires operating in there.

The lunar poles are of special interest to research with a focus of lunar south pole [38] [39]. The coverage times for grid points between 84°S to 90°S are analyzed in addition to the thirteen landing sites (Table 1). Each of the following graphs (Figure 13 to Figure 15) show grid points of one latitude.

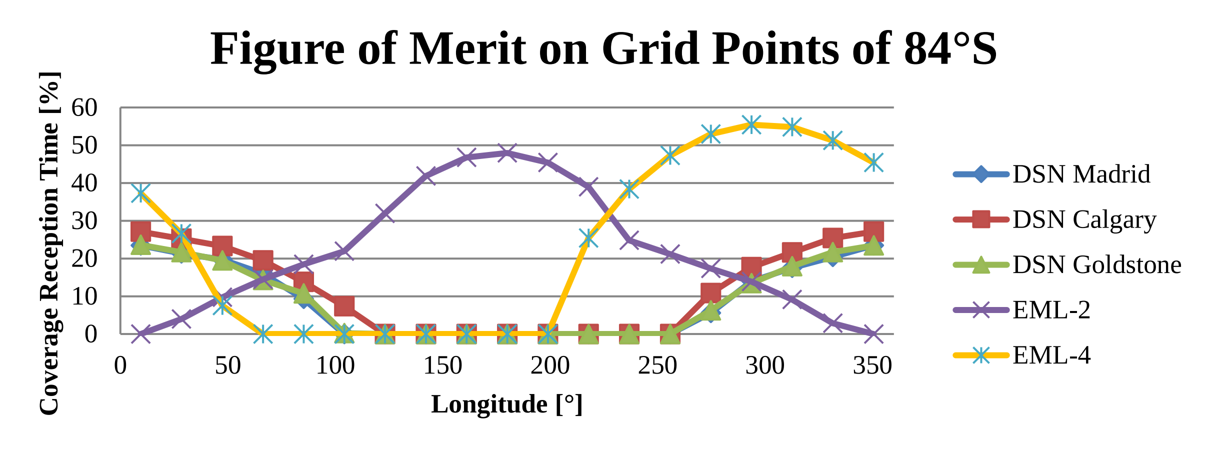

Figure 13: Figure of merit (coverage reception time) on grid points of 84°S

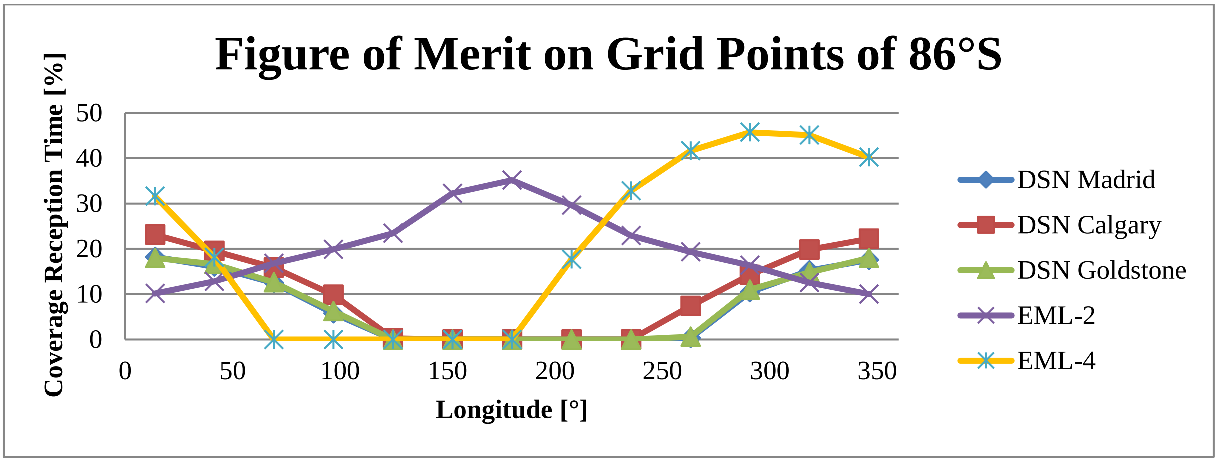

Figure 14: Figure of merit (coverage reception time) on grid points of 86°S

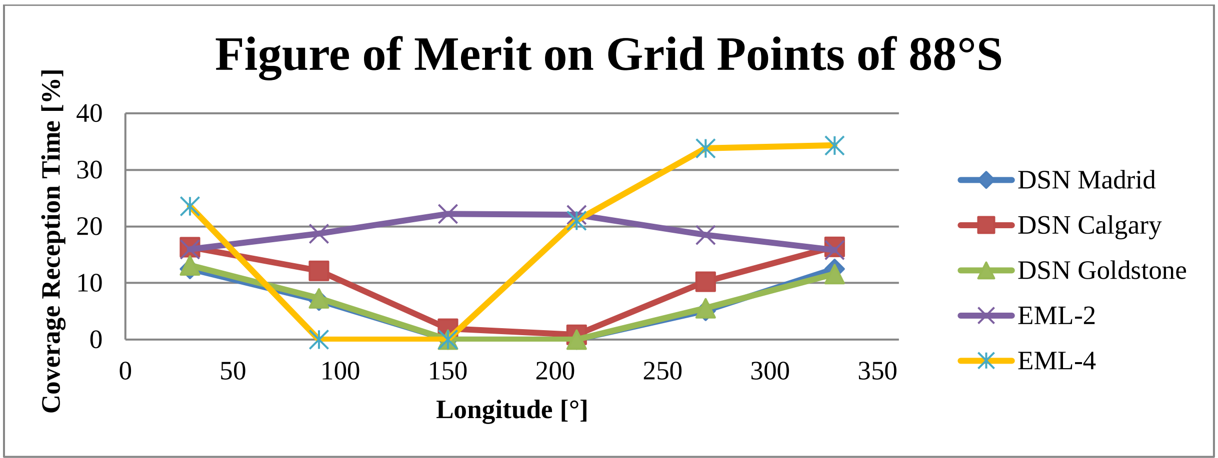

Figure 15: Figure of merit (coverage reception time) on grid points of 88°S

This latitude wise analysis shows that the latitude between 75°E and 160°W is not covered or only partly covered from EML-4. Only from an EML-2 halo orbit position all grid points receive coverage during a fraction of one Moon orbit. Nevertheless the coverage times of grid points with longitudes around 60°W is higher from EML-4 (55%) than the coverage times of grid points with longitude around 180°E from the EML-2 halo (45%). This is due to the out-of-plane period of the EML-2 halo orbit that only allows access to the poles of half of its orbit period.

Especially on the lunar poles low elevation for ground station or relay satellite visibility becomes important. In this pole area the roughness of the topography need to be taken into account that local topography features allow direct line-of-sight communication with very low elevation angles as analyzed for Next Lunar Lander [39]. A more detailed study has to be done for specific pole missions.

3.2.3.2 Coverage in Lunar Orbit and EML-2

For lunar orbiters or satellites EML-2 halo orbits black-out phases during communication is a planning point because during this time the satellite has to be self-operational. All acquired data cannot be sent during this period and has to be stored onboard instead until the orbiter is in direct line-of-sight of the ground station and in their communication cone.

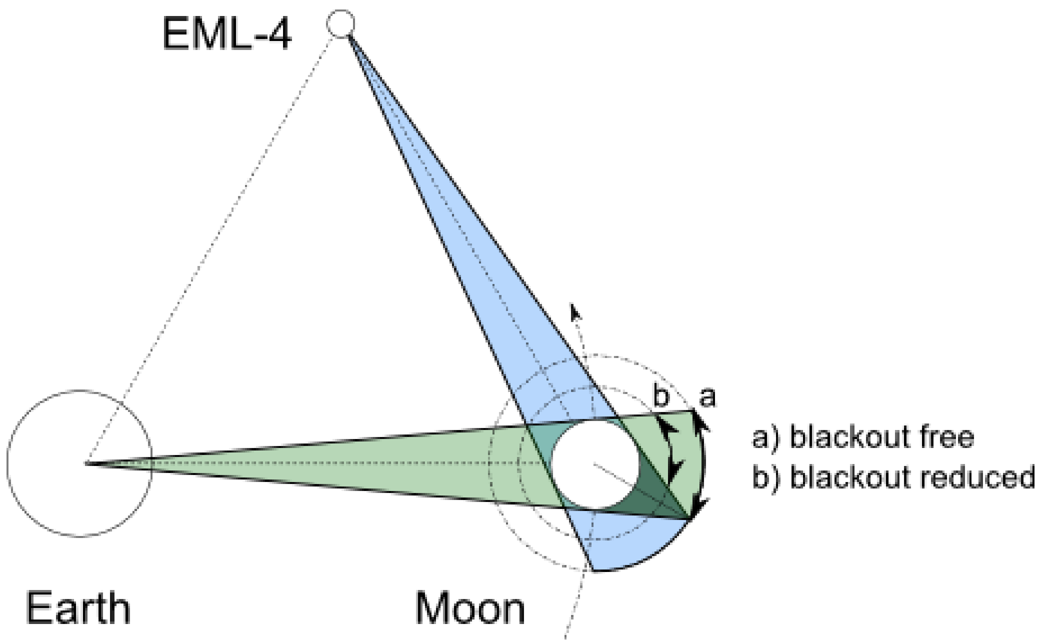

Figure 16: Communication black-out reduction of lunar orbiters via EML-4 relay communication

With an additional communication link provided from EML-4 position blackout phases can be decreased for lunar orbits with altitudes to 1765 km and is estimated with basic 2D-geometric calculations for spheres.

Above this altitude the orbiter is always in direct line-of-sight of either the Earth ground station or of an EML-4 satellite. To ensure communication the lunar orbiter needs to be within the EML-4 satellite’s propagation beam or the relay satellite has to be re-targeted to follow the orbiter when it leaves the nominal propagation beam.

Satellites in EML-2 position or with z- and y-axis amplitudes less than the Moon's radius are only reachable via an EML-4 relay in this configuration. These orbits in the shielded zone are of special interest to radio astronomy missions that use the Moon to block the satellite from artificial radio frequency noise from Earth.

3.2.3.3 Signal Latency

Lunar missions require different maximum signal latencies for their objectives. These depend on factors like real-time performance, data packaging or human voice communication.

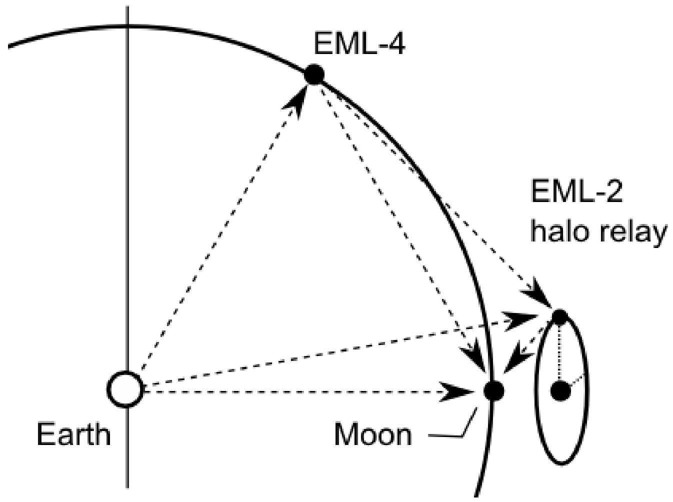

Figure 17: Signal propagation paths

Table 6: Delay times of a one-way signal propagation from Earth to the Moon and via relay stations

	Earth to Moon	Earth via EML-4 to Moon	Earth via EML-4 via EML-2 halo to Moon	Earth via EML-2 halo to Moon
Distance [km]	384400	768800	863295	449171
Propagation time [sec]	1.28	2.56	2.88	1.50

The Table 6 presents different signal routings and their propagation times. It is obvious that the signal routing from Earth via EML-4 to the Moon surface takes the longest time and is only surpassed by another relay routing via EML-2 before the signal reaches the Moon. This propagation time is one of the biggest influences in the signal latency budget. The budget contains latency times of all propagation paths and signal processing steps and it sums up to the round-trip statement.

Round-trip times are crucial for and tele-presence applications. Round-trip delay time is the time the signal takes to go to the satellite and return. This includes the complete signal delay generated by the signal propagation times and processing times of devices the signal passed in the satellite. For tele-robotics a rover or manipulator is directly operated and steered by personnel and there are concepts to reduce latency times for lunar missions by placing a space station in EML-1 and operate the robots from this nearer location [40]. The main focus of a relay satellite in EML-4 is a permanent signal routing for scientific and telemetry data. Depending on the processing like recorded data transmission or live video compression round-trip delay times may be between 5.5 and 6.5 seconds.

Nevertheless it is technically possible to send real-time data but it requires further planning and autonomous function to reduce the latency effects. So the Apollo astronauts communicated via audio channels with mission control center in Houston, Texas. The ITU recommends not to exceed a one-way delay of 400 ms regardless of the type of application (ITU-T Rec. G.114) [41] otherwise the user is dissatisfied.

This delay is also applied for the internet protocol packet delay variation (IPDV) used for the Internet on Earth [42]. Extensions of the internet protocol for space application are already active on the ISS with Internet Protocol (IP) Encapsulation (CCSDS 133.1-B-2) [43] [44] and there are concepts for further concepts with interplanetary internet [45] or NASA delay tolerant networking [46].

The signal delay budget shall respect an increased round trip time. The benefits of a direct, IP based data transfer from lunar networks into the reception network shall be respected with the implementation of a delay tolerant communication protocol for TMA-1, with minimizing routing delays and by buffering the data onboard of TMA-1. The complete round trip for the TYCHO mission includes future networks like the International Lunar Network (ILN). Via ILN different lunar missions are able to connect to each other and the signal shall be relayed via peer-to-peer (P2P) to central lunar communication terminals (LCT) on the surface, existing relay satellite networks and Earth based infrastructures. In this way a complete chain-of-transmission without conversion to different protocols is possible with a common standard protocol.

3.2.3.4 Field-of-View

From the EML-4 orbit the field-of-view to Earth and to Moon spans the maximum surface coverage. It can be used to define the half-power beamwidth (HPBW) angle that is needed to provide communication coverage from maximum transmit power on the center line to target until the radiated transmit power drops 3dB. The HPBW is also defined by the field-of-view (FOV) (Figure 18)

$$\frac{FOV}{2} = \tan^{-1}\left(\frac{Radius}{Distance}\right) = HPBW \qquad 3.50$$

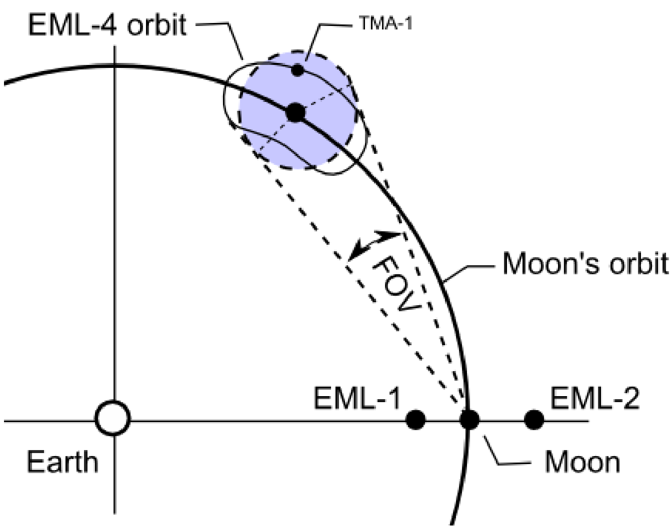

Figure 18: Field-of-view angle that covers the EML-4 orbit

The Table 7 shows the half-power beamwidth (HPBW) angle for covering Earth and even the GEO, in case for full GEO relay satellite reception, on the one link side. On the other link side it covers the Moon and lunar orbits until altitude of 2000 km to be able to give access to lunar orbiter.

Table 7: Half-power beamwidth angle from satellite to Earth, Moon and orbits

	Distance to Earth	R_{earth}	R_{earth}**+GEO**	R_{moon}	R_{moon}**+2000km**
	[km]	6371	42157	1737	3737
Periapsis	363300	1.005°	6.619°	0.274°	0.589°
Sem. Axis	384400	0.950°	6.259°	0.259°	0.557°
Apoapsis	405500	0.900°	5.935°	0.245°	0.528°

From the other direction (Earth or Moon) the HPBW angle is defined by the relative distance from TMA-1 to the EML-4. Table 8 shows results for orbits with distances analyzed in [47] and also used for the later design of the orbit keeping.

Table 8: HPBW angle from the Earth or Moon to a satellite with orbits of distances to EML-4

	Distance to Earth	**A**	**B**	**C**	**D**
	[km]	(0,0,0)	(5000,5000,0)	(10000,10000,0)	(45000,45000,0)
Periapsis	363300	0.00	0.788°	1.577°	7.061°
Sem. Axis	384400	0.00	0.745°	1.490°	6.677°
Apoapsis	405500	0.00	0.706°	1.413°	6.332°

Both directions identify maximum HPBW angles for the communication links with a full coverage of the celestial bodies. Nevertheless full coverage is not needed in every application. Smaller HPBW angles give the advantage of increased antenna gains and higher data-rates and the smaller angle can be compensated by retargeting the antenna due to small movements of the satellite or steerable antennas. Using steerable antennas (motor, phase array) can have a positive effect on the sensitive design of the communication link budget.

3.2.3.5 Perturbations

Each mass body in a multi body system is attracted by every other mass during their orbit run. If one body movement describes an orbit around a second body each additional mass' attraction is a perturbation that will change the orbit movement to a certain attempt that is proportional to the distance between both attracting masses. Besides the gravity induced perturbations there are additional perturbations that are generated by pressure acting on the body's surface, such as solar radiation pressure or atmospheric drag.

The trend shown in Figure 19, Table 9 and Table 10 taken from "Astronautics" [19] depict that the relevant perturbations acting on a satellite in EML-4 orbit are generated from Earth and Moon, from the Sun and solar pressure and from Jupiter. Because the Earth and the Moon are rotating around each other and the system is also rotating around the Sun, thus the perturbations on the satellite changes over time.

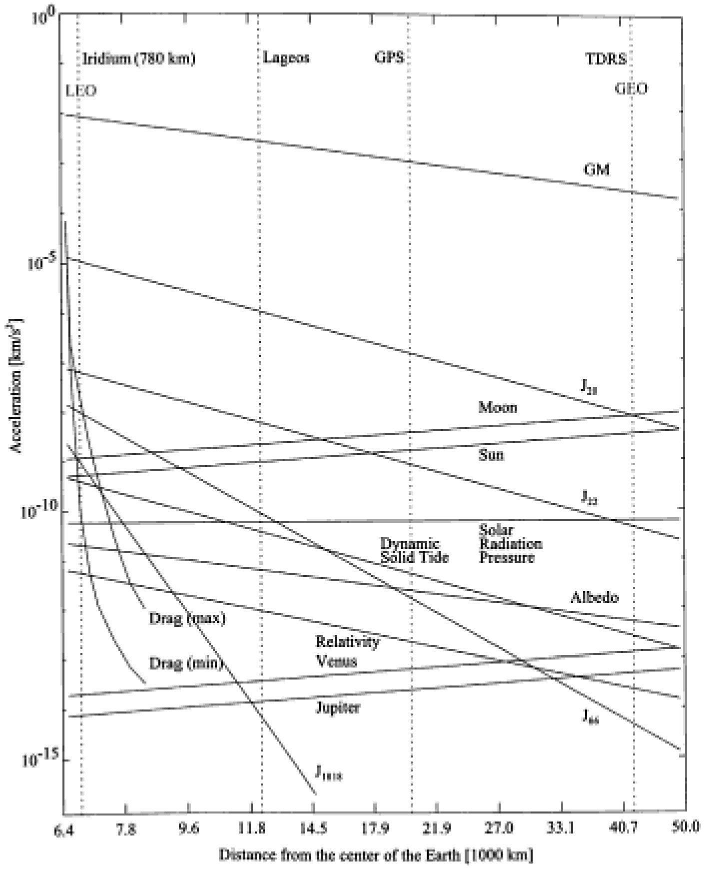

Figure 19: Magnitudes of different perturbations of a satellite orbit

Table 9: Magnitudes of perturbations (m/s²) on a S/C at a distance from Earth of 50000 km (1/2)

Perturbation	**GM**	**Moon**	**Sun**	**J2,0**	**Solar Radiation Pressure**	**J2,2**
Magnitude	2×10^{-1}	9×10^{-6}	7×10^{-6}	6×10^{-6}	$8 \times 10^{-8}\ (A_{\perp}/m)$	4×10^{-8}

[19]

Table 10: Magnitudes of perturbations (m/s²) on a SC at a distance from Earth of 50000 km (2/2)

Perturbation	**Albedo**	**Venus**	**Dynamic Solid Tide**	**Jupiter**	**Relativity**	**J6,6**
Magnitude	6×10^{-10}	3×10^{-10}	2×10^{-10}	8×10^{-11}	2×10^{-11}	1×10^{-12}

[19]

GM = regular gravitational force of the Earth
Jn,m = gravitational multi-poles
Relativity = relativistic deviations

During the orbit design these perturbations are included because they affect each orbit (transfer, orbit keeping and disposal). Besides the weak stability transfer, where the influence of Sun's gravity will be used for orbit plane changing, the most affected phase is orbit keeping. During orbit keeping the AOC system has to generate the delta-v to counteract the perturbations and to keep the satellite on the desired orbit. For the orbit simulation NASA General Mission Analysis Tool (GMAT) [48] is used with activated perturbations and including the ephemeris data for those bodies. It shows that during the orbit keeping phase around the EML-4 point the highest effect on the satellite is caused by the eccentricity of Moon's orbit around the Earth. Due to this the radial distances between both primaries changes over one orbit period. The libration points are located at distances that are just fractions of both primary masses and the current distance of the primaries. So when the distance changes thus does the position of the libration point. This means that even though the satellite is placed directly on the libration point position at the beginning the satellites start velocity components have to include this libration point movement. When the satellite leaves the EML-4 the restoring effects takes place but not at the magnitude to relocate it at EML-4 and it will follow the moving EML-4. The importance to include this effect is also explained in „A Survey Of Earth-Moon Libration Orbits: Stationkeeping Strategies and Intra-Orbit Transfers" by Folta and Vaughn [47] and is complex. The result of a not-adapted station keeping orbit can be seen with pulsating orbits that contracts and expands over time and finally in a drifting orbit. Generally the orbit keeping in EML-4 is a sophisticated problem which can be a thesis on its own.

3.2.3.6 Thermal Housekeeping

The temperature of satellite components is maintained within their specific limits. The thermal control subsystem (TCS) is responsible to keep all parts of the satellite in their operational or non-operational temperatures. This control system receives external energy from radiation from different sources (Figure 20).

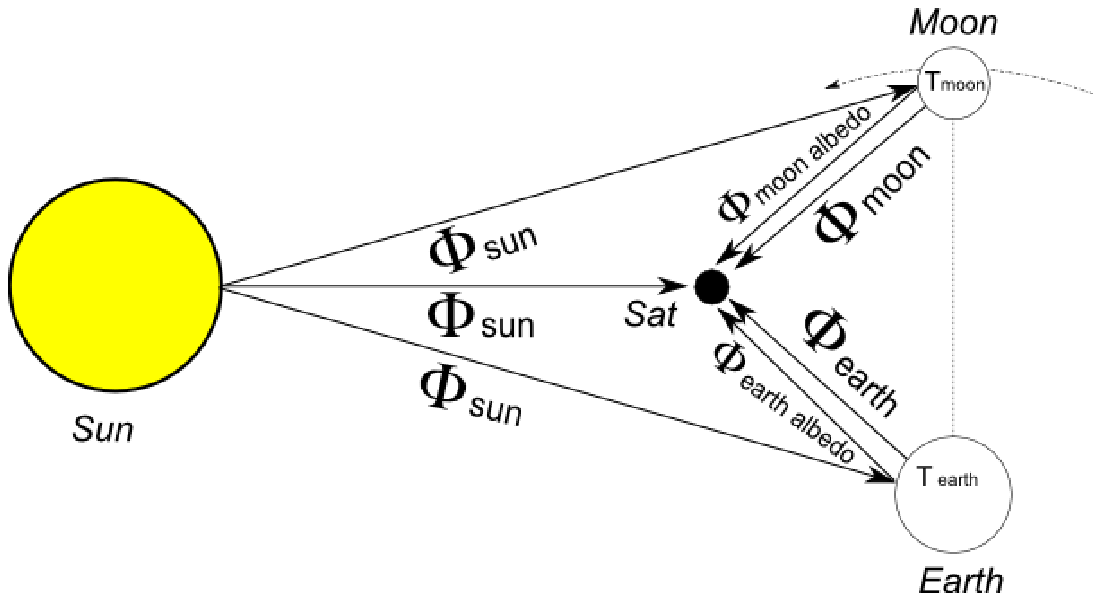

Figure 20: Radiation flux directions of Sun, Earth and Moon. Sketch not scaled.

The available sources are solar radiation and the temperature and albedo radiations of Earth and Moon. The radiation flux by the Sun Φ_{sun} is described by the solar constant S_0 on a sphere surface area A. In this case the area A is the surface of a sphere with a radius $r_{sun-target}$ that reaches from the Sun to the satellite or another target. The heat flux is on this surface is provided by the Sun's temperature T_{sun} directly on the Sun's surface radius r_{sun}.

$$\Phi_{\mathrm{sun}} = S_0 4\,\pi\, r_{sun-target}^2 = \sigma\, 4\,\pi\, r_{sun}^2 T_{sun}^4 \qquad 3.51$$

$$S_0 = \frac{\sigma\ r_{sun}^2 T_{sun}^4}{r_{sun-target}^2} \qquad 3.52$$

The solar constant decreases with the square of the distance of the source to the satellite.

This can be transferred to radiation fluxes on the Earth and Moon and according to the emissivity ϵ of the body and the Stefan-Boltzmann constant $\sigma = 5.670373 \times 10^{-8}\mathrm{Wm}^{-2}\mathrm{K}^{-4}$ one part of the incoming solar flux is transformed to the surface temperature of the body that also transmits radiation flux in infrared wavelength into space and the other part is reflected and described as albedo radiation. So the direct and indirect solar flux is transferred to the satellite. The magnitude of the flux is given by the distance to the radiation source r and its temperature T.

$$\Phi_{\mathrm{earth}} = \epsilon_{earth}\, \sigma\, 4\pi r_{earth}^2\, T_{earth}^4 \qquad 3.53$$

Table 11: Atmospheric properties of the Earth and the Moon

	Min. Temperature	**Mean Temperature**	**Max. Temperature**	**Albedo**
Earth	184 K	288 K	330 K	0.367
Moon	100 K	220 K	230 K	0.136

[49] [50] [51] [52]

Table 12: Radiation flux densities for direct and indirect radiation sources on the EML-4 satellite

	Sun to Sat	**Earth to Sat**		**Moon to Sat**	
	Direct	Albedo	Body radiation	Albedo	Body radiation
$q_{low}\ [W/m^2]$	1325	0.12	0.02	0.004	0.0001
$q_{high}\ [W/m^2]$	1420	0.14	0.18	0.003	0.03

The received radiation power per square meter q for maximum, minimum and the mean solar activity via all three flux directions (Sun, Earth and Moon) to the satellite in EML-4 is presented in the Table 12 (based on surface temperatures on Earth and Moon in Table 11).

It is obvious that at these altitudes the indirect specific solar radiation fluxes can be disregarded and only the direct Sun to satellite radiation flux defines the thermal housekeeping modes as well as the hot and cold case modes. Nevertheless the radiation influence of Earth has to be respected during the transfer phase when the periapsis of the GTO is close to Earth (altitude of 300 km) and the specific albedo radiation flux is in the magnitude of 500 W/m² and the specific infrared radiation flux in the magnitude of 600 W/m².

The received heat flux in the infrared range is important for the thermal design because that is also the frequency range where the satellite's radiators emit. With Kichhoff's law of equal absorption and emissivity $\alpha = \epsilon$ in the same frequency range this is a major design factor for the surface property selection of the thermal control system.

3.2.3.7 Shadow Phases

Even at positions and orbits at altitudes of the EML-4, shadow phases occur and are due to passages through the umbra and penumbra zones by Earth and Moon. This influences thermal housekeeping as well as the power system that is fed by solar power generator panels. Length and frequency of shadow phases are a typical design criterion.

Therefore an analysis of the EML-4 orbit (standard in plane and inclined) with respect to the shadow zone is conducted with AGI Satellite Tool Kit (STK) [37]. The analyzed orbits were modeled as ephemeris data and directly used by STK. The first model includes a placement of the satellite directly on the libration point without displacement over time. The second model includes a displacement of the satellite with a simple sine-cosine approach to change the z- and x-components with respect to the libration point coordinate frame to simulate the movement of an inclination with a z-amplitude of 8000 km. The analysis encompasses a time period of 10 years between January 2013 and January 2023 that respects the repeating nature of shadow phases.

The results in Table 13 (Figure 21) and Table 14 (Figure 22) show that Earth has the most influence on the sunlight time with respect to the umbra and penumbra shadow phase times. The satellite only transits the penumbra zones of the Moon shadow. The minimum sunlight duration shows that the satellite will pass through the Earth and Moon shadow zones during one orbit.

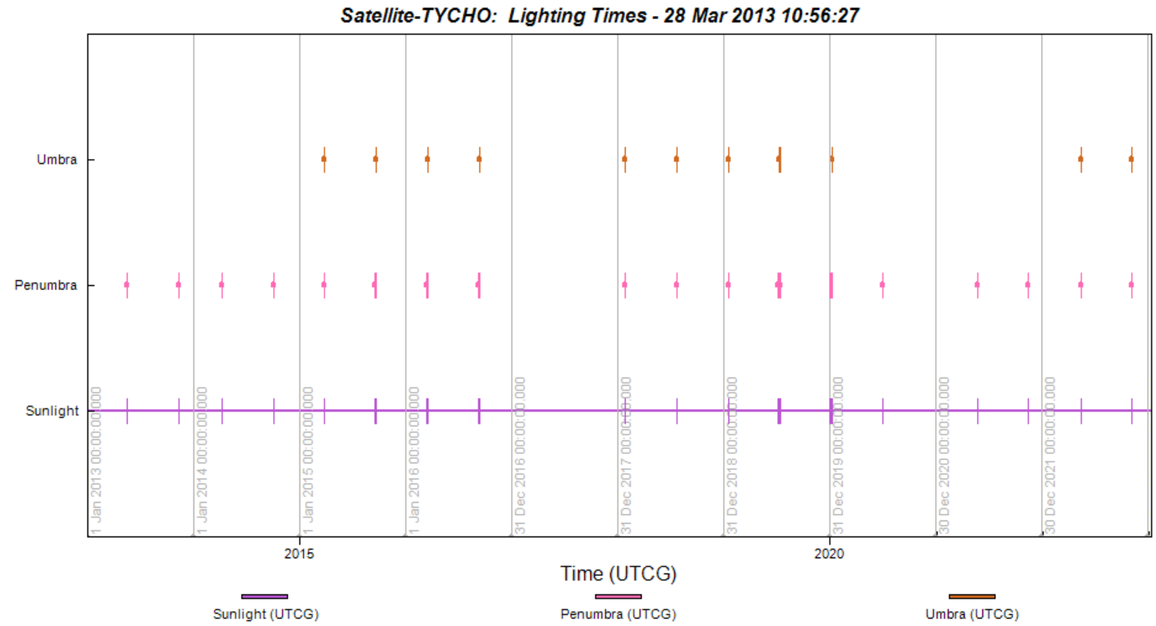

Figure 21: Lightning times for TYCHO satellite on EML-4 (in-plane)

Table 13: Sunlight conditions for TYCHO satellite on EML-4 (in-plane)

Sunlight Conditions on EML-4 (in-plane)					
Eclipse Bodies	Phase	Duration [sec]			
		Min	Max	Mean	Total
Earth + Moon	Sunlight	389255	43370164	13160756	315858158
	Penumbra	1473	14133	6007	204250
	Umbra	1816	10013	6835	75191
Earth	Sunlight	5642910	43370164	16625687	315888064
	Penumbra	3530	14133	6011	174344
	Umbra	1816	10013	6835	75191
Moon	Sunlight	15256501	95345600	52684615	316107693
	Penumbra	1473	8060	5981	29906
	Umbra	-	-	-	-

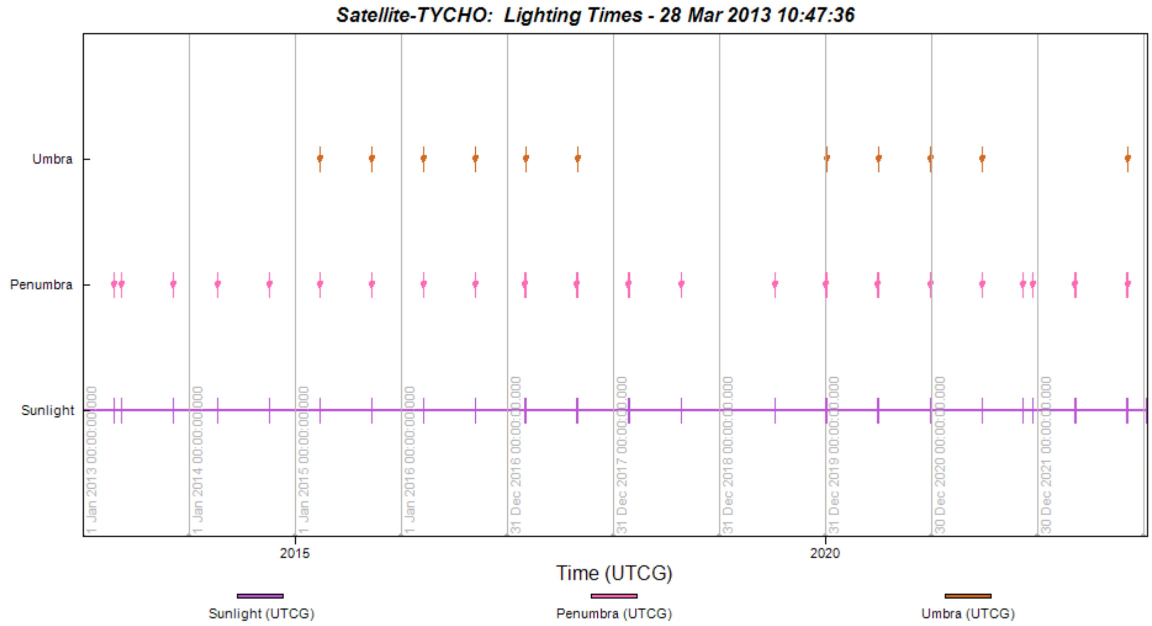

Figure 22: Lightning times for TYCHO satellite on EML-4 (out-of-plane)

Table 14: Sunlight conditions for TYCHO satellite on EML-4 (out-of-plane)

Sunlight Conditions on EML-4 (out-of-plane)					
Eclipse Bodies	Phase	Duration [sec]			
		Min	Max	Mean	Total
Earth + Moon	Sunlight	382729	28055489	10528704	315861120
	Penumbra	2101	13373	5880	235227
	Umbra	5506	9835	7677	84452
Earth	Sunlight	5686558	30574898	15796172	315923448
	Penumbra	2101	13373	5763	172899
	Umbra	5506	9835	7677	84452
Moon	Sunlight	6088599	104644081	28738042	316118472
	Penumbra	3602	8015	6232	62327
	Umbra	-	-	-	-

For the thermal housekeeping and the electrical power system, the maximum umbra and penumbra times of both shadow zones from Earth and the Moon shall be used. The longest shadow phases (14133 seconds and 10013 seconds) are used for the battery sizing and define the battery capacity. This defines the possibility of heat emission of the satellite and a drop in temperature.

Furthermore the minimum sunlight duration of 382729 seconds shall be used to design the ability to raise the temperature back to nominal level and to fully charge the batteries. The analysis of both orbits gives the opportunity to change the inclination according to the mission objectives.

The thermal control system design has to include a hot case during the sunlight phases and a cold case during the shadow phases. For the preliminary design the equilibrium temperatures in both sentences set the minimum and maximum temperatures for the thermal control design.

3.2.4 Case Study Focus on EML-4

This study selected the leading equilateral triangular libration point EML-4 as the target for the TYCHO demonstrator mission in favor of the following EML-5 for several reasons. The similarity of both points allows a demonstration of transfer, station keeping and end-of-life strategies in analogue manner. The direct transfer will bring the satellite in closer vicinity to the Moon and may be more influenced leading to more delta-v. Although communication link distances are equal more possible targets out of the ESAS top 10 list are accessible from EML-4. An additional analysis and evaluation of the effects on EML-5 is advised for the utilization of the proposed TYCHO TMA-1 satellite configuration for an operational mission to EML-5.

3.3 Requirements Elicitation and Analysis

The requirement elicitation and analysis is part of systems engineering and is used to identify the needs and conditions of future customers for the TYCHO operational mission, TMA-1. The user requirements are identified and shall be translated to mission requirements and hence being implemented as system requirements used in this thesis.

Requirement analysis is critical to the conceptual design with respect to the definition of baseline scenarios because the derived target and mission objectives characterize the TYCHO mission and distinguishes it from other communication relay missions. As well as it directly links to the overall mission costs by complexity and amount of new technologies which eventually need to be developed to fulfill the mission. The complete mission planning is based on the requirement elicitation and analysis and all decision documents can be traced back to the requirements.

3.3.1 User Requirements

Within the scope of user requirements is the identification of the general user needs in terms of communication between the Moon and the Earth. For lunar missions the expected requirements are availability, performance and a universal, standardized access of the communication system. Each of these major requirements is presented in this chapter and they lead to baseline scenarios defining the TYCHO mission requirements.

3.3.1.1 Communication Availability

In general users expect to be able to communicate during their mission. So the availability of communication opportunities is related to the mission duration, their mission objectives and their mission target.

The expected mission duration depends on the mission target of the user. For lunar missions it ranges from several days up to ten years. For Apollo type manned lander missions, the stay time was several days. This short time mission assumed as a possible scenario for proposed future manned lander missions by China National Space Administration (CNSA) and Indian Space Research Organization (ISRO). Medium time missions encompass lunar orbit missions. The prior lunar orbiter missions stayed in orbit up to six years (Luna program, Explorer program, Lunar Reconnaissance Orbiter). Long term stay up to ten years is assumed for proposed extended autonomous exploration with rovers and landers as well as for manned bases on the Moon of space stations on EML-2 halo orbit.

[UR100] communication shall be possible during the complete mission time with minimum 10 years for lunar bases

During the user mission time the communication link is able to transmit the telemetry and acquired payload data to Earth and receive telecommands and further data. With a broad range of possible costumers the demanded access can be periodically for e.g. autonomous rovers and orbiters or a permanent link for data intense missions or manned missions. For manned missions the human factor demands a permanent communication links for command and science briefings, safety and social aspects.

[UR101] Communication shall be permanent

The user mission target is identified for the last availability requirement. The user expects to be able to communicate within the target zone. For lunar missions this can be the complete lunar surface, lunar orbit and the EML-4 halo orbits.

It also includes position changes of the lunar surface missions with various radiuses. In these the communication is required to be possible. There are certain lunar regions with an accumulation of high-priority landing sites (see Chapter 3.2.3.1.). From these points of special interest the user is expected to communicate. Adding to that, the terrain in the user mission zone is a factor. The user requires communicating from their position in valleys, on lunar maria and even in craters.

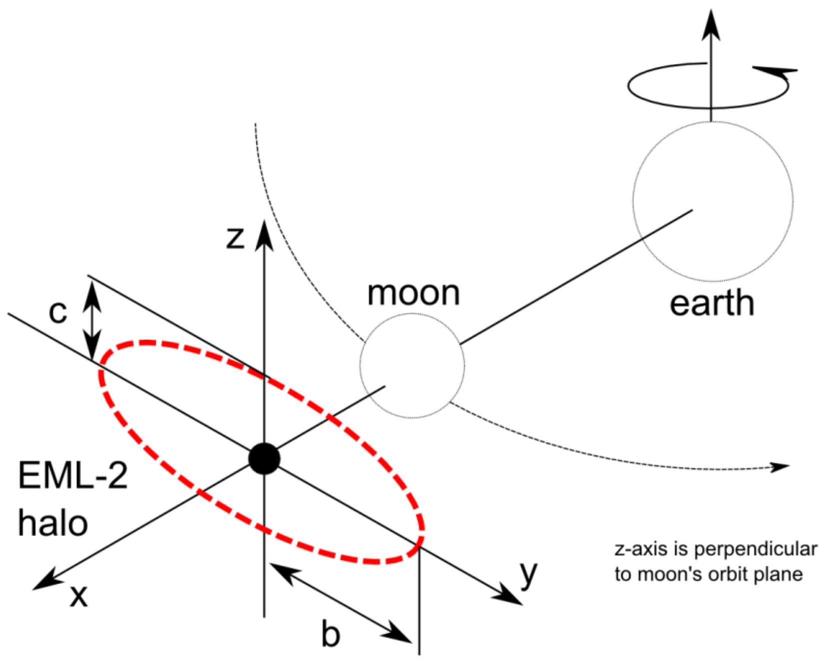

Figure 23: EML-2 halo orbit coordinates with y- and z-axis amplitudes b and c

In lunar orbit the line-of-sight to Earth is periodically blocked by the Moon and direct communication to Earth is not possible for a certain period. The EML-2 halo orbit can be completely blocked behind the Moon when the orbit z- and y-axis amplitudes are smaller than the Moon’s radius (Figure 23). Then direct communication is not possible for the user.

[UR102] communication coverage footprint shall be possible from the mission's lunar landing zone
[UR103] communication shall be possible from fixed and mobile positions
[UR104] communication shall be possible within every terrain (valley, maria, craters)
[UR105] communication coverage shall include points of interest for high-priority landing sites (see Chapter 3.2.3.1.)
[UR106] communication access should be possible within lunar orbits (low lunar orbits to high elliptical lunar orbits)
[UR107] Communication from halo and Lissajous orbits inside the shielded Moon zone shall be possible

3.3.1.2 Communication Performance

The user expects certain communication performances that involve certain technology related demands.

3.3.1.2.1 Data-Rate Recommendations

With a presented wide range of users a wide range of data-rates are required. There are recommendations of data-rates for future space research satellites to the libration points and communication networks by the International Telecommunication Union (ITU) and in the ESAS study for lunar missions. The data-rate survey is extended by analysis of data-rates of different present and future lunar missions as well as of relevant future space applications.

In the Recommendation ITU-R SA.1625* "*Feasibility of sharing between the space research service (space-to-Earth) and the fixed, inter-satellite, and mobile services in the band 25.5-27 GHz*" [53] a data-rate of 400 Mbit/s on the space-to-Earth link for space research satellites is assumed. These space research satellite (SRS) missions are assumed with equatorial orbits with some at geostationary altitudes and other at L1 and L2 libration points. The reference system of the libration points is not stated in the ITU recommendation but can be assumed to be in the Sun-Earth system. For the EML-2 point this recommendation can be adopted.

The halo orbit around Earth-Moon libration point EML-2 is attractive for relay satellites, space observatories and future space stations. The point itself offers a relative fixed position in space with respect to the Earth-Moon system that can be utilized for communication relay infrastructures providing access to the far side surface of the Moon or to other satellites in orbits around EML-2. Space observatories [54] target objects in the opposite direction and could take advantage of the Moon as a blocking body reducing the noise originating from Earth. Space stations in EML-2 offer both features and extend it with the human factor of flexible work and research.

The data-rates of various space observatories missions between 1977 and 2020 are presented in Table 99. For future observatories the data-rate development in Figure 24 shows a trend of 10 Mbit/s for 2020. This data-rate is anticipated to be the average data-rate of space observatories in EML-2 orbit that needs to be relayed to Earth via a relay satellite in EML-2 or -4. As for the analyzed missions the data transmission to Earth is not time critical and thus the data-volume shall be transmitted with respect to the satellite's onboard data storage.

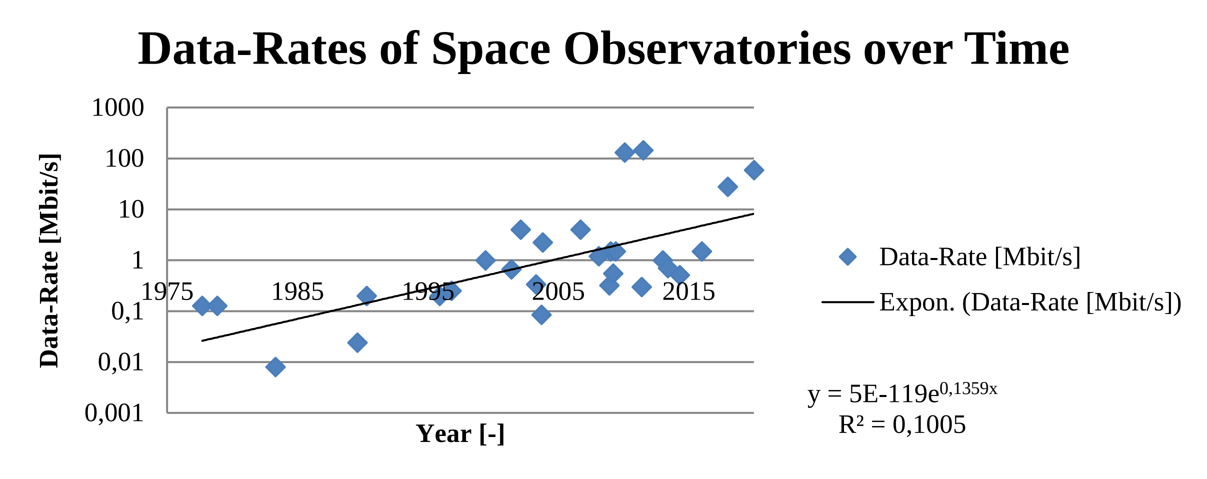

Figure 24: Data-rates of space observatories between 1977 and 2020 (Table 99)

Within the ESAS [35] scenarios data-rates depending on the mission are presented. For a mission including mobile habitats continual communication data-rates of 10-20 Mbit/s are stated. This data-rate even increases in case of a human outpost to 250 Mbps with a maximum of 300 Mbps of the lunar communication terminal providing the Earth gateway relay service. For sortie missions with a combination of astronaut fieldwork and robotic exploration the lunar communication terminal (LCT) would communicate with Earth providing one or two 100 Mbit/s channels with additional LCTs with one or two 25 Mbit/s channels. The channel frequency bands used for the LCTs in that scenario are in K/Ka-band. For science and robotic missions and during the stepwise expansion of the lunar habitats and outpost classes of data-rate levels are proposed. Table 15 presents an overview of these classes for the three types of lunar explorations (science & robotic, sortie, human exploration and outpost) for the long haul transmission from lunar surface to Earth.

Table 15: Link capacity requirements according to mission class for the long haul to Earth

	Science & Robotic(1)	**Sortie(2)**	**Human Exploration(3)**	**Large, High-Capacity, Base, Camp, Outpost LCT(4)**
Long Haul	0.2 Mbits	< 20 Mbit/s	< 20 Mbit/s	2 × 100 Mbit/s

(1) Science, monitoring, environment measurements, terrain
(2) Human survivability, science
(3) Survivability, science, locale, exploration
(4) Long-term human survivability

Another aspect is the connectivity of the relay satellite to other relay services. The European Data Relay Satellite Service (EDRS) will provide an overall downlink data-rate of 1.8 Gbit/s with four channels and thus 450 Mbit/s per channel [55].

For Earth to Moon communication the data-rate is based on the current output of the International Space Station (ISS) [56]. The Columbus module onboard ISS in low Earth orbit is representatively analyzed for the data-output of a space station. Columbus' average data-rate of 32 Mbit/s covers system and payload data. The science mission planning can allocate data-rates between 0 Mbit/s and 43 Mbit/s. It uses the ISS communication system to connect with TDRS satellites with an available maximum bandwidth of 150 Mbit/s via TDRS. The Ku-band coverage of TDRS to the ISS can be surmised to be 68 % of the orbit period [56]. The Luch Satellite Data Relay Network (SDRN) system provides also a bandwidth of 150 Mbit/s but with less coverage time per orbit [56] [57]. A future space station in an EML-2 halo orbit is considered to generate a data-volume per day of minimum the same volume as ISS.

The recommendations of data-rate by several organizations and missions set the last user requirements for the TYCHO mission [58].

The user requirements derived for data-rates are:

[UR200] the data-rate shall be up to 400 Mbit/s for Moon to Earth transmission
[UR201] the data-rate shall be up to 100 Mbit/s for Earth to Moon transmission

3.3.1.2.2 Multiple Access

Furthermore it is considered that there are multiple lunar missions on the surface and in orbits at the same time as depicted in ESAS [35]. With a further increase of scientific data volumes generated by orbiters, landers and rovers, the relay satellite service has to include their inputs to the link budget. Those missions include tele-operated missions from the human outpost or from operating centers from the Earth. So rovers and landers either access TMA-1 directly or via network architectures.

Current and future lunar missions from 2001 to 2026 were analyzed with respect of their communication data-rate or their daily data acquisition. A trend of data-rate development could not be observed (Figure 25 based on Table 100).

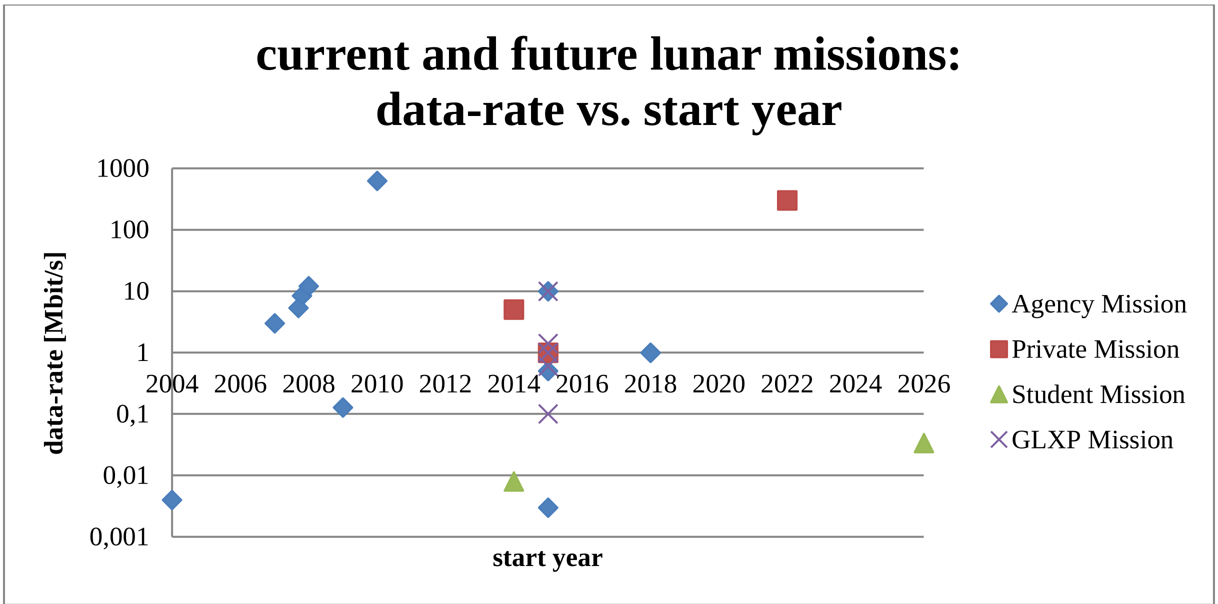

Figure 25: Data-rate distribution of different lunar missions

Those missions include space agency driven, university (BW-1, ESMO) and private (Google Lunar X-Prize, SpaceX) endeavors towards the Moon to provide an overview of the complete spectrum of operated or planned missions as possible clients. NASA's Lunar Atmosphere and Dust Environment Explorer (LADEE) mission uses an optical link with 622 Mbit/s per second and this magnitude is relatively high in contrast to the other analyzed missions. So the data-rate of 400 Mbit/s recommended by ITU and in ESAS shall be used. However it is assumed that several lunar missions will be operating on and in lunar vicinity at the same time.

[UR202] the user shall be able to communicate via the communication relay by multiple access method

3.3.1.2.3 Network Delay

The transmitted user data experiences a certain level of delay that is caused by processing, queuing, transmitting and the propagation. The biggest influence is the propagation delay as presented in Chapter 3.2.3.3 and the remaining delays are caused by the communication hardware performance like data-rate or the subsystem components.

The user requirements for network delay times ranges can be diverse and specific to the user mission. For remote controlled or semi-autonomous rover missions the network delay shall be as low as possible to minimize risks and maximize performance. For human mission with audio and video transmission the convenience of communication also decrease with longer delay times. For science-data transmission the delay time is not critical. The data is only required to be transferred completely and flawless.

[UR203] network delay shall be adequate to transmit the user's data completely

3.3.1.3 Standardized Universal Access

The user requires having a cost efficient and reliable way of communication. This is possible with a standardized and universal access. On the ground segment side on Earth the user benefits from using existing infrastructures (EDRS). On the mission side he can use standardized methods and off-the-shelf components that reduce costs and risks. On the infrastructure side he is able to collaborate in international projects like the International Lunar Network (ILN) on lunar surface or a permanent lunar orbital relay (Chapter 2.5) where synergetic effects can also reduce risks and be beneficial for the mission.

[UR300] the user shall be able to use standardized communication methods and technology

[UR301] the user shall be able to communicate via standardized communication relays

3.3.2 Communication Baseline

For the general user requirements the communication baseline is defined. The baseline definition includes the target zones, where the user mission will have access to the TMA-1 satellite, and a description of the possible user mission objectives in these zones.

3.3.2.1 Surface Missions

The high-priority landing sites presented in Table 1 can be grouped in three areas:

1. Exclusive Zone (80°W to 100°W and 85°N to 85°S)
2. Lunar Maria (Mare Imbrium, Oceanus Procellarum, Mare Cognitum and Mare Humorum)
3. North Pole (85°N to 90°N) and South Pole (85°S to 90°S)

Exclusive Zone:

The exclusive zone includes Mare Orientale which is of interest for geology (basaltic area) and considered as a landing site for sortie missions with sample-return. The Mare Orientale is an impact crater and can be used as shielding for area radio astronomy observatories that benefit from blocked radio frequency noise. Moreover the crater can provide areas of eternal darkness for the instruments cooling system.

As a long term projection presented in NASA’s ESAS [35], this area can serve as the starting point for mobile habitats and lunar bases [59] due to the transition zone between the near and far side of the Moon. For crewed mission the expedition fieldwork can include astronomy and high particle science as well as geology missions to the South Pole Aitken Basin. It is an area considered for a mobile outpost to explore the basin of the 2500 km diameter crater. It is the deepest crater in the solar system and exploration in that crater can test the lunar cataclysm hypothesis. The lunar cataclysm or the late heavy bombardment is a hypothetical event around 4.1 to 3.85 billion years ago (Ga), during which a large number of impact craters would have formed [60]. Exploration includes a wide range of different geological fieldwork tasks conducted by the crew. This area is also one target point for the Farside mission [38] interested in KREEP material. The far side position of the Aitken Basin is also of interest for chemistry since due to traces of water in the regolith and for astronomy as well.

This area is exclusively covered from EML-4 and the lunar landing mission can benefit from permanent communication access and a relatively fixed position with respect to the elevation and azimuth. The missions will generate a high volume of data due to observatories and manned missions. So the data-rate of up to 400 Mbit/s is required for this zone. Beyond that, the compatibility to the ILN (Figure 26) is required because the network can be used to extend the surface coverage further into the far side where the coverage from EML-4 is not possible (South Pole Aitken Basin). In this way no additional relay satellite in EML-2 or lunar orbit is needed.

Multiple accesses to the communication system are required. This includes the RF link with several channels and other techniques for several users to be able to communicate to Earth at the same time. This can be supported by an additional laser link that offers a single user to relay satellite connection and an independent target pointing with respect to the RF link that covers a wide area. This supports the user requirement of mobile communication.

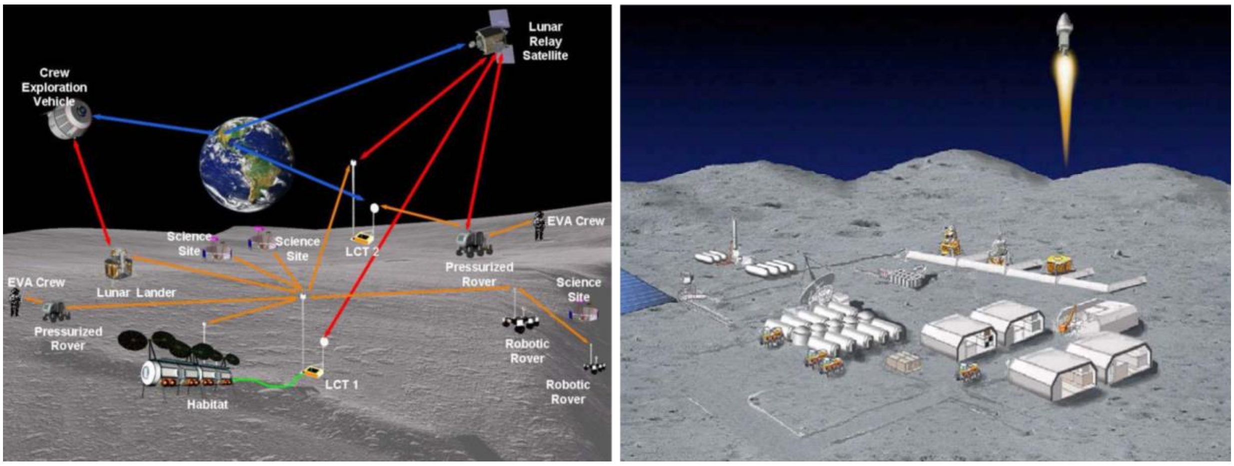

Figure 26: Artist impression of International Lunar Network (left) and modular lunar outpost (right)

Lunar Maria:

The lunar maria area compound of Mare Imbrium, Oceanus Procellarum, Mare Cognitum and Mare Humorum includes the landing sites of Aristarchus Plateau, Rima Bode, Copernicus Crater (Apollo 18), Oceanus Procellarum and Tycho crater (Apollo 20). This wide area is completely on the near side and interesting for geology and the evolution of the Moon.

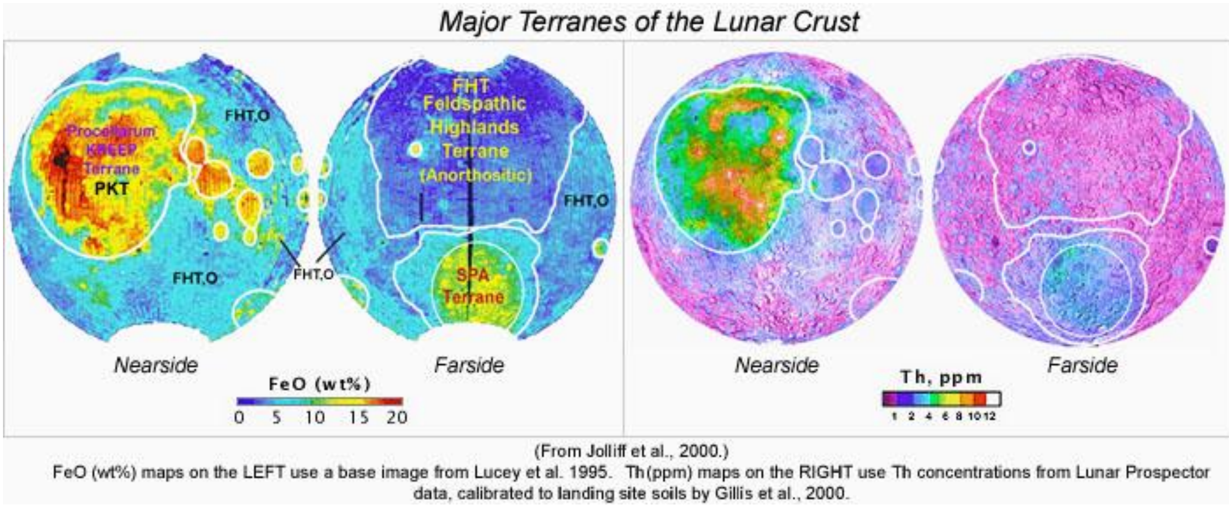

Figure 27: Major terranes of the lunar crust.
Feldspathic Highlands (FHT), Procellarum KREEP and South Pole Aitken (SPA) Terrane maps

FHT:	*includes its somewhat different outer portion (FHT,O); this terrane has low FeO & Th.*
KREEP :	*is characterized by high FeO and Th.*
SPA:	*has relatively moderate FeO and Th.* [61]

The maria area is an interesting goal for rovers to explore the geology of a buried volcano shield with radioactivity of the mantle and KREEP elements [acronym for K (the atomic symbol for potassium), REE (rare earth elements) and P (for phosphorus), a geochemical component of basaltic rocks and some lunar impact breccia] and also for research of lunar cataclysm and the late heavy bombardment hypothesis (Figure 27). The plane area supports rovers and landers and the relay in EML-4 can serve as communication redundancy and for mission extensions into craters like the Tycho crater and into the far side.

The data-rate for one rover are depicted as 0.2 Mbit/s in ESAS [35], however it is expected to have multiple parallel rovers and landers that cooperatively explore the maria area. For this multiple access to the relay satellite with ILN compatibility is required.

North Pole and South Pole:

The pole areas are only periodically accessible from Earth. With a relay on EML-4 the duration can be extended (Table 3). The pole areas are of interest for lander and rover missions because of water signatures under the surface that have been found via remote sensing missions and in craters with eternal darkness. This also includes sortie missions.

The North Pole area (85°N to 90°N) is of interest for seismic measurements and this is one objective for the International Lunar Network landing nodes ESAS [35]. In the South Pole area (85°N to 90°N) significant amount water ice was found in Cabeus crater by LCROSS, Kaguya and other missions [62]. The topography of both regions is categorized as high lands with a denser distribution of craters. These can also be used for radio astronomy and particle science.

The periodic access to the poles and expected high science data-volume requires high data-rates of 50 Mbit/s. Due to the periods where no access is possible laser communication is feasible as an addition to RF communication in K-band. This is due to the fact that the propagation beam of a laser can be narrower than a K-band communication and when the RF coil spans from pole to pole the signal power decreases to the poles. The laser can be used to switch to targets like the poles while the RF coil supports the parallel missions in the other two zones.

3.3.2.2 Lunar Orbit and EML-2 Missions

For lunar orbits and EML-2 missions high-data rates are assumed. This is due to the assumption that orbiters will multiplex the data from accompanying rover or lander missions and their own remote sensing data or even serve as a relay for the ILN [35]. The user requires permanent communication and a relay in EML-4 will reduce the communication black-out times. Furthermore high data-rates are expected for missions to EML-2 where space observatories and a space station are assumed for the communication baseline. The data-rate for these missions is also defined as up to 400 Mbit/s and for EML-2 missions within the shielded Moon zone the only line of communication is possible via another relay satellite. The user requirement of a simple communication access to a relatively fixed position is only fulfilled with a relay in EML-4 position.

3.3.3 Mission Requirements

In the following chapters the mission requirements of the TYCHO mission concept will be assessed and compared to the previously derived general user requirements for a lunar relay mission.

The EML-4 concept bears certain constraints, as all other lunar relay mission architectures. Thus, not all user requirements can be met, however it will be shown, that for certain users, the EML-4 mission provides significant advantages over other types of communication architectures.

3.3.3.1 General

Generally the mission concept envisages the compatibility of the TYCHO mission to other existing communication networks, ground station networks (e.g. DSN), data relay satellites (e.g. EDRS) or potential future lunar networks (e.g. ILN). This needs to be ensured by the use of suitable communication architecture and protocols. This leads to the first, general mission requirements:

[MR100]	TMA-1 shall provide communication relay functionality between Moon and Earth
[MR101]	TMA-1 shall provide standard communication interfaces
[MR102]	TMA-1 shall use as much as possible commercial-off-the-shelf technology
[MR103]	TMA-1 shall be able to make use of existing communication infrastructures

The mission time of TMA-1 is a combination of general and technology considerations about economic feasibility of the service.

The operational time of TMA-1 in phase E shall be minimum ten years. This is specified for technical and service reasons. This time span allows servicing a number of Moon missions, which is advocated to last 24 months. So the launch and operation start has to be defined according to missions happening during the operational period. The inauguration of TMA-1 can be combined with a specific Moon mission to the benefit of a shared launch or to directly support the Moon mission after TMA-1 has completed the system check in advance to the accompanied mission.

Ten years of operations are in-line with current communication satellites in GEO orbits. This gives the opportunity to use standard components or to build TMA-1 based on a standard GEO platform saving cost and development effort. Components like batteries, solar cells and on-board computers are qualified to restrain space conditions in GEO that are quite similar to those in EML-4 position. The transfer to EML-4 may include several passages through the van-Allen belt depending on the launch scenario. According to current state of knowledge the radiation environment is similar to the one encountered by a GEO mission, however only little data is available so far about the EML-4 environment, thus this mission (or its technology demonstrator TMA-0) offers also the opportunity to investigate the radiation environment almost during a complete solar radiation intensity cycle of eleven years. In addition the Kordylewski dust clouds are disputed in EML-4 that could have an effect on the satellite hardware. Thus the effort to qualify new hardware for radiation hardness or degradation can be reduced.

In addition regulatory aspects have to be taken into account. Frequency assignments and allocations of communication frequency bands with Earth stations are limited to 10 years and have to be renewed. Band allocation periods can also be shorter on request in case of a renewed assignment for an extended mission longer than 10 years [63].

[MR104]	TMA-1 shall have an operational mission lifetime of minimum 10 years

3.3.3.2 Orbit Position

The coverage of the targets on lunar surface, orbit and in EML-2 depends mainly on the orbit position of the relay satellite service. A relay satellite in EML-4 position can provide the almost fixed position with respect to the lunar surface and the permanent availability from certain regions of the Moon, as required by [UR102]. A detailed analysis of the coverage zones is presented in Chapter 3.2.3.1 and compared to other communication relay options.

The orbit position requires a station keeping strategy to keep the orbit position. Principally EML-4 provides a long-time stable orbit which allows missions times of ten years with less delta-v as orbiting lunar relays or as EML-2 relays, which is discussed in Chapters 3.2.1.2 and 4.2.3.

Completing the mission the TMA-1 shall perform a disposal transfer away from the EML-4 position so that the deactivated TMA-1 will not endanger future satellite missions to EML-4.

The operational TYCHO TMA-1 mission requirements for the orbit are:

[MR200]	TMA-1 shall provide communication from upon a satellite position on EML-4
[MR201]	TMA-1 shall provide a permanent communication relay function to the Moon‘s rim area (20°E - 140°W, 85°N - 85°S)
[MR202]	TMA-1 shall provide orbit keeping to stay within a to be defined distance to the EML-4 so that users are enabled to have a simple targeting of the satellite
[MR203]	TMA-1 shall not endanger future missions. There shall be a suitable end of life disposal procedure. General space debris should be minimize

3.3.3.3 Communication

The main objective of the TYCHO mission is to provide communication relay service between Earth and Moon segments. To fulfill the user requirements the maximum transmission data-rate from the Moon to the Earth shall be 400 Mbit/s [UR200] and the return channel shall provide 100 Mbit/s of data-rate [UR201].

TMA-1 shall provide communication links in radio frequency (RF) bands according to current state of the art technology and development progress towards higher RF bands but ensuring compatibility to already existing network infrastructures.

Additionally due to the technology development and interesting performance of optical communication with laser frequencies and the inauguration of the European Data Relay Satellite (EDRS) service that will include laser communication terminals (LCT) the TMA-1 satellite shall also provide optical transmission with high data-rate with LCTs. Steerable LCTs would enable the satellite to point to different targets, like lunar missions, locations on Earth or even beyond. The RF as well as the laser channels shall be able to support the high data-rates required by users. Implementing and EDRS compatible design enables also the use of EDRS ground stations which broadens the potential access to TMA-1 but also limits the need for dedicated costly ground station developments.

Besides the communication links, special features for the data transmission are required. The user segment is diverse and their demands of data-rates lie between several Kbit/s and up to the maximum of 400 Mbit/s. TMA-1 shall support flexible data-rate settings that can be changed according to the individual user's needs. It is assumed that a user is able to send during a long communication window or with a high data-rate during a short time span. This requires planning for accessing the service. Additionally users shall be able to use the communication link in parallel with multiplex methods like code division multiple access (CDMA) or alternatives.

More so, users shall be able to request higher priority status for their transmission in case the data has to be transferred immediately. Priority modes shall include that a user shall be able to allocate a complete channel and other users shall transmit with a low data-rate with the data stored in the satellite's buffer. One application could be given data from a manned mission high priority and a full RF channel and autonomous exploratory missions with uncritical communication the remaining channel as a shared medium or to support emergency case communication with one connected user. After the high priority phase is ended the stored data from the users shall be transmitted to the target. In this way permanent access is still possible for all users. The TMA-1 satellite manages the multi user access and the data transfer to the targets.

The RF-links towards ground segment shall be done in K-band since this provides a high bandwidth and there are allocated bands for Earth exploration satellite communication as well as inter-satellite communication by the International Telecommunication Union (ITU) and they are ground stations available at different locations on the Earth (Chapter 4.3.3). Moreover optical free space communication shall be done with a laser wavelength of 1064 nm since it also provides a high data-rate, the band is also allocated for Earth exploration satellite and it is compatible to the EDRS laser communication system.

On the Moon side of communication, the users require communication to the relay satellite via ILN gateway terminals besides direct-to-TMA-1 communication links. TMA-1 should be able to access ILN terminals.

The operational TYCHO TMA-1 mission requirements for communication infrastructure are:

[MR300]	shall provide communication links in radio-frequencies with a variable data-rate of up to 400 Mbit/s between the Moon and TMA-1 transmissions
[MR301]	shall provide communication links with optical transmission with a variable data-rate of up to 400 Mbit/s between the Moon and TMA-1 transmissions
[MR302]	shall provide communication links in radio-frequencies with a variable data-rate of up to 400 Mbit/s between TMA-1 and Earth ground stations
[MR303]	shall include priority modes for data transmission
[MR304]	shall support up to four parallel RF channels
[MR305]	shall include multiple access per RF channel
[MR306]	shall include flexible data-rate mode
[MR307]	shall be compatible to EDRS network
[MR308]	shall be compatible to International Lunar Network (ILN)

Those unique assets are the key design drivers influencing the mission and the satellite system. Optical laser communication link is expected to gain importance for space communication and is therefore included into this study [64].

Table 16: Traceability matrix for user and mission requirements ("1" stands for implementation)

	Mission Requirments [MR]																	
User Requirements [UR]	100	101	102	103	104	200	201	202	203	300	301	302	303	304	305	306	307	308
100					1	1		1										
101						1	1	1		1	1	1						
102						1	1											
103						1												
104						1												
105						1												
106						1												
107						1												
200										1	1	1						
201										1	1	1						
202													1	1	1			
203																1		
300																	1	1
301																	1	1

3.3.4 System Requirements

The system requirements identify technical requirements directly derived from either the user or mission requirements and there are additional general requirements that influence system complexity, the development time and costs. Within the scope of this study the system requirements are identified on the basis of the mission requirements presented in the previous Chapter 3.3.3.

General system requirements:

[SR100] TMA-1 shall follow the principle to rely on available, space qualified components with a high technology readiness level

[SR101] TMA-1 shall initiate technology development only where absolutely necessary to achieve critical mission points

[SR102] TMA-1 critical subsystem components shall be single-point-failure-free

[SR103] TMA-1 shall be designed, built, inspected, tested and certified to specially address the requirements for communication satellites

[SR104] TMA-1 should have subsystem components with European heritage

[SR105] TMA-1 shall have a minimum operational lifetime of 10 years

Communication system requirements:

[SR200] TMA-1 shall include K-band communication to support the high-data-rate and EDRS compatibility

[SR201] TMA-1 shall include four K-band channels

[SR202] TMA-1 shall provide K-band communication access for multiple assets (CDMA)

[SR203] TMA-1 should include flexible K-band access for the user missions (data-rate, FEC, transmit power)

[SR204] TMA-1 shall include laser communication to support the high-data-rate and EDRS compatibility

[SR205] TMA-1 shall include priority transmission modes and channel selection

[SR206] TMA-1 shall include a data buffer

Propulsion and attitude and orbital control system requirements:

[SR300] TMA-1 shall include a propulsion system that provides the delta-v for the transfer to EML-4

[SR301] TMA-1 shall include a propulsion system that provides the delta-v for the orbit keeping

[SR302] TMA-1 shall include a propulsion system that provides the delta-v for the disposal maneuver

[SR303] TMA-1 propulsion system shall be single-point-failure-free

[SR304] TMA-1 shall include AOCS components and strategies suitable for high data-rate communication

Table 17: Traceability matrix for mission and system requirements (“1” stands for implementation)

System Requirements [SR]	Mission Requirments [MR]																	
	100	101	102	103	104	200	201	202	203	300	301	302	303	304	305	306	307	308
100		1																
101		1																
102					1									1				
103					1													
104		1																
105					1													
200	1	1	1	1		1	1			1		1		1			1	1
201												1		1				
202												1			1			
203												1				1		
204	1	1	1	1							1						1	1
205													1					
206													1					
300						1												
301					1	1	1	1										
302						1			1									
303					1	1		1										
304					1	1	1	1										

3.4 TMA-1: Operational Satellite Concept and Operations

The TYCHO mission plan contains two satellite missions. The operational satellite TMA-1 shall serve as the service providing satellite. TMA-1 shall fulfill all requirements specified so far like provision of permanent communication links between Earth and the Moon’s rim surface area, lunar orbits and the EML-2 orbits. This shall be achieved from upon a satellite position on EML-4.

The TYCHO mission would bring the first communication relay satellite to EML-4. Such an inauguration mission possesses advantages but also critical mission points. To reduce the risk and to qualify certain technologies of an EML-4 mission, a demonstrator mission is envisaged. Its requirements will be derived from the requirements identified for TMA-1 scaling down where possible in order to reduce the mission cost but maintain the representability.

3.4.1 Critical Mission Points

The discussion on critical mission points is particular to each mission. It is necessary to design a mission and to identify possible design and performance drivers.

Identified critical points for the TMA-1 mission are:

a. transfer and injection into EML-4 orbit
b. attitude and orbital control
c. orbit form sensitivity
d. EML-4 environment
e. communication relay performance

The injection into EML-4 (a) has not been done before with a satellite mission. There were missions like Hiten who passed through it but no satellite can be used as a mission reference [65]. Hence the third-body perturbations and their influences on the injection are as yet not completely known. Only missions to Sun-Earth libration points can be consulted. During the transfer the satellite will cross the van-Allen belt. This area with high energy electron and protons can heavily influence the on-board electronic and cause degradation of the solar cells. The passage time should be as short as possible. And lastly the propulsion system of the satellite should be designed to accomplish the transfer. This means the propulsion system should avoid single point of failures. This should include redundancies of the thruster system.

Attitude and orbital control (b) during orbit keeping demands a specific control strategy. Pure east-west and north-south drift control used for GEO communication satellites cannot be used to compensate inclination and true anomaly changes. Finding an adequate strategy requires a surveillance of the accelerations provided by the third-body effects, solar pressure and the EML-4 environment. Even though there are known Trojan asteroids with inclinations up to 40° inclination, the out-of-plane stability of the EML-4 region and the sensitivity of the orbit parameters inclination and semi-major axis (c) are not completely known [20] [66] [67] [68].

Another aspect of the EML-4 mission is the environment (d) and its stability that can virtually trap masses. For the Sun-Jupiter libration points SJL-4 and -5 Trojan asteroids are known. In the EML system, the Kordylewski cloud is disputed. The particles will be small with the maximum size of millimeters but the relative velocity and the cloud density are unknown presently. This could have a degradation effect on the solar cells and further components of the satellite. As long as the cloud particle parameters are unknown it should be treated as a critical mission point that may have an effect maximum mission lifetime.

The main objective of the TYCHO mission is providing the communication relay performance (e). If this is not possible the unique selling point vanishes and the mission has no business case. So the high data-rate and the fail-safe strategy shall be respected. One option will be to include power margins for the communication links but also with using several channels and redundant components in the radio frequency distribution unit (RFDU). In addition the relay service shall be able to connect several assets on Earth and Moon. This is due to weather effects on Earth so that a permanent access is possible and to have several lunar missions that are possible to connect with the satellite relay in parallel.

3.4.2 TYCHO Mission Benefits

TMA-1 is perfect for permanent communication between Earth and the Moon‘s rim side (Chapter 3.2.3.1). Covering this rim area extends into areas where exploratory missions with the need for communication to Earth could not be sent before due to the lack of such direct Earth line-of-sight. These missions required an additional orbiter with communication link. However those links could not provide permanent connection. TMA-1 is able to provide this relay service for missions without the need of an additional orbiter for relay purposes. This will make missions possible that need to be behind the lunar horizon with respect to the Earth.

Four major aspects (communication, orbit, environmental science and operation) are identified which justifies the operation of an EML-4 relay compared to other lunar relay concepts.

Communication:

- permanent communication links to rim region (20°E - 140°W, 85°N - 85°S).
- coverage of exclusive regions (80°W - 100°W, 85°N - 85°S) on the Moon (compared to EML relays).
- periodically covering lunar poles with adequate inclination.
- no black-out phases (compared to lunar relay).
- radio frequencies and laser links and high data-rate to Moon for flexible service.

TYCHO’s advantage is to be at a stable libration point position for a long period of time, being able to establish permanent communication connections to all libration points and to be a communication satellite as a backer for single lunar exploration missions even to the pole areas and on the far side of the Moon.

Position:

- stable EML-4 orbit (compared to EML-2 relay)
- no orbit declination as lunar orbits (compared to lunar relay)
- less delta-v for transfer and station keeping (compared to EML-2 relay, lunar relay)
- interesting for long-time space weather observation (early warning system)
- no regulation of orbit position placement like in GEO

The position on the EML-4 is a unique feature and as important for relay satellite as the geosynchronous orbit. The ability to offer a satellite platform can be an advantage in the communication market.

Transfer:

- WSB transfer is an option, but with longer transfer times
- piggy-back option can reduce costs
- less delta-v than transfer to EML-2
- variety of launcher and launch options
- can be used for orbit with inclination (out-of-plane maneuvers)
- dedicated and share flights possible
- several transfer orbits as an option

The EML-4 position offers a wide range of launch and transfer options. Furthermore the transfer can be easier than transfers to EML-2 point, where comparable relay satellites can be operated.

Science:

- EML-4 environment mapping of trapped dust
- longtime solar radiation intensity measurement (on solar intensity cycle of approx. 11 years)
- longtime cosmic radiation measurement
- EML-4 position as early-warning system for lunar crew (depending on sensors in science payload)

The location and a satellite platform that is able to stay in EML-4 orbit are valuable for scientific research. In addition to the communication provision, a scientific payload will provide valuable data of the libration point environment and space weather. The EML-4 area is debated among scientists to contain the Kordylewski cloud with concentrations of space dust. The space dust detector will provide data of space dust parameters and whether and how it influences the operation capability of the satellite.

Another advantage is that the long duration of stay in the EML-4 makes it possible to investigate the solar activity, in case of the operational mission for one solar activity period. And furthermore the satellite can serve as an early warning system for solar or cosmic radiation for manned mission on the Moon because the satellite is outside the van-Allen radiation belt and is able to detect it and it gives response time for the crew.

Relay Provision Operation:

- first relay service of such kind
- the platform can mainly base of standard components and few technology development is needed
- creating a new service as support for other missions (communication, space weather)

A communication satellite's constraint is the selection of the operation window. The service is dependent on the partners using this service. Thus a suitable time frame has to be found in which enough partner missions will use the service to approve the mission efforts and maximize the cost efficiency with respect to amortization of the service.

3.5 TMA-0: In-Orbit Demonstration Satellite

The presented critical mission points constitute a high level of risk. With this uncertainty a mission start with the operational satellite TMA-1 could lead to long development times, a mission failure and/or high costs. To reduce the risks an in orbit demonstrator (IOD) satellite can qualify the mission and the operational satellite's hardware components and some relevant subsystems. The subsystem complexity of TMA-0 can also be reduced that can lead to a faster realization time of the satellite and an earlier launch and mission start. With a proven mission and qualified components the design margins for the operational mission can be reduced and will be more efficient with respect to payload capacity.

The main demonstration objectives are:

- Earth-based communication demonstration
- Target pointing demonstration
- Orbit insertion demonstration
- Orbit keeping demonstration

The operational TMA-1 satellite specifies the fundaments of the TMA-0 mission. This thesis describes the conceptual design of the TMA-0 demonstrator mission with respect to the operational mission requirements of TMA-1. The goal of the continuing chapter is to derive mission objectives for a mission demonstrating the performance of this concept. This culminates in the TMA-0 satellite design with its own set of requirements and scaled down approach. This can be achieved by direct requirement implementations or with methods to prove the capability of the satellite with alternatives. This chapter states the derived requirements from TMA-1 on TMA-0.

3.5.1 Definition of Demonstrator Mission Requirements

This sub-chapter describes only the differing requirements of TMA-1 and TMA-0. When the previously listed requirements are not described in this chapter they are still valid in that unchanged form.

3.5.1.1 Mission Time

The TMA-0 mission time shall be minimum three years instead of ten years of TMA-1. This mission time includes a set of specific demonstration runs that respect certain aspects of the TMA-1 requirements.

During the in-orbit demonstration (IOD) one of the main critical points is the orbit keeping. The demonstration requires a combined inclination and eccentricity correction can be demonstrated in separated steps qualifying both. The orbital maneuvers take place during one or several orbit periods that is equal to 27.3 days hence three years allows several runs of different demonstrations.

In parallel to orbit keeping demonstration with the attitude and orbital control system (AOCS), the communication verification shall take place independently from supported lunar missions, because it reduces cost by a down scaled system, requires less infrastructure preparation and there is no need of linking schedules of partnering missions with the TMA-0 mission. The communication testing is even possible within shorter times than AOCS testing that will take place during several orbits.

During the complete mission time scientific measurement shall be made simultaneously. This measurement is possible without conflicting with the technical demonstration schedule. The IOD mission times allows measuring one fourth of a solar intensity cycle and is adequate for dust detection and Kordylewski dust cloud observation. Kordylewski dust may be an important design information for the operational mission, e.g. with respect to the degradation of the solar array being caused by those particles.

After the demonstration mission of three years, TMA-0 shall be used as a communication relay with reduced operational capability instead of directly entering the disposal face. The two-way RF and laser links could be used for inter-satellite links. This shall be decided on the satellite condition after demonstration mission if such an operational mission is feasible and when a disposal phase F is still possible afterwards.

The three years IOD mission time also affects the storability of the propellants and the reliability of the propulsion system. AOCS hardware characteristics can be evaluated and the re-activation of the thrusters used for the disposal transfer can be demonstrated under long-time effects.

3.5.1.2 Communication Baseline

The IOD communication baseline shall be reduced in relation to the operational mission. This includes the communication link branches (just Earth, instead of Earth and Moon) and the number of channels.

The demonstration of the communication links reflects mainly the target pointing and accessibility. Because of the satellite position on EML-4 orbit from where the distances to Earth and to Moon are equal and the requirements of target pointing, data-rates and more for both branches is basically the same, only the Earth link branch shall be used for IOD communication demonstration. This also neglects the need for surface or orbital assets on the Moon for the demonstration.

TMA-0 shall qualify the link properties from Earth, the target pointing capability and the on-board data handling of buffered data (Figure 28). In this way the verification can be done from Earth ground stations or by satellites in Earth’s orbit. This also reduces the communication subsystem because the Earth branch of TMA-1 possesses RF links and the now redundant RF-links of the Moon branch are not needed. But the optical link of the Moon shall be demonstrated on the Earth branch site. This has to be respected due to atmospheric effects on the laser link that would not occur for laser links to the Moon. The main advantage is demonstration of the satellite features without the dependency of other lunar missions.

The optical link shall be realized as commercial-off-the-shelf (COTS) hardware. For the operational mission better terminals may be developed. The data-rate adapts to the distance and link access shall be verified. This demonstrates the target pointing capability of the laser link. This method offers the benefit of reduced development time of the laser communication terminal (LCT) and costs. There are LCTs available on the market with technology readiness levels of six and above and even some already space qualified LCTs (Tesat LCT-1).

The properties of now missing Moon link branch shall be verified with an additional optical measurement system to determine the target pointing of stated lunar targets of TMA-1 communication baseline requirement. Even though there is no need for communication links to the Moon the selected targets on lunar surface, lunar orbit and EML-4 shall be verified.

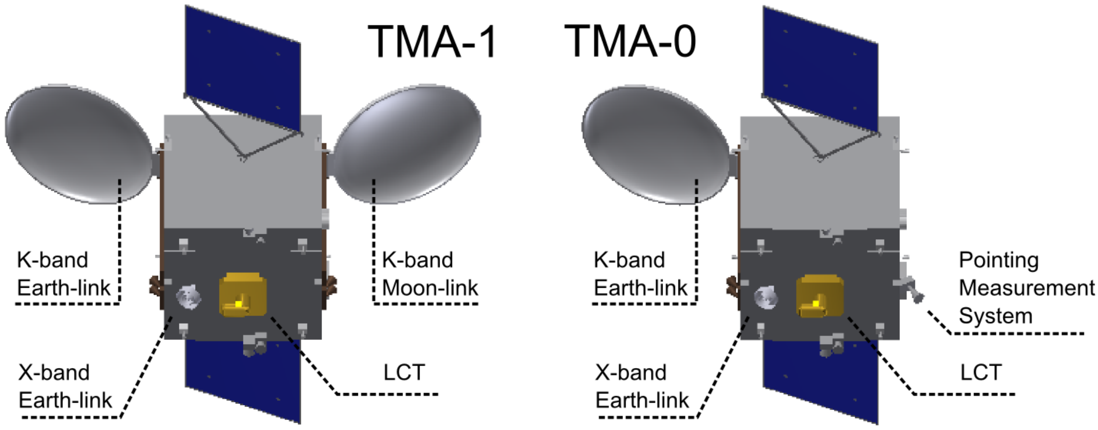

Figure 28: Operational TMA-1 and demonstrator TMA-0 satellites

The data-rate verification of the RF links shall be realized by an analysis of the data throughput per channel. The maximum of 400 Mbit/s for TMA-1 results from using several channels within the broadcasting bandwidth. Several channels' output is representative for the needed channels to achieve the maximum of 400 Mbit/s. The TMA-0 shall include at least one RF-channel with the same characteristics as the TMA-1channel. So the overall data-rate can be below that 400 Mbit/s but still qualifies the communication system of the operational mission. Additional qualification of the communication payload shall be achieved on-ground.

The permanent access of the communication link from Earth is not necessary for the demonstration. A hand-over of the signal of one ground station to another shall be demonstrated but several ground stations like in DSN configuration to guarantee permanent access shall be avoided to simplify the ground segment and reduce costs.

3.5.1.3 Earth-Moon Libration Orbit

The Earth-Moon libration orbit for TMA-0 shall be the same as for TMA-1, but it shall be demonstrated to change the orbit elements with respect to eccentricity and inclination. Therefore a sequence of orbit demonstration phases shall be conducted over a period of orbits. Moreover, station keeping shall be verified to allow targeting from and to TMA-0.

Attitude control demonstration shall include de-tumbling mode and target pointing mode. This shall be determined by the influence on the communication links and the Moon branch optical sensor to allow their requirements.

With TMA-0 the disposal transfer shall be qualified. For this crash landing on or near the lunar heritage sites like Apollo mission landing zones shall be avoided [69].

3.5.1.4 Environmental Constraints

Due to the unknown effects of the EML-4 environment on the satellite, scientific measurement shall be included in the IOD mission. Scientific instruments for the operational mission are optional but could be based on the instruments on-board TMA-0. With respect for space weather measuring and early warning system the instruments and results are important for TMA-1.

The scientific payload shall include a dust detector that will be used to determine the existence of particles and micrometeorites trapped in the EML-4 region that pose a possible threat to the satellite. As well, observation and surveillance of the Kordylewsky cloud are of inestimable values for science. community. Another degradation source for the solar cells is high energetic protons and electrons. These mainly occur during the transfer phase of TMA-0. An optional instrument should be considered to perform space environment sensing of magnetic fields of the Earth magneto-tail.

Additional measurement shall be conducted for solar intensity that can simply be done with the satellites solar cells and Sun sensors. This needs little development time because it’s already included within the AOCS and EPS systems.

As an optional scientific payload solar and cosmic radiation could be measured. This instrument on-board TMA-0 can directly be qualified for the operational mission and thus TMA-0 can serve as a test-bed. The qualified instrument can serve for the advance warning system of solar and radiation activity as a support of manned missions to the Moon.

3.5.1.5 Mission Costs and Development Time

For the demonstrator mission, the design shall be cost efficient and the development time shall be short in order not to delay the TMA-1 launch unnecessarily. This means the component selection shall be in favor of commercial off-the-shelf (COTS) and standard decisions rather than in development of new technology and experimental design, unless necessary for the full operational mission.

One of the big items in the cost budget will be the launcher service. The main and back-up launcher service shall be selected according to the lowest cost but should be able to deliver the satellite into orbit according to the mission time plan. In addition, the candidate list should include a European launcher due to an independent access to the orbit and due to international traffic in arms regulations (ITAR). Additional launchers are shortlisted for a flexible launch date scheduling.

3.5.2 Mission Drivers

From all mission requirements, some few represent mission drivers that influence the one or more decisions and architecture configurations. These drivers need to be identified and analyzed according to their influences and sensitivities. The main conceptual design work is spent on those drivers otherwise they could negatively affect the mission progress.

The identified drivers communication, orbit design as well as mission costs and timeline are explained in detail in the following sub-chapters.

3.5.2.1 Communication

3.5.2.1.1 Frequency Band Selection

The frequency band selection and allocation for the TYCHO mission is highly influencing the technical design of the communication subsystem and service, but also the legal design with respect to international laws and regulations.

The obvious influence is on the data-rate. With the requirement of high-data rate higher frequency bands have to be used. Otherwise the needed bandwidth would be too wide for already crowded bands so that a band allocation of a free and wide enough frequency band slot is not possible. Another effect is that the maximum allowed equivalent isotropically radiated power (EIRP) would be exceeded. That leads to selection considerations in bands higher than 8 GHz where complex, high-gain antennas are used or atmospheric damping will occur in the Earth links. The soft requirement of integration in a communication relay satellite network (like EDRS) also poses special needs on the frequency selection, modulation, polarization and more. All this creates a set of limits influencing the design of the subsystem and on the satellite outer shape where the antennas are able to be attached.

The regulatory aspect is an important selection criterion. Radio frequencies are a common good with a limited number of technically usable frequency bands. The International Telecommunication Union (ITU), as a specialized agency of the United Nations, coordinates the shared global use of the radio spectrum. The utilization is regulated within the band plan with bands associated with certain applications. The band selection for the TYCHO mission has to respect three categories [53] [70].

- It is a space research satellite (SRS) due to its scientific payload and the position in EML-4 that is at a higher altitude than GEO. Thus bands for space-to-Earth and Earth-to-space communication for SRS are suitable.
- It is also a relay satellite where inter satellite links have to be used that shall not interfere with communication on Earth surface, where those frequencies are sometimes used for point-to-point services.
- And the ground stations for TYCHO can be considered as fixed satellite services.

Selecting a frequency band that allows inter-satellite links and communication of SRS may reduce the system complexity but it limits the possible bands that can be used.

An additional aspect is that the assignment of the allocated frequency is tasked by ITU and their members. This process requires contacting the users of the neighboring frequencies by ITU during the year and up to the next assembly or meeting. The TYCHO satellite on EML-4 orbit passes the GEO plane several times at different places and the communication beam will propagate over several GEO and other satellites. Depending on the transmitted frequency, both signals could interfere. The frequency selection should respect the band allocation of those of GEO communication satellites so that both TYCHO's allocated frequencies are not interfering or blinding the GEO services. Because such a mission was not undertaken before the time needed to allocate a frequency is uncertain and the clarification and allocation of the band is the main first task to keep the mission development short and avoid a midproject change of frequencies, in case it cannot be granted.

One of the benefits of the TYCHO mission is to provide communication to the far side and shielded side of the Moon that is an asset area for radio astronomy. This zone is also regulated by ITU with consensus of the International Astronomical Union (IAU) in "Protection of frequencies for radio astronomical measurements in the shielded zone of the Moon" (Rec. ITU-R RA.479-5) [71] so that "[…] *frequencies that would be most acceptable to radio astronomers for transmissions on the Moon are the higher ones; i.e., the range above 25 GHz.*"

As presented the radio frequency band selection is not trivial and a discussion between ITU, IAU and TYCHO operating organization of a relay service between Earth and the Moon and its possible implication is advised here. In this thesis the selection of K-band represents the compromise of the given conditions and user requirements.

For the IOD there is an additional aspect. The communication links that would be used for the Moon branch on TMA-1 are demonstrated on the Earth link branch. Hence the frequency bands have to be useable for this.

3.5.2.1.2 Data-Rate

Another aspect of the communication as a design driver is the data-rate. This is important for the users of the relay service. They shall be able to fulfill their tasks in transmitting the data and therefore the expected data-rate has to be met. As a future relay service the data-rate has to respect the expected needs of the users in during the proposed mission time. The data-rate is selected according to the identified user requirements and official recommendations. Nevertheless a surplus-capacity leads to more complex solutions and higher mission costs and an undersupply cannot handle the service needs and can result in loss of users and thus a loss of financing.

The data-rate as a fixed request requires an adequate transmit power that is provided by the EPS. Hence the data-rate is a direct design driver for the solar generator and battery within the electrical power system. In addition, the data-rate of the relay service is the biggest item for the data handling (satellite telemetry and its own science payload are negligible) it drives the on-board data-handling (OBDH) subsystem in regards to the processing speeds, interfaces and storage capacity.

Moreover the variety of user requested data-rates is a design driver for the communication system. Typically the data-rate, modulation, error correction and transmit-power are fixed but this can lead to no-connections due to anything from too bad signal to noise ratios. In case the relay satellite service shall be able to give access to a broader range of users, it will drive the design of the radio frequency distribution unit and the receiver module.

3.5.2.1.3 Ground Segment

Leaving the user requirements that set the data-rates and the Moon link branch the Earth ground segment plays a role in the design. The receiver antenna gains influence depending on the received and sent data-rates. Although the transmit power is not limited, the availability of the ground stations and the possibility to work within the band is affecting the cost of the project.

3.5.2.2 Orbit Design

The transfer and target orbit selection drives the propellant demand and therewith the mass budget. This influences the launcher selection that can provide the starting orbit for the possible transfers and the propulsion system. The propulsion system design and the launcher drive again the cost budget.

The transfer to the target orbit influences the communication system that will be used for the Telemetry, Tracking and Control (TT&C) because it shall provide communication during all mission phases from Earth orbit to the target orbit. In case of a bi-elliptical or weak stability transfer (WSB), the propagation path length varies and the TT&C have to provide telecommunication modes for all distances. Commanding and monitoring the satellite is an essential mission part and thus driving the communication subsystem and ground segment.

3.5.2.3 Mission Costs and Timeline

The last mission drivers are mission costs and timeline in general as the all-encompassing drivers. They are the cause to separate the TYCHO mission in the in orbit demonstration and the operation mission.

3.5.2.3.1 Launcher

As required the TMA-0 mission shall be a low cost mission and the reduction in complexity supports it. The launcher selection still influences and thus is the start orbit and transfer, the satellite system dry mass as well as the dimensions and structure. With the launcher selection, the launching sites are appointed and even the heritage of the satellite components is determined due to regulations and restrictions.

3.5.2.3.2 Mission Start and Timeline

The mission start of TMA-0 is independent from other lunar missions, but is has to fully accomplish the mission before TMA-1 can be launched. This is due to the results of the demonstration shall be incorporated into the design. And the Timeline of TMA-1 is dependent from other lunar missions as user of the relay service. Hence there is an inter mission driver taking into account the timelines of the complete dual satellite TYCHO mission.

4 TMA-0 Demonstrator Mission Architecture

The mission architecture outlines the demonstration and science objectives for TYCHO TMA-0 satellite in further detail and defines references for the different satellite's subsystems. The specified goals and requirements are analyzed and evaluated between alternatives. In this way the presented references are the basis for the subsystem design and component pre-selection in the following Chapter 4.4: Demonstrator Satellite Configuration.

4.1 Launcher Systems and Start Concepts

This chapter is dedicated to the launcher selection and recommendations are made for launcher options in terms of the TMA-0 mission requirements like GTO injection, launch opportunity and cost-related aspects. As presented the launcher selection is one of the mission drivers for TMA-0.

4.1.1 Start Orbit

The multitude of available launcher vehicles offers a set of different start orbits in which the payload satellite can be placed in. Depending on the launcher the payload capacity covers delivery to low Earth orbit (LEO), geostationary transfer orbit (GTO), geo synchronous orbit (GEO) and highly elliptical orbit (HEO). All of these offer certain advantages and disadvantages for the TYCHO mission. These options are briefly discussed in Table 18.

Table 18: Start orbit options

Start Orbit	Advantage	Disadvantage
LEO		high launcher performance, high delta-v, few secondary payload options (mostly polar orbit)
GTO	standard orbit, frequent secondary payload options,	
GEO	standard orbit	few direct orbit injections, high delta-v requirement (lower orbit energy compared to GTO)
HEO	low delta-v	very few launches, dedicated launch with higher cost

The GTO is chosen as the start orbit for TMA-0 because it offers a compromise in delta-v and as a standard orbit with frequent launches it offers secondary payload options. All selected launchers shall provide payload capacity to GTO. Although the final apoapsis altitude is fixed the periapsis altitude and the orbit plane varies between all launcher options (Table 19).

Table 19: GTO orbit parameters of launcher candidates

Launcher	Apoapsis altitude	Periapsis altitude	Inclination
Ariane 5 ECS	35943 km	250 km	6.0°
Falcon 9 v1.1	35950 km	185 km	15.0° - 28.5°
GSLV	36000 km	200 km	18.0°
Soyuz (Baikonur)	35786 km	4200 km	23.3°
		2100 km	31.0°
Soyuz (Kourou)	35950 km	230 km	6.0°

[72] [73] [74] [75] [76]

The GTO orbit in the transfer simulation is modeled for a low periapsis to be risen from about 200 km to 400 km first. In this way it allows to stay on the GTO for several revolutions. A higher periapsis decreases atmospheric drag loss and the orbit decay is less. This shall be considered for the launch window planning where an in-orbit waiting time is used to adjust the transfer and injection into the target orbit (Chapter 4.2).

4.1.2 Launcher Candidates

The launchers taken into account provide payload capacity into GTO with satellite masses suitable for TMA-0. With regard of the operational TMA-1 satellite that will have a higher mass some launchers can even serve as a launch option for both missions. However the selection respects primarily the TMA-0 mission. The launcher capacity varies so that the initial GTO they shall provide differs with respect to the periapsis altitude and the inclination. This is already included in the orbit design (Chapter 4.2) with a 400 km altitude of the periapsis with an equatorial orbit plane (inclination = 0).

Considering the mission requirements for a cost effective launch, the launchers are also selected with respect to the yearly launch frequency and options of dedicated, secondary launch options. This allows a more flexible launcher selection for the demonstrator satellite.

Table 20: Launcher systems – launch masses and costs

Launcher	**Country of origin**	**Payload capability to GTO [kg]**	**Launch site**	**Launch cost [M€]**
Antares	USA	TBD	Wallops	40
Ariane 5 ECA	Europe	10600	Kourou	120
Ariane 5 ECA, secondary payload	Europe	3000 – 4500 kg*	Kourou	48 (40 % of 120)
Falcon 9 v1.1	USA	3000 - 4500	Cape Canaveral	42
GSLV	India	2000 - 2500	Satish Dhawan	35
Long March 3A	China	1000 - 2500	Xichang	37
Long March 3C	China	2500 - 3800	Xichang	37
Proton	Russia	3000 - 5000	Baikonur	70 - 77
Soyuz	Russia	1400 - 1800	Baikonur, Vostochny	58
Soyuz	Russia	3200	Kourou	70
Tsyklon-4	Ukraine	1600 - 1700	Baikonur, Alcântara	31
Zenitt-3 SL	Ukraine	5000 - 6000	Sea Launch (mobile)	66

Note: For launch costs in US-Dollars the currency rate from Euro is 0.77. [77] [78]
**Ariane 5 ECA: total payload capacity 10600 kg*
primary payload 5000 – 6500 kg, secondary payload 3000 – 4500 kg, Sylda 5 Adapter 425 - 535 kg

Possible launchers for the GTO transfer are listed in the Table 20 and these are technically able to transfer TMA-0 as a dedicated or secondary payload into orbit. Based on the list potential launchers are analyzed according to technical and program criteria of:

- Launch cost of not more than 70 M€
- Launch window and launch frequency
- Flexibility of the GTO orbit (periapsis, inclination)
- Availability for starting after 2016[1]
- Proven reliability expected after 2016 after several successful starts
- Political aspects (e.g. ITAR, heritage)

Table 21 presents the Soyuz as the baseline launcher with launching site in Kourou, French Guiana and the backup launcher candidates Soyuz (Baikonur, Kazachstan), GSLV, Ariane 5 ECS and Falcon 9 v1.1. The baseline launcher is the main mission and system driver. The dimension of the satellite still needs to fulfill the maximum payload dimensions of all launchers. Therefore the mission requirements of the baseline and backup options are directly influencing the mission requirements respectively the system requirements of TMA-0 and TMA-1. A later switch to another launcher is costly and time-consuming, if it is possible at all.

Table 21: Baseline and backup launchers

	Major Restriction	**Advantage**
Baseline Launcher		
Soyuz (Kourou)	Launch cost	Reliability, dedicated & secondary option
Backup Launcher Candidate		
Soyuz (Baikonur)	only dedicated launch for smallest satellite mass class, low first periapsis, relocation Soyuz launch to Vostochny after 2018	Reliability
GSLV	no major restriction identified	Cost
Ariane 5 ECS	Dual launch (cost driven), only secondary payload option.	Frequent launch opportunities, European heritage, supported lunar mission as primary payload (dual Moon mission) [TMA-1]
Falcon 9 v1.1	development schedule and reliability is questionable	Cost

The backup launcher option gives certain advantages. The risk of massive time delay is avoided if the chosen launcher is grounded due to technical reasons or dual flight reasons. The unsuccessful launch with Zenith from Sea Launch platform on January 30th, 2007 led to a rebuild of the platform and a delay of launches [79]. The reduction in launch cost demands to find a dual launch partner that can be complex due to the launch window and GTO parameter

[1] Some launch vehicles are not in production anymore and only stocked vehicles are expended

matching. General aspects of cost saving also come into play when there is a competition between several providers during the negotiation phase.

The discarded launchers in Table 22 are not considered due to high risks in costs, political reasons and capacity and are not suitable for the TMA-0 mission. The specific reason per launcher is provided briefly in the table.

Table 22: Discarded launchers and reasons

Discarded Launcher	Reason
Proton	cost > 70 M€
Ariane 5 ECA	cost > 70 M€
Zenith-3 SL	Launch delay risk
Long March 3A	ITAR Risk
Long March 3C	ITAR Risk
Antares	Unspecified payload capability
Tsyklon-4	Low payload capability

An additional aspect of the launcher selection is the availability of launch opportunities. The demonstrator mission shall be cost saving and this also means a flexible launcher selection. This is achieved by negotiation with launch system providers offering the most launches (including GTO launches) in the market. For the secondary payload launch option, the higher number of launches increases the chance finding a vacant secondary payload slot. Moreover the frequency of launches gives a flexible launch window selection during the year for dedicated and secondary launch options. The selected launchers are presented with their launches during a period in Table 23.

Table 23: Number of future launches per period

Launcher	Period	Launches (to GTO)	Launches per Year
Ariane 5 ECS	2010 - 2019	18 (16)	2
Falcon 9 v1.1	2013 - 2017	32 (3)*	8
GSLV	2010 - 2013	3 (3)	1
Soyuz-U (Baikonur)	2010 - 2014	19	4.75
Soyuz-2 (Baikonur)	2004 - 2013	8	0.9
Soyuz-2 (Kourou)	2010 - 2014	5	1.25

*Falcon 9 v1.1 inauguration flight in 2013, launch numbers from preliminary list.
Launches for specific GEO communication satellites in brackets
[80] [81] [82] [83]

The launchers are launched from different launch centers and can reach a certain range of inclinations from it. This is already referenced in Table 19. To the interest of this range, the WSB is also chosen that the transfer is independent from the launcher selection. Only the final launch and transfer start adjustments are affected by the launcher that only varies within a day between launch sites.

4.1.3 Launcher Recommendations

Overall the recommendations for the baseline and backup launch options are presented in this study. The decision needs to be verified in the following study and development phase when major technical changes will be made.

The baseline launcher is Soyuz with launch site in Kourou. Soyuz is a launcher system with a proven reliability, with a payload capability of the expected satellite mass and with an adequate launch cost. The launcher and launch sites are managed by European Arianespace. The Soyuz Launch Site (Ensemble de Lancement Soyuz – ELS) provides the same quality of services for combined launch vehicle operations with spacecraft as the remaining facilities. The ground industrial and launch vehicle teams responsible for the satellite integration are from Russian partners in collaboration with the teams of the Guiana Space Centre [72].

With respect to launch costs the Falcon 9 is a candidate. After the required reliability of several successful launches, the Falcon 9 can also be considered as a direct baseline launcher. The Soyuz backup launcher with launch site in Baikonur (or Vostochny) is an option with respect to costs. In case of generally grounded Soyuz systems, it cannot be used as the single alternative for Soyuz (Kourou) baseline launcher. The GSLV is a backup option due to costs, although the number of launches is low. The Ariane 5 launch option is interesting for TMA-0 as secondary payload. The high number of booked launches for GTO until 2019 gives the opportunity to find a main passenger that suits the launch window and a basis for cost negotiation. Ariane 5 even offers a proven system with GTO as the main target. Therefore special midnight launches are offered [84]. Ariane 5 is operated by Arianespace and launched in Kourou that also offers European legislation and support by the European Space Agency (ESA).

4.2 Orbit Design

The orbit design reflects the mission requirements of TMA-0. It is separated into the transfer orbit, the mission orbit around EML-4 and the end-of-life transfer. Each of these phases is separated into sub-phases. Several alternatives are analyzed and rated for different aspects.

4.2.1 Transfer Orbit Sequence

The satellite transfer is a sequence of different orbits and maneuvers bringing TMA-0 from the initial Earth's orbit provided by the launcher to the EML-4 target where the station keeping phase starts. The transfer orbit sequence is examined on aspects like transfer time, delta-v costs, environmental conditions and launcher options. There are multiple ways to transfer a satellite into the EML-4 orbit. The selected scenarios are a direct transfer, a bi-elliptical transfer within the Earth's sphere of influence (SOI) and in the weak stability boundary (WSB) (Figure 29).

The direct transfer (a) includes two or more changes of the spacecraft velocity. The first delta-v maneuver is initiated during the periapsis passage of the initial geostationary transfer orbit (GTO). The resulting orbit connects the initial periapsis altitude with the new apoapsis altitude directly into the target orbit. When the satellite reaches the apoapsis of the direct transfer orbit the velocity is corrected to increase speed and change the elliptical transfer orbit to the target orbit. For satellites with long ignition times and low thrust levels, the direct transfer contains several intermediate orbits. At each periapsis passage the orbit velocity is increased and the transfer apoapsis is raised until it also reaches the target orbit. In this way the gravity losses can be minimized at the expense of a longer transfer time.

The bi-elliptical transfer (b) makes three changes to the spacecraft's velocity in contrast to the direct transfer that can be completed with two change maneuvers. The first transfer trajectory orbit arc connects the initial orbit with an apoapsis that is greater than the desired final radius. At the apoapsis the second delta-v maneuver brings the spacecraft on another elliptical transfer orbit. The spacecraft is then transferred into the final orbit. When reaching the periapsis of the second transfer orbit, the third and final change in velocity is initiated. For the WSB transfer the sequence of the bi-elliptical transfer is used but with an apoapsis with a radius that lies outside the sphere of influence (SOI).

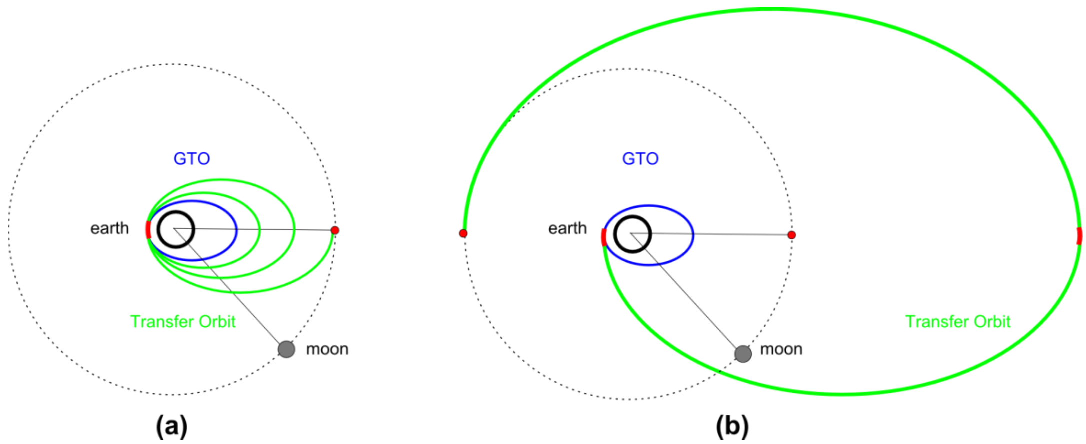

Figure 29: Transfer options from Earth to EML-4 target orbit
(a) direct transfer including several thruster ignitions, (b) bi-elliptical transfer or week stability transfer (WSB)

Both transfer strategies are described for coplanar orbit maneuvers. During the transfer the orbit plane can be changed. This is most efficient at the apoapsis when the orbit velocity is the lowest. The plane change can be achieved with a special delta-v maneuver. For the WSB transfer the plane change is supported by the Sun's gravity and can even be completely accomplished without a spacecraft maneuver. The target plane can be reached if the line of nodes of the transfer orbit and those of the target plane coincide. This can be achieved by either waiting time in the target orbit or with other target change maneuvers. As a co-passenger the latter two options are realistic [85].

For the TYCHO transfer concept a GTO as the starting orbit for all transfer scenarios. It offers a higher flexibility in launcher and launch window selection for TMA-0 as a secondary payload (piggy-back) satellite. There are well-planned standard midnight launches by Ariane 5 delivering communication satellites into GTO on a regular basis [84]. Further launcher systems like Soyuz, Zenith and others offer performances to deliver satellites on orbits with apoapsis of 42000 km.

Table 24 shows that a GTO with an injection into GEO and a following transfer orbit to EML-4 is discarded because it requires additional delta-v. So the transfer maneuvers are conducted during the periapsis passage of the initial GTO. The injection into an initial LEO orbit is also discarded because it requires the most delta-v to transfer the satellite to EML-4 in this comparison. An increase in delta-v leads to an increase in propellant on-board of TMA-0. In this way the satellite propellant can be reduced by the GTO to EML-4 transfer strategy.

Table 24: Delta-v budgets for impulsive transfers from LEO or GTO to EML-4

Transfer	Delta-V	Maneuvers
LEO to EML-4	3901 m/s	2
GTO via GEO to EML-4	3083 m/s	3
GTO to EML-4	1501 m/s	2

The orbit altitude of circular LEO and the periapsis altitude of the GTO are 400 km.
The circular GEO radius is 42157 km and the circular EML-4 orbit radius is 405500 km

The three transfer strategies, direct, bi-elliptical and the WSB contain the following sequence with the exception for the direct transfer, where the apoapsis lowering is not needed. For the trade-off the ideal transfer with impulsive maneuvers is used, so the midcourse correction will be effective for the simulation and is not applied for the ideal calculation.

Transfer Orbit Sequence:

0. GTO
1. Apoapsis Raising
2. Periapsis Raising
3. Plane Change
4. Midcourse Correction
5. Apoapsis Lowering and Plane Change/Correction

The three strategies (direct, bi-elliptical, WSB) are compared with theoretically impulsive velocity changes. The maneuvers bring a spacecraft from one orbit to another orbit on the same orbital plane. A transfer from GTO to the Moon faces the problem that there is a difference in inclination of 18°-29° between the Earth's equatorial plane and the Moon's orbit. Launching directly into the lunar transfer orbit with a rendezvous with EML-4 is only possible twice a month within the EML-4 orbit nodes. Otherwise an inclination change is required with an additional delta-v intensive maneuver. The comparison includes an inclination change of 7°. The transfer apoapsis radiuses reflects the direct transfer to the distance of the EML-4 that is the same as the Moon's orbit, to a distance beyond the sphere of influence (SOI) for the WSB and a distance with half of both distances. Therefore the distance to the edge of the SOI r_{SOI} is calculated

$$r_{SOI} = a\left(\frac{m_{em}}{M_{sun}}\right)^{\frac{2}{5}} = 929228\ km \quad 4.1$$

with the parameters for the masses of all three celestial bodies and the semi-mayor axis of Earth's orbit around the Sun [17].

$$M_{sun} = 1.989 \times 10^{30}\ kg \quad 4.2$$

$$m_{earth} = 5.974 \times 10^{24}\ kg \quad 4.3$$

$$m_{moon} = 7.349 \times 10^{22}\ kg \quad 4.4$$

$$m_{em} = m_{earth} + m_{moon} = 6.048 \times 10^{24}\ kg \tag{4.5}$$

$$a = 149600000\ km \tag{4.6}$$

The equation is describes a theoretical edge of the SOI where both gravitational forces acting on the spacecraft are equal. In reality this switch of the central gravity source is a fuzzy transition zone with a steady change of influences of the two main gravity sources and further perturbations. The distance when the spacecraft leaves this transition zone and is in the reference of the Sun is set to

$$r_{SOI} = 960000\ km \tag{4.7}$$

For each orbit used in the sequence (1-5) the corresponding orbit velocities are calculated and used for the delta-v budget of the complete mission sequence. For orbits with eccentricities $e \leq 1$the energy equation (Vis-viva equation) can be used to obtain the velocities v at a certain radius of a given orbit with semi-major axis a with

$$\frac{v^2}{2} - \frac{\mu}{r} = -\frac{\mu}{2\,a}\ (Energy\ Equation) \tag{4.8}$$

where μ is standard gravitational parameter and G is the universal gravity constant.

$$G = 6.67384 \times 10^{-11} \frac{m^3}{kg\ s^2} \tag{4.9}$$

$$\mu = G\ m_{earth} \tag{4.10}$$

For the transition of one orbit to another the energy of the orbit has to be increased and that is achieved by thrust maneuvers (impulsive for the ideal maneuver, with finite burning times for the real maneuvers) that changes the spacecraft's velocity by Δv. This has to be done for orbit changes and for the plane change. The amount of Δv is in relation to the spacecraft's current velocity v_1 and the velocity v_2 that has to be achieved for the next orbit.

$$\Delta v_{eccentricity\ change} = |v_2 - v_1| \tag{4.11}$$

$$\Delta v_{plane\ change} = \sqrt{v_1^2 + v_2^2 - 2\,v_1\,v_2\ \cos \Delta i} \tag{4.12}$$

The comparison of all three transfer options in Table 25 to Table 27 shows that the weak stability transfer is the less intensive delta-v transfer.

Table 25: Ideal impulsive direct transfer to EML-4

Direct Transfer (highest apoapsis 400000 km)							
#	**Maneuver**	**Radius [km]**		**Velocity [km/s]**		**Delta-V [km/s]**	
		Periapsis	Apoapsis	Periapsis	Apoapsis	Periapsis	Apoapsis
0	GTO	6771	42157	10.072	1.617		
1	Apoapsis Raising	6771	405500	10.762	0.180	0.689	
2	Periapsis Raising	4055000	405500	0.992	0.992		0.812
3	Plane Change of 28.6°						0.489
4	Midcourse Correction						
5	Apoapsis Lowering						
						Total	1.991

Table 26: Ideal impulsive bi-elliptical transfer to EML-4

Bi-Elliptic Transfer (highest apoapsis 680000 km)							
#	**Maneuver**	**Radius [km]**		**Velocity [km/s]**		**Delta-V [km/s]**	
		Periapsis	Apoapsis	Periapsis	Apoapsis	Periapsis	Apoapsis
0	GTO	6771	42157	10.072	1.617		
1	Apoapsis Raising	6771	680000	10.798	0.108	0.725	
2	Periapsis Raising	405500	680000	1.110	0.662		0.554
3	Plane Change of 28.6°						0.327
4	Midcourse Correction						
5	Apoapsis Lowering	405500	405500	0.992	0.992	0.118	
						Total	1.725

Table 27: Ideal impulsive WSB transfer to EML-4

Weak Stability Transfer (highest apoapsis 960000 km)							
#	**Maneuver**	**Radius [km]**		**Velocity [km/s]**		**Delta-V [km/s]**	
		Periapsis	Apoapsis	Periapsis	Apoapsis	Periapsis	Apoapsis
0	GTO	6771	42157	10.072	1.617		
1	Apoapsis Raising	6771	960000	10.814	0.076	0.741	
2	Periapsis Raising	405500	960000	1.110	0.662		0.420
3	Plane Change of 28.6°						0.245
4	Midcourse Correction						
5	Apoapsis Lowering	405500	405500	0.992	0.992	0.184	
						Total	1.590

For transfers from an orbit with radius r_1 to another orbit with radius r_2

$$R_r = \frac{r_2}{r_1} \qquad 4.13$$

the delta-v demand is lower for a bi-elliptical transfer compared to direct transfers for $R > 11.94$. This condition is given for a transfer from periapsis in LEO to EML-4 orbit. This advantage of an orbit transfer with less delta-v also leads to longer transfer times which have to be considered for the orbit design [86]. The WSB transfer is a special form of bi-elliptical transfer. The transfer apoapsis lies outside the SOI. In that region the Sun is considered as the main source of gravitational force and acting on the spacecraft. Now the spacecraft's trajectory is not with respect to the Sun's center of gravity and the gravitational pull is correcting the trajectory to fulfill this requirement of spaceflight dynamics. In that way the orbital plane of the spacecraft with respect to Earth is changed. This can be utilized to have a delta-v free plane change.

The spacecraft has to stay outside the Earth's SOI as long as the orbital plane reaches the target orbit plane. The calculation presented in Table 27 still include the inclination change of 28.6° because the Sun induced plane change depends on the actual position of the Sun. The actual delta-v for the WSB transfer can be even lower than the presented.

Despite the advantage of the WSB with respect of lower delta-v budgets, the operations during the passage of the WSB zone are complex. Maneuvers with small delta-v by either the satellite itself or external forces can have a big effect on the trajectory. Furthermore the transfer time is even longer than the classical bi-elliptical transfer within the Earth's SOI.

The direct, bi-elliptical and WSB transfer methods provide a useful first approximation of the delta-v needed for the EML-4 transfer. The Simulations are used to refine the estimates. The WSB transfer (without the plane change) was preliminary investigated with n-body software application, which was developed for TYCHO within this study and based on a code in "Orbital Mechanics for Engineering Students" by H. Curtis [17] [87] [88]. The simulation was processed on the Moon's orbit plane and with finite burn maneuvers. The results are shown in Figure 74 to Figure 77. The delta-v is in range of the delta-v for WSB without plane change in Table 27. The difference is due to gravity loss. Furthermore the importance of the correct location of the celestial bodies Earth and Moon by their ephemerides data can be seen. The starting location in Earth orbit and time is obvious by the ability into the target EML-4 orbit. Not all starting orbit parameters resulted in an insertion under the required conditions minimizing the target function. In addition the gravity effect by the Sun could not be completely modeled, which is needed for the transfer orbit plane change of the WSB. The lack of more adequate perturbation forces on the satellite in EML4 orbit did not result in the expected epicyclic orbit around EML-4 [19].

As the consequence, all three transfer scenarios are simulated with the professional GMAT simulation software offering these features and the approaches and results are presented in the next sub-chapter.

4.2.2 Transfer Simulation

The transfer of the TMA-0 satellite is simulated with NASA General Mission Analysis Tool (GMAT) [48]. Each orbit simulation includes variations of the satellite mass and thruster parameters. The result is a matrix of different delta-v budgets needed for the transfer that is used for the selection of the propulsion system, the launcher system and to determine the possible system dry mass. The latter result influences the satellite overall and subsystem mass budget.

The simulation models the WSB transfer orbit sequences. It includes finite thrust phases for the maneuvers to model the thruster parameters. The simulated satellite starts in GTO with a periapsis radius of 6771 km and an apoapsis radius of 42157 km. From this orbit (0) the transfer to EML-4 is initiated. The GMAT simulation finds the true anomaly positions before and after the periapsis to start and end the thrusting period for the apoapsis rising during sequence (1) as seen in Figure 30.

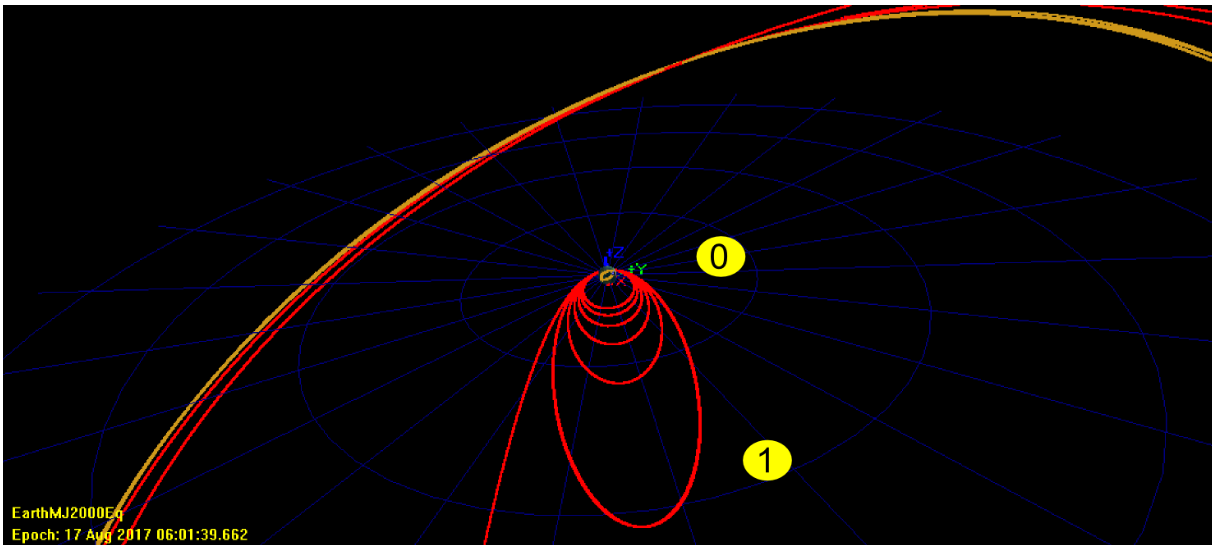

Figure 30: Transfer – GTO (0) and first five apoapsis rising orbits (1).

The number of thrust maneuvers is set to six. This respects the gravity losses that are higher for lower numbers of maneuvers because the thrust is applied outside the perfect position for an impulsive maneuver during the periapsis passage. With lower numbers the ignition time has to be longer and thrust is applied even further away from the periapsis and the delta-v is not only transferred to the rising of the apoapsis but also for turning the apse line of the orbit. The upper limit of maneuvers is influenced by the passages through the van-Allen belt and the transfer time. The model includes six maneuvers because the gravity losses are already converged, see Figure 31, and the ignition times are about nine minutes (Figure 32). For example Chandrayaan-1 transferred to the Moon with seven apoapsis rising maneuvers with about twelve minutes burning times of the 440 N thrusters. The simulation was processed with the TYCHO n-body application. The simulation is simplified on the Moon orbit plane and it was processed on the distributed computing platform Constellation [87].

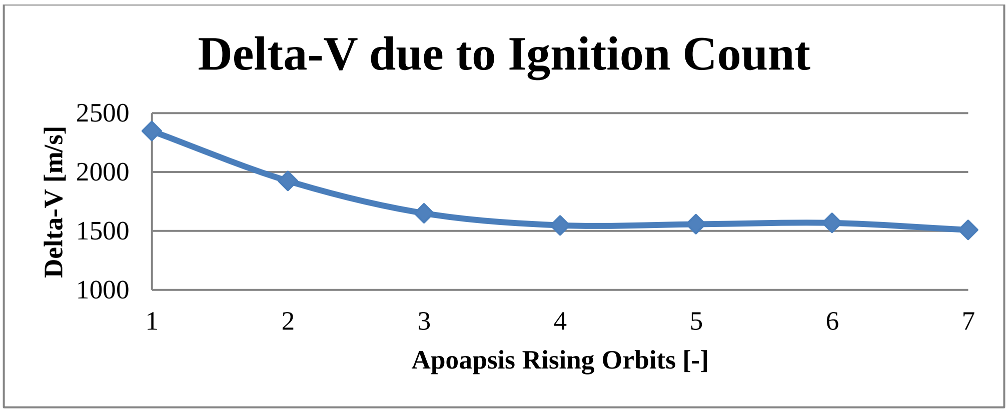

Figure 31: Gravity loss of delta-v with respect to rising orbits

TMA-0 sequence 1 also includes an additional revolution on each of the six orbits. This additional revolution is also included in the trajectory analysis of the “DLR-AMSAT P5 Moon” concept study that also use the WSB transfer and that is one basis of the TMA-0 orbit design [85]. It allows an external tracking and orbit determination that can be used for correcting the thrust maneuvers. The chosen thruster must be able to be re-ignitable for the number of maneuvers.

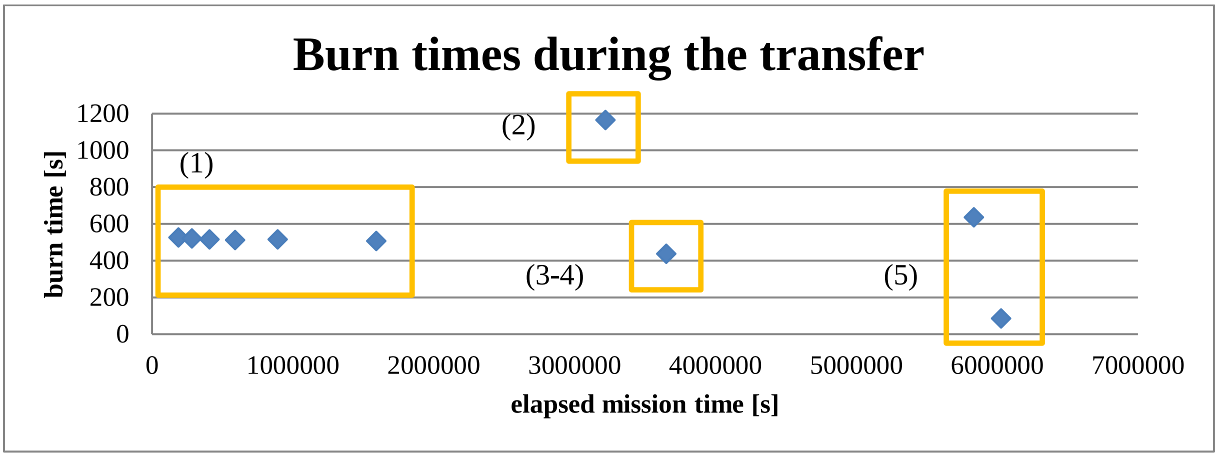

Figure 32: Burn times during the transfer for 5 sequences

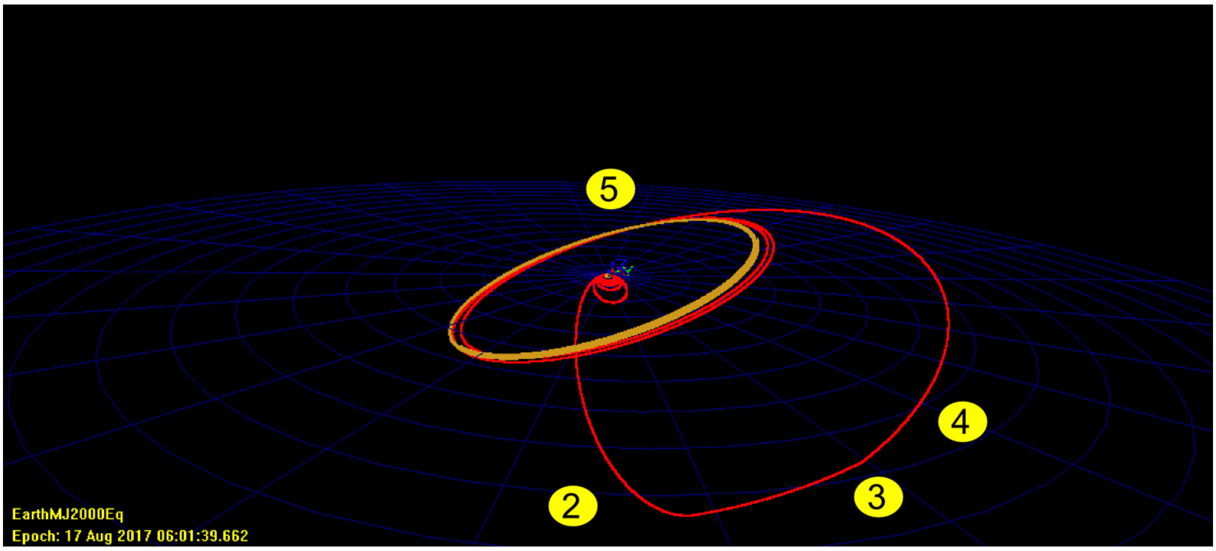

Figure 33: Transfer – periapsis rising (2) plane change (3), midcourse (4) and apoapsis lowering (5)

When the TMA-0 satellite reaches the apoapsis the periapsis raising maneuver (2) is initiated. This raises the following trajectory arc's periapsis to the same orbit altitude of that of the EML-4 orbit. This is also conducted with a finite burn time of the thruster. GMAT optimizes the burn time duration until the condition of the periapsis altitude is reached. No inclination change maneuver is proceeded and the satellite propagates only under the influences of Earth, Moon and Sun.

The propagation continues until the satellite will reach the target orbit plane (3). This should be in the vicinity of the previous apoapsis. On orbit positions near to the apoapsis the satellite's velocity is still slower than near to the periapsis and plane change maneuvers are more efficient. The coasting time until reaching the plane also allows the Sun and external perturbation to change the inclination in a positive and delta-v saving way. So the transfer time until reaching point (3) is one important factor for the mission and is also considered as a parameter for optimization. When reaching the target orbit plane the inclination is changed with finite burn maneuvers. This also means that the satellite cannot completely be injected on an orbit of the demanded plane. This is corrected within the following two maneuvers.

Directly after the plane change, the midcourse correction maneuver corrects the periapsis altitude to the demanded altitude (4). This is due to the fact that during the plane change, this could have been changed. Another aspect is that a certain time span lies between the first periapsis adjustment in (2) and the midcourse correction (4) during which the Moon also propagated on its orbit. Because of the elliptic orbit of the Moon the current orbit altitude changes. The GMAT model includes a method that includes the Moon orbits behavior and thus that of EML-4. After the midcourse correction finite burn maneuver in flight direction the satellite propagates to the periapsis.

At the periapsis, the apoapsis lowering maneuver is initiated (5) that fits the apoapsis altitude of that of the target orbit. After the finite burn maneuver the satellite propagates until reaching the target orbit plane again. This change in inclination could have happened during the transfer and caused by the previous maneuvers. When reaching the plane the last small finite burn maneuver is activated and the target orbit is finally reached.

The launch and transfer start is an additional parameter in the user set-up. The EML-4 has not the advantage of the Moon to attract the satellite and force it in an orbit around it. This means that no patched-conic strategy can be used. For the EML-4 target the satellite has to fill the described transfer sequence and after the last maneuver it has to be within an adequate distance to EML-4. If it is not the case, the Julian start date can be corrected until this condition is met. With further adjustment of the start date the plane change maneuver at (3) can occur near to the transfer apoapsis, where the maneuver is more efficient.

The satellite is modeled in GMAT with data for the propulsion system, the satellite dry mass and propulsion mass. The finite burn maneuvers require the data input for thrusters and masses so that the mass decrement is simulated and the adequate velocity changes during the maneuver times can be determined. For this, parameters for thrust and the initial specific impulse (ISP) and the satellite launch mass are used.

Table 28 shows a selection of available apogee kick motors as a basis for the simulation. EADS EAM 500N, HiPAT 445N and S400-12 420N are used for the trade-off to find a suitable main thruster system for the TMA-0 satellite. During the concept study the result of the simulation as well as further parameter like propellant combination and heritage are criteria for the thruster selection.

The transfer simulations include satellites with the thrusters EADS EAM 500N, HiPAT 445N and S400-12 420N. This corresponds with the three classes of thruster levels available on the market (500-490N, 450-445N and 425-420N). The ISP still differs according to the thruster and used propellant combination. This indicates that the delta-v needed for the transfer is sensitive to the chosen propulsion system.

Table 28: Apogee kick motors

Model-Name	Manufacturer	Application	Prop F/O	Thrust	ISP
EAM	EADS	Alphabus, Spacebus, Eurostar, SGEO	MMH / MON	500 N	325 s
R-4D, R-4D-11	Aerojet	HTV 1,2,4, ATV	MMH / MON	490 N	315 s
HBT-5	IHI	HTV 3,5,6,7	Hydrazine / MON	450 N	329 s
HiPAT 445N	Aerojet		MMH / MON	445 N	323 s
HiPAT 445N Dual Mode	Aerojet		Hydrazine / MON	445 N	329 s
Liquid Apogee Engine	Thales Alenia		MMH / MON	420 N	318 s
S400-12	EADS	SYMPHONIE, THOR-6	MMH / MON	420 N	318 s
S400-15	EADS	SYMPHONIE, THOR-6	MMH / MON	425 N	321 s

[89] [90] [91] [92] [93] [94] [95]

Moreover the satellite wet launch mass is analyzed for three options. The three options are 1500 kg, 2300 kg and 3100 kg. The mass classes are chosen according to limitations of possible launchers. The 3100 kg option is conform with the secondary payload transfer option onboard of Ariane 5 ECS (around 3300 kg) or for the dedicated launch option of Soyuz with a launch from Kourou, French Guiana (3200 kg) [96] [77] and others. The maximum mass of 3100 kg is also chosen in preparation for the TMA-1 mission so that the simulation results and the launcher selection are directly influencing the launcher selection. The minimum analyzed mass of 1500 kg reflects the capacity of Soyuz with launch site in Baikonur, Kazakhstan (1400 – 1800 kg depending on the demanded inclination) or of Tsyklon (1600 – 2000 kg) [78]. However the minimum mass is considered as the technological lower limit and thus the next mass step is set to 2300 kg. For all of these launch masses, launcher options will be described in detail in Chapter 4.1.

The thruster and wet launch mass properties are used in combination for the simulation. In this way the selection is more flexible when the following design decisions will lead to an excess of one thruster's performance. The selection process can then decide to take another thruster or to proceed to the next launch mass level. The results are presented in Table 29 to Table 31.

Table 29: Thruster performance - delta-v and satellite masses for direct transfer

Direct Transfer (highest apoapsis 400000 km)							
Thrust [N]	ISP [s]	Raising Orbits [-]	Mass0 (start) [kg]	Mass1 (end) [kg]	Delta-V [m/s]	Transfer Time [d]	Injection Distance [km]
420	318	6	1500	801	1954	35.9	4291
			2300	1238	1930	36.5	9499
			3100	1656	1954	36.4	2989
445	323	6	1500	813	1939	35.7	351
			2300	1268	1885	37.0	33940
			3100	1697	1908	36.9	12176
500	325	6	1500	811	1959	35.9	1892
			2300	1312	1787	36.2	12618
			3100	1683	1946	36.4	645

Table 30: Thruster performance - delta-v and satellite masses for bi-elliptical transfer

Bi-Elliptic Transfer (highest apoapsis 680000 km)							
Thrust [N]	ISP [s]	Raising Orbits [-]	Mass0 (start) [kg]	Mass1 (end) [kg]	Delta-V [m/s]	Transfer Time [d]	Injection Distance [km]
420	318	6	1500	818	1888	71.0	8315
			2300	1260	1877	85.2	6745
			3100	1709	1857	85.3	3098
445	323	6	1500	826	1889	71.1	10161
			2300	1271	1877	85.3	8856
			3100	1715	1874	84.4	5793
500	325	6	1500	828	1894	71.4	11159
			2300	1275	1879	85.6	10082
			3100	1721	1874	84.8	8022

Table 31: Thruster performance - delta-v and satellite masses for weak stability boundary transfer

Weak Stability Transfer (highest apoapsis 960000 km)							
Thrust [N]	ISP [s]	Raising Orbits [-]	Mass0 (start) [kg]	Mass1 (end) [kg]	Delta-V [m/s]	Transfer Time [d]	Injection Distance [km]
420	318	6	1500	932	1482	89.6	3350
			2300	1436	1468	89.8	7534
			3100	1938	1463	89.6	13285
445	323	6	1500	938	1484	89.7	4808
			2300	1446	1469	89.6	25321
			3100	1953	1463	89.7	2415
500	325	6	1500	940	1489	89.6	4246
			2300	1448	1475	89.7	3836
			3100	1955	1469	89.8	11989

Table 29 to Table 31 show the simulation results for the satellite mass at the end of the transfer Mass1 and the needed delta-v for all three transfer options. The transfer is accepted when the injection of the satellite in the target orbit takes place within a distance of less than 45000 km to EML-4. The transfer start was set according to this condition. The WSB transfer offers again the delta-v efficient transfer but also has the longest transfer time with 90 days. This is only about 5 days (6%) longer than the bi-elliptical transfer but offers about 410 m/s of saved delta-v (22%).

It is also obvious that the simulation is influenced by the starting day of the transfer. Although the majority of the results in each transfer option lie in the same range of delta-v, there are exceptions. In Table 29 for the thruster with 500 N and the satellite mass of 2300 kg the delta-v is 1787 m/s although all the other values are around 1950 m/s. For this particular simulation the start date was postponed for two days to meet the injection distance. This led to a closer Moon fly-by with additional gravitation pull that influenced the trajectory. In general the small variations in delta-v are due to small perturbations during the transfer, the accuracy of injection and the simulation and their numerical errors.

The results of the ideal and simulated transfers with respect to the needed delta-v of the EAM 500 N thruster for the 3100 kg satellite is presented in Figure 34 confirms the trend, but also the influence of the simulation, that includes several perturbations and a full n-body simulation. These influences are not included in the ideal calculation. So the magnitude of these parameters and for example the midcourse correction maneuver can be responsible for the difference. The interpretation of the delta-v for the WSB transfer includes the smaller delta-v consumption of the simulation because the plane change is supported by the Sun's gravity as expected.

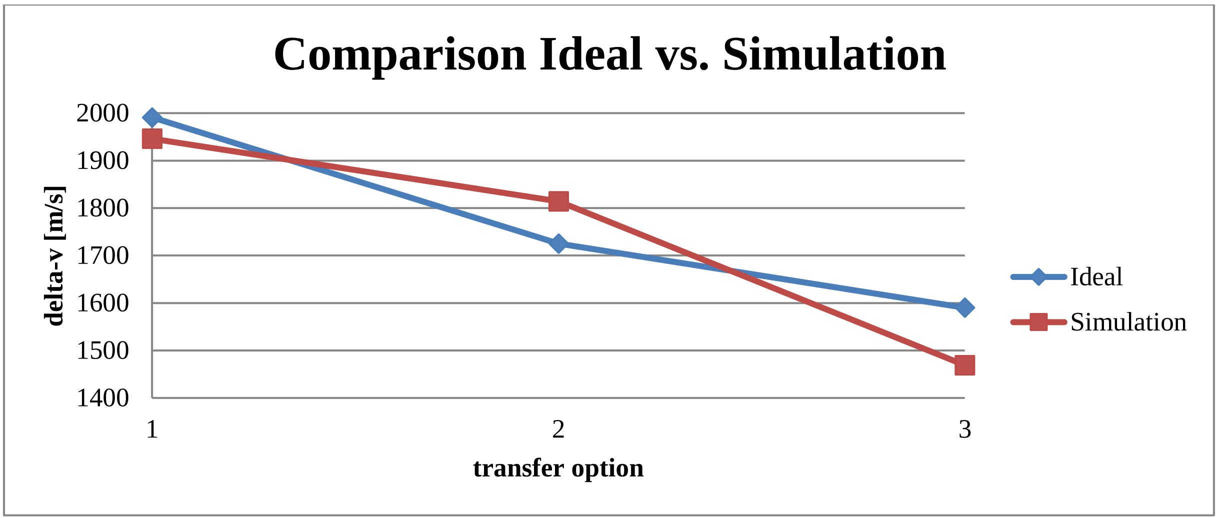

Figure 34: Comparison of the results of the ideal and the simulated transfer options
(1) direct, (2) bi-elliptical and (3) WSB transfer

For the following mission orbit around EML-4, the satellite masses at the end of the transfer with the EAM 500 N thruster are used (bolded in Table 31). The thrusters offer the highest satellite masses (Mass1) injected into the target orbit of all three initially launched satellite masses (Mass0). However the mass advantage compared to the other two thrusters is only in the range of a few kilograms.

4.2.3 Libration Mission Orbits

The last transfer maneuver inserts the spacecraft into the libration mission orbit. The orbit requires orbit keeping to stay the maximum allowed distance to the EML-4 point and also additional maneuvers to change the orbit for specific tasks of the demonstrator mission. The libration mission orbit is important for the communication position. The optimum position is exactly on the EML-4 point to meet the requirement of the fixed position with respect to the Moon and the Earth. Due to external perturbation or because the mission requires it, displacement away from EML-4 occurs. The relative movement around the EML-4 has to be limited to stay within the allowed region that allows the simple connection from the targets to the TMA-0 satellite and in order not to drift away from the EML-4 position.

Two station keeping maneuver strategies are tested with GMAT. The first strategy (1) lets the satellite propagate from the exact or near EML-4 position until it reaches the $y = 0\,m$ position in the rotating libration point frame (Figure 35). Then GMAT finds the thrust vector compatible to the spacecraft propulsion system that will allow the next periapsis to be also at $y = 0\,m$ and with the condition of $v_x = 0\,m/s$. This will lead to orbits around EML-4 as long as the orbit correction maneuvers take place. This strategy is simple and let the satellite propagate without further restrictions between the mentioned axis passages.

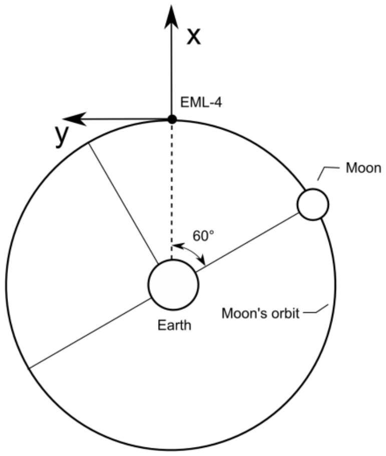

Figure 35: Co-rotating frame of reference with frame origin in EML-4

The second strategy (2) tested was to keep the satellite within a certain radius from EML-4. A simple phase-space control was coded for GMAT controlling the satellite radial velocity $\dot{r}$ to stay within a allowed radius r to EML-4. GMAT proved to be not suitable for the phase-space control of the orbital fine control because the accumulated delta-v budget exceeded the expected range of annual 100 m/s after 30 days.

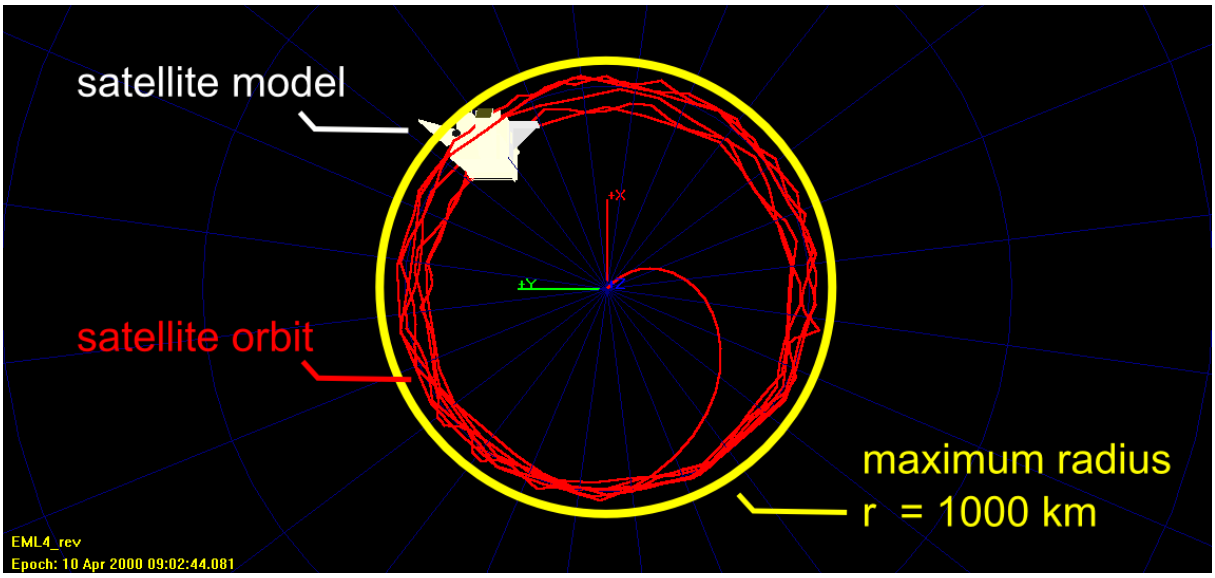

Figure 36: Phase-space control for a zone with maximum radius of 1000 km around EML-4

4.2.3.1 In- and Out-of-Plane

The advantage of the EML-4 position in comparison to the EML-2 position is that satellites can orbit on the same plane as the Moon while having direct line-of-sight to Earth. So the simulations are modeled for orbits in-plane. Indeed it is still possible to use out-of plane orbits that will allow other coverage conditions to the lunar pole areas and still benefit from the stability of the EML-4 position. There are Trojan asteroids in the Sun-Jupiter system that are inclined up to 40° and are long-time stable [20].

The station keeping strategy (1) is applied for out-of planes orbits with inclinations until 10°. The simulation shows that it can also be controlled (Figure 37 and Figure 38). The orbit starts to follow a more chaotic trajectory that is more difficult to determine. The satellite position is required to be fixed and/or easily predictable so that targeting from the user to the relay is simple. For the mission in-plane orbits and out-of-plane orbits with small inclinations of maximum 1.15° are considered. This still allows orbits that have an out-of-plane z-amplitude of 8000 km that is also used for the EML-2 halo orbit comparison in Chapter 3.2.3.1 [97]. With respect to the Moon this would mean a variation in position of the relay of also 1.15°.

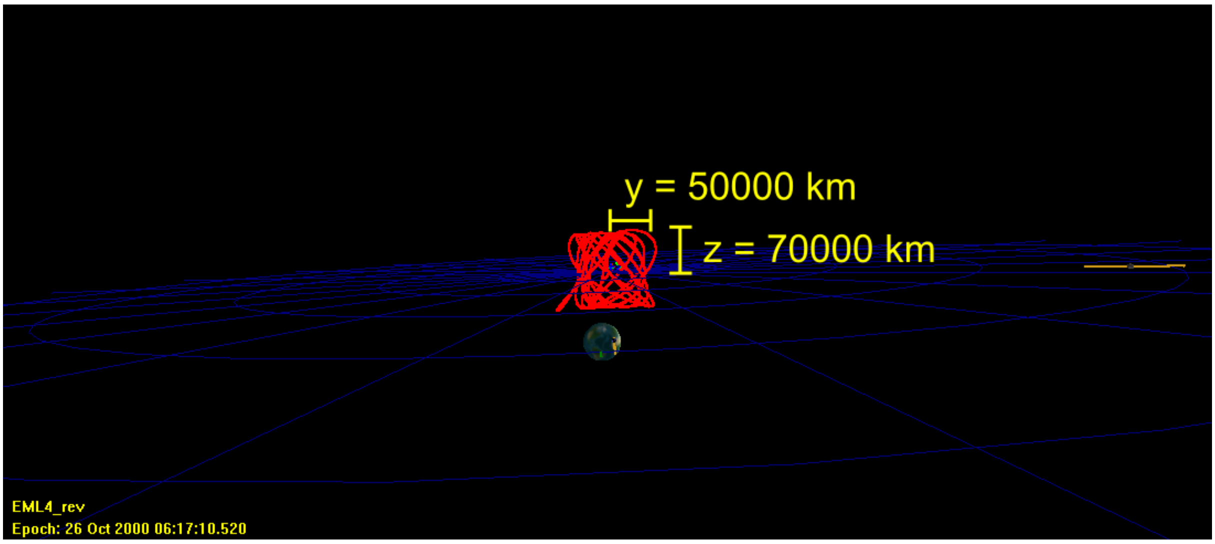

Figure 37: EML-4 out-of-plane orbit seen from Earth (orbit inclination = 10°)

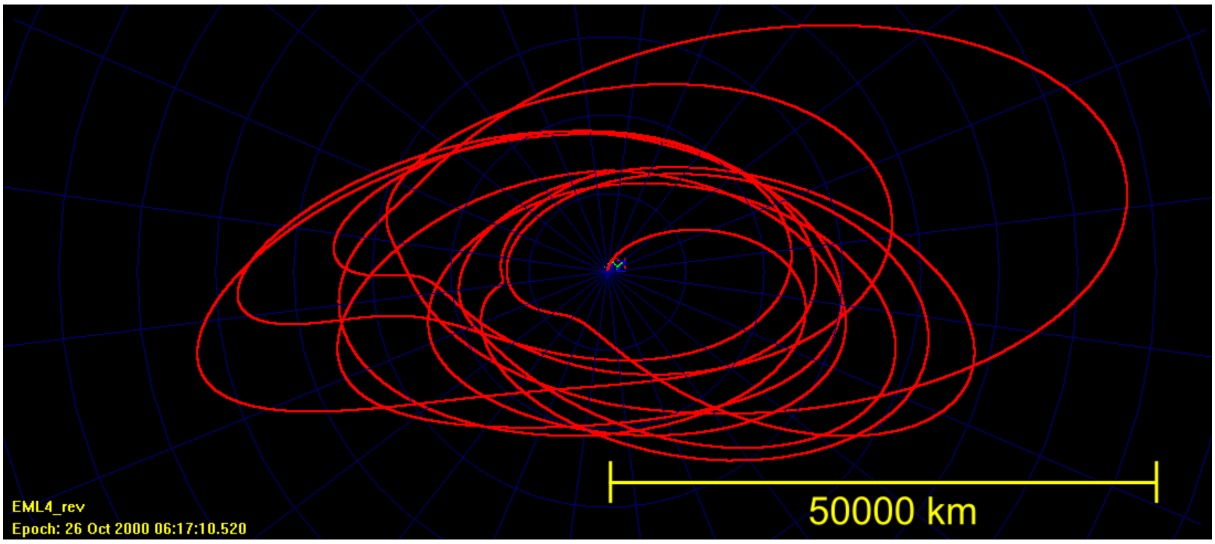

Figure 38: EML-4 out-of-plane orbit seen from z-direction (orbit inclination = 10°)

4.2.3.2 Station Keeping Orbit Simulation

The station keeping orbit is analyzed for two initial satellite positions. The first station keeping orbit begins directly in the EML-4 point. The second position uses the previously simulated injection position at a distance from EML-4 with 11989 km for the satellite with the EAM 500 N thruster and satellite launch mass of 3100 kg. Both simulations shall show the behavior of the satellite in and around EML-4 position.

For the station keeping common customary AOCS thrusters are analyzed (Table 32). For the simulation the Aerojet MR-111C and the EADS 22 N Bipropellant Thruster are used. The MR-111C represents the typical 4 N thruster segment and the mono-propellant system with the highest ISP. The EADS 22 N thruster represents the bi-propellant system with a European heritage and the upper level of ISP range. This provides candidate options for further decisions for the orbit maneuvers, in the propulsion system and purchase flexibility.

Table 32: Thrusters for attitude and orbital control

Model-Name	Manufacturer	Propellant F/O	MIBIT	Thrust	ISP
MR-103G	Aerojet	N2H4	13.3 mNs @15 ms	1 N	224 s
MR-103M	Aerojet	N2H4	0.7 mNs @1.6 ms	1 N	221 s
1 N Thruster	Thales Alenia	N2H4		1 N	221 s
1 N Thruster	ihi	N2H4	4-24 mNs @20 ms	1 N	222 s
1 N Thruster	Astrium	N2H4	10 mNs @10 ms	1 N	220 s
4 N Thruster	ihi	N2H4		4 N	225 s
MR-111C	Aerojet	N2H4	80 mNs @15 ms	4 N	229 s
4 N Bipropellant Thruster	EADS	MMH / MON	42 mNs @10 ms	4 N	285 s
10 N Bipropellant Thruster	EADS	MMH / MON	60 mNs @10 ms	10 N	291 s
10 N Thruster	Thales Alenia	MMH / MON		10 N	287 s
20 N Thruster	ihi	N2H4		17.6 N	236 s
22 N Thruster	ihi	MMH / MON		21.5 N	295 s
22 N Bipropellant Thruster	EADS	MMH / MON	90 mNs @10 ms	22 N	290 s
R-6D	Aerojet	MMH / MON	8.9 mNs @5ms?	22 N	294 s
MTT	Aerojet	MMH / MON	44 mNs @?	22 N	284 s
R-1E	Aerojet	MMH / MON	890 mNs @?	110 N	280 s

[91] [93] [98] [99] [100] [101] [102] [103] [104]

The direct injection into EML-4 (0) occurs with the conditions of $v_x = v_y = v_z = 0\ m/s$ in the rotating reference frame (Figure 35) that is placed in the libration point and the x-axis always pointing away from the Earth. Due to the permanent position change of the Earth and the Moon as seen in Figure 39 and Figure 40 the EML-4 also moves.

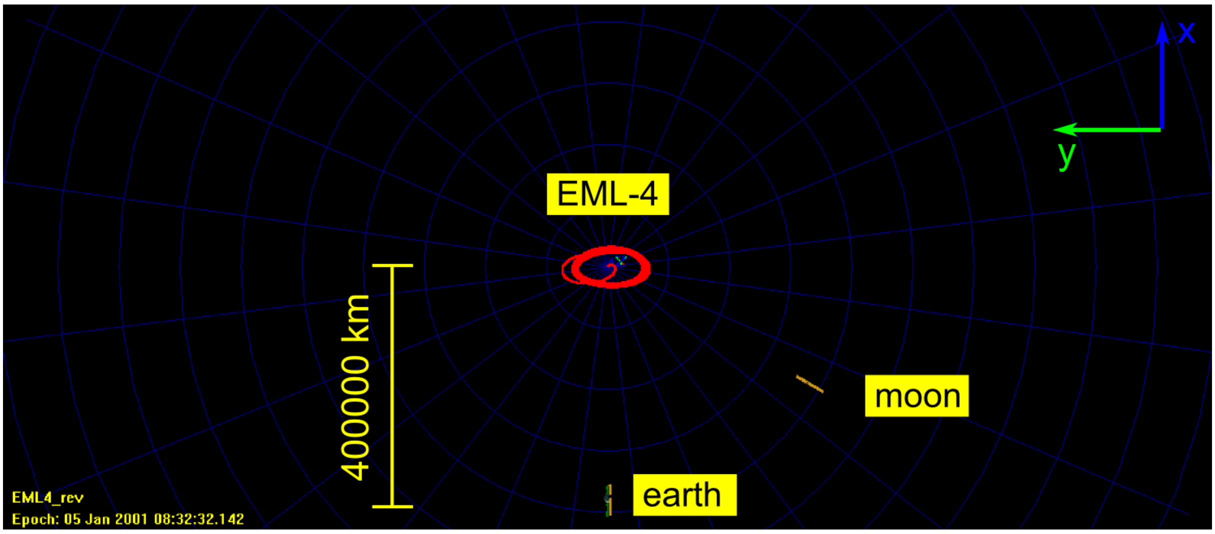

Figure 39: Station keeping orbit after direct injection into EML-4

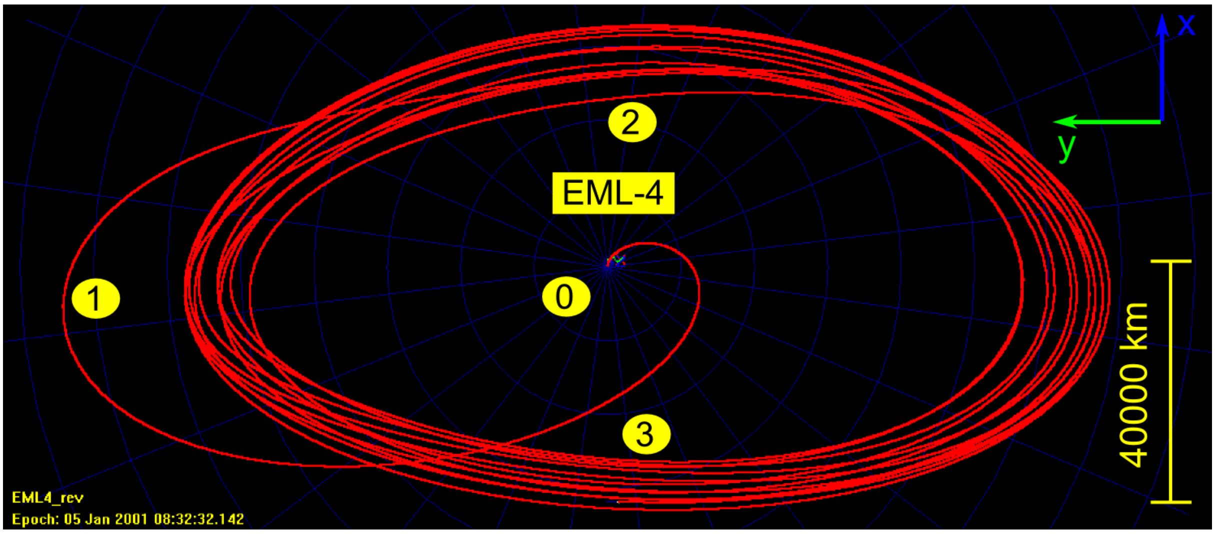

Figure 40: Station keeping orbit after direct injection into EML-4, zoomed

With respect to TMA-0 EML-4 moves away introducing a restoring force acting on the satellite generating acceleration. A trajectory around EML-4 is induced (1). In the inertial reference frame of the Earth the satellite orbit changes the eccentricity and the satellite drifts around the EML-4 position, which is shown in detail in the reference frame of EML-4 in Figure 40. The satellite now propagates to the apoapsis (2) and until the axis transition condition of $y = 0\,km$ is reached at periapsis (3). The GMAT simulation now varies the thrust vector by altering it components under the condition of $v_x = 0\,m/s$, which will allow another apoapsis and periapsis propagation (2-3). This sequence is then repeated.

The real thrust maneuver requires orbit determination of the position and velocity. A control law for the thrust vector control of the satellite is applied that compares the state with the set point values. The attitude of the satellite is changed and thus the direction of the thrust provided by the engine to minimize the difference between state and set point values.

The analyzed trajectories for satellites with different masses show the behavior that the satellites' trajectories stay within a ring area and near to the EML-4 orbit plane. This is due to the initial velocity components of the satellite and the changing position of the Earth and the Moon. The latter is the biggest perturbation influence as presented in Chapter 3.2.3.5 and it confirms the statement of Folta and Vaughn in "A Survey of Earth-Moon Libration Orbits: Station keeping Strategies and Intra-Orbit Transfers" [47]. The station keeping strategy keeps the TMA-0 satellite within a radius of about 60000 km for a simulated period of 10 years. This radial distance is above the specified distance of 45000 km and a shorter distance of smaller than 10000 km is preferred. A more efficient orbit keeping strategy shall be found in the following study.

The same station keeping strategy is applied after the simulated TMA-0 satellite is injected (0) within a distance of 11989 km to the EML-4 point (1) (Figure 41 and Figure 42). For the first revolutions on orbits around EML-4 the distance is better than before and staying within the allowed 45000 km range (2), but the Earth and Moon induced perturbations and the numerical method for the station keeping control leads to a drift-away of the satellite (3) until it also reaches the distance range as seen for the direct EML-4 injection simulation (4). Such orbits also showed a behavior of contraction and expansion as described in Folta and Vaughn [47]. The epicycle movement of the satellite around EML-4, that cannot be observed for ideal simulations with a circular Moon orbit (Chapter B.1 and "Astronautics" [19]), is observed.

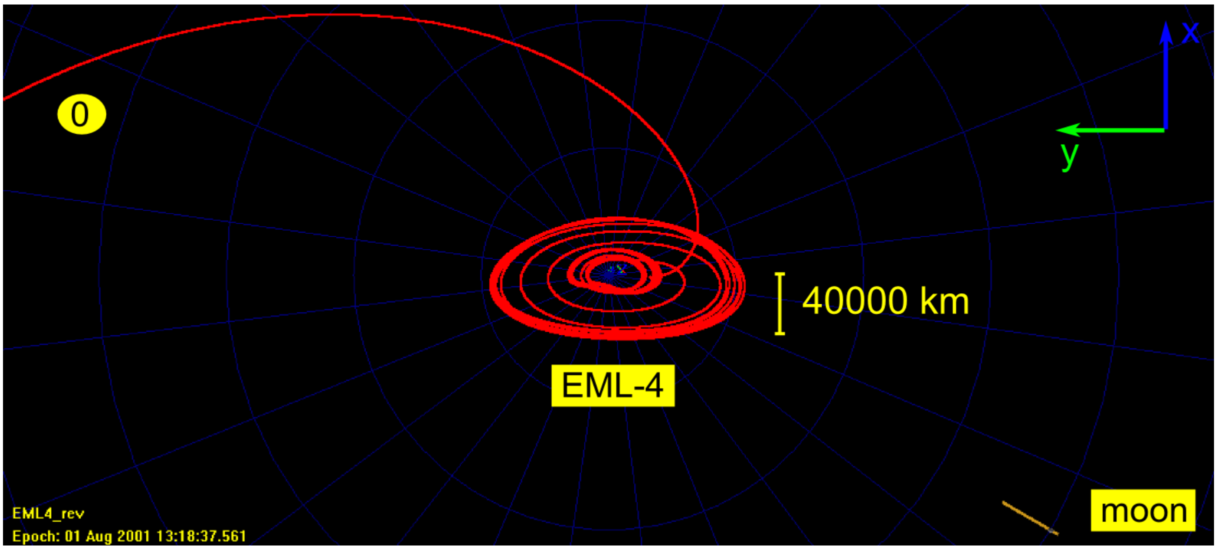

Figure 41: Station keeping orbit after injection within a distance to EML-4

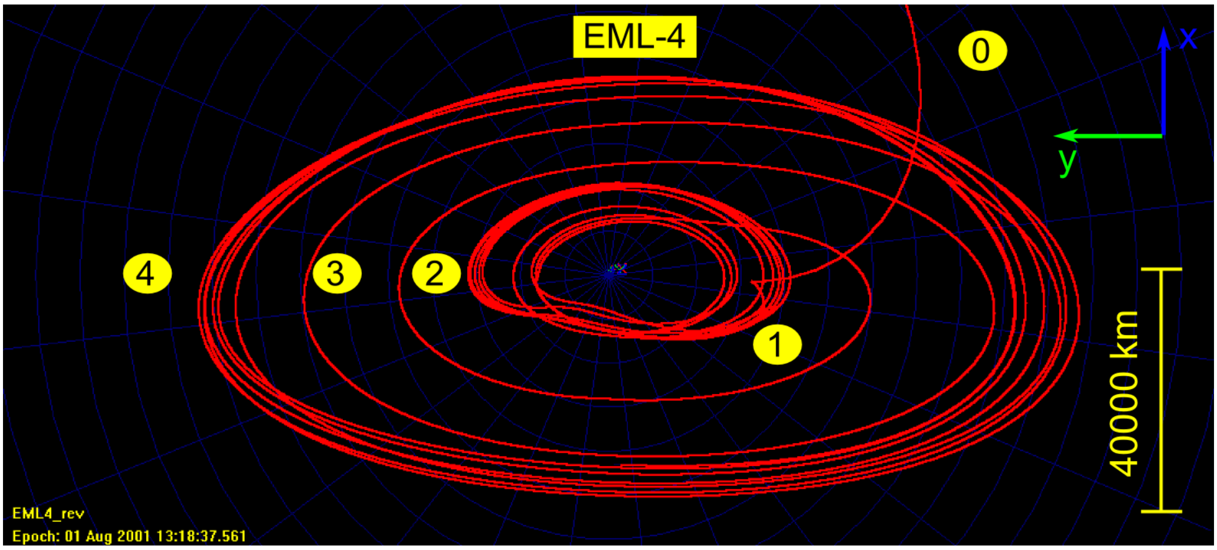

Figure 42: Station keeping orbit after injection within a distance to EML-4, zoomed

4.2.3.3 EML-4 Orbit Stability

When the TMA-0 satellite propagates freely without station keeping maneuvers that will keep it in the vicinity of EML-4 the external perturbation affects the satellite's trajectory and let the satellite drift-away from EML-4.

The mission time of three years (1095 days) are simulated without station keeping maneuvers and Figure 43 shows the satellite movement from the initial EML-4 position. The varying perturbation changes the satellite's orbit eccentricity in a pulsating way and increasing the distance to EML-4. Even though the EML-4 offers the benefit of stability, the satellite needs to have a station keeping strategy and chemical or electrical thruster systems. Furthermore the uncontrolled drift with expanding region around EML-4 bears the possibility to let the satellite return to the Earth or to bring it to the Moon. The required disposal phase shall avoid both uncontrolled trajectories and possible threats to Earth or satellites.

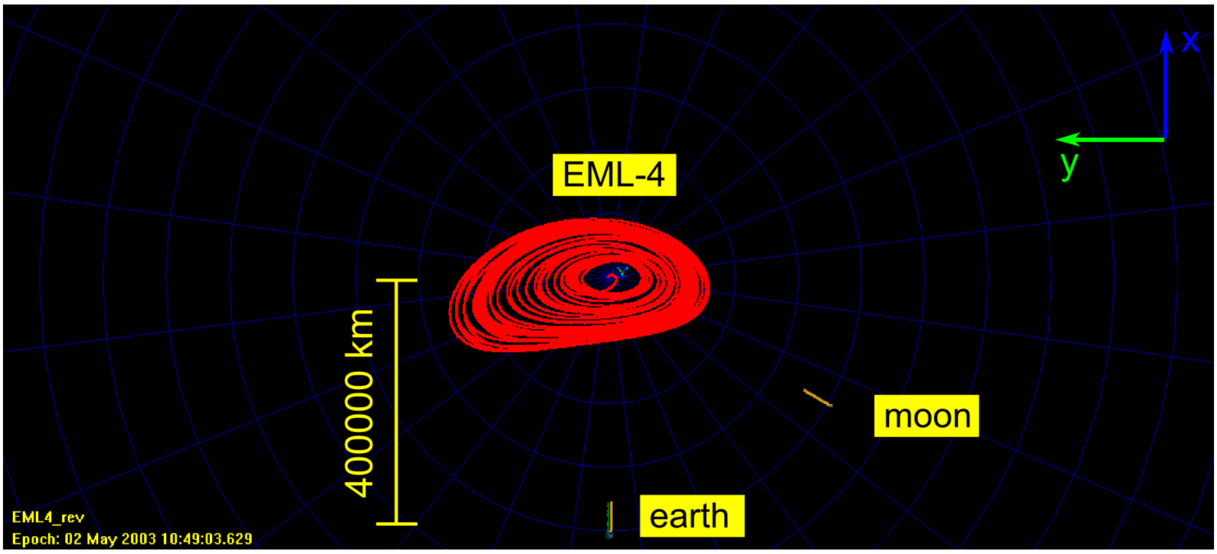

Figure 43: TMA-0 satellite propagation without station keeping maneuver for 1095 days

4.2.3.4 Station Keeping Orbit

The simulated station keeping trajectories left the allowed distance to EML-4 of 45000 km and GMAT does not offer a full feedback control needed for the phase-space control to proper model a more effective orbit control. For this reasons the station keeping orbit for TMA-0 is considered with the yearly delta-v budget of “A Survey Of Earth-Moon Libration Orbits: Stationkeeping Strategies and Intra-Orbit Transfers” by Folta and Vaughn [47].

For the simulations of the non-utilized station keeping strategies and for the following delta-v budget calculations, the Aerojet MR-111C 4 N mono-propellant and EADS 22 N bi-propellant thrusters are chosen (Table 32). The mono-propellant offer a simple design and usage in a dual-mode propulsion system (combined bi-propellant and mono-propellant thrusters). The bi-propellant thruster offers a higher efficiency and ISP. Both minimum impulse bit (MIBIT) are in the same region.

Table 33 and Table 34 give a comparison between Lissajous and halo orbits around EML-2 and in-plane orbits around EML-4 [47]. EML-4 offer less delta-v yearly costs (except for the first small lissajous orbits). The initial radiuses of the three EML-4 orbits are used for further purposes (e.g. Field-of-View analysis) and for the delta-v budget for the three year mission of TMA-0. Therefore the best case with 29 m/s and the worst case with 57 m/s delta-v are used.

Table 33: Station keeping yearly costs of EML-2 orbits

Orbit Location & Control	**Method**	**Station Keeping Yearly Costs (m/s)**			
		Small Lissajous	**Small halo**	**Large Lissajous**	**Large halo**
L2 x axis	M1	26.13	305.07	198.06 (213 days)	316.21
L2 y axis	M1	41.90	279.80	58.50 (111 days)	397.83
L2	M2	60.87	61.00	59.88	59.86

M1: differential correction station keeping yearly cost with navigation and solar radiation pressure (SRP), and delta-v errors

M2: discrete linear quadratic regulator (dLRQ) station keeping yearly cost

Table 34: Station keeping yearly costs of EML-4 orbits

	Station Keeping Yearly Costs (m/s)			
Initial Conditions Relative to L4 [km]	At L4 (0,0,0)	(5000,5000,0)	(10000,10000,0)	(45000,45000,0)
Station Keeping Δv	30.00	29.00	57.00	31.00

The decrement of satellite mass is calculated for both cases and for both chosen thrusters [105]. It includes the thrust *F* and *ISP* of the thrusters and the standard gravity g_0.

$$\dot{m} = \frac{F}{ISP\ g_0} \quad 4.14$$

With the exit velocity v_{exit} of the thruster exhaust gases and the general rocket equation (Tsiolkovsky rocket equation) with the given delta-v Δv, satellite initial mass before ignition m_1 the satellite mass after the station keeping phase m_2 is yielded.

$$F = \dot{m} * v_{exit} \quad 4.15$$

$$\Delta v = v_{exit} * ln\left(\frac{m_1}{m_2}\right) \quad 4.16$$

Table 35 shows satellite masses (Mass2) for the three satellite mass classes (1500 kg, 2300 kg, 3100 kg) after three years considering

- for the best and worst case station keeping orbit
- for initial satellite masses of all the transfers.

Table 35: Satellite masses after station keeping of three years for best & worst case of two thrusters

		ISP			
		229 s		**290 s**	
		29 [m/(s*a)]	**57 [m/(s*a)]**	**29 [m/(s*a)]**	**57 [m/(s*a)]**
#	**Mass1 [kg]**	**Mass2-1 best [kg]**	**Mass2-1 worst [kg]**	**Mass2-2 best [kg]**	**Mass2-2 worst [kg]**
19	933	897	864	904	878
20	1436	1381	1331	1393	1352
21	1938	1864	1796	1880	1825
22	939	903	***870***	910	884
23	1446	1391	***1340***	1402	1361
24	1953	1878	***1809***	1894	1839
25	940	904	871	911	885
26	1454	1398	1347	1410	1369
27	1955	1880	1811	1896	1840

Note: Table 35 is shortened. Full list is presented in Table 101

The satellite masses *#22-24 (bolded)* are used because it is derived from the chosen WSB transfer (Chapter 4.2.24.2.1) offering the highest satellite mass reaching the target orbit (Mass1). Furthermore it is the middle value of the three kick motors that still allows taking the second apogee kick motor, Aerojet HiPAT 445N (Table 28). The chosen three end masses (Mass2) by HiPAT 445N are also the lowest because they are derived for the worst case of the AOCS thruster with the lower ISP. This marks the lower satellite mass for the design.

Baseline:

AKM:	EADS EAM 500 N bi-propellant thruster
AOCS Thrusters:	EADS 22 N bi-propellant thruster
Satellite dry Mass:	1446 kg to 1340 kg
Station Keeping Orbit:	10000 km distance to EML-4

4.2.4 End of Life Transfer

After the operational phase E a disposal plan for TMA-0 is mandatory according to European Cooperation for Space Standardization ECSS–M–30A [106]. Removing the satellite from the operational position makes room for successor missions in the same orbit area and also decreases the possibility of debris production caused by collisions between other space debris or other objects with the defunct TMA-0. A space debris free EML-4 orbit is taken serious for future usage of this valuable position. At the orbit altitude and due to the stable position of this potential field area a self-cleaning effect is not effective [86].

Four disposal scenarios were analyzed and will be discussed in the following: back to Earth, graveyard behind Moon orbit, out of Earth's SOI and lunar Impact.

1. Back to Earth

A back to Earth transfer involves a maneuver that will lower the periapsis to reach into the Earth's atmosphere. This is a rather delta-v intensive maneuver of about 1500 m/s delta-v. During the transfer the TMA-0 satellite transits all technical and operational orbits (from GEO to LEO) and a chosen trajectory has to include an analysis of possible close encounters with other spacecraft. Moreover the satellite has to be disposed in an unpopulated or low populated region or ocean area. The targeting and correction maneuvers are complex and the timing is important. With respect to the high delta-v, the technical and human risks and due to insurance reasons the back to Earth strategy is not selected.

2. Graveyard behind Moon orbit

A proven method for GEO satellite is the transfer to a graveyard orbit. For GEO the graveyard orbit lies above the synchronous orbit with a distance of minimum 235 kilometers [107]. In this zone (sometimes also called supersynchronous orbit, junk orbit or disposal) the satellites are decommissioned. The delta-v required for this transfer is about 11 m/s. The international telecommunication union (ITU) recommends and the federal communications commission (FCC) requires satellites in GEO orbit to be carried out into the graveyard orbit by this code of conduct agreement. The satellite decommission shall be carried out avoiding RF interference with active satellites and by releasing as little space debris as possible into GSO [108]. For the EML-4 orbit a graveyard orbit is not defined yet.

The minimum distance for the GEO graveyard orbit varies depending on the agency. If the same minimum distance of about 235 km as proposed by ITU/FCC is used for the higher EML-4 graveyard orbit, it still lays within the EML-4 region. All the perturbations are acting on the now defunct satellite and an uncontrolled drifting around EML-4 will take place as seen in Chapter 4.2.3.3. This uncontrolled movement within the EML-4 zone should be avoided.

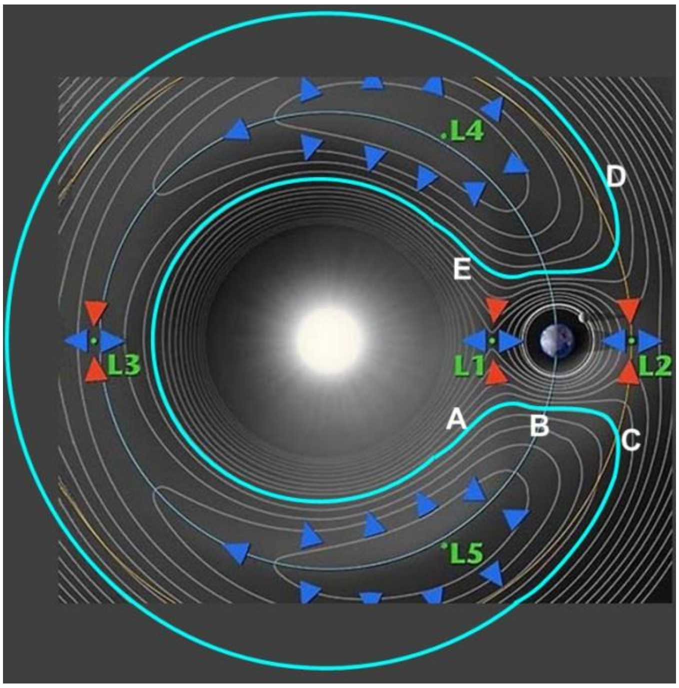

Figure 44: Satellite in uncontrolled horse-shoe orbit (A-E) [109]

If the satellite is transferred in an even higher orbit outside the EML-4 zone, the satellite will phase on this orbit and can drift towards the Moon. Then it can either be attracted to crash land on it, or swing-by and leave the Earth-Moon system or even enter a horse-shoe orbit. The horse-shoe orbit is a special kind of orbit as seen in a rotating reference frame of a restricted three-body system. The satellite periodically approaches within a closer distance (Figure 44). Without a defined graveyard orbit for EML-4 and the possible Earth approach this option is also not applicable for TMA-0.

3. Beyond Earth's Sphere of Influence

Leaving the Earth-Moon system is a solution that does not include several uncontrolled close Earth fly-bys. This either means leaving the SOI in a direct transfer with more delta-v or with the additional support of a lunar swing-by for a transfer with less delta-v. This also offers the option to use the satellite as an interplanetary probe for dust or other scientific measurements even after the expected mission time as long the satellite is operational.

For this operation phase new requirements arise for planetary protection. The planets and Moons in the solar system are protected by the UN Outer Space Treaty [110]. Missions to those planets have to fulfill certain standards of biological cleanliness and further conditions according to the category of the targeted celestial body. These regulations are set to avoid organic-constituent and biological contamination by the spacecraft [111]. In case the TMA-0 satellite mission contains an interplanetary trajectory with the chance of being attracted on the surface the requirements of cleanliness rises above category one, which would apply for lunar missions. The trajectory can be analyzed and prepared to avoid close fly-bys to other planets. The effort for the trajectory and cleanliness is disproportionate to the main mission. So this disposal transfer is not favorable.

4. Lunar Impact

The optimal solution with respect to delta-v and space debris mitigation is the graveyard on Moon scenario (Figure 45 and Figure 46). It requires less delta-v for the disposal and it takes out TMA-0 as a possible source of new space debris by disposing it on the Moon. Planetary protection is regulated by the UN Outer Space Treaty [110] and it classifies the Moon as Category I. A disposal is allowed with the lowest level of satellite sterilization during final ground assembling in mission phase D. Nevertheless precautions have to be made to target a lunar area away from historical landing sites such as Apollo and lunar remote explorations [69]. These can be considered as world heritage sites and have to be protected by man-made influences. And in consideration of the TMA-1 mission the target site has also be away from major sites of scientific interest.

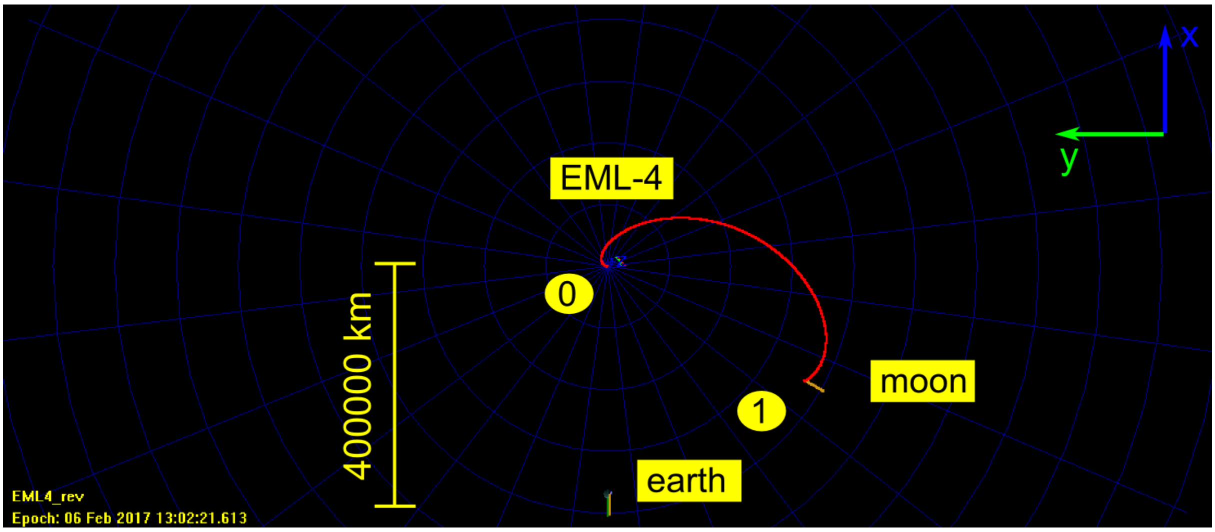

Figure 45: End-of-life transfer to the Moon in EML-4 rotation reference frame

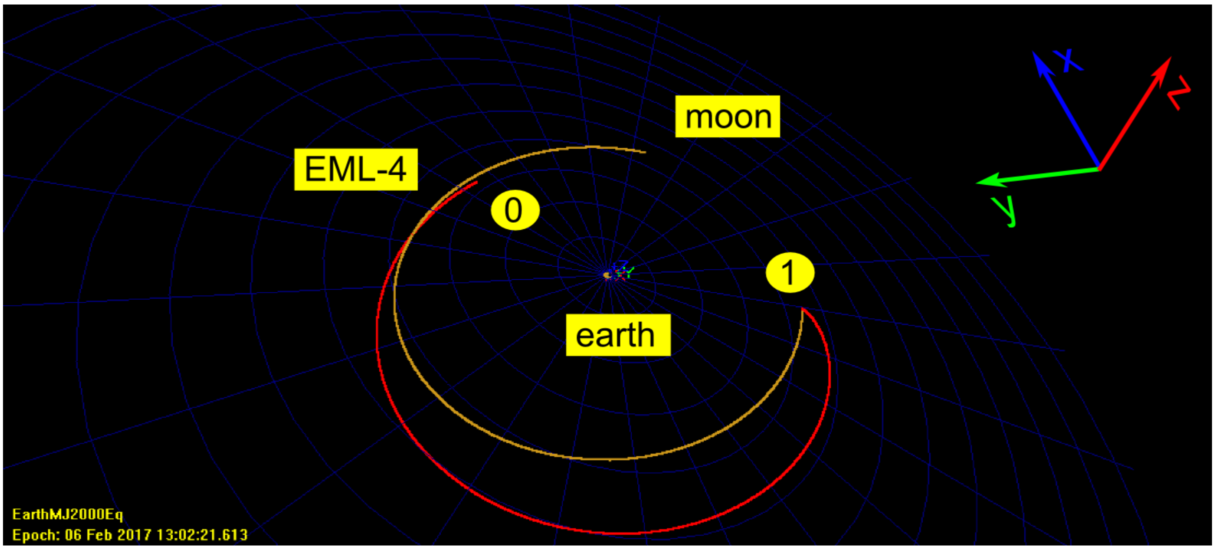

Figure 46: End-of-life transfer to the Moon in Earth inertial J2000Eq reference frame

The end-of-life (EOL) transfer of TMA-0 is simulated with GMAT from an initial position on EML-4 (0). The finite thrust maneuver is applied as a phasing orbit that raises the apoapsis and TMA-0 is transferred to the Moon within the next periapsis passage (1). The timing and apoapsis radius of the phasing orbit is important for the targeting. They allow a targeted crash landing on the Moon (Figure 45 and Figure 46).

The simulations include an analysis of the crash landing and lunar swing-by transfer. The simulated satellite achieved the distance of 1700 km and 3000 km from the Moon’s center of gravity. The first condition respects the lunar surface distance and the second allows a swing-by trajectory. The results show that the amount of delta-v for a crash landing on the Moon and for lunar swing-by is almost the same for all satellite initial mass classes and thrusters (Table 36). So both transfers are possible without major changes.

Table 36: Satellite delta-v consumption for the disposal options Moon Impact and Lunar Swing-by

		Moon Impact			**Lunar Swingby**		
		4N/229s	**22N/290s**	**500N/325s**	**4N/229s**	**22N/290s**	**500N/325s**
#	**Mass2-1 worst [kg]**	**DeltaV-3-1 [m/s]**	**DeltaV-3-2 [m/s]**	**DeltaV-3-3 [m/s]**	**DeltaV-3-4 [m/s]**	**DeltaV-3-5 [m/s]**	**DeltaV-3-6 [m/s]**
22	870	49.83	49.68	50.03	51.67	51.51	51.48
23	1340	49.93	49.69	49.65	51.78	51.53	51.48
24	1809	49.70	49.71	49.64	51.88	51.55	51.48

With this transfer the final mission orbit is accomplished and the satellite’s dry mass is determined. This dry mass of the satellite with the “4N/229s“ thruster is used for conceptual design because represents the worst case dry mass (Table 37).

Table 37: Satellite masses after disposal options Moon Impact and Lunar Swing-by

		Moon Impact			**Lunar Swingby**		
		4N/229s	**22N/290s**	**500N/325s**	**4N/229s**	**22N/290s**	**500N/325s**
#	**Mass2-1 worst [kg]**	**Mass3-1 [kg]**	**Mass3-2 [kg]**	**Mass3-3 [kg]**	**Mass3-4 [kg]**	**Mass3-5 [kg]**	**Mass3-6 [kg]**
22	870	851	855	856	850	854	856
23	1340	1310	1316	1319	1309	1315	1318
24	1809	1770	1778	1781	1768	1777	1780

The following mass budget for the satellite system Table 38 is created with respect to the three satellite mass classes. The maximum satellite dry mass is determined by the propellant masses for each phase (transfer, station keeping, end-of-life). The propellant masses include design maturity mass margins and propellant residuals according to the Margin Philosophy for Science Assessment Studies (SCI-PA/2007/022/) [112]. The 2% propellant residuals are not part of the other margins and are included to model the unburned and remaining propellant in the tanks and pipe-work.

The dry masses in Table 38 will be further analyzed in the overall system mass budget in Chapter 4.4.8. In there, additional masses like for the launch adapter and the 20 % system margin to respect the launcher performance are included further reducing the usable satellite dry mass for the satellite system and subsystem design. If one satellite wet mass reaches the next higher launch mass class, the next higher mass class is used for the design.

Table 38: TMA-1 dry & propellant masses for three satellite classes derived from propellant masses

Launch Mass [kg]	1500		2300		3100	
	Best [kg]	**Worst [kg]**	**Best [kg]**	**Worst [kg]**	**Best [kg]**	**Worst [kg]**
Propellant Masses						
Transfer	560		846		1145	
Station Keeping	28	69	44	106	59	143
End-of-Life	14	19	21	29	28	40
Margin Masses						
Transfer (5%)	28.0		42.3		57.2	
Station Keeping (20%)	6	14	9	21	12	29
End-of-Life (5%)	0.68	0.95	1.04	1.47	1.40	1.98
Propellant Residual (2%)	13	14	19	21	26	28
Total Masses						
Propellant Mass	691	704	981	1067	1328	1444
Dry Mass	851	796	1319	1233	1772	1656

In Figure 47, the satellite's dry and propellant mass is compared to the initial launch mass. The propellant mass of the TMA-0 satellite is almost half of the initial launch mass of the satellite. This assumption can be used for further design considerations before another simulation case is modeled. Furthermore there is only a small range within 3 % points between the best and worst case dry mass and the selection of an adequate thruster for the propulsion system is a sensitive influence of the dry mass.

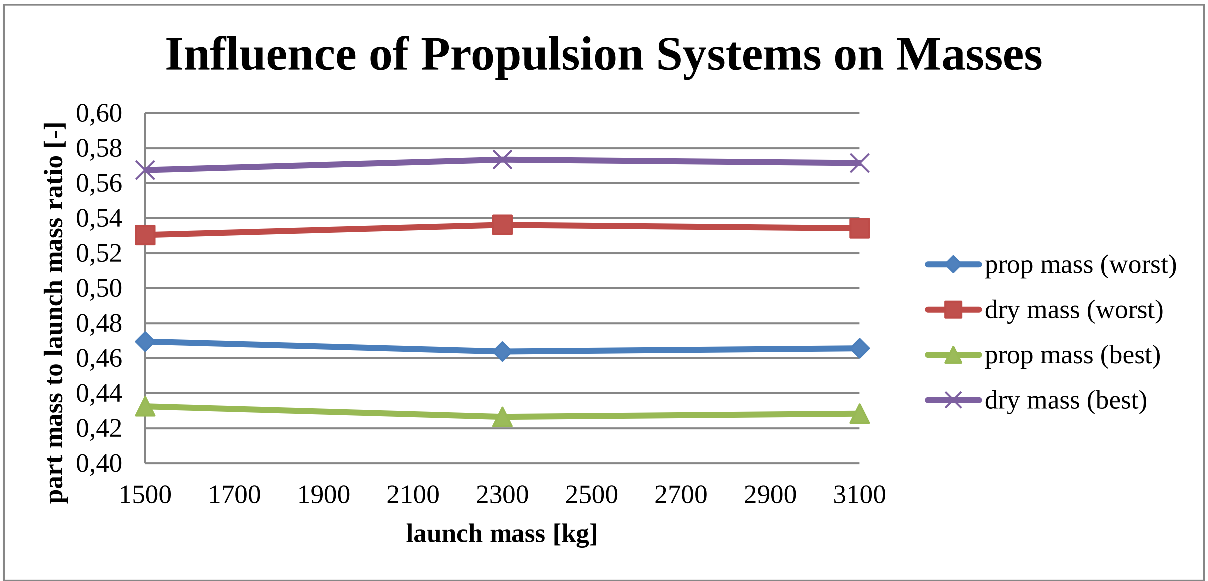

Figure 47: Ratio of dry and propellant mass to initial satellite launch mass

Baseline:

AKM:	EADS EAM 500 N bi-propellant thruster
AOCS Thrusters:	EADS 22 N bi-propellant thrusters
Satellite Mass:	1340 kg to 1316 kg
Disposal:	Impact on Moon

4.3 Communication Architecture

The communication architecture is driven by the data-rate required by the users and by international regulations by the International Telecommunication Union and their members. The presented architecture is designed to include the system drivers and restrictions to fulfill the IOD mission requirements (Figure 48).

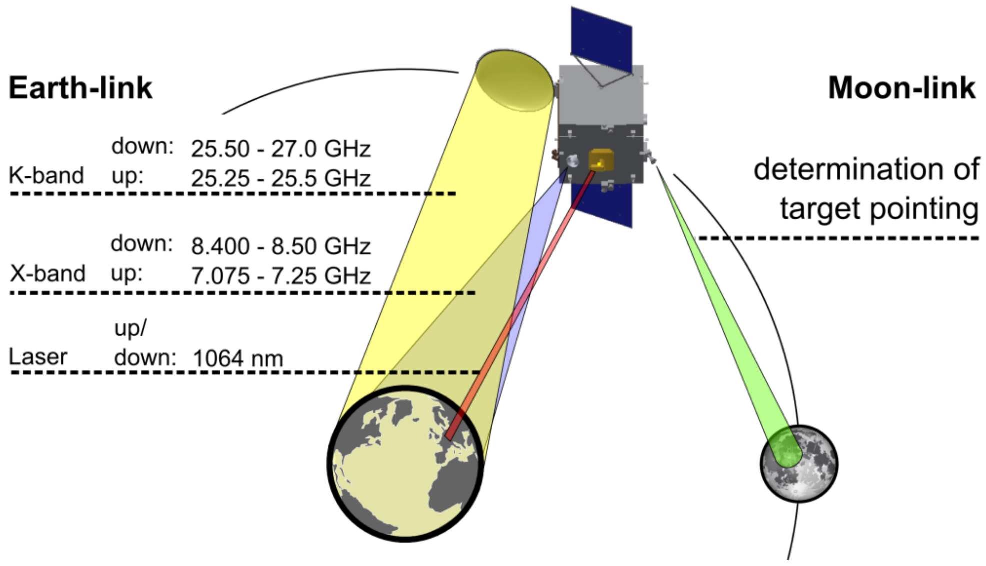

Figure 48: Communication architecture for Earth- and Moon-link

4.3.1 Band Selection

The frequency band selection proved to be a complex task in this thesis. The interconnection of regulations, subsystem design, relay network integration, ground-segment selection and finally user requirements for the high data-rate link is challenging. The selection and allocation of the designated frequency can be considered a time critical mission point and shall have a high priority a later preliminary design phase A (ECSS) [113].

4.3.1.1 High Data Rate: Radio Frequency

The TMA-1 frequency band of 25.5 GHz (K-band) for up and download is selected for TMA-0.

On the technical side, the frequency band's limitations on maximum emissions and for isotropic emissions can be handled and the maximum bandwidth around the center frequency is adequate for 400 Mbit/s even in one channel. Furthermore the K-band is selected to respect the requirement of an integration of the TYCHO satellite in a communication relay network. The frequency is used by EDRS for data-downlink. For TYCHO the feeder link is also selected in K-band.

The uplink and downlink frequencies (Table 39) are selected to stay close to their common border of 25.5 GHz so that the same high-gain antenna can be used and the losses of one or both links are minimal. The uplink frequency band shall be 25.25 – 25.5 GHz and downlink frequency band shall be 25.5 - 27.0 GHz. The rule of thumb to take a higher frequency band for uplinks cannot be followed due to the utilization plans and the absence of an allowed uplink in close vicinity of the downlink. A higher frequency is dampened more by the atmosphere than lower frequencies so that the flexible power adjustments of ground station can compensate it. In this case it is obsolete. The propagation path through the atmosphere is also not as affected as frequency bands of 11 GHz.

For the band selection the ITU "Radio Regulations Volume 1 (2008)" [114] is used and checked with the "Frequenznutzungsplan" (frequency utilization plan) of the German Bundesnetzagentur of 2011 [70]. The allocation to service regulations of ITU is the basis for the selection.

Table 39: High data-rate frequency allocation in K-band (25.5 GHz)

High Data-Rate Frequency Allocation		
	Uplink	Downlink
Band Plan ID:	381	382-383
Frequency Band:	25.25 – 25.5 GHz	25.5 – 27.0 GHz
Mode:	civilian	civilian
Frequency Utilization:	FIXED INTER-SATELLITE 5.536 MOBILE Standard frequency and time signal-satellite (Earth-to-space)	EARTH EXPLORATION-SATELLITE (space-to Earth) 5.536B FIXED INTER-SATELLITE 5.536 MOBILE SPACE RESEARCH (space-to-Earth) 5.536C Standard frequency and time signal-satellite (Earth-to-space) 5.536A

The band selection also enables the demonstration of the inter satellite capacity with Earth-space links in both directions. The utilization of inter-satellite links [115] is allowed on request.

Further recommendations by ITU concern the space research satellites (SRS) in Rec. ITU-R SA.1625 [116]. The ITU recommends due to the small number of expected SRS Earth stations that:

> *that sharing between transmitting SRS satellites and receiving data relay satellites (DRS) operating in the ISS near 26 GHz is feasible given the following constraints:*
>
> *– SRS satellites in an orbit that is near to the orbits of the DRS user satellites should not produce a pfd greater than –155 dB(W/m2) in 1 MHz at any location on the GSO for more than 0.1% of the time;*
>
> *– SRS satellites in orbits other than that mentioned above should not produce a pfd greater than –155 dB(W/m2) in 1 MHz at any location on the GSO for more than 1% of the time;*
>
> *that, when designing SRS systems, the probability of receiving brief periods of interference from DRS user satellites in the ISS should be taken into account. This interference should exist for less than 0.1% of the time;*

The interference with other satellites has to be minimized because it could influence the TYCHO mission. The communication link budgets has to respect the maximum power flux density of –155 dB(W/m2) in 1 MHz in GSO of 1% of the orbit period time and take actions like emit power reduction. For the operational mission, that does not include a laser communication terminal for communication with Earth, the usage of the LCT for Earth transmission shall be considered as an option to bypass this regulation. The laser frequency does not interfere with the RF frequencies and it can provide a narrow propagation beam and target pointing that excludes passages of satellites in GSO from the passage through that cone.

Lastly as an additional aspect in the frequency selection, the bordering up- and downlink frequencies shall have an adequate frequency gap band. This helps minimizing the creation of interferences by the incoming signal at the relay satellite on the transmitting system of the relay satellite. The offset distance between the frequency flanks of both bands is set at the -3dB threshold respecting the HPBW angle. For the conceptual frequency design a bandwidth gap of 1 MHz offset is used.

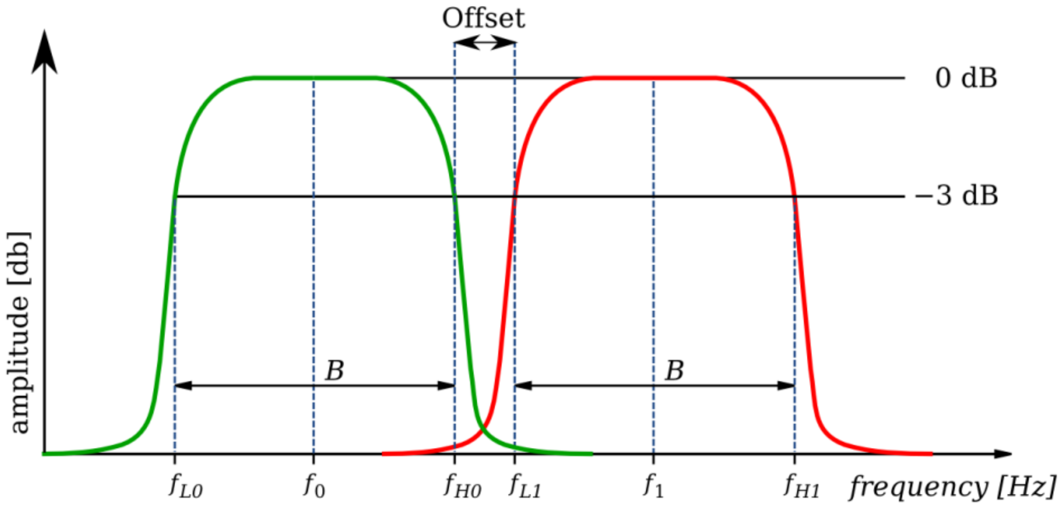

Figure 49: Frequency allocation for downlink (left) and uplink (right)

f:	*center frequency*	*B:*	*bandwidth or half-power beamwidth*
fL:	*lower cutoff frequency*	*fR:*	*upper cutoff frequency*

4.3.1.2 High Data Rate: Laser Wavelength

Optical free-space communication is a rather new technology with respect to the application in high-data-rate satellite-to-satellite and satellite-to-ground communication. In 2001 the first European satellite-to-satellite transmission was established. The CNES Earth observation satellite Spot-4 established a transmission link (LEO-to-GEO) with the Artemis satellite using the SILEX system (Semiconductor-laser Inter-satellite Link EXperiment) and a data-rate of 50 Mbit/s was reached [117]. Since 2008 space-to-ground links have been performed with NFIRE (USA) and TerraSAR-X (Germany) [118]. Further satellite missions will use LCTs onboard like LADEE (NASA) and EDRS (Europe).

For higher data-rates, higher frequencies have to be used that means small wave-lengths for the carrier frequency shall be selected. The SILEX experiment uses wavelength of 830 nm but the current development of LCT technology is in favor of 1064 and 1550 nm wavelength (Table 40). The wavelength of 1064 nm provides a higher efficiency and 1550 is well developed for fiber communication [119].

Table 40: A few satellites with LCT and the utilized wavelengths

#	Satellite	Wavelength [nm]
1	Artemis (SILEX)	830
2	Spot-4 (SILEX)	830
3	NFIRE	1064
4	TerraSAR-X & Tandem-X	1064
5	Alphasat I / Inmarsat I-XL	1064
6	EDRS	1064
7	LADEE	1550

The wavelength selection for TYCHO favors 1064 nm because of the efficiency and thus leading to higher data-rates, the high technology readiness level (TRL) of LCT that are already space qualified, the higher number of possible satellites using this wavelength and the integration of TYCHO into the EDRS network. Moreover the wavelength can be used for inter-satellite links as well as space-to-ground because the wavelength in the infrared spectrum is still not that affected by the atmosphere and is not as near to the visible spectrum, which is important for the optical ground station (OGS).

4.3.1.3 Telemetry, Tracking and Control: Radio Frequency

The satellite telemetry, tracking and control (TT&C) is primarily transmitted via separate communication links. The high data-rate K-band links can be used for TT&C during the transfer phases. However the accessibility of the satellites shall still be possible even during tumbling and miss-pointing. It requires a wide HPBW angle. For this, omni-directional transmission and reception with low data-rate shall be used as the primary TT&C channel.

The frequency selection favors X-band instead of S-band. S-band is currently mainly used for space research satellites because of standard subsystems and good ground station availability with DSN and further infrastructure. However the S-band spectrum is already crowded with space and civilian Earth applications in near-Earth orbit that increases the possibility of interference [120]. The selection of X-band allows higher emit power, wider bandwidth and thus higher data-rates during a weak stability transfer with apoapsides with distances of more than 960000 km. During the apoapsis and midcourse maneuvers, telecommand and telemetry data is essential. And lastly the Moon shielded zone needs to be protected from radio frequency pollution. With an omnidirectional transmitter on EML-4 that sends out signals to Earth will also be received on the Moon. Some of the most interesting and heavily studied spectral lines of great astrophysical interests lie within the 0.3 to 3 GHz range and so does S-band (2 - 4 GHz). Within the 3 – 20 GHz lie less frequency bands with lines of importance for astrophysics. This region is also increasingly used by airborne and satellite services [71].

The up- and downlink frequencies in X-band (Table 41) are selected by the frequency band plan [70] and they use band for allocation for services for space research satellites. The upload band with 8.4 to 8.5 GHz is also used by radio astronomers for deep space observation but the transmission from Earth does not interfere with Earth based observation and the shielded Moon zone stays also unaffected. And finally even though the data-rate is lower within 1 – 100 Kbit/s, there currently are fewer limitations for bandwidth sizes and maximum power flux densities in X-band than there are for S-band.

Table 41: TT&C frequency allocation

TT&C Frequency Allocation		
	Downlink	Uplink
Band Plan:	328	317
Item:	328002	317003
Frequency Band:	8.400 – 8.500 GHz	7.075 – 7.250 GHz
Service:	space research service (direction Earth-space) D465	D460: space research service (direction Earth-space)
Mode:	civilian	
Frequency Utilization:	space research: communication with space vessels, typically for data transmission, with a scope of scientific or technical research	
Frequency Space:	8.400 – 8.500 GHz	7.145 – 7.235 GHz

4.3.2 Network Integration

The TYCHO mission requirement is to provide a universal and open relay service. This means on the one side that users in Moon vicinity and beyond can use it for their communication towards Earth. On the other hand it also demands for integration into different networks to be able to route the signal to the user satellite's operation center. Therewith the complete signal route can be closed.

The most prominent relay satellite service currently available includes the systems available for ISS like Tracking and Data Relay Satellite (TDRS, USA) or the Luch Satellite Data Relay Network (SDRN, Russia). There are programs from other space agencies deploying relay satellites in GEO with EDRS the most promising for the TYCHO mission. The advantage is that the TMA-0 satellite shall be able to either establish connection with the satellite itself or to directly use their ground segment infrastructure. It offers the benefit that there is no need to invest in a specific ground segment for TYCHO and reducing costs and mainly time.

EDRS is favored even though the first satellite will be launched in 2014. It offers a data-rate of 1.8 Gbit/s in four Ka-band channels for the Earth downlink. This suits the TYCHO mission requirement of 400 Mbit/s that is not possible with the current generation of TDRS with 150 Mbit/s. Furthermore it is a European endeavor that will use ground segments that are open for servicing satellites besides EDRS. Hence the downlink radio frequency of 25.5 GHz is selected with respect to EDRS. The inter-satellite link for EDRS uses an optical wavelength. The LCT is built by Tesat and offers target pointing via two axes offering access to objects on a half sphere field-of-view and a full sphere by additional attitude control maneuvers of the EDRS satellite. The TDRS satellites in GEO possess steerable high-gain antennas but with propagation coils towards the Earth that makes connections to even further orbits complex. In this way, the EDRS LCT could either be used to establish connections to the single TMA-1, to transmit data to lunar missions via the Ka-Band link to the Moon, or the TMA-1 LCT transmits data to an EDRS satellite that can downlink it to an Earth ground station. An additional LCT onboard of TMA-1 is only needed for a gapless laser routing between the Earth and the Moon. For the in orbit demonstration with TMA-0, the targeting and connection shall be qualified.

The routing on Earth from ground stations to the mission operation centers and the routing in space can rely on well-known and tested infrastructure. Private satellite operator SES conducted a market study to analyze the possible market growth of data relay services [121] and Eutelsat will place the EDRS-A payload on the commercial Eutelsat 9b as within a public private partnership [122].

On the other link side there are plans for an International Lunar Network (ILN) that will provide the capability to span communication meshes from one participating lunar vessel to another and finally connecting to a lunar communication terminal (LCT) that serves as the gateway to Earth or a relay satellite in a lunar orbit [16]. TMA-1 shall expand this network by offering an alternative route between Earth and the terminals or even directly to the vessels.

4.3.3 Ground Segment

The IOD satellite TMA-0 shall be qualified with existing ground stations. For this available ground stations for K-band with 25.5 GHz support are presented in Table 42. These ESA stations already have or will have support until 2014 and are representatively used for the TMA-0 study. For the in orbit demonstration with TMA-0, only one station is needed with another one serving for the handover testing. The global distribution of the ground station locations also allows for a permanent access with three ground stations. The analysis of the Deep Space Network configuration is presented within the coverage zone identification in Chapter 3.2.3.1. The presented ground stations also allow such a configuration with angular distances of 120°.

Table 42: Ground stations with K/Ka-band antennas (ESA)

Ground Stations with K/Ka-band Antennas (ESA)				
#	**Name**	**Country**	**Additional**	**Antenna Diameter**
1	Malargüe	Argentina	DSA 3	35 m
2	Cebreros	Spain	Euclid, DSA 2	35 m
3	Kourou	French Guyana	Euclid	15 m
4	New Norcia	Australia	Euclid, DSA 1	35 m
5	Maspalomas Station	Spain	Euclid	15 m
6	Harwell	UK	EDRS	-
7	Redu	Belgium	EDRS	13.5 m
8	Weilheim (DLR)	Germany	EDRS	13 m

[123] [124] [125]

For optical ground stations (OGS) there is the Observatorio del Teide (OT) on Tenerife, Spain where ESA conducted several optical communication connections with NFIRE, TerraSAR-X and others. It will also be used by ESA and NASA for the LADEE mission [126] (Table 43).

Table 43: Optical ground stations (ESA)

Optical Ground Stations (ESA)				
#	**Name**	**Country**	**Additional**	**Aperture Diameter**
1	Observatorio del Teide	Spain	ESA & NASA	1.016 m

Current stationary OGS by Tesat have apertures of 60 mm and they currently develop mobile and stationary LCTs with 250 mm and 400 mm aperture that will also be used in observatories (Table 44). Laser communication is heavily influenced by atmospheric conditions and mainly clouding. Thus an additional ground stations shall be found for the operational TMA-1 satellite. For optical demonstrations with TMA-0 a single optical ground station is adequate because the laser testing is not time critical and can be postponed for a better weather phase. For the operational mission multiple OGS locations shall be considered to be able to target another OGS in case of no availability of one OGS due to weather conditions.

Table 44: Optical ground station aperture diameters

	Current stationary	**Future mobile**	**Future stationary**
OGS telescope aperture	60 mm	250 mm	400 mm

This chapter does not include additional parameters like availability due to yearly weather conditions, altitude, wind condition, RF or light pollution. It summarizes the design conditions for the communication link budgets. The selection of the RF and optical ground station shall be part of a continuing study.

4.3.4 Communication Links and Data-Rates

The TMA-0 shall demonstrate the communication links from TMA-1 with respect to capabilities of signal quality, stability and data-rates. For this the radio frequency and optical link budget for the Earth link has to be analyzed. This is done with different approaches due to different signal propagation of the RF-band (K and X) and optical band's electromagnetic wave and different signal detection.

4.3.4.1 Radio Frequency Link Budget

The radio link budgets for up and downlinks are modeled after "Space Mission Analysis and Design" by W. J. Larson and J. R. Wertz [127] and "Satellite Communications" by C. Nöldeke [128] and is only presented in abbreviated form.

Received power P_r at a ground station antenna is influenced by a chain of signal damping and amplifying components on the transmitter side (index t & l), the free-space propagation and environment (index s & a) and the receiver side (index r) decreasing the transmitted power.

$$P_r = P_t L_d \, L_l G_t L_a G_r \left(\frac{\lambda}{4\,\pi S}\right)^2 = P_t \, L_d L_l G_t L_a G_r L_s = (EIRP) L_a G_r \, L_s \qquad 4.17$$

The link budget includes on the satellite site the transmit power P_t, the losses inside the radio distribution unit L_d as well as line loss L_l to the antenna and the transmit antenna gain G_t. These four terms are also combined as the equivalent isotropically radiated power (EIRP). During the signal propagation the space loss L_s, that includes the wavelength λ and the path distance S, and the atmospheric losses L_a are damping the signal. The resulting power density is then amplified by receiver antenna gain G_r.

The link budget design is mainly designed around the frequency f [GHz] and the allowed transmit power P_t [W] outlining the maximum data-rate. The selection of the frequency is also based on international regulations that specifies the usage of certain frequency bands for certain applications, such as satellite to satellite interlinks [129], and maximum allowed energy density and power transmission by either the regulations or further satellite subsystem design like maximum power budget.

With a selected transmit power it is used in logarithmic scale with

$$P_t = 10\log(P)\ [dB] \tag{4.18}$$

to respect the equation in decibels and the transmitter line loss L_l [dB] and transmit antenna beamwidth θ_t[deg] are specified by the transmitter hardware. The peak transmit antenna gain is obtained with the half-power beamwidth along the major axis to θ_x and θ_y [deg] for noncircular beam antennas.

$$G_{pt} \approx 44.3 - 10\log(\theta_x\theta_y)\ \ [dB] \tag{4.19}$$

The given equation is for peak gain and the receiver antenna might not be perfectly targeted in the center of the transmitter antenna beam. This is respected with the transmit antenna pointing offset e_t [deg] and with narrow beamwidths the transmit antenna pointing loss

$$L_{pt} = \ -12\ \left(\frac{e_t}{\theta_t}\right)^2\ \ [dB] \tag{4.20}$$

increases and can lead to a noticeable reduced gain. The transmit antenna diameter is obtained by the empirical relationship for circular antenna beams

$$\theta_t = \frac{21}{f_{GHz}D_t}\ [deg] \tag{4.21}$$

influenced by the antenna's diameter and applied frequency. The net transmit antenna gain is a combination of the peak gain reduced by the pointing loss.

$$\mathrm{G_t} = \ \mathrm{G_{pt}}\ \ + \ \mathrm{L_{pt}}\ \ [dBi] \tag{4.22}$$

The equivalent isotropically radiated power (EIRP) characterizes the amount of power that would be transmitted by a theoretical isotropic antenna with an emitted peak power density in the direction of the maximum antenna gain. It includes the line and feeder losses L_l and the losses inside the radio frequency distribution unit L_d.The latter includes losses that occur after the carrier frequency amplification so that the transmitted power is influenced by switches, insulation, filters as devices and during the passages through waveguides and flanges where the losses occur along the guide tubes before it exits the RFDU for the feeder.

$$EIRP = P_t + L_d + L_l + G_t\ [dBW] \tag{4.23}$$

By now the signal exits the transmitter and propagates in free-space. The power density is now reduced by the propagation path length S_p [km] due to an increased projected area of the propagation coil and formulated by space loss

$$L_s = \left(\frac{\lambda}{4\,\pi\,S}\right)^2 = \left(\frac{c}{4\,\pi\,S_p\,f}\right)^2 = 20\log(3\times10^8) - 20\log(4\,\pi) - 20\log S_p - 20\log f \tag{4.24}$$

Further space environments and the transfer through Earth's atmosphere result in additional losses included in propagation and polarization loss L_a [dB] (Figure 78). For services with high availabilities of 99.9% or 99.99% ITU recommends rain margins in ITU-R P.618 [130]. For the K-band channel this was set to 10 dB and is for worst case scenario. This must be corrected when the ground station location and their altitude and typical rain rates (mm/h) are known. As a comparison the rain rates for the representative power compensation margin for the 12 GHz band of 10 dB are 50 mm/h with 99.99% availability and more than 60 mm/h for 99.9% availability [131]. In rain precipitation measurement a rate of more than 50.0 mm/h is considered extreme rain.

The signal is now interfacing the receiver and the receive antenna gain (net) is modeled

$$G_{pr} = 20\log\pi + 20\log D_r + 20\log f + 10\log\eta_r - 20\log c \;\; [dBi] \qquad 4.25$$

with geometric properties of the antenna as receive antenna diameter D_r [m] antenna efficiency $\eta_r = 0.55$ (for typical parabolic antennas) and physical parameters with applied frequency and the speed of light c in free-space $= 3 \times 10^8 \frac{m}{s}$

The receiver antenna beamwidth is obtained in similar fashion like the transmit antenna diameter before

$$\theta_r = \frac{21}{f_{GHz} D_r} \; [deg] \qquad 4.26$$

And is used to calculate the receiver antenna pointing loss with a known receiver antenna pointing error e_r [deg]

$$L_{pr} = -12\left(\frac{e_r}{\theta_r}\right)^2 [dB] \qquad 4.27$$

The effective receiver antenna gain also includes the peak gain reduced by the losses.

$$G_r = G_{pr} + L_{pr} \qquad 4.28$$

The signal propagation now enters the antenna but is overlaid with a broadband environmental noise by the system noise temperature T_s [K] ([SMAD] Table 13-10). The received energy-per-bit to noise-density *Eb/N0* now specifies the signal quality and whether or not it is possible to receive a set data-rate *R* [bps].

$$\frac{E_b}{N_0} = P_t + L_l + G_t + L_{pr} + L_s + L_a + G_r + 228.6 - 10\log T_s - 10\log R \;\; [dB] \qquad 4.29$$

the signal to noise ratio describes the sensitivity of the receiver and includes in addition to the already stated path components the Boltzmann constant that includes the related energy at different levels of temperature of the receiver.

$$10\log k = -228.6\frac{dBW}{Hz\,K} \qquad 4.30$$

We can now find the carrier-to-noise density ratio used for demodulation.

$$\frac{C}{N_0} = \frac{E_b}{N_0} + 10 * LOG(R) \; [dB - Hz] \qquad 4.31$$

The final step includes selecting a bit error rate *BER* [-] with respect of how robust a data stream reception shall be and how many received bits over a communication channel are allowed to be altered due to interference, noise, bit synchronization and distortion. Furthermore the required *Eb/N0* [dB] (Figure 78) and implementation loss L_{imp} [dB] have to be selected (often estimated -2 dB) to obtained the system margin.

$$\frac{E_b}{N_0} - Req.\frac{E_b}{N_0} + L_{imp} \tag{4.32}$$

Typically a *system margin* of $\geq\ 3\ dB$ is aimed for to account for additional environmental effects damping the signal and guaranteeing a certain level of accessibility of the signal.

4.3.4.2 Radio Frequency Up- and Downlinks

The communication link design includes the high data-rate channels and the TT&C link.

It includes the data-rate, for up- and downlink, for 35 m and 15 m ground station antennas as found for the EDRS ground segment and alternatives and for distances to the EML-4 target orbit in a distance of 400000 km. For the TT&C links, the furthest distance at the transfer apoapsis at 960000 km is also considered due to telecommands and telemetry during the transfer.

The link budgets for K-band in Table 45 to Table 50 can be considered as worst case scenarios because the rain margin is set for heavy rain for the high-data rate channel and the distances from the EML-4 orbit includes the maximum allowed station keeping orbit around EML-4 with 45000 km. Additionally, the high data-rate channels are analyzed for the feasibility of usage during the transfer apoapsis where typically the X-band channels are used for communication. This is done for redundancy in case X-band cannot be used.

Table 45: Link-budget: high data-rate link (K-band) – EML-4 orbit (1/3)

High Data-Rate Link (K-band) – EML-4 Orbit (1/3)							
				Downlink		**Uplink**	
Item	**Symbol**	**Unit**	**Source**	**35 m GS Antenna**	**15 m GS Antenna**	**35 m GS Antenna**	**15 m GS Antenna**
Frequency	f	GHz	input	25.701		25.449	
Transmitter Power	P	W	input	60.0		50.0	
Transmitter Power	P_t	dBw		17.78		16.99	
RF Distrib. Unit Loss	L_d	dB	Table 59	3.16		0.0	
Transmitter Line & Feeder Loss	L_l	dB	input	0.5		2.8	
Transmit Antenna Beamwidth	θ_t	deg		0.4		0.024	0.055
Peak Transmit Antenna Gain	G_{pt}	dBi		52.26		76.85	69.49
Transmit Antenna Diameter	D_t	m	Ch. 4.4.1.1.1, Ch. 4.3.3	2.04		35.0	15.0
Transmit Antenna Pointing Offset	e_t	deg	input	0.05		0.005	
Transmit Antenna Pointing Loss	L_{pt}	dB		0.19		0.54	0.1
Transmit Antenna Gain (net)	G_t	dBi		52.07		76.31	69.39
Equiv. Isotropic Radiated Power	EIRP	dBw		66.19		90.5	83.58

Table 46: Link-budget: high data-rate link (K-band) – EML-4 orbit (2/3)

High Data-Rate Link (K-band) – EML-4 Orbit (2/3)							
				Downlink		**Uplink**	
Item	**Symbol**	**Unit**	**Source**	**35 m GS Antenna**	**15 m GS Antenna**	**35 m GS Antenna**	**15 m GS Antenna**
Propagation Path Length	S_p	Km	input	451000		451000	
Space Loss	L_s	dB		233.72		233.64	
Propagation & Polarization Loss	L_a	dB	Figure 80	0.4		0.4	
rain margin	L_{rm}	dB	(ITU-R P.618-8), [132]	10.0		10.0	

Table 47: Link-budget: high data-rate link (K-band) – EML-4 orbit (3/3)

High Data-Rate Link (K-band) – EML-4 Orbit (3/3)							
				Downlink		**Uplink**	
Item	**Symbol**	**Unit**	**Source**	**35 m GS Antenna**	**15 m GS Antenna**	**35 m GS Antenna**	**15 m GS Antenna**
Receive Antenna Diameter	D_r	m	Ch 4.3.3, Ch. 4.4.1.1.1	35.0	15.0	2.04	
Peak Receive Antenna Gain (net)	G_{pr}	dBi		76.89	69.53	52.12	
Receive Antenna Beamwidth	θ_r	deg		0.023	0.054	0.4	
Receive Antenna Pointing Error	e_r	deg	input	0.005		0.1	
Receive Antenna Pointing Loss	L_{pr}	dB		0.55	0.1	0.74	
Receive Antenna Gain	G_r	dBi		76.33	69.42	51.39	
System Noise Temperature	T_s	K	Figure 79	424.0		763.0	
Data-Rate	R	bps	input	4×10^8	1×10^8	1×10^8	2.5×10^7
Signal-to-Noise Ratio	E_b/N_0	dB		15.23	14.32	17.74	16.84
Carrier-to-Noise Density Ratio	C/N_0	dB-Hz		101.25	94.32	97.62	90.7
Modulation & Coding		-	Figure 78, [132]	64 APSK		QPSK	
Required E_b/N_0	Req. C/N_0	dB	Figure 78, [132]	9.0		7.5	
Implementation Loss	L_{imp}	dB	estimate	2.0		2.0	
System Margin		dB		**4.21**	**3.32**	**8.12**	**7.22**

The system margins for up- and downlink for both ground station antenna sizes are above the required 3 dB. Nevertheless it shows that in case of the 15 m Antenna the data-rate is 100 Mbit/s instead of the required 400 Mbit/s. With respect of the redundancy requirement of splitting the bandwidth for several channels, this already requires four separate channels. In that case two channels will share one frequency with circular polarization. So for TMA-1 all four channels are used and TMA-0 shall qualify two channels on the same frequency with the filtered polarization. The ground station selection is also more flexible because of the availability of 15 m ground stations of EDRS and an option to use DSN 35 m antennas.

Table 48: Link-budget: high data-rate link (K-band) – transfer orbit (1/3)

High Data-Rate Link (K-band) – Transfer (1/3)							
				Downlink		Uplink	
Item	**Symbol**	**Unit**	**Source**	**35 m GS Antenna**	**15 m GS Antenna**	**35 m GS Antenna**	**15 m GS Antenna**
Frequency	f	GHz	input	25.701		25.449	
Transmitter Power	P	W	input	60.0		50.0	
Transmitter Power	P_t	dBw		17.78		16.99	
RF Distrib. Unit Loss	L_d	dB	Table 59	3.16		0.0	
Transmitter Line & Feeder Loss	L_l	dB	input	0.5		2.8	
Transmit Antenna Beamwidth	θ_t	deg		0.4		0.024	0.055
Peak Transmit Antenna Gain	G_{pt}	dBi		52.26		76.85	69.49
Transmit Antenna Diameter	D_t	m	Ch. 4.4.1.1.1, Ch. 4.3.3	2.04		35.0	15.0
Transmit Antenna Pointing Offset	e_t	deg	input	0.05		0.005	
Transmit Antenna Pointing Loss	L_{pt}	dB		0.19		0.54	0.1
Transmit Antenna Gain (net)	G_t	dBi		52.07		76.31	69.39
Equiv. Isotropic Radiated Power	EIRP	dBw		66.19		90.5	83.58

Table 49: Link-budget: high data-rate link (K-band) – transfer orbit (2/3)

High Data-Rate Link (K-band) – Transfer (2/3)							
				Downlink		Uplink	
Item	**Symbol**	**Unit**	**Source**	**35 m GS Antenna**	**15 m GS Antenna**	**35 m GS Antenna**	**15 m GS Antenna**
Propagation Path Length	S_p	Km	input	960000		960000	
Space Loss	L_s	dB		240.29		240.2	
Propagation & Polarization Loss	L_a	dB	Figure 80	0.4		0.4	
rain margin	L_{rm}	dB	(ITU-R P.618-8), [132]	10.0		10.0	

Table 50: Link-budget: high data-rate link (K-band) – transfer orbit (3/3)

High Data-Rate Link (K-band) – Transfer (3/3)							
				Downlink		**Uplink**	
Item	**Symbol**	**Unit**	**Source**	**35 m GS Antenna**	**15 m GS Antenna**	**35 m GS Antenna**	**15 m GS Antenna**
Receive Antenna Diameter	D_r	m	Ch 4.3.3, Ch. 4.4.1.1.1	35.0	15.0	2.04	
Peak Receive Antenna Gain (net)	G_{pr}	dBi		76.89	69.53	52.12	
Receive Antenna Beamwidth	θ_r	deg		0.023	0.054	0.4	
Receive Antenna Pointing Error	e_r	deg	input	0.005		0.1	
Receive Antenna Pointing Loss	L_{pr}	dB		0.55	0.1	0.74	
Receive Antenna Gain	G_r	dBi		76.33	69.42	51.39	
System Noise Temperature	T_s	K	Figure 79	424.0		763.0	
Data-Rate	R	bps	input	5×10^7	1×10^7	2.5×10^7	1×10^7
Signal-to-Noise Ratio	E_b/N_0	dB		17.68	17.19	17.08	14.14
Carrier-to-Noise Density Ratio	C/N_0	dB-Hz		94.67	87.19	91.06	84.14
Modulation & Coding		-	Figure 78, [132]	64 APSK		QPSK	
Required E_b/N_0	Req. C/N_0	dB	Figure 78, [132]	9.0		7.5	
Implementation Loss	L_{imp}	dB	estimate	2.0		2.0	
System Margin		dB		**6.68**	**6.19**	**7.58**	**4.64**

The high data-rate communication is checked for the behavior of the link margins. As expected the data-rate has to be decreased to be able to communicate from this further distance. It is still in the range of 25 to 50 Mbit/s for downloads but the most important aspect is the accessibility by ground station via the uplink for an optional TT&C channel.

In addition this shows another argument of demand for a flexible data-rate selection via the K-band link. As described before, the heterogeneous demand for data-rates by possible users would be supported with a flexible set-up of the communication set-up. Usually the channels are fixed to certain predefined modes. With a flexible, telecontrollable reconfiguration of the communication setting both, the users and the transfer can be served. This requires a modulator that can change the data-rate and frequency according to the commando sent from mission operation. Such a modulator is currently in development under the name “TeTra” by Tesat [132] and is presented in the “Communication” Chapter 4.4.1.1.

Table 51: Link-budget: TT&C link (X-band) – EML-4 orbit (1/3)

TT&C Link (X-band) – EML-4 Orbit (1/3)							
				Downlink		**Uplink**	
Item	**Symbol**	**Unit**	**Source**	**35 m GS Antenna**	**15 m GS Antenna**	**35 m GS Antenna**	**15 m GS Antenna**
Frequency	f	GHz	input	8.44		7.19	
Transmitter Power	P	W	input	10.0		50.0	
Transmitter Power	P_t	dBw		10.0		16.99	
RF Distrib. Unit Loss	L_d	dB	Table 59	0.0		0.0	
Transmitter Line & Feeder Loss	L_l	dB	input	1.0		2.8	
Transmit Antenna Beamwidth	θ_t	deg		140.0		0.083	0.195
Peak Transmit Antenna Gain	G_{pt}	dBi		1.38		65.87	58.51
Transmit Antenna Diameter	D_t	m	Ch. 4.4.1.1.1, Ch. 4.3.3	0.018		35.0	15.0
Transmit Antenna Pointing Offset	e_t	deg	input	20.0		0.005	
Transmit Antenna Pointing Loss	L_{pt}	dB		0.25		0.043	0.008
Transmit Antenna Gain (net)	G_t	dBi		1.13		65.83	58.5
Equiv. Isotropic Radiated Power	EIRP	dBw		10.13		80.02	72.69

Table 52: Link-budget: TT&C link (X-band) – EML-4 orbit (2/3)

TT&C Link (X-band) – EML-4 Orbit (2/3)							
				Downlink		Uplink	
Item	**Symbol**	**Unit**	**Source**	**35 m GS Antenna**	**15 m GS Antenna**	**35 m GS Antenna**	**15 m GS Antenna**
Propagation Path Length	S_p	Km	input	451000		451000	
Space Loss	L_s	dB		224.05		222.66	
Propagation & Polarization Loss	L_a	dB	Figure 80	0.4		0.4	
rain margin	L_{rm}	dB	(ITU-R P.618-8), [132]	0.03		0.03	

Table 53: Link-budget: TT&C link (X-band) – EML-4 orbit (3/3)

TT&C Link (X-band) – EML-4 Orbit **(3/3)**							
				Downlink		**Uplink**	
Item	**Symbol**	**Unit**	**Source**	**35 m GS Antenna**	**15 m GS Antenna**	**35 m GS Antenna**	**15 m GS Antenna**
Receive Antenna Diameter	D_r	m	Ch 4.3.3, Ch. 4.4.1.1.1	35.0	15.0	0.018	
Peak Receive Antenna Gain (net)	G_{pr}	dBi		67.21	59.85	-0.066	
Receive Antenna Beamwidth	θ_r	deg		0.07	0.17	164.34	
Receive Antenna Pointing Error	e_r	deg	input	0.005		1.0	
Receive Antenna Pointing Loss	L_{pr}	dB		0.06	0.01	0.0	
Receive Antenna Gain	G_r	dBi		67.15	59.84	-0.067	
System Noise Temperature	T_s	K	Figure 79	135.0		614.0	
Data-Rate	R	bps	input	$\mathbf{1 \times 10^4}$	$\mathbf{4 \times 10^3}$	$\mathbf{1 \times 10^4}$	$\mathbf{2 \times 10^3}$
Signal-to-Noise Ratio	E_b/N_0	dB		20.1	16.77	17.6	17.3
Carrier-to-Noise Density Ratio	C/N_0	dB-Hz		60.1	52.79	57.6	50.3
Modulation & Coding		-	Figure 78, [132]	QPSK		QPSK	
Required E_b/N_0	Req. C/N_0	dB	Figure 78, [132]	10.5		10.5	
Implementation Loss	L_{imp}	dB	estimate	2.0		2.0	
System Margin		dB		**7.6**	**4.27**	**5.08**	**4.75**

Table 54: Link-budget: TT&C link (X-band) – transfer orbit (1/3)

TT&C Link (X-band) – Transfer (1/3)							
				Downlink		**Uplink**	
Item	**Symbol**	**Unit**	**Source**	**35 m GS Antenna**	**15 m GS Antenna**	**35 m GS Antenna**	**15 m GS Antenna**
Frequency	f	GHz	input	8.44		7.19	
Transmitter Power	P	W	input	10.0		50.0	
Transmitter Power	P_t	dBw		10.0		16.99	
RF Distrib. Unit Loss	L_d	dB	Table 59	0.0		0.0	
Transmitter Line & Feeder Loss	L_l	dB	input	1.0		2.8	
Transmit Antenna Beamwidth	θ_t	deg		140.0		0.083	140.0
Peak Transmit Antenna Gain	G_{pt}	dBi		1.38		65.87	1.38
Transmit Antenna Diameter	D_t	m	Ch. 4.4.1.1.1, Ch. 4.3.3	0.018		35.0	0.018
Transmit Antenna Pointing Offset	e_t	deg	input	20.0		0.005	
Transmit Antenna Pointing Loss	L_{pt}	dB		0.25		0.043	0.25
Transmit Antenna Gain (net)	G_t	dBi		1.13		65.83	1.13
Equiv. Isotropic Radiated Power	EIRP	dBw		10.13		80.02	10.13

Table 55: Link-budget: TT&C link (X-band) – transfer orbit (2/3)

TT&C Link (X-band) – Transfer (2/3)							
				Downlink		**Uplink**	
Item	**Symbol**	**Unit**	**Source**	**35 m GS Antenna**	**15 m GS Antenna**	**35 m GS Antenna**	**15 m GS Antenna**
Propagation Path Length	S_p	Km	input	960000		960000	
Space Loss	L_s	dB		230.61		229.22	
Propagation & Polarization Loss	L_a	dB	Figure 80	0.4		0.4	
rain margin	L_{rm}	dB	(ITU-R P.618-8), [132]	0.03		0.03	

Table 56: Link-budget: TT&C link (X-band) – transfer orbit (3/3)

TT&C Link (X-band) – Transfer (3/3)							
				Downlink		**Uplink**	
Item	**Symbol**	**Unit**	**Source**	**35 m GS Antenna**	**15 m GS Antenna**	**35 m GS Antenna**	**15 m GS Antenna**
Receive Antenna Diameter	D_r	m	Ch 4.3.3, Ch. 4.4.1.1.1	35.0	15.0	0.018	
Peak Receive Antenna Gain (net)	G_{pr}	dBi		67.21	59.85	-0.066	
Receive Antenna Beamwidth	θ_r	deg		0.07	0.17	164.34	
Receive Antenna Pointing Error	e_r	deg	input	0.005		1.0	
Receive Antenna Pointing Loss	L_{pr}	dB		0.06	0.01	0.0	
Receive Antenna Gain	G_r	dBi		67.15	59.84	-0.067	
System Noise Temperature	T_s	K	Figure 79	135.0		614.0	
Data-Rate	R	bps	input	$\mathbf{4 \times 10^3}$	$\mathbf{5 \times 10^2}$	$\mathbf{2 \times 10^3}$	$\mathbf{4 \times 10^2}$
Signal-to-Noise Ratio	E_b/N_0	dB		17.52	19.24	18.01	17.67
Carrier-to-Noise Density Ratio	C/N_0	dB-Hz		53.54	46.23	51.02	43.69
Modulation & Coding		-	Figure 78, [132]	QPSK		QPSK	
Required E_b/N_0	Req. C/N_0	dB	Figure 78, [132]	10.5		10.5	
Implementation Loss	L_{imp}	dB	estimate	2.0		2.0	
System Margin		dB		**5.02**	**6.74**	**5.51**	**5.17**

4.3.4.3 *Laser Frequency Link Budget*

The link budget for optical free-space communication shares similarities to that of radio frequency but is based on a different concept. The simplest laser detection method is direct detection and basically counts the number of received photons on the detector sensor area, thus it is sometimes colloquially called “photon-bucket” technique.

The received power P_r is the consequence of transmit signal P_t degradation. Like its RF counterpart, it encompasses loses (L_t, L_r, L_s), attenuation and amplification of transmitter and receiver gain (G_t, G_r) [133] [134] [135] [136].

$$P_r = P_t \eta_{ot} \eta_{or} \left(\frac{\lambda}{4\,\pi S}\right)^2 G_t G_r L_t L_r \ [W] \qquad 4.33$$

The equation includes the optical efficiency of the transmitter η_{ot} and receiver η_{or}. The optical efficiencies represent the quantum number of the sensors. The transmitter and receiver gain *G* is given by

$$G = \left(\frac{\pi D}{\lambda}\right)^2 \qquad 4.34$$

and is influenced by the selected wavelength λ and the diameter *D* of the optical antenna. Pointing losses contributes to signal degradation when the system transmitter uses a laser diode with narrow-divergence angle θ_t and when the receiver has a narrow field-of-view angle θ_r. Both pointing loss factors can then be approximated by

$$L = \exp(-G\,\theta^2) \qquad 4.35$$

The transmitted power is then received on the detector and is equivalent to a certain number of photons with the specific wavelength. The energy per photon E_{ph} is given by

$$E_{ph} = h\,\lambda\,[J] \qquad 4.36$$

where h is the Planks constant. The sensor sensitivity than states the number of photons have to be detected for one bit with photons-per-bit N_{ph} and the data-rate *R* is acquired with

$$R = \frac{P_r}{N_{ph} E_{ph}} \ [bps] \qquad 4.37$$

This is a basic free-space link budget without atmospheric losses like scattering and scintillation. The current budget can be used for the Moon link of TMA-1. The Earth link, which shall be provided by TMA-0, uses a COTS laser communication terminal (LCT) with known data-rates from specified low Earth and geosynchronous orbits to Earth ground level (Table 57). Hence the data-rate is corrected by the different free-space losses of the new distance and includes atmospheric passage. TMA-0 is able to demonstrate target pointing, data-rate and signal stability in this way with a loss of maximum data-rate as described in the following Chapter 4.3.4.4.

Table 57: Parameters of Tesat and RUAG laser communication terminals

	Tesat LCT-1	**Tesat LCT-2**	**RUAG Optel-μ**
Link:	LEO-LEO	LEO-GEO	LEO-LEO
Data-Rate R:	5.625 Gbit/s	1.8 Gbit/s	2.5 Gbit/s
Distance:	1000-5100 km	$> 45000\ km$	1000 km
BER:	$< 10^{-9}$	10^{-8}	10^{-9}
Wavelength	1064 nm	1064 nm	1550 nm
Optical Transmit Power:	0.7 W	2.2 W	1.0 W
Telescope Aperture:	125 mm	135 mm	60 mm
Mass:	35 kg	50 kg	5.0 kg
Power Consumption:	120 W	160 W	45 W
Volume:	$0.5 \times 0.5 \times 0.6\ m^3$	$0.6 \times 0.6 \times 0.7\ m^3$	5600 ml

[137] [138] [139]

The ground station selection is also effected and a multiple ground station separated by region approach is recommended due to atmospheric conditions blocking the signal (clouds, rain, thermic) or sensor saturation due to sunlight at one location.

4.3.4.4 Laser Frequency Up- and Downlinks

The data-rate of a given LCT is corrected [140] for distance LEO to EML-4 with the correction distance factor as a fraction of the reference distance and the new distance yielding a decrease of data-rate for increasing distances from the specified laser distance d_{laser} for a give data-rate R to the new distance d_{eml4} to the EML-4. The equation then yields

$$R_{cor} = R\left(\frac{1}{s_{cor}}\right)^2 = R\left(\frac{d_{laser}}{d_{eml4}}\right)^2 [bps] \quad 4.38$$

Table 58 shows the corrected data-rate with respect to the further distance of the Tesat and RUAG LCTs in Table 57.

Table 58: Corrected data-rates of laser communication terminals for distances of 406000 km.

	Tesat LCT-1	**Tesat LCT-2**	**RUAG Optel-μ**
Link:	LEO-EML-4		
Distance:	406000 km		
Data-Rate:	$8.876 \times 10^{-4} Gbit/s$	$2.211 \times 10^{-2} Gbit/s$	$1.517 \times 10^{-5} Gbit/s$

The Tesat LCT-2 could provide a data-rate of about 20 Mbit/s from a lunar distance to Earth. The configuration of the transmitting and receiving telescope and the transmit power of the diode stayed untouched. With a modification for high power LEDs, with bigger telescope aperture sizes and sensitive photon detectors the data-rate could be increased. For the TMA-0 satellite the LCT-2 is selected to be used as a COTS component. It is based on LCT-1 and it is partly space qualified. As the laser communication terminal for the EDR-Satellites, LCT-2 will be deployed and qualified for operation in 2014.

The RUAG Optel-μ is currently in development and has a tech readiness level of 6. The corrected data-rate is the lowest but it can serve as an alternative LCT. The laser wavelength can be changed from 1550 nm to the required 1064 nm by changing the laser source. The optical apparatus is almost not affected by this [55] [141]. RUAG conducted studies with applications for Optel-μ with distances to the Moon that even includes small satellites like ESMO [142] [143] [144]. Furthermore RUAG will provide parts of the optical ground station of ESA and NASA in Tenerife for the reception of signals from the LADEE mission [142] [145]. The telescopes that will be developed for the space and ground segments can serve as an alternative to the Tesat LCT-2 system.

The presented correction does not go into detail about atmospheric effects like refraction, scintillation, polarization and other sources of losses. TMA-0 shall demonstrate target pointing and signal handover. The achieved data-rate during demonstration shall be used to define the requirements of TMA-1 and to initiate further technology development.

4.4 Demonstrator Satellite Configuration

The phase 0 study of TYCHO focusses on the configuration of the demonstrator satellite mission TMA-0. The discussed components shall be qualified with the TMA-0 mission. Further modifications on the component or configuration are eventually to be done for the operational TMA-1 satellite. This chapter presents the demonstrator satellite configuration for the payloads, subsystems and a discussion about an alternative architecture based on available standard busses.

4.4.1 Payload

A set of instruments for inclusion in the TMA-0 satellite are presented in this chapter. These instruments address objectives related to the high data-rate communication service, to the EML-4 environment observation and the demonstration of the key technologies of the future TMA-1 satellite. In case that the entire accommodation of the instruments cannot be achieved the instruments are prioritized. Priority 1 instruments are the core payload for the minimum required payload for TMA-0 ensuring the technology demonstration.

4.4.1.1 Communication: Radio Frequency

There are two communication payloads for K-band and X-band frequencies. The link budgets are presented in Chapter 4.3.4.2. Typical settings for both systems are presented in this chapter.

High Data-Rate:

The assumption for each high data-rate channel via K-band is made for a simple, cold redundant system with switching between modulators and between the microwave power modules. Due to the link budget requirement of 400 Mbit/s and the system margin constraints each channel is planned for 100 Mbit/s and two channels with to circular polarizations are applied. For qualification one channel with both polarizations are used and it also allows redundancy. The K-band communication payload includes two radio frequency distribution units (RFDU). Both interface the same high-gain parabolic antenna. The high data-rate system is priority 1.

Inside the RFDU the electromagnetic wave is guided through WR34 wave guides that are specified for frequencies from 22 GHz to 33 GHz [146]. The lower frequency limit is fixed due to the geometrical constraints for the frequency propagation as an electromagnetic wave. The interaction of the electromagnetic wave and the metallic wall is the reason why the inner coating shall be gold or silver. The coating with these metals causes lower damping and losses, although the costs are higher. Nevertheless loss reduction directly at the RFDU source positively influences the link budgets. The assumptions on losses for different sections in the RFDU are presented in Table 59 [147].

Table 59: Losses for different sections in the RFDU

	Waveguide (silver, gold)	Waveguide flange	Switch & coupling network
loss	0.36 dB/m	0.1 dB	~ 2 dB

The K-band communication system for TMA-0 with one channel and two polarizations for transmission (TX) and reception (RX) including the redundancy concept is presented in Figure 50. For TMA-0 two radio frequency distribution units have to be multiplexed to the antennas and two additional receiver lines have to be diplexed. This concept already includes the Tesat TeTra modulator. The communication concept is based on a proposal by U. Beyermann (Tesat) [132] of a solution for the variable data-rate communication required for the TYCHO mission [132].

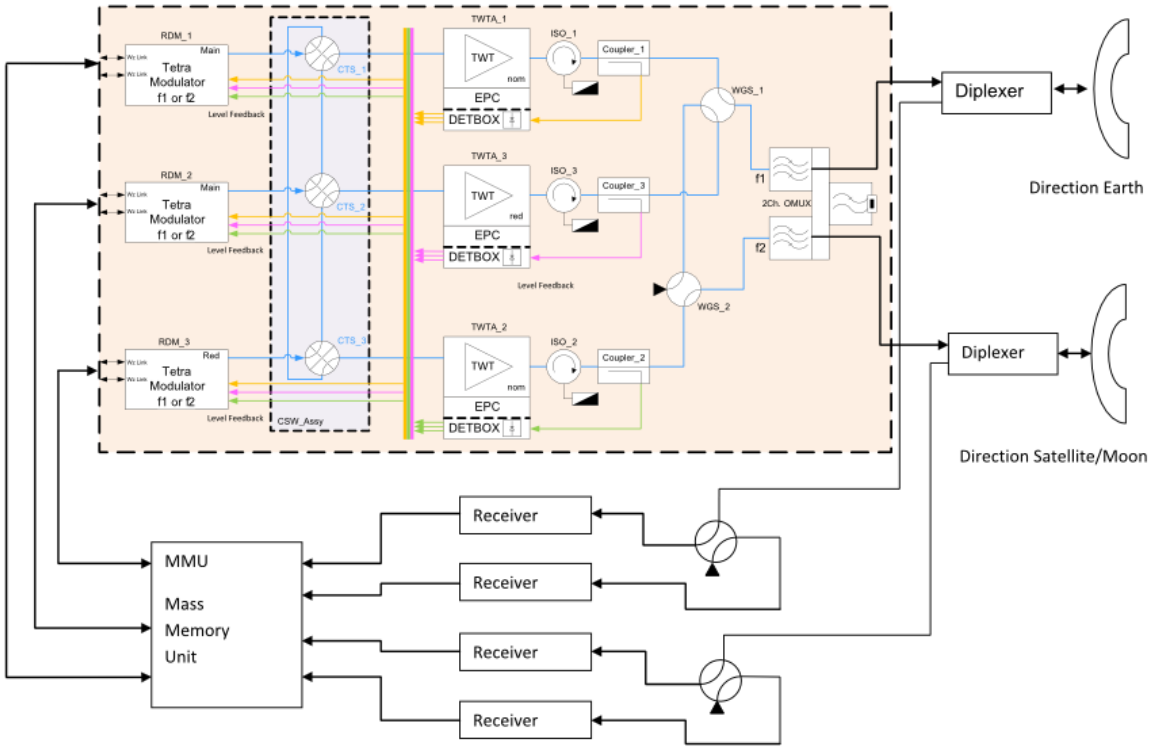

Figure 50: K-band communication system for TMA-0.

TWT: Travelling Wave Tube
EPC: Electric Power Conditioner
ISO: Isolator and Terminator
WGS: Wave Guide Switch

The system TeTra modulator is in development for a release in 2016. It offers a flexible setting of the data-rate as well as the frequency that can be changed by telecommand. It is currently the first world-wide in development that can offer it as stated by Tesat. This functionality shall be used to provide access to a wider range of users. By this modulator, users with smaller receiver antennas and lower data-rate can receive TMA-0 signals. Otherwise the system margin would have been fixed to certain broadcasting modes that would exclude users that are not compatible to those modes. An adaptive transmitter and receiver system solves this critical point. TMA-0 could also serve as a test bed for technology demonstration of the TeTra system.

TT&C

The TT&C communication payload in X-band shall comprise two systems with receivers in hot redundant mode and two transmitters in cold mode that are switched by a high priority command. The systems include Solid State Power Amplifiers (SSPA) and hybrid couplers. The RF is guided to two omnidirectional antennas that offer full 360° hemispherical coverage. The antenna design is considered as a corrugated flange (choke ring) waveguide or as helix antenna with wide coverage [148]. Typical data for the TT&C electronic equipment is used from space qualified “TTC X-Band Flexible Transponder” by Thales Alenia Space [149] and from Small Deep Space Transponder (SDTS) by JPL and General Dynamics [150] [151]. The TT&C system for this mission is considered to be a standard component as COTS hardware. The TT&C system is priority 1.

4.4.1.1.1 Steerable Antenna

The data-rate requirement of 400 Mbit/s requires a high-gain antenna with a diameter of 2.04 meters to achieve the needed system margin (Chapter 4.3.4.2). The resulting half-power beamwidth (HPBW) angle of 0.4°would be adequate to cover the Moon, but it does not cover the Earth (Chapter 3.2.3.4). The difference of 0.6° can be compensated by either changing the satellite’s attitude due to using the momentum wheels or by steerable antenna. Antenna pointing mechanisms shall be used because they can be used independently for each antenna from the attitude control. Furthermore they can be used to point to targets in Earth’s or Moon’s orbits. It requires pointing with even larger displacement angles of 6.6° [152] [153].

Larger antenna diameters would even narrow the HPBW and thus increasing the system margin. However the antenna diameter of is one of the factors for the payload envelope check that has to be derived from the selected launchers (Chapter 4.1). The payload envelope is defined by the smallest payload compartment of the launcher candidates. The current size allows the deployment of an unfolded antenna instead of a folded antenna, which reduces deployment risks. The single antenna concept for transmission and reception is a possible source for single point of failure. A medium gain horn antenna could be directly mounted and operated without deployment mechanisms.

$$d_a = \sqrt{3\lambda L} \tag{4.39}$$

Where d_a is the diameter of the cylindrical horn aperture, λ is the wavelength and L is the slant length of the cone from the apex. The length of the optimum conical horn with the same diameter and gain for reception would result in a slant length of 116.8 meter for a receiver horn antenna that is not applicable for 25.5 GHz.

To this extent, the TMA-0 satellite uses a high gain parabolic reflector dish antenna with a feeder/receiver horn because it is a compact size system with high gain reception and transmission. The optimum horn antenna can only provide a high gain transmission and a medium gain reception. Moreover, there are standard communication satellite busses like A 2100, Alphabus, BSS, LS 1300, SGEO and Spacebus with proven reliability and antenna systems [154] [155] [156] [157] [158] [159].

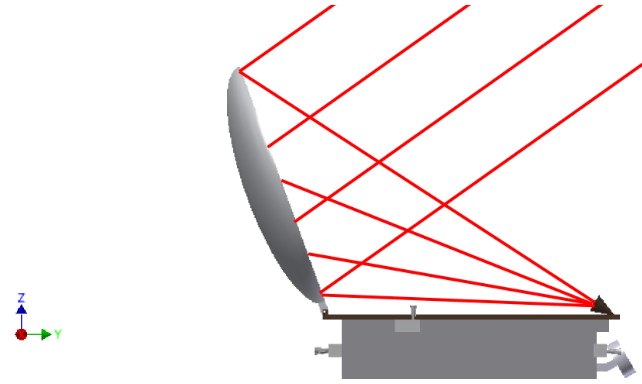

Figure 51: Parabolic antenna with offset feed

The antenna type should be an off-axis or offset feed. This allows a compact launch configuration with the antenna attached to the satellite's hull and deployed to sending configuration when the satellite is operational [160] [161].

4.4.1.1.2 Accommodation Requirements

The accommodations of the communication components have to fulfill the requirements of the communication links as well as the thermal conditions of the components. The parabolic antenna has to be mounted on the outside of the satellite in a way that it can be space-saving during launch and deployed before the operational phase (Figure 52).

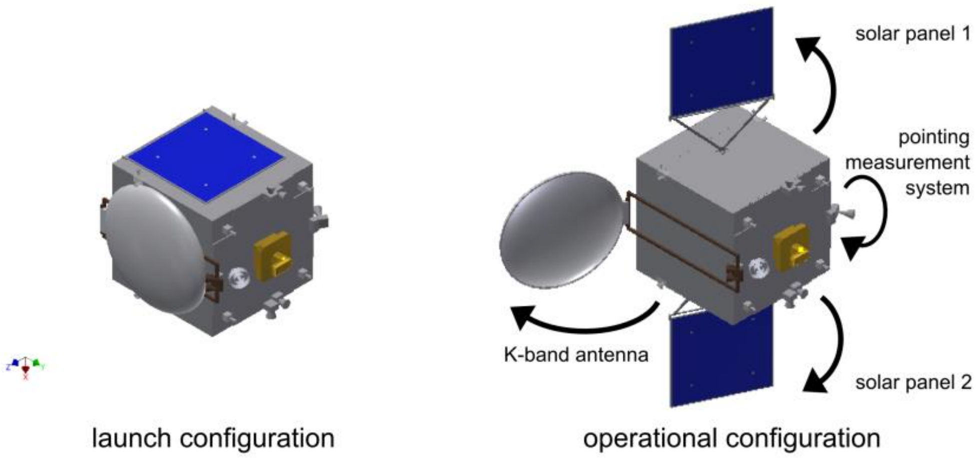

Figure 52: Launch and operational configuration

The mounting location of the communication electronics in the equipment compartment shall be interfacing the hull. This is due to high thermal loads generated by the electronics. The interfacing can be either achieved by mounting the travelling wave tubes (TWT) on the radiator if the thermal design concept requires it, or by heat pipes and loop heat pipes interfacing the elsewhere TWT and then conducting the heat to the radiators.

The thermal loads are typically between 60 – 65 % of the power consumption and this has to be radiated into space. Therefore a location at the hull interfacing a radiator is required for the TMA-1 TWTs (Figure 53). A side effect will be that due to the radiator the switch-on temperature of the TWT is under-run. A heater is required to bring the electronics temperature back to the specified switch-on temperature. Otherwise the electronics are run beyond the specification and the manufacturer guarantee expires.

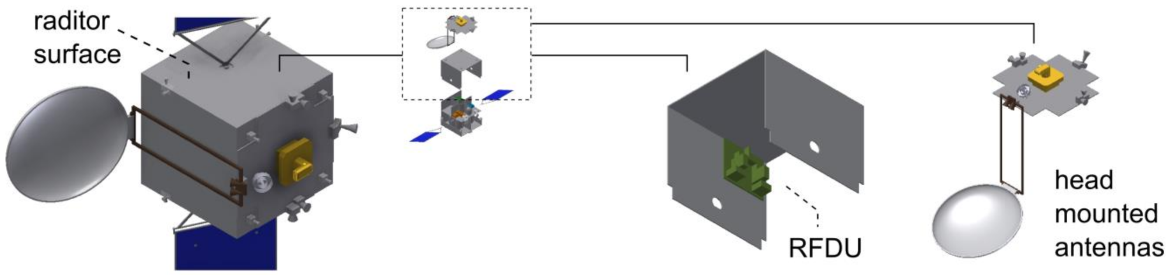

Figure 53: Radio frequency distribution unit allocation under radiator surface

4.4.1.2 Communication: Laser

The laser communication terminal for TMA-0 shall be COTS hardware. Tesat LCT-2 was selected in Chapter 4.3.4.4 due to the highest data-rate of all three candidates in Table 57 with 22 Mbit/s. Importantly, it will be space-qualified with the application onboard of EDR-Satellites until 2014 and thus several copies have been built. This will keep development time and costs low. The RUAG Optel-μ could be a backup candidate in case of modification to change the wavelength from 1550 nm to the required 1064 nm and in case of modifications that will provide higher data-rates.

All analyzed LCTs already include 2-axis control for high-precision targeting which is required for demonstrating the flexible retargeting between several communication access points. The LCT system is priority 1.

4.4.1.2.1 Accommodation Requirements

The LCTs are rather bulky and cannot and should not be placed on the hull area, where the parabolic antenna is mounted. Otherwise it interferes with the antenna in transport configuration and can be blocked by it. It cannot be used as a redundant communication link then. The LCT should be mounted on the front end of TMA-0 where it is possible to target the Earth as well as other targets. This location on TMA-1 would also allow targeting locations on Earth as well as on the Moon, because the other hull areas are reserved for the second antenna, the solar panels and the apogee kick motor and adapter ring. To respect this configuration the TMA-0 location reflects this aspect (Figure 54).

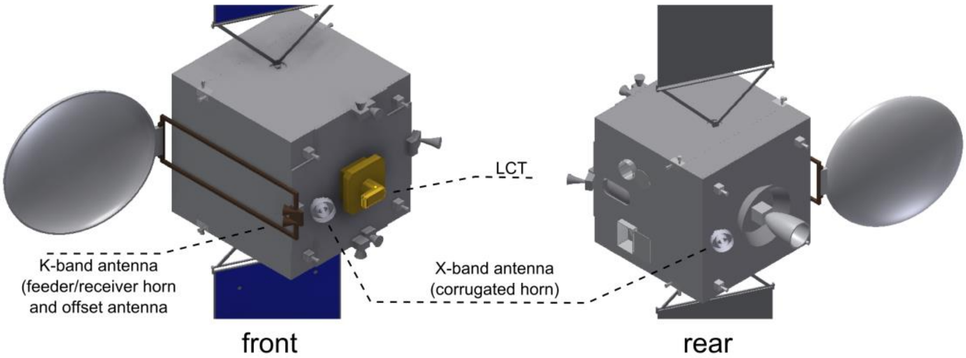

Figure 54: Antennas accommodations

4.4.1.3 Pointing Measurement System

TMA-0 demonstrates the communication links only towards Earth. Nevertheless the pointing accuracy of the satellite and thus the RF link towards Moon has to be determined. This shall be realized with a combined measurement with the inertial measurement unit (IMU) on board and an additional camera system. The IMU includes acceleration and rotation measurements, Sun- and star trackers for the attitude control. This can be used for the pointing-knowledge accuracy [162].

The additional camera system shall be mounted on the location instead of the second parabolic antenna for the Moon link, that is not demonstrated with TMA-0. The camera system shall provide a direct pointing accuracy of the satellite pointing mechanism. In this way both pointing direction, the active RF link to Earth and the virtual link to the Moon can be determined. The camera shall be optical and COTS to keep the costs low for this additional measurement.

Table 60: Camera systems for optical Moon pointing measurement

	MSSS: ECAM-C50	**SSTL: VHRI 250**	**GOMspace: NanoCam C1U**
	CMOS array sensor for 450 nm – 750 nm	Linear imager for 450 nm – 1000 nm	CMOS array sensor for 450 nm – 1000 nm
Pixel	2560 x 1944	~5312	2048 x 1536
Focal length	customized	3360 mm	35 mm
FOV	15°	±0.84° x ±0.23° (±0.87° diag.)	9.22°
GSD	46.39 km	1.29 km	35.51 km
Power	1.75 W (idle), 2.5 W (imaging)	55 W	0.36 W (idle), 0.63 W (imaging)
Mass	0.256 kg + 0.1 Kg	41 kg	0.166 kg

[163] [164] [165] [166]

The pointing determination system is used for visual positioning of the Moon and pattern recognition on the lunar surface. So the cameras in Table 60 are chosen for the optical range of 450n – 750 nm. In addition the systems are off-the-shelf products.

The SSTL VHRI 250 is a linear imager and is categorized as an instrument class by its mass and power consumption. It is solely respected for the imaging of the lunar surface during the libration tumbling and when if the TMA-0 satellite is on the maximum allowed orbit distance to EML-4. Then the Moon's libration period of also 27.3 days and the relative movement of the satellite allows to measure with VHRI 250. It can be considered as a full separate payload and is not considered for TMA-0.

The GOMspace NanoCam C1U array sensor camera offers the most cost saving option, but it is not yet space qualified.

The ECAM-C50 system of Malin Space Science Systems (MSSS) is a space qualified CMOS (Complementary Metal Oxide Semiconductor) system, that was the basis for the Lunar Reconnaissance Orbiter Camera (LROC) [163] [164]. It is designed for a radiation dose of 5 years in GEO and a design life of 10 years under radiation environment. MSSS custom optics can be from 15 to 180° and additional motorized focus adjustment and zoom lenses can be included [167].

$$GSD = \frac{\tan\left(\frac{FOV}{2}\right) * d}{n_{pixel}} \qquad 4.40$$

The ground sample distance (GSD) is derived from the geometrical relation of the field-of-view FOV of the camera and the distance d to the observed object and the number of pixels (row or column) n_{pixel} of the sensor [168]. With the minimum FOV of 15°and a distance of 405000 km, the GSD is around 40 km. So optics with a smaller FOV or a mechanical zoom should be considered in case topographic features have to be clearer. With respect to the camera reference frame the center of Moon can be used for the pointing accuracy determination [169] [170].

The presented camera systems do not fulfill the requirement for the pointing measurement system. The target pointing accuracy of the satellite shall be within the range of $\pm 0.001°$. This shall be provided by the reaction wheels and pointing mechanism. This allows a target pointing of the peak transmit power on a ground sample distance of about ± 7 km on the Moon from EML-4. With the 2048 pixels of the sensor the required FOV would be about 4°. So the optics of the camera should provide the maximum FOV or smaller. The presented FOV and GSD can be used for digital image processing for the determination of the center of the Moon surface and a determination of the relative angular position of the center of the Moon to the camera pointing direction. The GSD is also small enough to resolve the categorized impact craters in Table 61 with several pixels [171]. These can be used for markers on more precise determination of pointing and rotation angles [169].

Table 61: Lunar crater categorization

Type	Archetype Crater	Diameter
ALC	Albategnius C	$\leq$ 10 km
BIO	Biot	10 – 15 km
SOS	Sosigenes	15 – 25 km
TRI	Triesnecker	25 – 50 km
TYC	Tycho	$>$ 50 km

The visual sensing of the Moon supports the target pointing determination and is an option. The attitude and orbital determination sensors are the main source for the attitude and thus for target pointing determination. The required information for the target pointing accuracy determination can be derived from the navigation and tracking data alone. In the following study it could be decided to withdraw the camera system.

4.4.1.4 Dust-Detector

The disputed Kordylewski cloud in EML-4 could pose a threat to the satellite and the mapping of the surrounding and the influence of the satellite is an important part of the TYCHO demonstrator mission. The expected dust particle movement is in the range of 10 – 100 m/s relatively to the satellite because the satellite is also moving in the stable zone of the EML-4 point. The other dust particle or micro meteorite class is planetary or stellar particles. Their velocities range from 10 – 40 km/s.

For the detection of both particle classes, three dust detectors have been identified in collaboration with Dr.-Ing. Ralf Srama from the Institute for Space Systems (IRS) at University of Stuttgart and Max Planck Institute for Nuclear Physics (MPIK) [172] (Figure 55).

The Phobos Dust Detector (a) from von Hoerner & Sulger GmbH is a trajectory sensor composed of different grid layers, which are charge sensitive. The position at each layer and the time of the particle transition is measured and the measurement is stopped when the particle hits the impact detector. It was designed for the Phobos Grunt Sample Return Mission (SRM) [173]. For dust detection in clouds it can measure impacts with low kinetic energies on a wide sensor area.

In general, a relatively wide and sensitive sensor area is beneficial for the planned measurements. A sensor area with only 10 cm x 10 cm dimension is too small for all particle populations (Clouds, interplanetary, interstellar). The Small Leopard (SLEO) (b) dust detector developed at the IRS and MPIK combines a trajectory sensor (squarish part) with an impact spectrometer (round part). It allows a measurement of the direction and relative velocity as well as the kinetic energy and mass of the particle expected from the cloud [174].

Solar Orbiter Dust Analyser (SODA) (c) is in development at Astrium and Institut für Astrophysik Göttingen. It is a highly sensitive impact ionization dust detector. It combines a mass analyzer and a trajectory sensor for sub-micron-sized particles (10^{-17} kg at 20 km/s). It is derived from the Stardust CIDA and Cassini CDA instruments. The detector is considered for the detection of planetary dust due to the sensitivity in their velocity range [175].

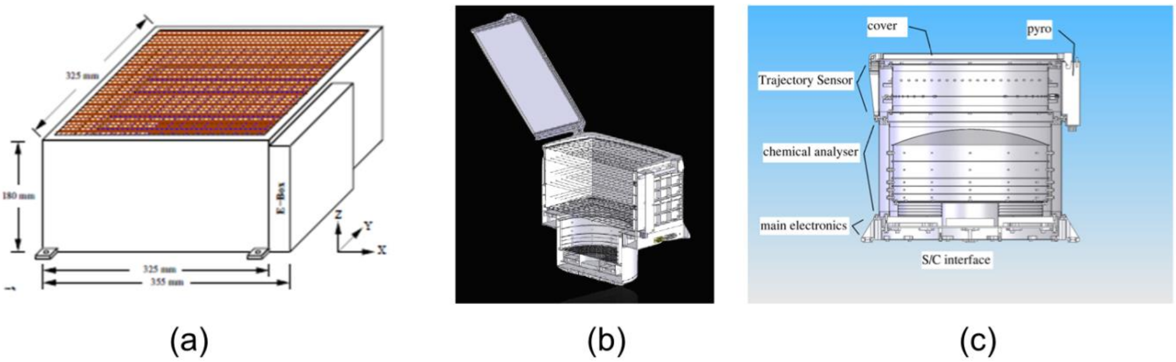

Figure 55: Dust detectors
(a) Phobos Dust Detector, (b) Small Leopard (SLEO), (c) Solar Orbiter Dust Analyzer (SODA)

As a combination of (a) and (c) the SLEO detector (b) is recommended as priority 1 for the science payload. SODA (c) has priority 2 for accommodation because the main detection objective is the Kordylewski cloud and because of the current development status (Table 62).

Table 62: Dust detector system parameters

	Phobos Dust Detector	**SLEO**	**SODA**
Sensor Type	Trajectory/Impact	Trajectory/Impact and Mass Analyzer	Trajectory/Impact and Mass Analyzer
Particle Mass Velocity	$10^{-16} - 10^{-7}$ kg at 0.5 - 10 km/s	$10^{-18} - 10^{-9}$ kg at 0.01 – 2.0 km/s	10^{-17} kg at 20 km/s
Dimensions	355x325x180 mm³	tbd	⌀263x237 mm³
Mass	2.5 kg	4.3 kg	2.7 kg
Power / Voltage	9.53 W / 28 V	10 W / 28 V	9.8 W / 28 V
Data-Rate	1 Kbit/s	16.8 Kbit/s	8.2 Kbit/s

4.4.1.4.1 Accommodation Requirements

The positions of the detectors are rather flexible due to their small dimensions and the possibility to attach them on the outer hull (Figure 56). The detectors' particle intake opening are facing towards space and they are not in close distance to covering antennas or solar panels. The current models for the Kordylewski cloud dust density are not validated and density, particle sizes and velocity vectors are still disputed. Thus a preferred direction of the particle impact is still to be determined. For this reason the position of the detector is either independent from the flight direction or a multi sensor approach on different mounting positions has to be considered because the preferred impact direction cannot be fully eliminated. The current design includes the SLEO and SODA sensors on the remaining uncovered satellite side in opposition to the flight direction. An attitude change for pointing the inlets to other directions relative to the flight directions is required for the dust impact direction measurement. Determination of the dust density and velocity vector of the particles are of scientific interest as well as for the TMA-1 design.

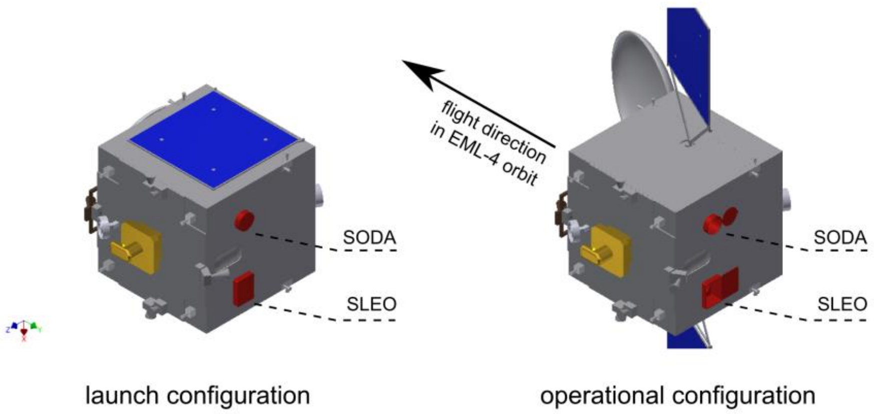

Figure 56: Dust detectors accommodation in TMA-0 and opening mechanism

4.4.2 Propulsion

The propulsion system design is one of the main aspects of this study because it influences several mission objectives. Besides offering the ability to reach the target orbit it affects the orbit design with station keeping and the disposal phase. It is used in combination with the attitude control for desaturation of the reaction wheels and as reaction control system (RCS). Attitude control thrusters improve redundancy for those reaction wheels. It also affects the mission lifetime with respect to storable propellants or the capability for re-ignitions of the engines. And lastly safety aspects for ground handling during fueling and costs have to be considered.

For the TYCHO mission a bi-propellant propulsion system with Mixed Oxides of Nitrogen and Monomethylhydrazine (MON/MMH) propellant combination for the main apogee kick motor and the AOC system has been selected instead of another bi-propellant, mono-propellant, cold-gas or electrical systems. Furthermore a brief outlook of applications and implications of green propellants for both systems is given.

4.4.2.1 Propellant Combination

The selection of the oxidizer and fuel combination for the propellant system shall fulfill the mission requirements of re-ignitions during transfer, station keeping and disposal phase, it shall be storable during the operational mission time of 10 years and of course allow transferring and injecting the satellite into the target orbit within mission time. Alternative options are briefly discussed in the following paragraphs.

Cryogenic propellants like hydrogen and oxygen provide a higher ISP, due to the small molecular weight of the propellants and their reaction products, are stored under cryogenic conditions and a certain percentage of leakage occurs due to boiling and degassing losses. This combination also needs an additional ignition by hydrazine or an ignition system. For the TMA-0 mission this introduces additional complexity, without providing additional benefits and was thus discarded.

Electrical propulsion offers the highest ISP and can also be used for perturbation compensation in the station keeping orbit and is increasingly used on GEO satellites. But the transfer as well as the injection into the EML-4 orbit takes either noticeable longer time or an additional chemical propulsion system. In case of ion drives the propellants are most often halogen gases with higher asset costs for the gas. In addition, the requirements for the electrical power system and electronic systems are higher. Thus the additional complexity also does not provide additional benefits and was thus discarded.

Hypergolic propellants are recommended for the TYCHO mission. The hypergolic properties allow chemical reactions on contact with both reaction partners or even with contact of one with a catalyst. They can be stored under standard temperatures over a long period of time and the thruster and propellant feed lines are simpler systems with proven heritages on telecommunication satellites. They also demand special handling within strict safety regulations due to their adverse health effects because they can be carcinogenic or corrosive even with organic molecules (Registration, Evaluation, Authorisation and Restriction of Chemical substances REACH [176]). Further future implications of REACH are discussed in Chapter 5.1.1.2.

Besides the hypergolic propellants that are used in bi-propellant thrusters there are also mono-propellant thrusters using propellants that are only passed on a catalyst which causes decomposition of the molecule into gaseous components. Mono-propellant thrusters are simpler systems compared to bipropellant systems and provide a high reliability. The mono-propellant systems are discarded for the following reasons:

- providing less ISP (Table 32) than bi-propellant system
- leading to more complex designs when used in dual mode (different propellant tank sizes)
- no possibility of redundancy thrust concept for the orbit maneuvers

Both, hypergol and monergol propellant can be either conventional propellant or the upcoming green propellant. Green propellants offer the same basic chemical reactions and similar or even higher ISP levels. In this regard they are less harmful to our environment, have fewer operational hazards and are government-funded to replace the conventional propellants (REACH) [176] [177]. Green propellants are still disregarded for this concept due to the current low technology readiness level, but should be analyzed as an application for TMA-1 during the following study.

For TMA-0 the analyzed propellants are chosen according to thrusters available on the market. For the apogee kick motor and the AOCS thrusters the propellant combinations of consideration are Mixed Oxides of Nitrogen and Monomethylhydrazine (MON/MMH) or Mixed Oxides of Nitrogen and Hydrazine (MON/N2H4).

4.4.2.2 Chemical Propulsion Concepts

The propulsion system can be designed as a universal mono-propellant, a universal bi-propellant system or in dual-mode

In dual-mode the high efficiency of bi-propellant systems is combined with the reliability and simplicity of mono-propellant systems. The propulsion system works in bi-propellant mode during the orbit-raising maneuvers when high-impulse is needed to reduce gravity losses. After injection into the target orbit the mono-propellant system is used for propulsion during AOCS trading a higher impulse against reliability. In case of a MON/Hydrazine dual-mode both propellants are used for the transfer and only hydrazine for AOCS reaction thrusters.

Dual-mode offers an advantage when the delta-v needed for transfer is significantly higher than that of the station keeping phase. For the TYCHO mission a universal bi-propellant system with MON/MMH shall be used. This is due to the fact that a dual system would favor a propellant combination of MON/Hydrazine because of the higher ISP compared to MON/MMH. But the analysis shows (Table 65 and Table 66) that even though some mass of propellant can be saved during transfer, the less efficient mono-propellant system with hydrazine needs more propellant during station keeping than the MON/MMH bi-propellant system. On the other side dual-mode is considered when simple and reliable systems are required. They also able to provide low thrust levels of 1 - 4 N and thus smaller MIBITs due to the simple reaction or even due to intentionally aborted decomposition of the propellant, whereas bi-propellant thrusters provides thrust levels of 4 N and more (Table 32). In this way more precise attitude and orbital control is possible.

Another advantage of the MON/MMH bi-propellant system is the combustion besides the stoichiometric mixture ratio. Stoichiometric combustion is the ideal combustion but does not lead to the highest ISP that is possible with the propellant combination. Nevertheless the reaction happens at maximum combustion temperature. The ISP can be modified by a change in mixture ratio when the generated energy is applied to the velocity of unburned propellant products. This results in higher ISP for products with smaller average molecular weights. This is accompanied with lower combustion temperatures that are advantageous for the nozzle and system life-time.

An analysis of ISP, temperatures and density with NASA Chemical Equilibrium with Application (CEA) [178] software is used for the system trade between MON/MMH and MON/Hydrazine. The trade is made with respect to the recommended mixture ratio, where fuel and oxidizer allow a reaction of the same volumes of both reaction partners. This offers the usage of tanks with equal sizes for both propellants. Table 63 shows that the stoichiometric combustion of MON/Hydrazine is near to the required volumetric mixture ratio. Due to the ideal combustion of both reaction partners, the temperatures in the injector and the nozzle exit are higher compared to the temperatures of the MON/MMH combustion with volumetric mixture ratio.

Table 63: Propulsion mode comparison for ISP and temperatures

Propulsion Mode Comparison				
	MON / MMH		MON / Hydrazine	
Oxidizer / Fuel	N2O4	CH6N2	N2O4	N2H4
Density [kg/m³]	1443	880	1443	1021
Molar Mass [kg/kmol]	92.001	46.07	92.001	32.045
	stoichiometric	volumetric 1:1	stoichiometric	volumetric 1:1
Mixture Ratio O/F	2.27	1.65	1.4	1.41
Ideal Vacuum ISP [Ns/kg]	3356	3261	3387	3386
Temperature Injector [k]	3174	3023	3076	3072
Temperature Nozzle Exit [k]	1362	912	1176	1171

Typically the mixture ratio of MON/Hydrazine is 0.85 to lower the temperatures (Table 64). This lead to an ISP that is comparable to that of MON/MMH with 1.65 mixture ratio (Figure 57). However the mixture ratio does not allow equal tank sizing.

The trade-off for the propulsion mode is based on the thrusters in Table 64. The highest ISP for the apogee kick motor and the lowest ISP for the AOCS thruster is found for the dual mode system with MON/Hydrazine propellant combination.

Table 64: Thruster operation parameters

Thruster	Name	Oxidizer	Fuel	O/F	Thrust	ISP
TH1	EADS EAM	N2O4	CH6N2	1.65	500 N	325 s
TH2	EADS 22 N	N2O4	CH6N2	1.65	22 N	290 s
TH3	Aerojet HiPAT DM	N2O4	N2H4	0.85	445 N	329 s
TH4	Aerojet MR-103M	-	N2H4	-	4 N	221 s

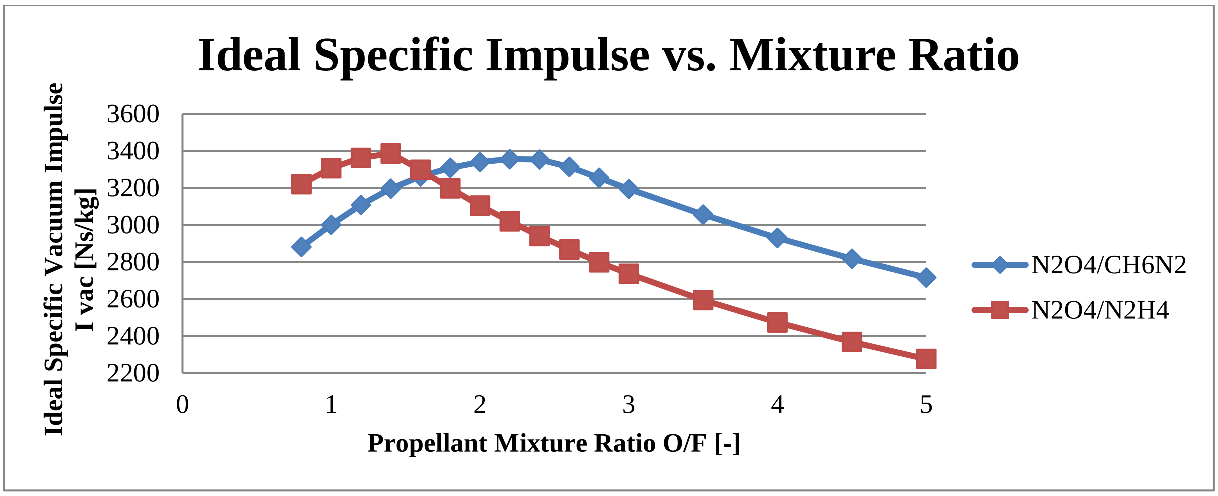

Figure 57: Ideal specific impulse of a MON/MHH and a MON/Hydrazine thruster
with chamber pressure *Pc*=9bar and exit-to-thrust-area ratio *Ae/At* = 45 for each data point

Besides the high flight heritage, one major advantage of a universal MON/MMH system for transfer and station keeping is that the volumes of both propellants are equal. The analysis in Table 65 shows that the mixture ratio of 1.65 during all maneuvers leads to the same propellant volumes in both tanks. In Table 66 the dual-mode system using MON/Hydrazine with the typical mixture ratio of 0.85 is presented. It is shown that both fuel tanks have different sizes. Equal tank sizes are very attractive from configuration point of view because this leads to the same sized tanks for oxidizer and fuel reducing efforts for tank design, placing, procurement and lastly weights.

Table 65: Propulsion system – universal bi-propellant mode

Phase	Thruster	$\boldsymbol{m_0}$ [k]	$\boldsymbol{m_{ox}}$ [kg]	$\boldsymbol{m_{fuel}}$ [kg]	$\boldsymbol{vol_{ox}}$ [m³]	$\boldsymbol{vol_{fuel}}$ [m³]
Transfer	TH1	2300	547	331	0.379	0.337
AOCS	TH2	1422	62	37	0.043	0.043
EOL	TH2	1323	50	31	0.035	0.035
Total Propellant			659	399	0.457	0.457
Tank Mass (a)			29	29		
Propellant + Tank Mass			**1116 kg**			

Note: Including margins for Transfer and EOL (5%) and AOCS (20%)
(a) Tank: "235 to 516 Litre Bi-propellant Tank: Model OST 01/X" (EADS)

Table 66 Propulsion system – dual mode

Phase	Thruster	$\boldsymbol{m_0}$ [k]	$\boldsymbol{m_{ox}}$ [kg]	$\boldsymbol{m_{fuel}}$ [kg]	$\boldsymbol{vol_{ox}}$ [m³]	$\boldsymbol{vol_{fuel}}$ [m³]
Transfer	TH3	2300	400	470	0.277	0.461
AOCS	TH4	1430	-	129	-	0.128
EOL	TH4	1301	-	103	-	0.102
Total Propellant			400	703	0.277	0.690
Tank Mass (b,c)			21	40		
Propellant + Tank Mass			**1164 kg**			

Note: Including margins for Transfer and EOL (5%) and AOCS (20%)
(b) Tank: "700 to 1108 Litre Bipropellant Surface Tension Tank" (EADS)
(c) Tank: "282 Litre Bipropellant Surface Tension Tank" (EADS) [179].

All tank masses are added into the propulsion subsystem budgets. The combined tank and propellant mass is obviously less for the universal bi-propellant mode leading to a higher satellite dry mass. As yet another valid point, the selected tank for dual mode can be scaled according to the propellant volume. For the propulsion system budget the tank mass is scaled, but it also offers a flexibility to customize the tank.

The pre-selected tanks and thrusters are manufactured by EADS Astrium and are space qualified, are specified for the storage of the hypergolic propellant for minimum 10 years and offer a European heritage. With respect to the Aerojet thrusters, they do not offer less propulsion mass, require to different sized tanks and do not have a European heritage. The recommended thrusters and tanks are therefore for the universal bi-propellant MON/MMH propulsion mode (Table 65). The structural design in phase B, the redundancy by using the AOCS thrusters instead of the apogee kick motor and the reduced costs for development of the tanks and propulsion system all benefit from the MON/MMH mode.

As an additional note the tanks have to be conditioned to not contain traces of organic molecules like fat or lubricants because of the aggressive corrosiveness of the hypergolic propellants. Contact with organic molecules causes heavy reactions that also influence the tank material. Special handling is required.

4.4.2.3 Propulsion Subsystem

4.4.2.3.1 Thrusters

The apogee kick motors presented in Table 28 are analyzed with respect to their efficiency. The simulation results are presented as the ratio of the effective thrust F for apoapsis rising over the initial mass m_0 in relation of the velocity increment Δv, mass decrement Δm and burn time t_{burn} required for the transfer. This shows the performance of each thruster.

$$\frac{F}{m_0} = \frac{\Delta m}{t_{burn}\, m_0} \Delta v \qquad 4.41$$

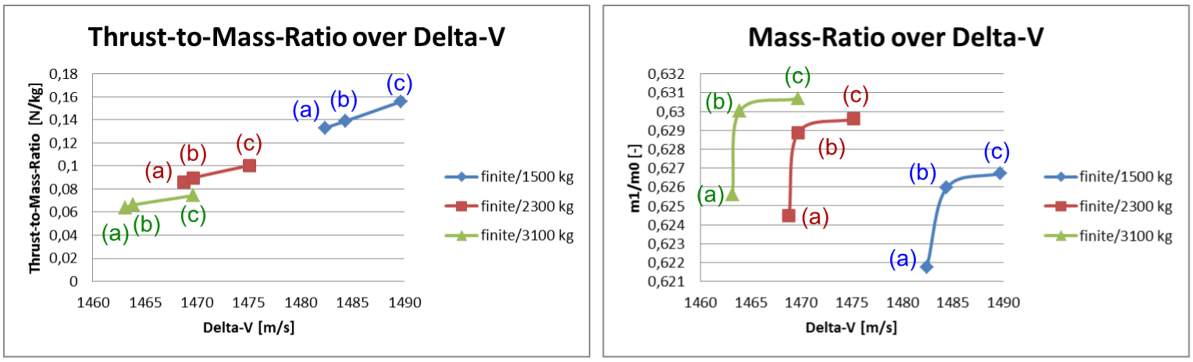

Figure 58: Thruster performance comparison between simulations with finite burns
Thrust to mass ratio over delta-v and mass ratio delta-v
Thrusters: (a) S400-12 420 N, 318 s (b) HiPAT 445 N, 323 s (c) EAM 500 N, 325 s

Figure 58 shows for each satellite mass class (1500 kg, 2300 kg, 3100 kg), the thrust-to-mass ratio over delta-v and the mass-ratio over delta-v for the realistic finite simulations. The delta-v is calculated with the Tsiolkovsky rocket equation from the mass ratio m_1/m_0 of the end mass to the initial launch mass of the simulated transfer and also from the thrusters' exhaust gas exit velocity v_{exit}. In this way it includes losses due to finite burns and gravity.

$$\Delta v = v_{exit} \ln\left(\frac{m_1}{m_0}\right) \qquad 4.42$$

The delta-v range for all nine data points are in a close range between 1460 m/s up to 1490 m/s and the results for each mass class are in delta-v range of 10 m/s. Even though the burn times of the 1500 kg satellite mass class are shorter and the required delta-v is higher leading to higher demands in propellant and thus to a lower m_1/m_0 ratio. The results indicate an optimization problem between the burn duration and the velocity increments of the transfer. Also the mass class is affected.

The EAM 500N thruster with an ISP of 325 s is selected for the design because it offers for each mass class the highest efficiency and the highest end mass m_1. The selection of thrusters with higher ISPs is also considered for the AOCS thrusters and the propulsion mode. The higher ISP of bi-propellant thrusters compared to mono-propulsion thrusters is another advantage.

Besides the EADS EAM 500 N thrusters as an apogee kick motor, the EADS 22 N Bipropellant Thruster is recommended for the attitude and orbital control system (AOCS) (Figure 59). The final selection for the 22 N Bipropellant Thruster also requires a later affirmation for the minimum impulse bit as an additional selection criterion in the AOCS Chapter 4.4.3.2. In case of re-design of the propulsion system during the following study the EADS 10 N Bipropellant thrusters are the alternative selection. All thrusters are or will be space qualified in 2013, fulfill the bipropellant requirement and have European heritage.

4.4.2.3.2 Propellant Feed

The propellants have to be transported from the tanks to the combustion chamber. This shall be done with a regulated pressure system instead of a blow-down system. The pressure stays constant and gives a constant propellant flow and thus thrust. The pressure gas is stored in one or more separated tanks that can be systematically placed to balance the satellite system. With a blow-down system the gas is stored within the propellant tanks and the pressure will decrease with the propellant consumed. It also needs larger and heavier propellant tanks [105]. With larger tanks and a free surface of the liquid propellant sloshing has a bigger effect on the satellite system and dynamics right from the beginning. This can be minimized by tank bladders or diaphragms for blow-down systems. Minimal sloshing effects are also an advantage of mono-propellant propulsion systems.

The pressure gas shall be helium instead of nitrogen because the density and thus the gas mass are smaller (Table 67). By this the supply tank volume can be smaller. The regulated pressure system feeds pressure gas into the propellant tanks as long as the complete propellant volume is replaced with the pressure gas. This is achieved with a high-pressure gas in the reservoir tanks that is higher than the operational pressure of the thruster. By this the propellant fluids are pressed into the feed lines and to the combustion chambers.

For the design the maximum operational pressure (MEOP) is used that results in the maximum amount of pressure gas mass. The “235 to 516 Litre Bipropellant Tank: Model OST 01/X” has a MEOP of 17.5 bar that allows to feed the EAM 500 N thrusters with an operational pressure range between 11 and 18 bar. The pressure gas tanks store gases with 310 bar [180]. The amount of the replacement pressure gas is designed to fill the empty propellant tank with 17.5 bar. At the beginning the propellant tank pressure is lower to be able to compensate the increasing pressure by temperature changes. This is controlled by a pressure regulator system.

For the calculation of the pressure gas masses and volumes in Table 67 the NIST software by National Institute of Standards and Technology is used [181]. The storage is assumed to be under 313.25 K and with isothermal properties.

Table 67: Physical properties of pressure gases helium and nitrogen

	Density	
Pressure	**Helium**	**Nitrogen**
17.5 bar	2.6519 kg/m³	18.711 kg/m³
310 bar	41.687 kg/m³	286.11 kg/m³

The calculation is done for one propellant tank, because storing the gas in two tanks would increase the total tank mass. The helium mass is considerably smaller than nitrogen with a similar tank volume (Table 68). Due to additional volumes where the pressure gas will be in (feed lines and the pressure tank itself) or due to losses, the fill pressure will be a little bit higher than 310 bar or the tank volume will be slightly bigger. Nevertheless this gas mass and the tank mass itself has to be added to the mass budget. This additional propellant mass, which is not considered for the combustion before, reduces the satellite dry mass. For the small volume needed, it can be decided to use one pressure tank or to split the volumes and distribute it among several tanks with the advantage of using this tanks for balancing the satellite (Figure 59).

Table 68: Pressure gas mass and volume comparison between helium and nitrogen

	Helium		**Nitrogen**	
Propellant Tank @ MEOP	Mass	Volume @ 310bar	Mass	Volume @ 310bar
0.914 m³	2.42 kg	0.058 m³	17.1 kg	0.059 m³

Note: Tank volume from Table 65

The presented pressure tanks by ATK [182] (Table 69) are composite overwrapped pressure vessels with a space qualified Selene tank and with space qualification of the Small GEO tank in 2014. ATK offers rescaling of the tanks for TMA-0. Both tanks are candidates, because the Selene tank offers less mass and the Small GEO tank is used for European missions. However the Small Geo tank volume is too small and needs customizing. So the masses for helium and the pressure tank are included in the mass budget.

Table 69: Helium pressure tanks by ATK

Helium Pressure Tanks by ATK			
Program	**Volume**	**Operating Pressure**	**Mass**
Selene	0.067 m³	310.26 bar	10.16 kg
Small GEO	0.051 m³	309.98 bar	12.47 kg

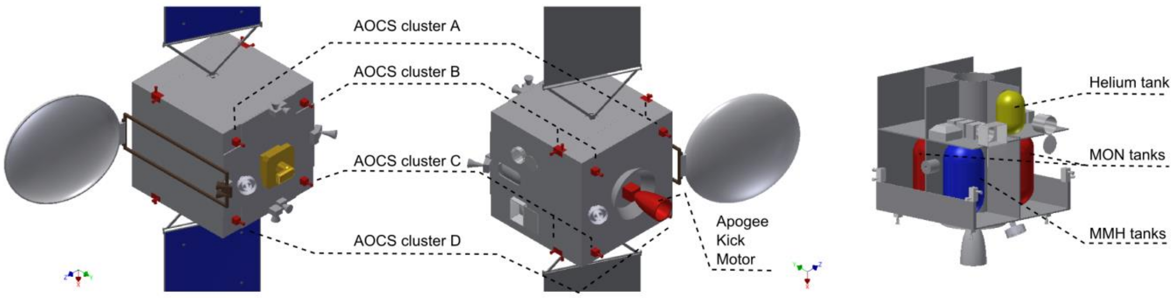

Figure 59: Accommodation of apogee kick motor, AOCS thruster clusters and propellant tanks

The propulsion system layout is presented in Figure 60. It includes the propellant and pressure gas tanks, the feed lines and the apogee kick motor and AOCS thrusters. For redundancy and safety during filling procedures or during operation, the pyro valves and pressure transducers are included. Several service valves are included for fuel the different tanks. The layout is in the style of the EADS Alphabus system [159].

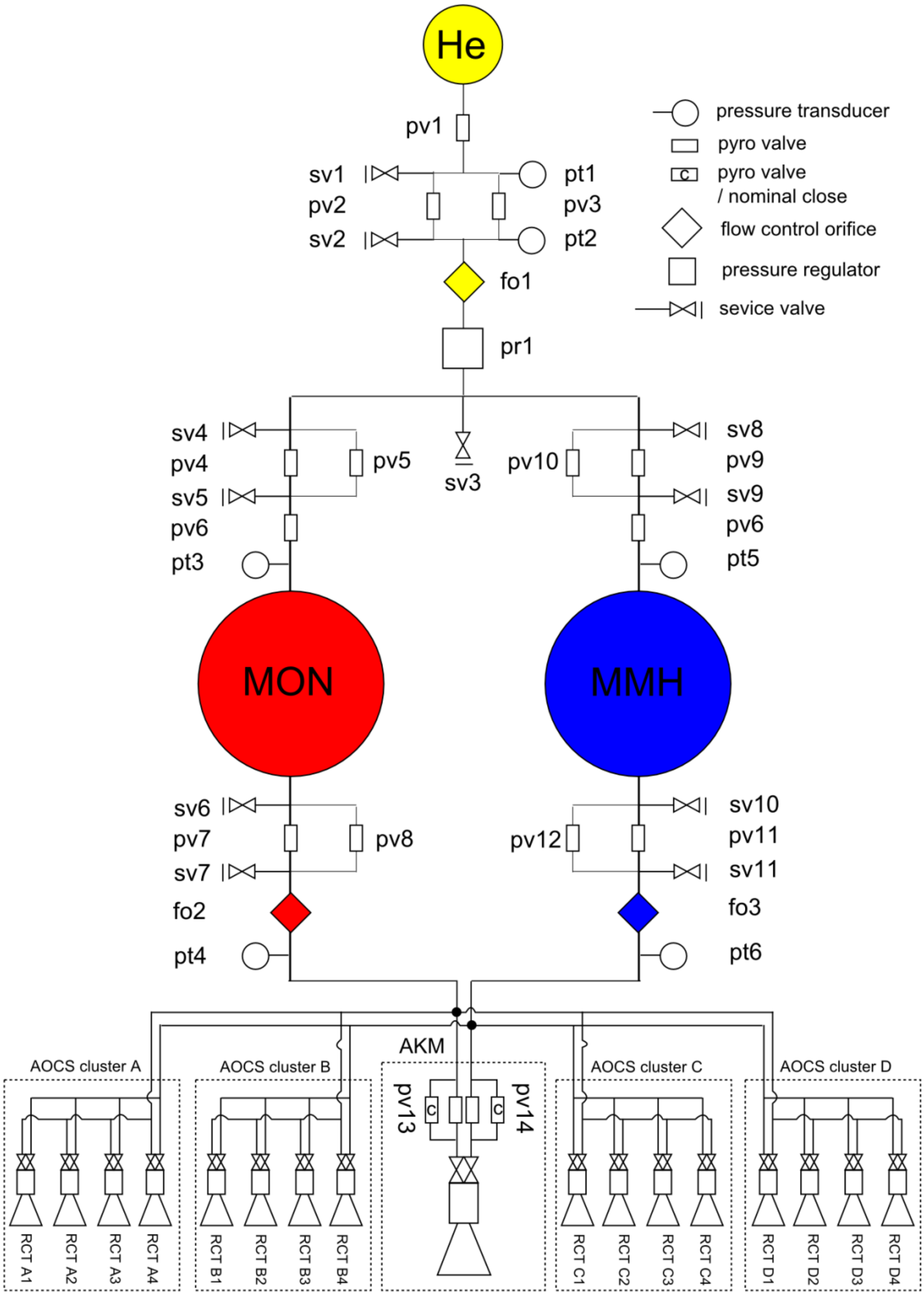

Figure 60: Propulsion system layout

4.4.2.3.3 End-of-Life Maneuver Consideration

For the TYCHO mission a disposal trajectory is part of phase F. After the three years of demonstrator mission time, the TMA-0 satellite will be transferred to the Moon and crash landed on the surface. For this transfer the apogee kick motor shall be used. Certainly the motor was put into secure condition. In this mode the main propellant feed lines where closed with pyro valves so that no remaining propellant can accidentally get into the combustion chamber and ignite or can be expelled. For the disposal transfer the motor has to be activated again and thus a second feeder line valve for each propellant has to be opened to allow propellant transport to the injectors of the main kick motor (AKM). The two valves are set to nominal open and nominal closed for the transfer (pv13 and pv14 in Figure 60). The first pyro valve closes the valve and secures the motor and the second pyro valve will open the feed line again for the end of life disposal. The remaining residual propellants in the tanks after the transfer maneuver [112] also have to be kept inside the tanks and feeder lines.

4.4.3 Attitude and Orbital Control Subsystem

The TMA-0 satellite requires an attitude and orbital control subsystem (AOCS) (Figure 61) for determination of the satellite's attitude and orbital position. With the information of attitude and orbital position the actuators are used to control the satellite's orientation and orbit to perform the relay communication functions. The actuators also compensate external disturbance torques such as solar pressure and gravitational forces by the Earth, Moon, Sun and others.

The functions include target pointing with the RF and laser communication links at the Earth ground stations and the Moon, pointing the solar arrays at the Sun and aligning the main kick motor and AOCS thrusters for the orbital maneuvers during transfers and station keeping. With off-the-shelf hardware for GEO satellites, the attitude and orbital position can be determined and controlled very precisely at low costs [183].

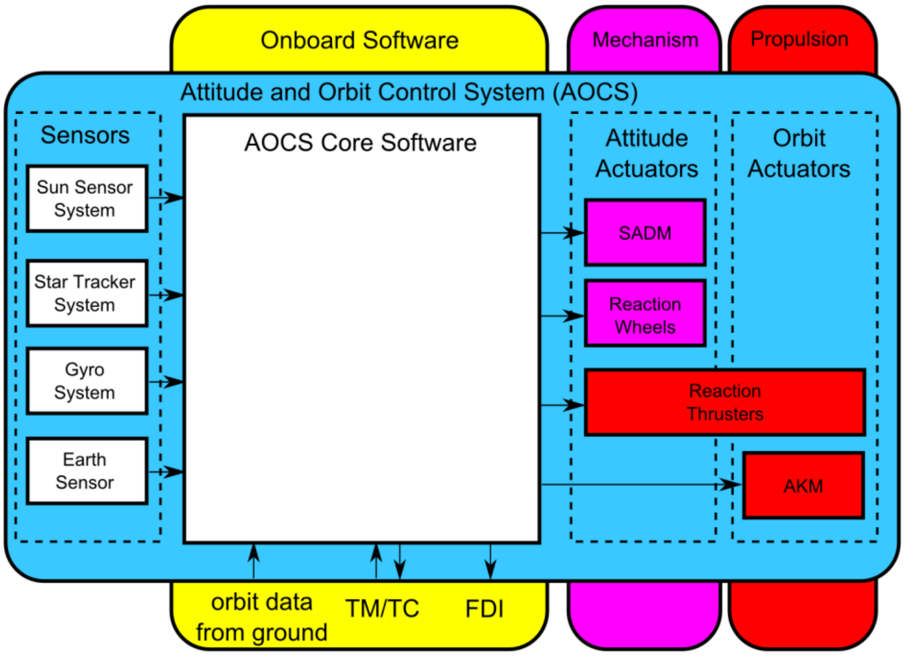

Figure 61: AOCS system layout

4.4.3.1 *Attitude Control*

As long as the final distribution of the subsystem components is not finished the satellite moment of inertia can be assumed as a homogenous distribution of the total launch mass at mission start and of the dry mass at target orbit injection. The satellite geometry and dimension selection shall reflect the shape of typical satellites thus reducing the options to a circular cylinder (a), a circular cylindrical shell (b) and a rectangular parallelepiped (c) [17].

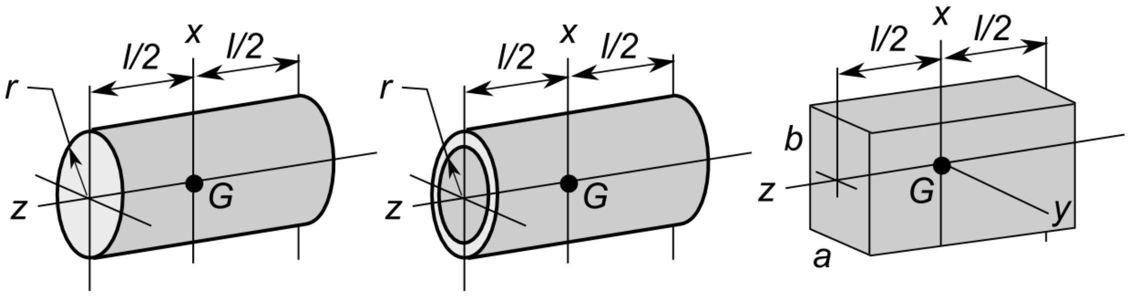

Figure 62: Moments of inertia for three common homogeneous solids of mass m.

(a)

$$I_x = I_y = \frac{1}{4}mr^2 + \frac{1}{12}ml^2$$
$$I_z = \frac{1}{2}mr^2$$

(b)

$$I_x = I_y = \frac{1}{2}mr^2 + \frac{1}{12}ml^2$$
$$I_z = \frac{1}{2}mr^2$$

(c)

$$I_x = \frac{1}{12}m(a^2 + l^2)$$
$$I_y = \frac{1}{12}m(b^2 + l^2)$$
$$I_z = \frac{1}{12}m(a^2 + b^2)$$

4.43

The satellite shall set its attitude in a way that it is able to target Earth and Moon during the orbit run. This means the satellite has to perform a rotation around one of its body fixed axis in relation to the current angular momentum of the satellite's center of mass on the orbit around the center of gravity. This is shown as the average angular velocity around z-axis of the satellite (x-axis in Figure 62) is related to the orbit's period

$$\omega_z = \frac{2\pi}{T_p} \tag{4.44}$$

The angular velocity of the satellite is generated by the reaction wheels and the attitude and stability around this rotation axis are provided by a three-axis stabilization of the satellite. Due to the lack of a technically usable magnetic field, AOCS thrusters instead of magnetic torquers are used to generate the counter momentum during the spin-up time of the wheels. When the reaction wheels angular velocity is constant, no momentum is induced. Nevertheless external perturbations occur during orbit run that need to be compensated by the reaction wheels changing their rotation velocity. For this reason the reaction wheels have to be desaturated when they exceed their specification limits. To apply this, the same AOCS thruster and method can be used like for spinning up.

As stated, TMA-0 is on an elliptical orbit on which the satellite's velocity and position radius changes. With this the reaction wheels have to change their rotational velocities as well to generate a momentum allowing to actively turn the satellite for re-targeting. The minimum and maximum satellite rotation are obtained with the orbital velocity v_{orbit} at the periapsis or apoapsis and their radiuses R

$$\omega_z = \frac{v_{orbit}}{R} \tag{4.45}$$

The change of the satellites angular velocity (Table 70) requires being within the target pointing accuracy. So the steering laws have to include either a permanent adjustment that can be provided by reaction wheels or a re-adjustment when the pointing vector leaves the specified range that could be either done by reaction wheels or thrusters.

Table 70: Satellite angular velocity ω_z at the periapsis and apoapsis

	Periapsis	**Apoapsis**	**Average**
R [km]	363300	405500	384400
ω_z [rad/s]	2.9615×10^{-6}	2.3772×10^{-6}	2.6694×10^{-6}

The thrusters' minimum impulse bit (MIBIT) and the control law limits the ability of re-adjustment. The set of two thrusters mounted with a distance l from the center of mass has to provide the MIBIT needed for the angular acceleration $\dot{\omega}_z$ of the satellite.

$$I_z \dot{\omega}_z = 2l\ |MIBIT| \quad 4.46$$

In the presented case, a MIBIT of 3.8×10^{-10} Ns would be needed for a satellite with 2300 kg, the assumed dimension of $2m \times 2m \times 2m$ and the average angular acceleration $\dot{\omega}_z$ during half the orbit's period. The MIBIT performances of the AOCS thrusters in Table 32 are above the stated MIBIT magnitude. Thus they are not capable of providing the same performance. The best thruster, MR-103M, provides 7×10^{-4} Ns and the recommended 22 N Bipropellant Thruster provides 9×10^{-2} Ns. Furthermore the angular acceleration changes over time so that thrusters would have to adjust the satellites velocity several times per orbit. For this reason reaction wheels are chosen for attitude control of the target pointing and AOCS thrusters shall be used for desaturation of the reaction wheels.

In addition to the target pointing requirements, the perturbations acting on the satellite have to be compensated. External and internal perturbations influence the design of the AOCS strategy. External perturbations include solar pressure acting on the surfaces, gravity gradient acting on the mass distribution and even the magnetic field of Earth acting on the material of the satellite itself. For altitudes of Moon orbit, the main external perturbations are induced by solar pressure and gravity gradient. The main perturbation however is induced by internal perturbations of misaligned thrusters and moving hardware of the satellite. During orbit control thrusting, a pair of thrusters has to be used. In case of a small difference in thrust vectors or thrust times, rotation is induced to the satellite.

Moreover moving hardware includes solar panels and steerable antennas and terminal. Alignment of the solar panels towards the Sun (solar array drive mechanisms SADM) with alpha or beta angle is continuously done during the orbit period but with small rotation rates corresponding to the satellite's orbit period. This could even be a positive perturbation factor because in case of solar panels mounted in z-axis direction and even rotating around this axis, they induce a counter rotation to the satellite supporting the reaction wheels.

Reaction wheels are selected for the three-axis attitude control due to several reasons. They can provide the small accelerations and changes of acceleration needed for the satellite's orientation towards the targets due to better variations of the electric motor inputs (voltage, ampere) with almost step-less settings within the limit compared to chemical thrusters (except electrical thruster systems). For faster re-targeting of the communication links the rotational movement shall be supported by steerable communication antennas itself.

The TMA-0 environment with respect to solar induced perturbations is comparable to GEO satellites (Chapter 3.2.3.5) and reaction wheels with torques between 70 to 100 mNm at a nominal speed of 3000 revolutions per minute (RPM) are recommended [183]. The wheel configuration shall be a pyramid or tetrahedron position to provide redundancy in case of one failing reaction wheel. It is also mandatory that the 3-axis stabilization offers higher accuracy pointing [184]. The nominal speed is also chosen to have an availability of the satellite reaction wheels of 95 % and only 5 % is used for momentum management when the wheels are desaturated.

Table 71: Reaction wheels with motor torque between 70 and 100 mNm

	Rockwell Collins			**Honeywell**	
	RDR 57-0	**RDR 68-3**	**RSI 45-75/60**	**HR14**	**HR16**
Performance					
Angular momentum	57 Nms	68 Nms	45 Nms	25,50,75 Nms	50,75 Nms
Operational speed	±5250 rpm	±6000 rpm	±6000 rpm	±6000 rpm	±6000 rpm
Motor torque	90 mNm	75 mNm	75 mNm	100 mNm	100 mNm
Physical Specs					
Diameter	345 mm	345 mm	310 mm	366 mm	418 mm
Height	118 mm	118 mm	160 mm	159 mm	178 mm
Mass	7.6 kg	7.6 kg	7.7 kg	7.5,8.5,10.6 kg	9, 10.4 kg
Total Mass	9.05 kg	8.85 kg	-	-	-
Power					
Standby	5 W	5 W	5 W	-	-
Steady state	20 W	20 W	22 W	22 W	22 W
Maximum torque	90 W	90 W	90 W	105 W	105 W

[185] [186]

The reaction wheels in Table 71 fulfill the torque range requirement, are space qualified and both companies have European branches. The following study and development, the AOCS design shall include an in-detail analysis of AOCS on basis of the pre-selection. This data is representatively used for the mass and power budgets. The baseline candidate is RDR 68-3 by Rockwell Collins offering the highest ranking in the decision matrix (Table 102).

4.4.3.2 Orbital Control

The orbital control serves three purposes. The main task is station keeping around the libration point EML-4, as support of attitude control and as back-up thrusters for the apogee kick motor for target orbit transfer and the final end-of-life transfer.

The configuration of orbital control thrusters are four clusters with four thrusters (4x4) in crossed direction with two of these clusters mounted on opposite sides of the satellite’s hull (Figure 60 and Figure 59). With a configuration of 2x4 a satellite is controllable around all three axes by a series of rotations. The additional thrusters in the 4x4 configuration allow direct rotation into the final position without a sequence of single rotations. And the additional thrusters improve redundancy with minimal cost of additional propellant feed lines (Figure 59).

Orbital control for station keeping on the orbit around EML-4 requires several maneuvers during the year compensating perturbation that changes the orbital parameters and keeping the satellite within the target zone of 45000 km (Chapter 4.2.3.4). Therefore the thrusters have to be specified with a total impulse count suitable for this. The analysis of the station keeping strategy is not within the scope of this concept and the yearly delta-v costs for three station keeping orbits are presented in Chapter 4.2.3.4. Hence the selection of thrusters in this concept has to be refined in the following study. The calculations for the propellant masses and performance are done for two AOCS thrusters that are all suitable for this task (EADS 22 N Bipropellant Thruster, Aerojet MR-111C). The thruster system is decided to be a bi-propellant as presented in Chapter 4.4.2 reducing the selection to thrusters with more than 4 N of thrust (Table 32). Due to the fact that the high accuracy attitude control is performed by reaction wheels, the recommended thruster is EADS 22 N Bipropellant Thruster for several reasons. It can be used with the same propellants like the main thruster, it is space qualified thrusters with adequate life time and it has a European heritage. As a backup-thruster, the EADS 10 N Bipropellant Thruster shall be considered because it provides a similar ISP and the same qualification and heritage (Table 32).

Furthermore four of these thrusters could serve as back-up thrusters to the main apogee motor. In case of a failed main motor, these thrusters allow a transfer to EML-4. Although the transfer time will be longer, the mission does not fail due to a single point of failure. This is only possible when the main engine and the AOCS thrusters are fed by the same propellant tanks, otherwise the required total delta-v could not be generated by the AOCS thrusters alone. If this backup system is considered, additional propellant margins for the higher propellant consumption during transfer due to lower ISP of the AOCS thrusters must be included in the design.

And lastly the AOCS thrusters can accomplish the end-of-life transfer in case of the main apogee motor cannot be reactivated at the end of the phase E.

Besides orbital control these thrusters are also used for desaturation of the reaction wheels. The external and internal perturbation can increase the rotational velocity of the reaction wheels beyond the nominal range. When this transition range is reached, the thrusters shall be used to reduce the angular velocity of the wheels back to the nominal level. At least one pair of thrusters must be able to provide enough thrust to generate an adequate torque compensating the extra angular momentum that is used for the desaturation. The angular momentum of two thrusters $2H$ is obtained with $C = I_z$ as the moment of inertia around the satellite's x-axis, the satellite's angular velocity ω_z, the changed reaction wheel angular velocity $\omega_{transition}$, the wheel's nominal speed $\omega_{nominal}$ and the gimbal angle of each of the four wheels θ [17].

$$2H_{thruster} = -4(C\omega_z + C\omega_{transition}\, cos\theta) + 4(C\omega_z + C\omega_{nominal}\, cos\theta) \qquad 4.47$$

$$|H_{thruster}| = l\, F\, t_{burn} \qquad 4.48$$

When two AOCS thrusters are used for desaturation with their thrust F, at a distance from l of 1 m to the center-of-mass and a burn time t_{burn} of 1 second, the satellite's angular velocity will be changed. Afterwards the wheels motor torque M_T is applied and can decrease the stored angular moment by decreasing the revolutions per minute back to the nominal speed [183].

$$t_{despin} = \frac{2l\ F\ t_{burn}}{M_T} \qquad 4.49$$

With two 22 N thrusters and the RDR 68-3, which offer the minimum torque but can store more angular momentum than RSI 45-75/60, it takes about the de-spin time t_{despin} of 9.9 minutes to reduce the additional angular momentum applied by the thrusters. Even with a four wheel configuration, the de-spin time will be less than 5 % of the mission time for the momentum management [183].

In addition to chemical propulsion systems electrical propulsion systems shall be analyzed in the following study. Electrical propulsion systems offer even lower minimum impulse bits and lower thrust levels. This is considered as advantageous for the station keeping within the vicinity of EML-4 with an expected range of 100 km instead of 10000 km that is currently assumed. Pulsed plasma thrusters (PPT, sometimes referred to as iMPD) are considered as propulsion type thrusters candidates due to the fact that these high precision maneuvers are not continuously needed. They offer MIBITs of around 100 – 1400 µNs, the power requirement of about 40 – 130 W is lower than Stationary Plasma Thrusters (SPT) (>1KW) and the cost efficient and solid propellants, which does not require tank structures, can be used. A possible candidate is the iMPD ADD SIMP-LEX developed at the Institute of Space Systems at the University of Stuttgart (Figure 82) [187]. The PPT system can also be used in the WSB zone where only minimal impulses are needed for the orbit transition.

4.4.3.3 Attitude Determination and Control Systems

The attitude determination system determines the position and orientation of the satellite. The requirements regarding accuracy are similar to that of GEO communication satellites and of-the-shelf determination components can be used for TMA-0 [183].

The TMA-0 satellite shall determine the accurate three-axis attitude as well as the orbit parameters. For this, two star trackers shall be used. Each of them can determine the three-axis attitude and two of them shall be used due to redundancy. They shall be used for the target pointing to Earth and the Moon because high precision attitude determination for a long period of time is needed. The star trackers are the primary sensor for attitude determination, because they offer star determination in more hemispherical areas than it is possible with Earth and Moon sensors. The integrated star catalogue of the complete hemisphere gives the advantage that it is even possible to determine the position when the Earth or the Moon is not within the associated sensors. Furthermore it gives information of the satellite attitude angles. Possible star trackers fulfilling the requirements are presented in Table 72.

Table 72: Star trackers

	Jena Optronik		Selex ES	
	Astro APS	**Astro 10**	**A-STR**	**AA-STR**
Performance				
Acquisition time (from lost in space)	10 s	8 s	6 s	9 s
Attitude accuracy (xy-axis)	1 arcsec	1.5 arcsec	3.6 arcsec	3.3 arcsec
Attitude accuracy (z-axis)	5 arcsec	12 arcsec	21 arcsec	15.6 arcsec
Power and Mass				
Idle	6 W	8 W	8.9 W	5.6 W
Maximum	10 W	11 W	13.5 W	12.6 W
Mass	1.98 kg	3.37 kg	3.55 kg	2.6 kg
Heritage	Small Geo, Alphabus	Tandem-X	Herschel, Planck	Alphabus, Spacebus 4000

[188] [189] [190]

The inertial position and attitude shall be determined with two inertial measurement units (IMU) including three-axis accelerometers and gyroscopes. They shall be used for the orbit control during transfers and station keeping. The EML-4 orbit requires high precision determination because small delta-v maneuvers are executed. Typical GEO communication gyros suitable for TMA-0 are presented in Table 73.

Table 73: Inertial measurement unit

	Honeywell	Astrium	
	MIMU	**Astrix 1090/1120**	**Astrix 200**
Performance			
Bias	< 0.005 °/hr	< 0.01 / 0.003 °/hr	< 0.0005 °/hr
Noise	< 0.005 °/rt-hr	< 0.005 / 0.002 °/rt-hr	< 0.0002 °/rt-hr
Power and Mass			
Average	22 W		
Maximum	32 W	12 W	6 W per ON channel
Mass	4.7 kg	4.2 kg	13 kg
Heritage	SGEO		Aeolus, MTG

[191] [192] [193]

TMA-0 shall also include a minimum of eight course Sun sensors. Theese are attached on each hull segment to be able to determine the Sun direction even during tumbling or safe mode. Sun sensors are not expensive and do not require electrical power. This it gives a cost effective and basic attitude sensor array with redundancy. The Sun sensors shall be used for the course where the IMU is supported by the Sun’s position in relation to the satellite’s attitude. It is also used for the solar array orientation towards the Sun in safe mode. For higher precision determination, fine Sun sensors shall be used for target pointing to the Earth and the Moon. They shall also be used for solar array orientation. Possible sensors are presented in Table 74.

Table 74: Sun sensors

	Astrium	**Bradford**		
	Coarse Bi-Axis	**Coarse Sensor**	**Cosine Sensor**	**Fine Sensor**
Performance				
FOV	+/- 90° (2 axis)	+/- 90° (2 axis)	+/- 80 (2 axis)	128° x 128°
Sun detection	+/- 15°	+/- 12°	+/- 3 arc sec	< 0.03 arcsec
Power and Mass				
Power	passive	passive	passive	0.25 W
Mass	0.065 kg	0.215 kg	0.037 kg	0.375 kg
Heritage	BASS7, BASS17	Alphabus	EDRS, SGEO, Galileo-FOC	Galileo-IOV/FOC

[194] [195] [196] [197]

The last pre-selected sensors are Earth sensors. Earth sensors detect the infrared Albedo radiation from Earth so the range of operation is limited according to the received infrared (IR) (see Chapter 3.2.3.6). So the proposed operation is during the transfer phase. Two representative sensors are show in Table 75. The Sodern STD 15 can also be used for altitude determination within a distance between 15000 and 140000 km from Earth. For further distances, the sensor can be used for an Earth presence sensor [198]. The accuracy of the attitude angles determination is less precise than the accuracy of the given start trackers in Table 72. Therefore the Earth sensors can be used for additional attitude determination in combination to the star sensors for the transfer.

Table 75: Earth sensors

	Sodern	**NEC/Toshiba**
	STD 15	**Earth Sensor Assembly**
Measuring	Pitch, Roll, Altitude	Pitch, Roll
Performance		
IFOV	1.5°	1.3°
Bias, Noise	0.035°, 0.015°	0.03°, -
Attitude Range	15000 – 140000 km	-
Power and Mass		
Power	6.5 W	4.0 W
Mass	3.4 kg	1.95 kg

[199] [200] [198]

The set of determination components provide a higher accuracy and a redundancy between different components. In case of one star tracker fails additional information provided by the Sun sensors is used.

The selection of the components is representative because standard off-the-shelf components can be used for TMA-0. As standard components, they are not critical to the mission. The presented components will be used for the mass and power budget. A further selection decision shall be included directly in the subsequent study. The baseline candidates offering the highest ranking in the decision matrices are Astrix 200 by EADS as IMU (Table 103) and Astro APS by Jena Optronik as star tracker (Table 104).

4.4.4 Command and Onboard Data Handling

The Command and Onboard Data Handling (OBDH) of the TMA-0 satellite is responsible for the processing of commands received from ground station on Earth, the processing of the satellite's telemetry data and the data handling and distribution between all subsystems.

It is the central subsystem for the relay service to receive, store and forward the user data between the lunar target and the Earth ground station. To simplify the development and increase the reliability, the choice is an OBDH system with flight heritage and with small modifications in the mass memory unit (MMU) providing the recording capability for users transmitting with different priority modes.

4.4.4.1 Radiation Shielding

During the mission time of 3 years, the TMA-0 satellite has to stand a dose of radiation and the electronics have to function under the environmental conditions. The transfer and station keeping phases are analyzed with the Space Environment Information System (SPENVIS) [201].

The radiation sources and effects are analyzed for trapped proton and electron fluxes (including anisotropy), short- and long-term solar particle fluxes, galactic ray fluxes and shielded fluxes. These sources are acting on the simulated simple geometry of an aluminum solid sphere containing standard silicon as the detector [202].

The analysis showed that the biggest part of the dose is received during the transfer when the satellite passes through the different radiation belts. At altitudes above 80000 km, the high energy particles in Earth's magnetic fields are not significant anymore and only a small level of radiation acts on the satellite.

The resulting ionizing dose on the silicon detector is presented in Figure 63. Typically communication satellite electronics are specified to be resistant to a dose of 100 Krad mostly [203]. An aluminum shielding thickness of 2 mm would be sufficient. However this analysis does not include the effects of braking radiation (Bremsstrahlung). For this reason the shielding is assumed to be 5 mm and the electronics components should not be mounted directly to the hull or the components shielding, because the braking radiation flux is more intense at the braking source.

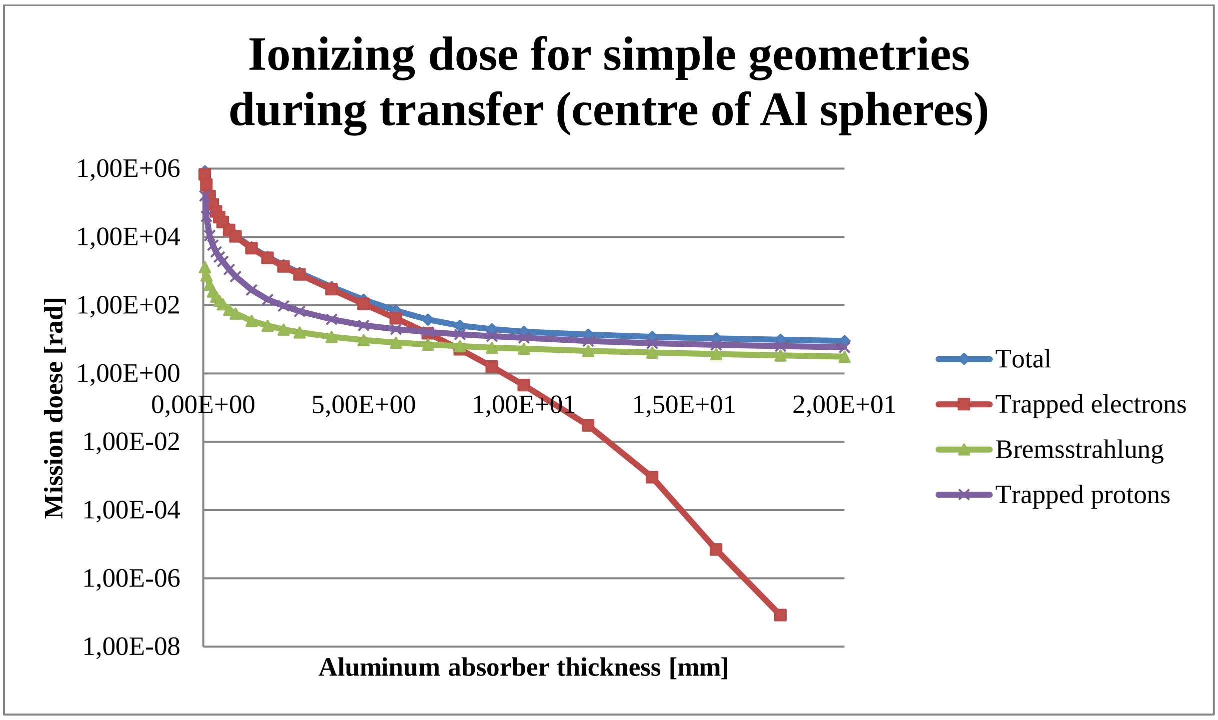

Figure 63: Ionizing dose for simple geometrics during transfer (center of Al spheres)

The effects of high energetic particles and radiation can cause damages or changes in the physical states in the circuitry. It can cause Single event upsets (change of state), single event latch-ups (short circuit) or even single event burnouts (circuit destruction). The selected electronics shall be radiation hardened or shielded by the component cases. For this reason space qualified and standard OBDH systems should be used for TMA-0. These components are specified for harsher radiation environments in GEO.

4.4.4.2 Mass Memory Unit

The mass memory unit (MMU) shall provide adequate recording capability to store the data sent by the users during communication outage times with Earth or when one user's transmission is directly relayed via high priority mode. Other users shall still be able to connect via low priority mode to the TMA-0 satellite but the data is stored for a later transmission.

The International Space Station (ISS) is specified for access times of 68 % during one orbit [56]. This leads to a MMU capacity of 19 TBytes that can store the data received via the 200 Mbit/s communication links. This would be sufficient enough for storing during the outage times during one Moon orbit. However the coverage time for the ISS is based on the connection to TDRS satellites and the ISS antennas. During one ISS revolution in low Earth orbit the links to TDRS satellites in GEO are blocked by ISS solar panels and further station components. Furthermore the TDR-Satellites are not completely covering the Earth and thus LEO [204]. This leads to the depicted access time for TMA-0 being based on the access time to one Earth ground station. So the storage capacity has to respect only 12 hours which leads to about 350 Gbytes. This fulfills the requirement of the permanent access to the Moon. The users are able to permanently sent data to TMA-0 and it will be forwarded when the access can be re-established. The MMUs shall be a scalable system that can be extended during the following design phase. Optionally, the number of mass memory unit can be increased for the operational TMA-1 mission with the space qualified MMUs onboard of TMA-0.

4.4.4.3 Onboard Computer

The tasks of onboard computers are payload data handling, housekeeping control, attitude and orbit control management and managing of all subsystem data. The system shall provide a high availability. This can be done with either a central or distributed computer system. For the TMA-0 satellite concept an available and proven system shall be used. Two systems are presented in Table 76 that serve for the pre-selection for this phase of the study and are used for the mass and power budget.

Table 76: Command and onboard data handling

Manufacturer	**Astrium**	**RUAG**
Product	**OSCAR & ICDE-NG**	**Command & Datahandling**
Processor	26 MIPS @ 32 MHz	65 MIPS at 80 MHz.
Interfaces	2x SpaceWire (160 Mbit/s), MIL-STD, 1553, UART, CAN	SpaceWire (160 Mbit/s), MIL-STD, 1553, UART, Synchronous serial link
Internal Memory	2.5 Gbytes (+12.5 Gbytes)	32 Gbytes
Radiation	10 Years in LEO 20 Years in GEO Single event upset tolerant Latchup immune	Reliability: >0.99 over a 3-year mission using class B components* >0.97 over a 15-year mission using class S components*
Mass	5 kg (+13.6 kg)	16 kg
Power	15 W (+35 W)	40 W (average) 60 W peak
Heritage	Galileo (Giove-B), TerraSAR-X, Tandem-X	SGEO, Aeolus

**component classes defined in MIL-STD-883 "Test Method Standard, Microcircuit"*
[205] [206] [207] [208]

The TMA-0 satellite includes two communication channels with 100 Mbit/s and two channels with 25 Mbit/s. The number of interfaces between the communication payload and the MMUs shall respect this data rate. Modifications of these preselected systems shall be conducted or alternatives have to be found. For the TMA-1 satellite the capability has to be scaled. This can be done with several stacks of onboard computer systems.

With a decentralized computer architecture the performance can be scaled with additional processors (CPU) and specialized hardware for the payload and the satellite control. The presented Astrium and RUAG systems could serve as satellite control and additional computer systems could serve for the payload data handling and transmission (PDHT). This decision should be made according to the computing requirement of the relay communication and storing requirement. This could lead to a customized solution or off-the-shelf computer boards like the PROTON series by Space Micro [209]. Specialized components like the PROTON are used for image and science data processing onboard of satellites. They provide advanced processing capability of several 100 MIPS (Million Instructions Per Second). Although the computing topology is more complex, a distributed increases reliability with redundancy. Due to the requirements for high data-rate and low delay times during the relay communication, two PDHT units are included in the mass and power budget as pre-selection. The usage has to be discussed further in the following design.

4.4.5 Electric Power Subsystem

The electrical power subsystem is responsible for the generation, storage and distribution of power within TMA-0. The subsystem includes solar generators, batteries and electronic devices for power conditioning and distribution to the components.

4.4.5.1 Power Modes

The TMA-0 mission consists of several phases and demonstration tasks that require different components to be active. For the power budget, different modes are defined according to the mission tasks [210].

Mode 0 – GTO:

After launcher separation the TMA-0 satellite shall automatically activate the detumbling procedure after a certain time. Furthermore the TT&C channel shall be switched from silent mode to active and send out a beacon signal and basic telemetry data. During this mode, the TT&C modem shall wait for commands.

Mode 1 - Safe Mode:

In safe mode, the satellite shall orient the solar panel in direction to the Sun and charging the batteries. This is the most basic mode that can be used during all phases. In this mode, the TT&C system shall listen for further commands to go back into higher modes. This mode shall also be used during eclipse times with reduced solar array pointing.

Mode 2 - Transfer Mode:

The satellite shall orient the solar panels in Sun direction to directly power the thruster systems. The TT&C is fully active. The apogee kick motor and the reaction thrusters are used. The reaction wheels are active to align the thrusters for the transfer and stabilization.

Mode 3 - Idle:

The TMA-0 satellite is operational but unused in target orbit. The solar panels are actively pointed to the Sun with the solar array drives and the satellite’s orientation is controlled with the reaction wheels. The batteries will be charged most efficiently that way and the satellite is ready to carry out operations in the pointing modes immediately. The idle mode can also be used during the transfer when no maneuvers are conducted.

Mode 4 – Science:

During the science mode, the science payload is active. The satellite provides the orientation and power for the environment mapping with the dust sensors and the Sun sensors.

Mode 5 – Operational with RF:

The satellite performs the operational objectives for the demonstrations. Both high data-rates and the target pointing mechanisms are active. The attitude control and the solar array drives orient the satellite for the data transmission and the solar array towards the Sun. The science payload is also active and the dust sensors and the Sun sensors shall perform environment mapping.

Mode 6 – Operational with RF and Laser:

In addition to mode 5, the laser communication terminal is active. In this mode, the inter satellite demonstration shall be performed. This is the most power intense mode and poses the highest demands on the thermal housekeeping.

4.4.5.2 Solar Power Generator

The solar power generators consist of the solar cells mounted on solar panels. The panels shall allow independent tracking of the Sun, which is controlled by solar array drive mechanisms (SADM) for orienting the panels towards the Sun. The direct contact with solar radiation and other space environment conditions, the solar cell selection includes the end-of-life efficiency (EOL).

The space radiation is analyzed again with SPENVIS [201]. The damage equivalent fluences for solar cells (EQFLUX) are representatively processed for Azur 3G28 in Table 77. It shows the electron fluences for the cells with different cover glass thicknesses.

Table 77: Summary of 1 MeV equivalent electron fluences (cm^{-2})

Coverglass thickness	**Total**		
[micron]	P_{max}	V_{oc}	I_{sc}
0.0	3.291E+16	2.091E+16	3.334E+16
25.4	2.681E+14	2.131E+14	2.204E+14
76.2	3.489E+13	3.396E+13	2.423E+13
152.4	1.029E+13	1.085E+13	6.468E+12
304.8	3.136E+12	3.502E+12	1.817E+12
508.0	1.192E+12	1.389E+12	6.548E+11
762.0	6.041E+11	7.177E+11	3.309E+11
1524.0	1.771E+11	2.172E+11	9.513E+10

The high energetic particles and radiation lead to a degradation of the solar cell and the photo effect. The cover glass thickness protects the material to a certain extent. The equivalent electron fluences for the glass thickness of the generic solar cell candidates in Table 78 determine the end-of-life parameters. The baseline candidate offering the highest ranking in the decision matrix is Azur 3G30C (Table 105).

Table 78: Solar cells – end-of-life parameters with respect to MeV equivalent electron fluences

	Azur Space		**EMCORE**	
	3G30C	**3G28C**	**ZTJ**	**BTJ**
Design				
Cell Area	30.18 cm²	30.18 cm²	26.60 cm²	26.60 cm²
Average Mass	86 mg/cm²	86 mg/cm²	84 mg/cm²	84 mg/cm²
Electrical Data				
Avg. Open Circuit $\boldsymbol{V_{oc}}$	2616 mV	2560 mV	2617 mV	2619 mV
Avg. Short Circuit $\boldsymbol{I_{SC}}$	518.5 mA	500.9 mA	458.2 mA	454.9 mA
Voltage @ max. Power $\boldsymbol{V_{mp}}$	2345 mV	2276 mV	2362 mV	2299 mV
Current @ max. Power $\boldsymbol{I_{mp}}$	503.2 mA	482.1 mA	434.5 mA	433.6 mA
Avg. efficiency $\boldsymbol{\eta}$	28.6 %	26.6 %	28.1 %	27.1 %

[211] [212] [213] [214]

The satellite system shall use the satellite standard voltage of 28 V as the de facto industry standard voltage. The limits of variation between 32 V and 22 V allow the end of charge voltage (EOCV) and end of discharge voltage (EODC) of the batteries to be counteracted by the solar cells via the power conditioning unit. Further electrical properties can achieved with DC/DC converters.

The solar cell grid configuration (see Table 79) to obtain the needed voltage and amperage depends on the overall power consumption presented in the power budget (Chapter 4.4.8). The solar generator is the primary source of power and shall provide the basic power level for the satellite system at all times. The excess power shall be used to charge the batteries during the sunlight phases so that during the eclipse times (Chapter 3.2.3.7), the needed power level is fed by the batteries.

The solar generator is a solar panel that can be folded into the transport configuration and has to be deployed after GTO injection. The panel itself shall be off-the-shelf and includes the deployment mechanism. To avoid a single point of failure, two independent panels shall be used [215]. A body mounted solar array cannot generate the required power, although it would avoid deployment and a single point of failure. The SADM also conducts the electrical power from the solar arrays to the satellite. The SADM interface shall handle power flux in the range of 1427 W (see Table 79) provided by the full solar panel area based on the system power of 1200 W in operational mode 6 (power budget in Chapter 4.4.8).

The driving case for the solar array sizing is the satellite system power level for the operational mode 6 because this level is required for the demonstrations with the satellite and RF and laser communication payload. The derivate designs of the electrical power system also fulfill the power demands of the remaining power modes 0 – 5 that require lower power levels than mode 6.

The orientation of the panel towards the Sun, the sunlight and eclipse times and physical properties of the solar cells are the main influences of the generated power. The solar array area must generate power P_{sa} during sunlight condition for the entire orbit. The analysis of shadow phases in Chapter 3.2.3.7 shows that there is no periodic sunlight –eclipse cycle per orbit. For this reason the maximum penumbra and umbra phases that occurred during the test period of 10 years is used as the eclipse duration for the design. The power level provided by the arrays is higher than the required level because of the occurrences of eclipse times. The power difference is stored in the batteries and can be used during the eclipse phases. Thus the power levels during daylight P_d and during eclipse P_e are equal to guarantee the same operation power level P_s of the satellite. As worst case assumption, one orbit of 655 hours is modeled as about 648 hours of daylight and 7 hours of penumbra/umbra (Chapter 3.2.3.7), representing the longest eclipse occurring in the modeled period for T_e. For battery charging the shortest daylight T_d duration is used.

The influences of the paths from the arrays through the batteries to the consumers and the path directly from the arrays to the consumers are represented by the efficiency terms X_e and X_d (0.8, 0.85).

$$P_{sa} = \frac{\frac{P_e T_e}{X_e} + \frac{P_d T_d}{X_d}}{T_d} \qquad 4.50$$

The solar array area A_{sa} required to generate this power level is then influenced by the orientation of the panels towards the Sun, so the ecliptic angle ϵ_e and the panel misalignment α_p are included. Also the EOL properties of the solar cells (efficiency η) and degradation δ (temperature 0.85, design and assembly 0.85) of the cells are used. The solar radiation flux is respected with the minimum solar constant S_0.

$$A_{sa} = \frac{P_{sa}}{\cos(\epsilon_e)\cos(\alpha_p)\,\eta\,\delta\,S_0} \qquad 4.51$$

For the estimation the triple junction cells 3G30C from Azur are used. They offer the highest EOL performance and less panel area usage which leads to lower structural mass of the panel.

The minimum solar panel properties for TMA-0 are presented in Table 79 and the solar area power P_{sa} of 1427 W provides the average system power P_s of 1200 W. For this 12 solar cells with 147 strings are needed to provide the power level with system voltage of 28 V. The panel area is distributed on two panels.

Table 79: Solar panel properties

Power	Panel Area	Misalignment	Ecliptic	Cells	Cells Configuration for 28 V
1427 W	5.3 m²	10°	5°	1764	12S147P

The panel construction including the folding and deployment mechanism shall be off-the-shelf. The Eurostar 3000 solar array family by Astrium is a candidate because of the heritage and the “off-loading” concept. This modular concept allows the adaption of the panel to customer needs [216]. The different modules shall be sized for the TMA-0 outer hull area. The panel area also respects a single string failure due to the sizing for the misalignment. In case of a half deployed panel, the power generated with one optimally oriented panel can provide power for the operational mode 6 during the first year (Table 80). The typical power of the depicted Eurostar 3000 panel family ranges between 6 to 23 KW so the panels for the TMA-0 satellite can be based on this expertise but will require modification [216].

Table 80: Solar panel properties for case of one half deployed panel

Power EOL	Power BOL	Degradation	Panel 1 Power BOL	Panel 2 Power BOL
1427 W	1975 W	0.85 x 0.85 = 0.7225	713.5 W @ nominal	504.5 W @ 45°

Panel 1 oriented under nominal, Panel 2 half oriented under 45° condition towards the Sun

4.4.5.3 Secondary Battery Pack

The secondary battery block has to provide power during the eclipse (umbra and penumbra) times. The permanent communication relay service requires to provide the satellite power level of mode 6 during the shadow phase. Thus the battery energy storage capacity C_e is obtained with

$$C_e = \frac{P_{sm}\,T_e}{DoD}\ [Wh] \tag{4.52}$$

where P_{sm} is the system power level of the mode, T_e is the eclipse time and DoD is the depth of discharge. The DoD influences the number of discharge cycles for the battery (DoD: 0 = full, 1 = empty). The smaller the DoD, the longer is the life time. When the life time increases, the capacity and thus the required battery mass for providing the required usable energy increases (see Figure 83 to Figure 85 for battery capacity over GEO cycle for LiOn-batteries with different DoD).

The battery capacity C_e in Table 81 shows the maximum capacity needed to maintain the power level for the full operational mode. The minimum capacity is obtained when the satellite operates in the safe mode 1 when only the very basic systems are online. The battery selection is based on the energy capacity of 16097 Wh for mode 6 but there is the option to save mass by reducing the battery’s capacity to reduce mass.

Table 81: Battery capacity for mode 1 and 6

Mode	P_{sm}	T_e	DoD	C_e
6	1200 W	24146 s	0.5	16097 Wh
1	616 W	24146 s	0.5	4131 Wh

Another battery design criterion is the charging time. The battery shall be completely chargeable from the depth-of-discharge level during the shortest sunlight phase (Chapter 3.2.3.7). The power generated by the solar arrays P_{sa} exceeds the satellite power mode level P_{sm} so that it is used for charging the battery pack. The charging losses are already included as X_e in the calculations for P_{sa}. The charging time T_c yields

$$T_c = \frac{C\ DoD}{P_{sa} - P_{sm}} \tag{4.53}$$

The charging times for both modes in Table 82 fulfill the condition of $T_c \leq T_{e(\min)}$. The battery selection can be decided on the capacity C and the system average voltage of V 28. The battery configuration has to amplify the voltage by connecting a certain number of battery cells in series. The total battery pack capacity is then reached with several series of cells in parallel connection. The power conditioning unit, to which also the solar panels are directly connected, are providing constant system voltage that changes over time.

Table 82: Battery charging times of battery pack with minimum and maximum capacity

Mode	P_{sa}	P_{sm}	**C**	$T_{e(min)}$	T_c
6	1427 W	1200 W	16097 Wh	389255 s	127488 s
1	1427 W	616 W	4131 Wh	389255 s	35715 s

The secondary battery technology should have a high specific energy density. In this way the number of cells can be reduced. Compared to nickel-cadmium (NiCd) and nickel hydrogen (NiH2), lithium-ion technology offers a significant energy density advantage and a wider operating temperature range [127] [217]. For these reasons, lithium-ion technology is recommended for the battery selection. Nevertheless it requires certain safety regulation in handling and transport due to explosion risk (REACH, NASA) [218] [219].

The battery pack configurations with Saft VES 180 & VL 48E and ABSL 18650NL battery cells are in a close mass range (Table 83), so a flexible selection is possible. The pack containing VES 180 cells give the advantage of the lowest mass and highest energy capacity (Table 84). All of these packs require casing and an integrated heating and radiator system, because the lithium-ion cells are sensitive to operation outside their temperature specification. The additional mass and power are added to the system budgets.

Table 83: Lithium-ion secondary batteries for GEO

	Saft Batteries			**ABSL Space**	**Quallion**
	VES 180	**VL 48E**	**VES 16**	**18650NL (8S10P)**	**QL075KA**
Mean voltage	3.6 V	3.6 V	3.6 V	28 V	3.6 V
Energy	180 Wh	170 Wh	16 Wh	1398 Wh	260 Wh
Specific Energy	165 Wh/kg	150 Wh/kg	105 Wh/kg	155 W/kg	148 Wh/kg
Mass	1.11 kg	1.13 kg	0.155 kg	9.0 kg	1.82 kg
Qualification	TRL 9	TRL 9	TRL 8	TRL 9	TRL 9

[220] [221] [222]

A Saft VES 180 battery pack including the cells, heater and casing for a 8S1P configuration with mass of 14 kg is used as a basis for the mass budget. The VES 1800 is the baseline candidate offering the highest ranking in the decision matrix (Table 106). Furthermore the charging requires this to be regulated. This can either be done by the power conditioning and distribution unit (PCDU) or directly within the battery pack system. Saft Batteries offers off-the-shelf systems with regulators and heaters [223] [224].

Table 84: Secondary battery pack capacity and mass

	Saft Batteries			**ABSL Space**	**Quallion**
	VES 180	**VL 48E**	**VES 16**	**18650NL (8S10P)**	**QL075KA**
Configuration	8S12P	8S12P	8P126S	8S112P	8S8P
Energy Capacity	17280 Wh	16320 Wh	16128 Wh	16776 Wh	16640 Wh
Mass	107 kg	109 kg	156 kg	108 kg	116 kg

4.4.5.4 Satellite Inauguration

After the launcher separation and geosynchronous transfer orbit injection the satellite is in mode 0. It self-activates the detumbling procedure and the TT&C system and waits for commands. During this phase the electric power is mainly fed by the battery because the solar panels are still in transport configuration. Depending on the panel folding, the solar cells could serve as body mounted panels which are periodically lighted by solar radiation. The battery pack shall serve as the main power source. The solar panels shall be deployed automatically and charge the batteries. The batteries are not completely charged due to safety reason [210]. At that point, the electric components shall be activated by commands in a specific sequence to avoid power consumption above the excess power generated by the solar panels. The battery charging time is influenced by the power level provided by the safe mode in Table 82. The satellite inauguration shall be controlled by mission control before the transfer phase preparation is initiated. The TMA-0 battery capacity and the orbit design respects this additional waiting time.

4.4.6 Thermal Control Subsystem

All spacecraft and payload components have specific operational and survival temperature limits. The thermal control subsystem (TCS) is required to maintain the temperature within these limits for each mission phase. The temperature control is achieved by passive control approaches with materials, coatings and finishes or by active control with heaters or thermo-electric coolers.

For TMA-0 active and passive control is required because there is high power dissipation (amplifiers and the laser communication terminal in the communication payload) and radiation input on large solar panel areas as well as the satellite compartment hull. For the thermal subsystem design information of the satellite's power budget, the satellite's form and the space radiation environment are used. The range of temperature that occurs during the mission is set for the hot, cold and eclipse case. The hot case scenario is defined for the maximum space radiation intensity of the direct solar radiation and the radiation of the Earth and the Sun. Because the satellite has to be transferred from Earth to the EML-4 position, the hot case also includes the radiations from the Earth on the Satellite in the GTO periapsis altitude of 300 km. The cold case is defined for the minimum space radiation intensities in the EML-4 position. The hot and cold cases define the thermal control system design of material selection and radiator design that are required to keep the temperature within the operational limits of 0 °C – 40 °C. The special case of the eclipse time defines further requirements for the heaters when the space radiation is reduced below the design limits of the hot and cold phases for a short time period. It is then the additional heat is provided by heaters to keep the temperatures within the survival or operational limits.

The approximation of the expected temperature is acquired by the steady-state equilibrium temperatures for the hot and cold case. This includes the dependence of emissivity and the solar absorptivity of the satellite surface material. The general selection of the passive thermal control material is based on the equilibrium temperature limit.

$$Q_{in} = Q_{out} \tag{4.54}$$

$$Q_{external} + Q_{internal} = Q_{sat} + Q_{radiator} \tag{4.55}$$

The equilibrium temperature is described by the absorbed power Q_{in} and the emitted power Q_{out} of the satellite. There sources for the power input are external radiation and internal power dissipation of the electronic components. The absorbed power can be emitted by the satellite's compartment section Q_{sat} and the radiator $Q_{radiator}$.

As for the satellite design the assumption is that the satellite shall stay within the survival temperature limits when there is no internal power dissipation and all power is radiated from the satellite compartment section. The solar cells and radiators are almost fully decoupled from the satellite's compartment without heat transfer towards the compartment.

$$Q_{sun} + Q_{earth} + Q_{moon} + Q_{internal} = \mathrm{Q_{sat}} \qquad 4.56$$

$$Q_{sun} = \alpha_{sat} S_0 A_p \qquad 4.57$$

$$Q_{earth} = \alpha_{sat}\, S_{eAlbedo} \mathrm{A_p} + \epsilon_{\mathrm{sat}}\, S_{eIR} A_p \qquad 4.58$$

$$Q_{moon} = \ \alpha_{sat}\, S_{eAlbedo} \mathrm{A_p} + \epsilon_{\mathrm{sat}}\, S_{eIR} A_p \qquad 4.59$$

$$Q_{sat} = \epsilon_{\mathrm{sat}}\, \sigma\, 4\, \mathrm{A_p}\left(T_{sat}^4 - T_{space}^4\right) + \epsilon_{\mathrm{radiator}}\ \sigma\, 2\, A_p (T_{sat}^4 - T_{space}^4) \qquad 4.60$$

The satellite receives radiation directly from the Sun Q_{sun} and in addition it receives radiation from the Earth and the Moon due to reflected sunlight, albedo, and the emitted radiation in infrared wavelength [225]. The received infrared radiation is due to the celestial bodies' own surface temperatures Q_{earth} and Q_{moon}. The absorption is modeled with the absorptivity α_{sat} of the material on the surface area $\mathrm{A_p}$ and the radiation intensity S of the celestial body. According to Kirchhoff's law the absorptance of a satellite to planetary radiation is equal to the emittance $\alpha_{sat} = \epsilon_{sat}$ because both radiations occur in infrared wavelength. The satellite is able to emit the received power against the black space via four surfaces $\mathrm{A_p} = 2 \times 2\ m^2$ of the hull.

Accounting for the two compartment surfaces, where the solar panels are mounted, are also used for the radiator areas. These two areas with also $\mathrm{A_p}$ are only covered by sunlight with an angle of only 5° due to the orbit's ecliptic. The solar panels orientation is out of the orbit's plane to be able to orient it towards the Sun. This also means that the compartment surfaces are perpendicular to the solar panels and hardly covered by sunlight. In this way there is the opportunity of minimum of input radiation and maximum emitted radiation. Accordingly, these areas are selected for the radiators and the material has another material and thus emissivity $\epsilon_{radiator}$. than the other four compartment areas. Therefore the materials for all six surfaces are specially selected on the basis of their emissivity ϵ_{sat} and $\epsilon_{\mathrm{radiator}}$ to perform their functions. According to Kirchhoff's law, the absorption and emissivity coefficients are equal when the received radiation wavelength is equal to the emitted wavelength of the satellite's surface. This is applied to the infrared radiation of the Earth and the Moon.

$$F_{view} = \frac{\Omega_{\mathrm{a}}}{\Pi} \approx \frac{A_{clestialbody}}{\pi r^2} \qquad 4.61$$

The view factors F_{view} from the satellite in EML-4 orbit to the Sun ($F_{sun} = 2.2 \times 10^{-5}$) to the Earth ($F_{earth} = 2.5 \times 10^{-4}$) and to the Moon ($F_{moon} = 1.8 \times 10^{-5}$) with solid angles

$\Omega_a \leq 0.2$ allow the assumption of heat radiation of all satellite surfaces against the cold space with a temperature of T_{space} = 3.5 K [226]. The radiation intensities of the Sun S_0, Earth ($S_{eAlbedo} + S_{eIR}$) and Moon ($S_{mAlbedo} + S_{mIR}$) are explained in Chapter 3.2.3.6. Hitherto, the surface property selection for the satellite hull defines the absorptivity α_{sat} and emissivity ϵ_{sat} and thus the equation can be solved for the satellite equilibrium temperature T_{sat}

$$T_{sat} = \sqrt[4]{\frac{Q_{sun}+Q_{earth}+Q_{moon}+Q_{internal}}{(\epsilon_{sat}\,\sigma\,4\,A_p+\epsilon_{radiator}\,\sigma\,2\,A_p)} + T_{space}^4} \qquad 4.62$$

As the first design, the satellite equilibrium temperature is also assumed to be the temperatures of the radiators. For a later in depth analysis, the radiator temperature shall be 20 K lower to allow a heat flux to the radiator surfaces. The satellite temperatures are now examined for different surface materials in the following section.

4.4.6.1 Satellite Equilibrium Temperature with Electrical Power Dissipation

The satellite equilibrium temperature is calculated for the hot and cold cases for three surface properties of the satellite's hull and one radiator's properties are derived. As materials, anodized aluminum and aluminized kapton foil as multi-layer insulation (MLI) are used. Anodized aluminum is a typical basic material for sandwich structures for the compartment and the optical properties can be controlled during the finish procedure. The kapton foil is also a typical insulator for satellites because it is a light material and is flexible for easy fitting. These two materials in combination are also used for the third surface property. The ratio of aluminum and kapton foil surface area is used for adjusting the equilibrium temperature.

Table 85 gives the properties for the hot and cold cases of the satellite thermal design. The hot case respects the transfer phase in GTO where the Earth's maximum infrared and albedo radiation affects the satellite due to the closer distance of 300 km to Earth. Hot case is only active for several days until the satellite is leaving the GTO and transferred to EML-4. The cold case is calculated in the final target orbit of 405000 km and for minimum solar activity and system power dissipation. It follows that the operational temperature in EML-4 orbit lies between the hot and cold case temperatures.

Table 85: Hot and cold case data

Case	Power Dissipation	Distance to Earth	Distance to Moon	Solar Constant
Hot	500 W	6671 km	386600 km	1420 W/m²
Cold	400 W	405000 km	405000 km	1320 W/m²

Note: Additional data for surface temperatures and albedo of celestial bodies is used from Chapter 3.2.3.6

The following material selection in Table 86 to Table 88 respects the hot and cold case phases and is representatively processed for typical thermal surface material of polished anodized aluminum and of kapton foil as multi-layer insulation (MLI).

Table 86: Equilibrium temperature for surface covered with 100% polished anodized aluminum

Case	α_{sat}	ϵ_{sat}	$\epsilon_{radiator}$	Temperature
Hot	0.24	0.08	0.44	311 K
Cold				280 K

Table 87: Equilibrium temperature for surface covered with 100% 1/2 mil. kapton foil

Case	α_{sat}	ϵ_{sat}	$\epsilon_{radiator}$	Temperature
Hot	0.4	0.63	0.44	285 K
Cold				239 K

The radiated surface with 100% aluminum in Table 86 offers a cold case temperature of 7°C within the operational temperature range, but also the hot case temperature of 38°C is almost reached with the maximum operational limit (40°C). The hot case temperature of the satellite with radiated surface material of 100% kapton foil in Table 87 is 12°C and within the operational mode. However the cold case temperature of -34°C is below the operational limit (0°C).

The satellite with aluminum cover reaches temperatures too close to the maximum operational temperature and the cold case temperature for of the kapton covered satellite is too low. So a combination of surfaces partially covered with aluminum and kapton foil is applied to lower the hot case temperature and to raise the cold case temperature. This still allows a passive cooling during the hot case and the use of the onboard heating system to raise the cold case temperature with less power.

$$\alpha_{sat} = 0.85\ \alpha_{aluminum} + 0.15\ \alpha_{kapton} = 0.264 \qquad 4.63$$

$$\epsilon_{sat} = 0.85\ \epsilon_{aluminum} + 0.15\ \epsilon_{kapton} = 0.163 \qquad 4.64$$

The given equations represent a simple distribution of both materials on the satellite hull. The ratio between surface area covered with aluminum and kapton and the emissivity of the radiator material is selected to keep the hot case temperature below the maximum limit for the survival mode of 50 °C and the cold case temperature in the operational mode between 0°C and 40°C.

Table 88: Equil. temp. for surface covered w/ anodized aluminum & w/ 1/2 mil. kapton foil

Case	α_{sat}	ϵ_{sat}	$\epsilon_{radiator}$	Temperature
Hot	0.264	0.163	0.44	302 K
Cold				268 K

85% anodized aluminum, 15% 1/2 mil. kapton foil

The hot case temperature is now further below the maximum operational temperature and the small temperature difference between the cold case temperature and the minimum operational temperature in the Table 88 can be compensated by heaters or the satellite power modes. The surface material for the two radiator areas is selected in accordance with the temperature limits generated by the combined satellite hull materials and also used before for the satellite surfaces in Table 86 and Table 87.

The radiators are on the two compartment surfaces where the solar panels are mounted (Figure 64) and they cover $\mathrm{A_p} = 2 \times 2\ m^2$. The emissivity of the radiators $\epsilon_{radiator} = 0.44$ can be achieved by several materials or paints. Aluminized kapton (0.5 mil) offers 0.5 and the emissivity of anodized aluminum also ranges between 0.04 and 0.88 [127]. In this way the satellite's hull and radiator design can be flexible and modified during the following design phases. In this configuration, a white paint is used.

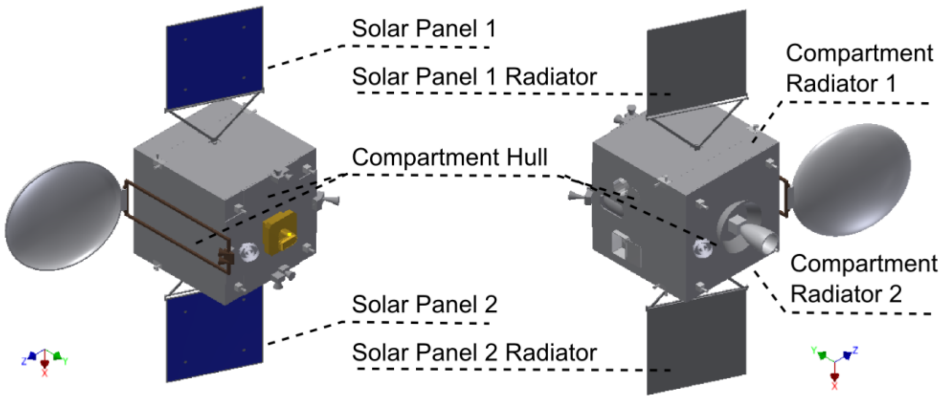

Figure 64: Thermal control surfaces on TMA-0

4.4.6.2 Heating and Special Radiators

The previously presented hot and cold cases define the temperatures that shall stay inside the operational temperature range. The control of the final temperature adjustment is possible with heaters and special radiators. These methods are applied during the solar eclipse case and for special components onboard the satellite with special temperature requirements.

During the hot and cold cases and for small temperature differences below the maximum operational temperature, the heater systems or the other electronic equipment can increase the internal heat input and adjust the temperature. The lowest equilibrium temperatures occur during the solar eclipse phases and when the main radiation input by the Sun is not radiating on the satellite's surface.

Table 89: Equilibrium temperature during solar eclipse

Solar Radiated Surface Material	α_{sat}	ϵ_{sat}	$\epsilon_{radiator}$	Temperature
100% aluminum	0.24	0.08	0.44	196 K
100% kapton	0.38	0.67	0.44	151 K
85% aluminum, 15% kapton	0.226	0.116	0.44	184 K

The satellite temperatures for the three surface properties are shown in Table 89. It respects the cold case conditions for internal power input and radiation by the Earth and the Moon and without the solar radiation. These temperatures would be reached after an infinite amount of time, but the solar eclipse durations are about two hours in average and maximum four hours. For this reason the internal heat energy stored in the entire component materials has to cool down from their operational temperature and this is time sensitive. The eclipse case temperatures shall be used for the heater design but the needed power shall be analyzed in detail for the instationary condition in the following design phase when the components and their specific heat capacity are known. The equilibrium temperature equation is used and the heater power Q_{heater} is added.

$$Q_{heater} = (\epsilon_{sat}\, \sigma\, 4\, A_p + \epsilon_{radiator}\, \sigma\, 2\, A_p)\left(T_{sat}^4 - \mathrm{T}_{\mathrm{space}}^4\right) - Q_{sun} - Q_{earth} - Q_{moon} - Q_{internal} \quad 4.65$$

The theoretical heater powers in Table 90 could raise challenges for the heater design in case the heat capacity of the satellite is drawn out before the solar eclipse phase ends. The design would be effect the battery pack capacity sizing to provide this high amount of power. The heat power is generate at specific local points in the satellite where high temperatures could effect the components and even structure.

Table 90: Theoretical maximum heating power

	Eclipse Temperature	Heated Temperature	Heating Power
100% aluminum	196 K	273 K	1112 W
100% kapton	151 K		3883 W
85% aluminum, 15% kapton	184 K		1527 W

The heater performance shall be designed to respect the maximum heating power conditions, however the nominal heating occurs during the cold case phase (Table 91). For the 100% aluminum satellite hull, the cold case temperature is above the required temperature of 273 K and no power is required. The combined case (85% aluminum, 15% kapton) requires a temperature increase of 5 K which requires 128 W. The 100% aluminum or the 85% aluminum, 15% kapton surface options are candidates as a basis for the following studies.

Table 91: Heating power during cold case

	Cold Case Temperature	Heated Temperature	Heating Power
100% aluminum	280 K	273 K	0 W
100% kapton	239 K		1763 W
85% aluminum, 15% kapton	268 K		128 W

Besides the heating systems, certain equipment requires special thermal control approaches. The travelling wave tube amplifiers (TWTA) of the high data-rate payload generate heat losses between 40% and 60% of the electric power. For each channel line it is about 78 Watts that has to be transferred to radiators. This means the position near to the satellite's hull is important and eventually another surface material than the previously presented has to be used. The radiator affects the starting procedure of the TWTA because without the internal heat the component temperature drops below the switch-on temperature, so an additional heater has to be mounted near to the TWTA to heat it up before initiation.

Furthermore the laser communication terminal (LCT) has high heat losses of about 50 Watts. The LCT is already mounted on the outside hull of the satellite and can directly radiate into space. This could also result in temperatures below the switch-on or even the survival temperatures. LCTs offer thermal interfaces for active-loop or passive-loop heat-pipes used for controlling the component temperature [227]. However, the LCT can be modified by the manufacturer respecting the TMA-0 conditions and TMA-0 shall offer the thermal interfaces. The interface between the LCT and the satellite shall also be a structure element including radiating properties and shall have a low heat transfer rate. In this way the heat is not transferred into the satellite compartment.

This interfacing method shall also be used for the solar panel mounting. The temperatures of the solar cells are in a region of 90°C, thus the transfer into the compartment section has to be minimal and can be solved by material selection, radiating surfaces and shapes with small profile sections.

The solar panel temperatures are Table 89 are for a solar panel with GaAs solar cells on the front panel side with area A_{panel}. This side is always oriented towards the Sun and absorbs the solar radiation and additional radiation sources. The front and back panel areas are emitting the radiation power in infrared generated by the equilibrium temperatures. Then two emissivity coefficients for the cells $\epsilon_{sp-front}$ and for the radiator side $\epsilon_{sp-back}$ with black paint are used.

Table 92: Solar panel temperature for GaAs cells on front, and black paint on back panel

Case	A_{panel}	$\alpha_{sp-front}$	$\epsilon_{sp-front}$	$\epsilon_{sp-back}$	**Temperature**
Hot	5.3 m²	0.88	0.08	0.8	366 K
Cold					314 K
Solar Eclipse					34 K

4.4.7 Structure

The satellite structure shall provide mechanical support and sufficient mounting area to accommodate all components. It has to withstand the highest loads and most severe conditions like vibrations and axial and lateral accelerations during the launch. The mounting areas are split into several sections for the different payload and subsystem modules. This should allow a simple and parallel build and integration for a fast satellite delivery [228]. The options for satellite structures consist of central tube or cylinder structures or shear wall structures.

The shear wall structures provide support to the box-like compartment as well as the top and bottom floor walls. It can be extended to a central wall cross or even a tube structure to increase the total stiffness. The plane walls allow mounting of the components in a simple and space efficient manner. The tube structure can also be used for integrating the propellant tanks. This offers the design advantages of a variety of standard tanks that can be placed in the satellite center. The shear walls also allow the mounting of fold-out solar panels and the parabolic antennas in the transport configuration to fit under the launcher fairing.

The central tube structure, as used in Alphabus and SGEO [229] [230], provides a higher stiffness against vibration and the launch environment. The structure is the main load path of the satellite and it carries the load from the external walls to the launcher interface. It also offers a simpler interface to the launcher via the cylindrical launch adapter ring that generates lower load peaks at the interface ring.

For the TMA-0 satellite, the shear wall structure with a supporting central structure is recommended. It is a typical structure for telecommunication satellites [228] and allows the solar panels, parabolic antenna and LCT to be mounted on the outside. It has shear walls where the communication payload can be attached for the thermal control. The other components can be placed with more flexibility on the plane walls and sections and the tanks can support the stiffness. The detachable shear walls give access for parallel work on several sides which is a benefit for a faster satellite delivery time. The estimated satellite compartment dimension of $2 \times 2 \times 2\, m^3$ allows the transportation with all launcher candidates in Chapter 4.1 and it also includes the bulky antennas and panels in transport configuration. The shear walls can be manufactured as honeycomb sandwich structures. This composite structure is light weight while it is also damping shocks. It can be used for banks with small deformations allowing the surface material to be finished with respect to the recommended thermal properties in Chapter 4.4.6.

The supporting central structures analyzed for TMA-0 are a shear web and a shear web with central tube (Figure 65). The shear web is also carrying a middle plate that separates the sections and also holds the tanks and bears the tank forces. The central tube reduces the peak loads at the interface because it is placed on the launch adapter. The tube also contains one central tank and two tanks are placed in diametrically opposed sections. In this way there is more space in the satellite than just placing the two tanks in two sections.

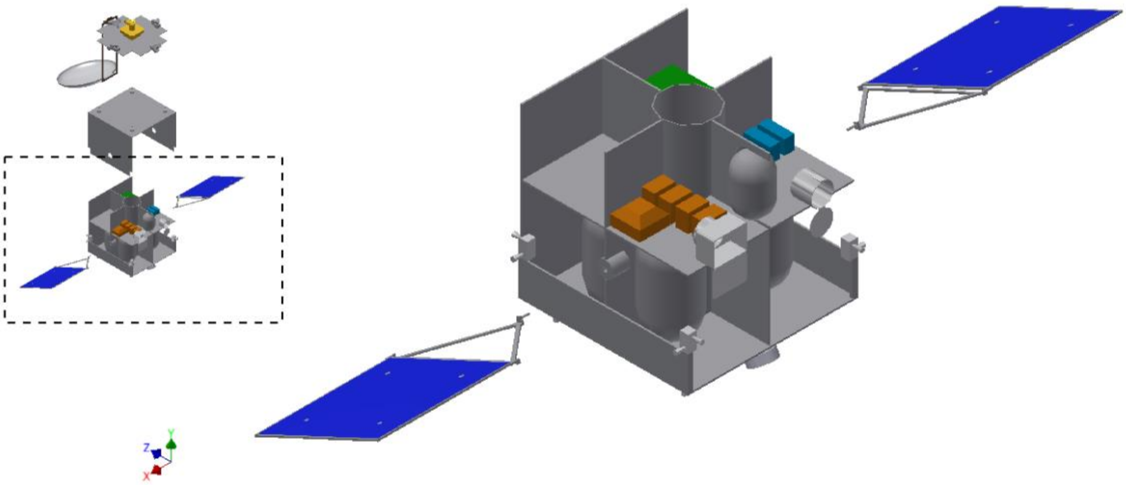

Figure 65: TMA-0 structure with shear web and central tube

The dimensionally check showed that the original equal tank size concept for the bipropellant propulsion system has to be extended from two to four tanks due to balancing. Only two tanks with the same propellant volume but different masses due to the propellants' densities would result in an unbalanced satellite. This cannot be counterbalanced by the remaining components. To avoid this, two oxidizer and two fuel tanks are placed according to their propellant species. In the shear web structure the different tanks counterbalance each other on opposing sections. In the central tube structure two tanks of the same propellant are mounted in the central tube and the other two tanks counterbalance each other on opposing sections as well.

Both solutions provide a balanced tank array and it offers a better attitude and orbital control. For this reason the small increase in off-the-shelf tank mass by four instead of two tanks is accepted. The tanks can remain as the proposed EADS “235 to 516 Litre Bi-propellant Tank: Model OST 01/X” [179] or also MT Aerospace “metal tank for Eurostar 2000” [231]. Both tank volumes of about 260 liters are suitable for the maximum filling level of 95 %.

The structure shall be designed further in the following studies and analyzed for the launch environment for the launcher candidates. This also includes the integration of the launch adapter specified or provided by the launcher provider.

4.4.8 Mission and System Budgets

All decisions that have been made for the system architecture until this stage culminate in mission and system budgets. These budgets include satellite mass, power and dimension and they affect different mission aspects.

The satellite dry mass effects the delta-v budget for the launcher and orbit maneuvers during the mission. It also effects the propulsion system selection and amount of propellant mass. The power budget effects the parallel operation of different electronic components and thus the mission planning. Just as important, the satellite dimension effects the size of certain equipment like the antenna and solar panels that can be used and the launching option. For the piggy-back or secondary launching option, the satellite’s dimension has to be within the limits for the launchers that offer this launch opportunity. In this way the launcher selection for TMA-0 remains flexible when the satellite’s dimension and mass is suitable for secondary and dedicated launch option. Suitable compromises are found for the budgets and decisions.

4.4.8.1 Mass Budget

Figure 66 presents the mass per subsystem of TMA-0. The launch mass of 2020 kg includes a 20 % system margin. This is a typical margin for a feasibility study and accounts for potential unknowns in the overall design. The platform and payload components already include component margins according to their development status [ECSS-E-10-02A [112] [232]] between 5% for COTS equipment, 10% for small delta development and 20% for major re-design or new designs.

The satellite launch mass (including a launch adapter of 100 kg) is above the first satellite launch mass class of 1500 kg so the orbit design for the next launch mass of 2300 kg is used. It also results in a reconsidering of the launcher candidates in the next iteration of the study. If the satellite launch mass cannot be reduced and remains in this mass range the Tsyklon-4 (max. 1700 kg) and the Soyuz (max. 1800 kg) launchers with launch sites in Baikonur do not provide the required payload capacity. The communication system is the main payload and the processing functions are proved by the PDHT subsystem [233]. The average component margin is also higher than the rest of the subsystems. There are payload components that need modifications or development. For example, the modulator shall provide flexible data-rate however modulators with this feature are still currently under development. The remaining components are off-the-shelf products according to the TMA-0 design principle.

The allocation of mass per subsystem presented in Figure 66 can be checked for plausibility by means of comparing it with prior satellite designs of the same mission class. Table 93 shows the dry mass and mass distribution among the subsystems for GEO communication satellites launched between 1990 and 1995. This data serves as the basis for the verification. The resulting average payload mass (PLM) to vehicle dry mass (VDM) ratio of 28.4% is in range of the relationship VDM = 3.6 PLM given by C.D. Brown for GEO communication satellites [234]. This approximation was also used for the first design decision of the three sat launch mass classes of 1500 kg, 2300 kg and 3100 kg in the orbit design in Chapter 4.2.

Subsystem	Nominal [kg]	Margin [%]	Total [kg]
Electrical Power Subsystem	213,9	0,1	224,6
Onboard Data Handling Subsystem	40,0	0,1	42,0
Payload Data Handling	20,0	0,1	21,0
TT&C Subsystem	6,2	0,0	6,5
Attitude and Orbit Control Subsystem	60,3	0,1	63,3
Electric Propulsion Subsystem	0,0	0,0	0,0
Chemical Propulsion Subsystem	95,0	0,1	99,8
Thermal Control Subsystem	24,9	0,2	29,9
Harness	46,2	0,2	55,4
Structure	129,3	0,2	155,2
Platform total	**635,8**	**0,1**	**697,7**
Repeater Subsystem	0,0	0,0	0,0
Antenna Subsystem	17,1	0,1	18,0
Payload	80,6	0,1	86,2
Payload total	**97,7**	**0,1**	**104,2**
Spacecraft dry mass	**733,5**	**0,1**	**801,8**
System margin		0,2	160,4
Spacecraft dry mass + Margin			**962,2**
Propellant mass			1058,0
Spacecraft launch mass			**2020,2**

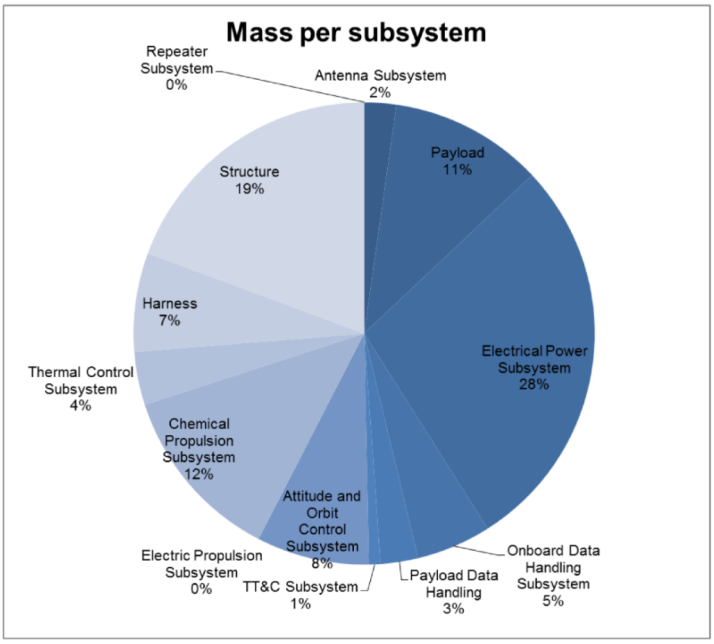

Figure 66: TMA-0 mass budgets – mass per subsystem and in total (dry and launch masses)

The result of the introduced analogy based on mass data of prior GEO communication satellite in Table 93 gives evidence that most of the TMA-0 subsystems lie within the normal mass range for a communication demonstrator satellite. The thermal, TT&C and propulsion subsystems masses lie outside the deviation that is the result of the different mission architecture. The deviation of the thermal control subsystem is the reason of the different environment. The propulsion system mass is higher due to higher delta-v for the mission and higher propellant demand leading to a bigger propulsion system compared to GEO communication satellites. The lower mass of the TT&C subsystem could be the result of the further distance and further driving design criteria.

Table 93: Dry mass by subsystem comparison between average GEO com. satellite and TMA-0

Satellite	**Dry Mass by Subsystem Comparison between average GEO Communication Satellite and TMA-0**							**Dry Mass**
	Payload	Structure	Thermal	EPS	TT&C	AOCS	Propulsion	[kg]
Average	28.4%	17.1%	5.0%	29.5%	3.1%	6.9%	8.7%	1209.1
Standard Deviation	8.0%	3.6%	1.1%	4.6%	1.6%	2.5%	2.4%	378.8
TMA-0	**27.8%**	**19.3%**	**3.7%**	**28.0%**	**0.9%**	**7.9%**	**12.4%**	**801.8**

Full information in Table 107

The mass allocation by subsystem is based on the equipment pre-selections and candidates discussed in Chapter 4.4. The detailed budget list is presented in Table 107 in the appendix.

4.4.8.2 Power Budget

Besides the mass budget, the power budget is influences the design of TMA-0. The analysis is based on the power modes of Chapter 4.4.5.1. The power consumption of each subsystem during each mode and the total power are presented in Figure 67 and Figure 68. The design of the electrical power system is based on mode 6 “Operating, RF & Laser” with a total power of 1200 W. The total power also includes the system margin of 20 % for a feasibility study and each component include component margins according to their development status [ECSS-E-10-02A [112] [232]].

Subsystem	Mode consumption [W]							Average consumption
	GTO	Safe mode, eclipse	Transfer	Idle	Science	Operating, RF	Operating, RF & Laser	
Electrical Power Subsystem	72,5	72,5	72,5	72,5	72,5	72,5	72,5	72,5
Onboard Data Handling Subsystem	67,2	63,0	67,2	67,2	84,0	84,0	84,0	82,5
Payload Data Handling	0,0	0,0	2,1	2,1	2,1	21,0	21,0	19,2
TT&C Subsystem	56,7	56,7	56,7	56,7	56,7	56,7	56,7	56,7
Attitude and Orbit Control Subsystem	177,5	177,5	177,5	177,5	177,5	177,5	177,5	177,5
Electric Propulsion Subsystem	0,0	0,0	0,0	0,0	0,0	0,0	0,0	0,0
Chemical Propulsion Subsystem	1,1	10,5	10,5	10,5	10,5	10,5	10,5	10,5
Thermal Control Subsystem	0,0	133,2	37,2	37,2	37,2	37,2	37,2	37,2
Harness	---	---	---	---	---	---	---	---
Structure	---	---	---	---	---	---	---	---
Platform total	**374,9**	**513,3**	**423,6**	**423,6**	**440,4**	**459,3**	**459,3**	**455,9**
Repeater Subsystem	0,0	0,0	0,0	0,0	0,0	0,0	0,0	0,0
Antenna Subsystem	0,0	0,0	0,0	2,3	2,3	15,8	15,8	14,3
Payload	0,0	0,0	21,8	77,6	78,4	388,9	525,4	416,3
Payload total	**0,0**	**0,0**	**21,8**	**79,9**	**80,7**	**404,7**	**541,2**	**430,6**
Subtotal	**374,9**	**513,3**	**445,4**	**503,5**	**521,1**	**864,0**	**1000,5**	**886,5**
System margin	75,0	102,7	89,1	100,7	104,2	172,8	200,1	177,3
Total	**449,8**	**616,0**	**534,5**	**604,2**	**625,3**	**1036,7**	**1200,5**	**1063,8**

Figure 67: TMA-0 mode consumption, per subsystem and in total

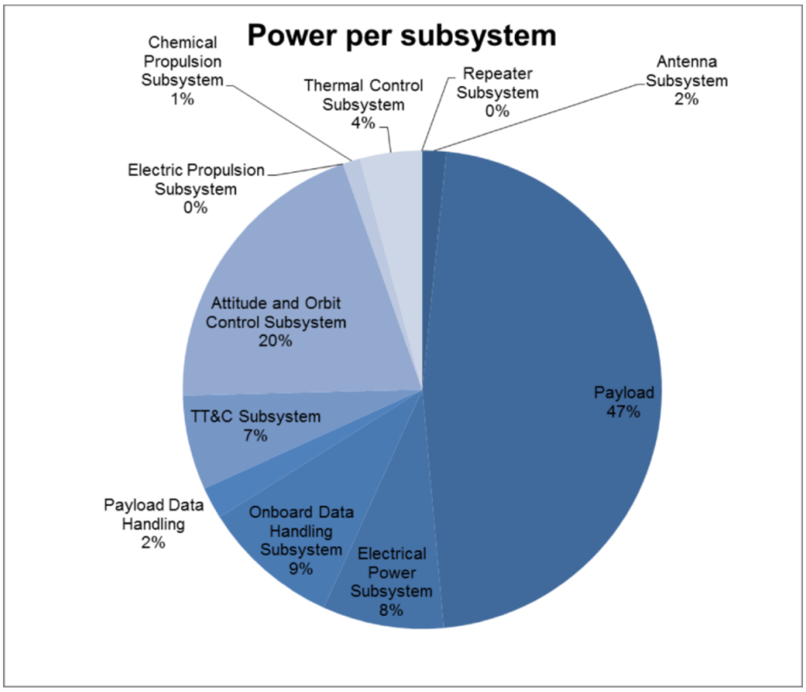

Figure 68: TMA-0 power per subsystem

Mode 6 is used for the analysis because all communication payload equipment is active and the duty cycle is 45 % of the mission. A detailed equipment power consumption and activation plan is presented in Figure 87 and Figure 88.

The total power is also checked for plausibility based on prior communication satellites. The prior GEO communication satellites in Table 108 lead to the linear regression function shown in Figure 69 which is used for the plausibility check of the power system. For this, the payload power P_{pl} is set into relation to the overall satellite system.

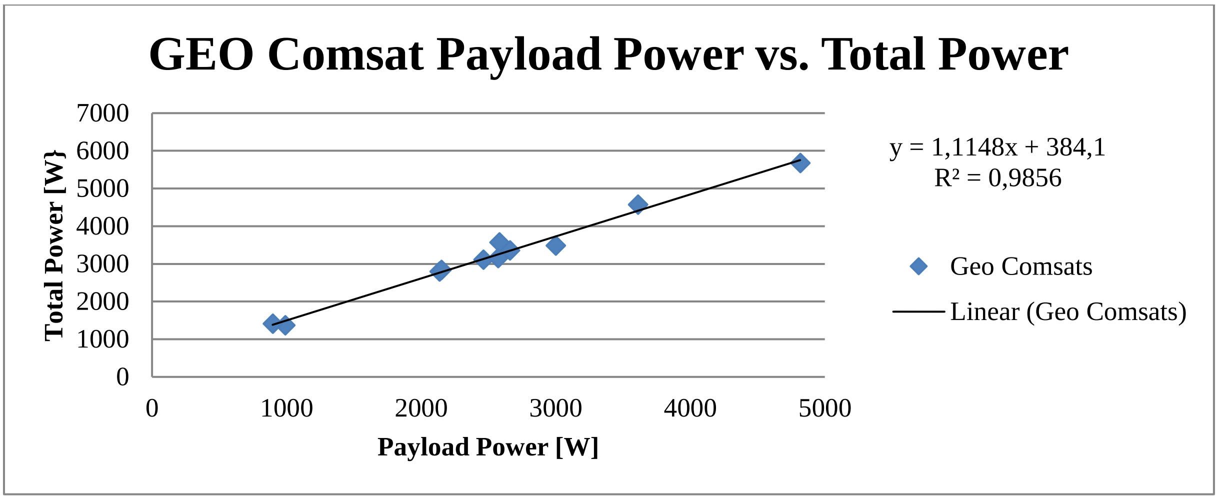

Figure 69: GEO comsat payload power vs. total power

$$P_{total} = 1.115 \times P_{pl} + 384.1W \tag{4.66}$$

The current TMA-0 power budget $P_{total-budget}$ includes margins according to each consumer component. Based on the linear regression function of prior satellites, the total power budget is 21% bigger than the estimated power $P_{total-estimated}$ (Table 94). The demonstrator satellite TMA-0 is a scaled down system based on the operational TMA-1 satellite consisting of a payload with only two out of four high data-rate channels. For the operational TMA-1 satellite, the power demand for the four high data-rate channels payload increases significantly and the power demand of the platform remains on the same level. The TMA-1 total power would then follow closer to the given trend. For this reason the payload and total power budget of the demonstrator TMA-0 mission is plausible.

Table 94: Total system power based on prior GEO com. satellites and TMA-0 system budget

P_{pl}	$P_{total-estimated}$	$P_{total-budget}$	$P_{total-budget}/P_{total-estimated}$
541 W	987 W	1200 W	1.21 (+21%)

5 TMA-0: In-Orbit Demonstration Conclusion

This chapter concludes the TMA-0 satellite architecture design. It presents an overview of the implications of the chosen architecture, a first draft of the mission timeline and the perspective of the demonstrator mission. The conclusions shall be used for the next iterations of the conceptual design and for further studies of the demonstrator satellite.

5.1 Demonstrator Mission Architecture Summary

The current TMA-0 mission architecture is mainly based on off-the-shelf components and no showstopper for the demonstrator mission has been identified in this study. The satellite mass budget allows a delivery into orbit with available launchers as well as transfer from Earth to EML-4 orbit. Nevertheless, at this early design stage there are still certain satellite components and regulations that need additional research to provide certainty about the system capabilities and behavior.

5.1.1 Technology Development and Considerations

In respect to the power, thermal and onboard data-handling subsystems standardized components with heritage can be used because the selection is based on missions with similar requirement. However, the communication payload items are identified that require higher technology readiness levels or further research before the TMA-0 is considered fully functional and fulfilling the mission requirements. The propulsion subsystem is also based on standard components but with an uncertainty of the amount of delta-v for the station keeping which requires an additional study.

5.1.1.1 Communication Payload

The high data-rate channel via the K-band link shall provide a flexible data-rate. The state of the art modulators do not provide the required data-rate range. The Tesat TeTra system presented in Chapter 4.4.1.1 is stated for a market release in 2016. It is the first system with this flexible and adaptive data-rate and frequency feature for K-band in development [132]. Possible consequences are to respect the availability in the mission time line which could lead to postponements or to initiate collaboration with the modulator manufacturer to foster the directed development. The decision depends on the final TYCHO demonstrator mission design start. For this reason, the availability of the modulator only results in a time critical point.

The frequency regulation and allocation procedure could pose another time critical point. As presented in Chapter 4.3.1, the allocation procedure could require a coordinated approval of different ITU sections and frequency band users. The relay service from EML-4 is a new application about which only several parties have to be heard.

The last communication development concerns the laser communication terminal. For the TMA-0 satellite, an available LCT is used to qualify certain requirements like the target pointing. It does not provide the required data-rate of 400 Mbit/s in this configuration and this leads to further developments in the transmit power output of the laser and the telescope sizes on board of the satellite as well as for optical ground stations. As stated in Chapter 4.3.3, larger aperture sizes for stationary and mobile telescopes are in development. Collaboration for fostered development could be a solution.

5.1.1.2 Station Keeping Strategy

The study shows that additional research for the station keeping requirement shall be conducted because the AOCS propellant demand is based on the study “A Survey Of Earth-Moon Libration Orbits: Stationkeeping Strategies and Intra-Orbit Transfers” by Folta and Vaughn [47] that has yet to be confirmed. This leads to the station keeping maneuver strategy requiring a model with more detail than in this study. Station keeping strategies of satellites in the Sun-Moon-libration points could be used as a basis. The current status for TMA-0 is that the station keeping in EML-4 feasible.

A general propulsion issue can arise from REACH (Registration, Evaluation, Authorisation and Restriction of Chemicals) [176]. The bi-propellant prolusion system relies on hypergol propellants that have a long space heritage for GEO communication satellites and other spacecraft. These were selected because of the heritage and the performance they offer. Nevertheless, the propellant MMH is classified as substances of very high concern (SVHC) due to their potential negative impacts on human health or the environment. Those chemicals are regulated by REACH with respect to the annual production and import as well as the utilization. This could negatively affect propulsion systems based on MON/MMH propellants in general by means of availability, handling and costs. REACH will enter into full force in 2018 that could affect the propulsion design with a risk that REACH will make hydrazine derivates obsolete. ESA initiated the development of “green propulsion” technologies to substitute substances on the SVHC list with less toxic substances for space applications [235]. There is a roadmap to find a MON/MMH replacement with green propellant (G61C-004MP) within this “Clean Space” initiative. The activity shall foster a European MON/MMH replacement with green bi-propellant to technology readiness level 6 until 2018. For these reasons the following TMA-0 study shall include research for a propulsion system with green propellant as an alternative due to the long-time strategy for the TYCHO mission.

Besides the Clean Space initiative by ESA, a high performance green propulsion (HPGP) system based on Ammonium Dinitramide (AND) is already flown onboard of Prisma (SNSB) in 2010 and a Hydroxyl Ammonium Nitrate (HAN) bases system is planned for the Green Propellant Infusion Mission (NASA) in 2015. Green propellants could also be an advantage due to several propellants offer similar or even higher ISPs than MON/MMH [236] (ADN/Al/GAP 335 s instead MON/MMH 330 s) [237]. Both systems use green mono-propellants making the TMA-0 propulsion system design not limited on the current bi-propellant system and could take advantage of a simpler system with similar or even higher performance.

5.1.2 Alternative Architectures

Instead of designing a new satellite architecture, the design can be based on existing standard platform busses. This approach further reduces delivery time of the satellite and mission risk.

The comparison of the SGEO, Spacebus 300 and Alphabus architectures with that of TMA-0 in Table 95 is made due to the fact that all three have European heritage. Each of them provides a platform servicing a special market segment that could reduce development time and costs. Lastly, the payload requirements and the propulsion system are critical points for TMA-0 making them necessary to be compared.

Table 95: Communication satellite architecture comparison (TMA-0, SGEO & Alphabus)

	TMA-0	**SGEO**	**Spacebus 3000**	**Alphabus**
Design Mission Life Time	3 years	15 years	15 Years	15 years
Payload Mass	104 kg	300 kg	500 kg	1500 kg
Payload Power	541 W	3000 W	6500 W	12000 – 18000 W
Propulsion System	Bi-Propellant with MON/MMH			
Apogee Kick Motor	EADS 500N	EADS 500N	EADS 400N	EADS 500N
AOCS Thruster	22 N	10 N	10 N	10 N
Launch Wet Mass	2020 kg	3200 kg	4100 kg	8800 kg
Dimension	2x2x2 m³	2x1.8x2.5 m³	2.4x3.2x2.4 m³	3x2.3x9 m³

[158] [159] [238] [239] [240]

It is obvious that SGEO matches the TMA-0 properties better because the Spacebus 3000 and Alphabus platforms serve other market sections that are not comparable to that of the TYCHO mission. The propulsion system and the apogee kick motor of SGEO and Alphabus are the same. The requirements of TMA-0 for the transfer can be fulfilled. The AOCS thruster requirements as discussed in Chapter 4.4.3 can also be fulfilled by the 10 N thrusters instead of the 22 N thrusters. The dimension mainly differs in the height that is due to additional parabolic antennas on top of Small GEO (SGEO). By considering the dimensions and the launch wet mass, a SGEO based TMA-0 satellite could be transported by the same launcher.

The payload mass and power design of SGEO exceeds those of TMA-0 and that makes SGEO a better candidate for the operational TMA-1. However, a further scaling of the payload mass and power of the SGEO could make platform compliant to TMA-0's requirements. This modification should result in less development time and costs rather than a new satellite development. It should be discussed in the following study if there is an advantage in development costs and time to directly use the SGEO architecture.

5.2 Demonstration Mission Timeline

The preliminary mission timeline for the demonstrator satellite TMA-0 should identify the main schedule in absolute terms when the TMA-0 mission will be realized. Furthermore, it will also influence the development start of the following TMA-1 satellite that is influenced by the results made during the demonstration.

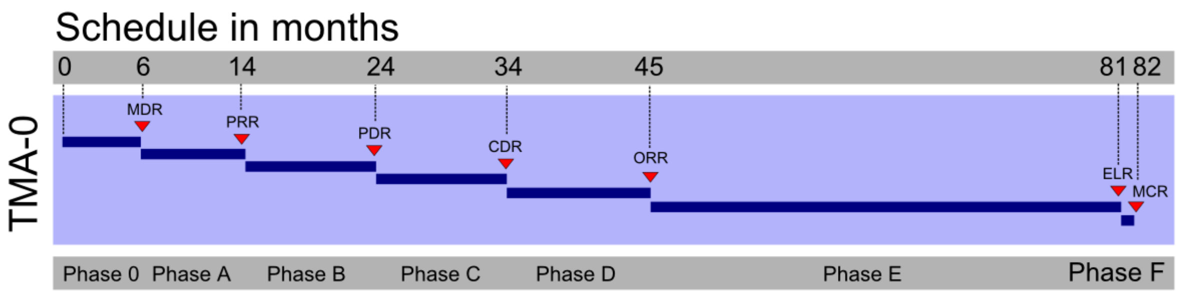

Figure 70: Preliminary key milestones in the TMA-0 demonstrator mission timeline (when satellite is based on platform)

Table 96: Preliminary distribution of development time per phase

	Satellite based on platform	**New development***
Phase A	8 Months	8 Months
Phase B	10 Months	12 Months
Phase C	10 Months	24 Months
Phase D	11 Months	24 Months
Phase E	36 Months	
Phase F	1 Month	

*(optimistic) [241] [238]

The development times per phase presented in Figure 70 and Table 96 are based on the EDRS-C satellite development phase and it serves as a first estimation due to the facts that it includes similar RF and laser payloads and it is based on SGEO, that shares a matching propulsion and power system [241].

5.2.1 Phase E and F Activities

Phase E consists of the satellite launch and demonstrator mission operation. Besides the standard procedure for satellite launch and mission preparations and reviews, the demonstrator mission shall perform a certain sequence of demonstration activities. These demonstration activities shall qualify the satellite components and the performance of the relay and science mission in general.

Table 97: Mission phase E and F activities

	Phase E	
0	**Launch preparation, launch and GTO inauguration**	1 Month
1	**Transfer and target orbit commissioning**	3 Months
2	**Demonstration Sequence A**	8 Months
	Orbit in target plane and relative position to EML-4 in target distance. Determination of station keeping orbit behavior	
3	**Demonstration Sequence B**	8 Months
	Orbit in target plane and relative position to EML-4 with varying target distance. Determination of station keeping orbit sensitivity with respect to semi-major axes.	
4	**Demonstration Sequence C**	8 Months
	Orbit with varying inclinations and relative position to EML-4 in target distance. Determination of station keeping orbit sensitivity with respect to inclination.	
5	**Demonstration Sequence D**	8 Months
	Orbit with varying inclinations and relative position to EML-4 with varying distance. Determination of station keeping orbit sensitivity with respect to inclination and to semi-major axis.	
6	**Mission Extension**	TBC
	The End of Life Review (ELR) shall clarify a mission extension to use the TMA-0 satellite after the demonstrator mission. The TMA-0 can either be used as a back-up relay for lunar missions or as an interplanetary science probe.	
	Phase F	
0	**End-of-Life Transfer**	1 Month

Table 97 shows a preliminary time line for the phases E and F. It includes transfers and the in-orbit demonstration sequences. During all phases, dust sensing is performed. The demonstration sequences are based on the delta-v maneuvers that need to be qualified. They will determine the sensitivity of the EML-4 orbit so several orbit periods shall be used for each demonstration sequence allowing a variation of parameters and a precise orbit parameter measurement. The activities shall include adequate delta-v as well as propellant margins in case of unexpected events that result in repetition of the activity.

Each of the demonstration sequences A to D consists of a set of communication demonstration tasks (Table 98). The communication demonstration set shall determine the influence of the orbit parameter on the communication performance characteristics.

Table 98: Set of communication demonstration tasks for each demonstration sequence A-D

	Performance	**Task**
0	Pointing accuracy	to Earth, Moon, EDRS
1	Connection and access	to Earth ground stations and EDRS
2	Connection handover	from ground station to ground station
3	Connection quality	flexible data-rate performance and delay time
4	Signal relay	RF to RF, RF to Laser, Laser to RF, Laser to Laser
5	Multi user access	Priority modes and data buffer

For each demonstration sequence this set shall be performed allowing a statistical evaluation and result that qualifies the mission requirement for communication points. When this result is achieved, the TMA-0 shall still perform the station keeping orbit of the demonstration phase to allow the orbit parameter determination.

When the demonstration sequences A to D are executed, the end of life review shall decide whether or not a mission extension is possible. This mission extension could be used to set the TMA-0 satellite into safe mode. It provides the option to use the satellite as a back-up relay for later lunar missions (Chapter 5.3.4). When a mission extension is not possible, the final orbit parameter determination shall be performed and the end of life transfer with a target Moon landing shall be performed and ending the TMA-0 mission.

5.3 Demonstration Mission Perspective

Summarizing the TMA-0 demonstrator satellite concept, on the one hand it is feasible to demonstrate key mission requirements for the operational TMA-1 satellite mission within the TYCHO concept. The components of the subsystems can be modified or off-the-shelf products. On the other hand, there are technology development initiations needed for the communication payload and for the attitude and orbital control subsystem. Such a mission with these requirements for both subsystems has never before performed by a satellite.

With the remaining uncertainty in the subsystem performance and in the availability of possible users of the relay, the division in a precursor mission that demonstrates the mission requirements independently from other lunar missions is a logical consequence. It reduces the financial risks for the operational mission and offers a qualification of the main components needed for the operational TMA-1 satellite.

5.3.1 Demonstration Mission Cost

The estimated mission cost of the satellite is about 140 M€ based on existing GEO communications satellites. This number was derived by using a specific cost of 70 K€/kg, as it is derived in [127] [242]. This seems to be low, however the platform of the EDRS-C, a small GEO communication satellite, is stated with cost of 160 M€ [243]. The cost range is thus feasible as the first estimation. The estimated combined cost of 230 M€ is distributed between

- 140 M€: satellite research, development and assembly
- 70 M€: baseline launcher – Soyuz (from Kourou)
- 20 M€: operation (ground segment and personnel)

The demonstration mission cost reflects one part of the overall TYCHO mission cost of two satellites. The demonstrator mission shall help to reduce the development costs of the operational mission. The overall two satellite mission is a compromise between cost and risks. The reduced risks for the operational TMA-1 mission is beneficial for granting of funds and thus the demonstration TMA-0 is required and even allows an optional-out decision before initiation of the TMA-1 development and still acquiring valuable scientific data and results.

5.3.2 Demonstration Mission Start

TMA-0 offers a schedule that is only possible with a demonstrator mission. The mission start is independent from other lunar mission and TMA-0 can be flexible scheduled for a launch that even offers a hiatus between phase D and F.

5.3.3 Research, Demonstration and Qualification

The TMA-0 concept will enhance the knowledge of the EML-4 environment and the influence on satellites hardware as well as on the station keeping orbit. It will serve as a demonstrator platform for the qualification of modified or new technologies like laser communication terminals. It will also influence the design of the operational TMA-1 satellite that could be the first permanent relay service between Earth and the far side of the Moon.

Besides the required research and demonstration of the TYCHO mission, the TMA-0 satellite could be used as a platform for qualification of further instruments and components. This test-bed option requires additional allocated budgets (power, mass, dimensions and location). In this way, TMA-0 could be a platform for demonstration and qualification and raising third-party funds. This is a unique possibility for exposing hardware to effects in the target location.

5.3.4 Extended Mission Time and Back-up Relay

By adopting the specification of EDRS for the RF and laser communication links, the TMA-0 is already prepared to be an operational relay satellite within the EDRS network. Though at this point, the demonstrator mission does neither provide a RF to RF nor a laser to laser link from the Earth to the Moon (Figure 3), the satellite can be used as a repeater and convert RF to laser and vice versa. This is possible due to the LCT and its ability of independent pointing with respect to the satellite body and thus the body mounted RF high-gain antennas. In this way space research missions designed for EDRS could also use TMA-0 with an adapted data-rate due to the further distance or data routed through the EDRS network could also be supported by TMA-0. This is an option if TMA-1 is functional after the primary demonstration mission. A hibernation strategy shall be considered that will extend the mission time to provide this back-up relay option within EDRS. The extended mission time also give the possibility for further scientific measurements. This shall be considered as long as the end-of-life disposal on the Moon is not affected.

6 TYCHO Mission Conclusion

The overall conclusion of the study is that the general TYCHO mission could be a future building block for the communication infrastructure between the Earth and the Moon needed for the exploration and development of the Moon. The TYCHO mission objectives are in-line with studies from the international telecommunication union (ITU) and similar plans by NASA for the utilization of EML-4 and the far side of the Moon.

This last chapter will give an encompassing summary of the study and the results, recommendation of the following steps as well as a perspective for the TMA-0 and TMA-1 satellites of the TYCHO mission.

6.1 Mission Perspectives

6.1.1 Relay Service Perspectives

The study shows that achieving this goal requires technology demonstration with TMA-0 to gather foreknowledge about critical mission points to minimize the risks of the operational TMA-1 mission. Henceforth, the selection for the earliest mission start for TMA-1 depends on the demonstrator and the mission results. The chosen dual satellite approach for the TYCHO mission leads to a TMA-1 operational mission start (phase E) not earlier than 2025. This assumption is based on the mission timeline in Chapter 5.2 if the development of TMA-0 and -1 is based on an existing satellite platform.

The extrapolated market and customer section for a relay system like TYCHO is demanding. Figure 71 (based on Table 109) shows a total of 50 completed, planned and proposed lunar missions. The missions classified as “proposed” include missions where the mission status is in a proposal or study phase as well as all private endeavors (like Google Lunar X-Prize and space tourism activities). The figure gives an overview that there are currently no space agency operated lunar missions for the TMA-1. However this may change when one of the next exploratory objectives and milestones is selected by the different space agencies. The decisions for the key milestones for space explorations are set by executive organs like the ESA ministerial council (Space Council) or President of the United States and the United States Congress. These organs evaluate the current space missions and provide orientations for the next objectives. Herein exists an opportunity for TMA-1 to be launched and fully operational for possible future lunar missions after 2025. By use of concurrent engineering concepts, the elapsed time required for the development phases A-D of TMA-1 could be reduce by parallelization of tasks. Concurrent engineering is an option and is not considered in this study due to increased costs. It is also an option to implement TMA-1 as part of a partnering lunar mission. It requires additional efforts for alignment of planning schedules but offers the advantage of a direct first costumer.

There are commitments by several ambitious space agencies in emerging space technology countries such as China and India who declared that their final goal for lunar missions in the culmination for manned exploratory missions and even bases. Besides the early stage and the proposal status of these missions, this could increase the ambitions of these and other space organizations for lunar missions.

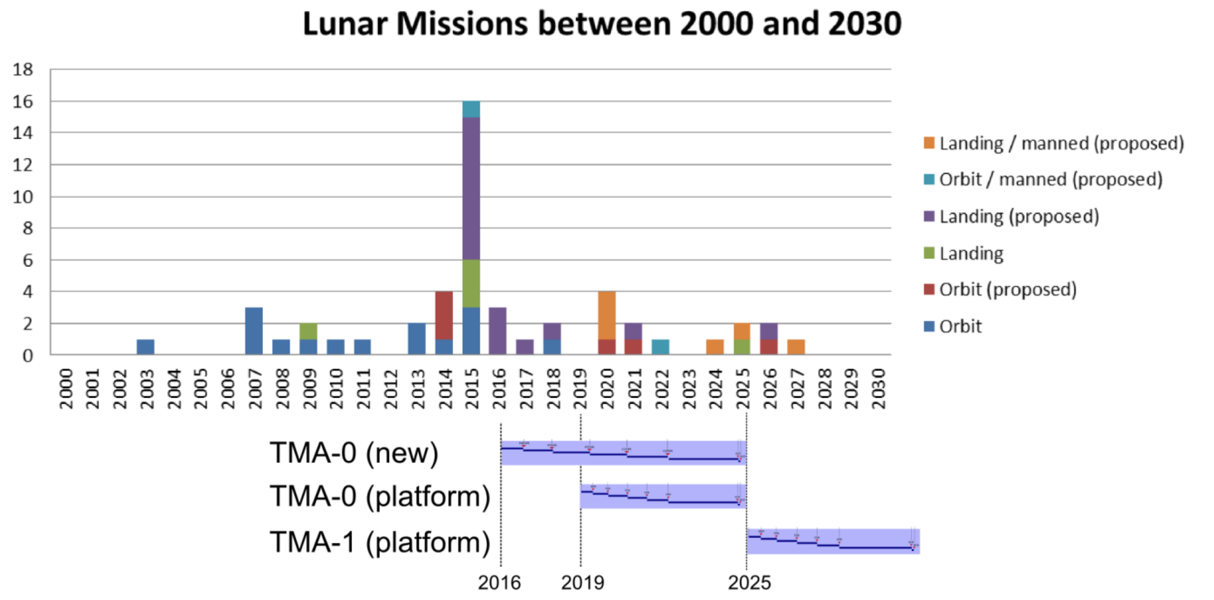

Figure 71: Lunar missions in relation to TYCHO mission time-line (full list in Table 109)

This also leads to the conclusion that the decision of an independent demonstrator, on which a possible TMA-1 can be based, is financial and technical logical. Furthermore, it leads to two scenarios where the TMA-1 is directly paired with another lunar mission as a customer. This requires a cooperation agreement and further organizational endeavors or a combination of both missions into one program. With or without this initial companion approach, the establishment of an available infrastructure can be the spawning point for customer commitments, which will use the service. Eutelsat S.A., that was founded for the commercialization of ESA communication satellites [244], could serve as a model to support the initial founding and marketing of the TMA-1 satellite. An open standard satellite service that allows a simple and universal utilization is mandatory whereby the costumers consist of governmental as well as future private missions.

Another obvious aspect is the commitment of private space companies like SpaceX, Golden Spike, and several others to develop technology for lunar missions. Their goals also include offering space tourism for suborbital flights on Earth but there are also proposals for manned missions to lunar orbit or even on the surface. The “*The Economic Impact of Commercial Space Transportation on the U. S Economy in 2009*” report by the Federal Aviation Administration in 2010 predicts space tourism “could become a billion dollar market within 20 years” [245]. TMA-1 could also partner with such a private endeavors and it could also include a public private partnership for the establishment of an infrastructure for both public lunar exploratory missions and private commercially driven missions [122]. The customer base, the market prediction and the price charged for service is a matter for further research [246].

6.1.2 Satellite Platform Perspectives

Besides the communication relay mission, the satellites TMA-0 and TMA-1 are designed for the EML-4 and -5 orbits that are also of interest for other purposes than communication services. Obtaining scientific and technological investigation will lead to knowledge that can be used for other EML-4 and -5 missions. The satellite design can even be a basis or a platform satellite mission serving as lunar navigation satellite systems (LNSS) for automated transfer vehicles between the Earth and the Moon, space observations or further mission in those target orbits. This is an additional advantage of the development of the TYCHO mission.

6.1.3 Integration in Lunar Exploration Joint Initiative Mission

The operational TMA-1 is proposed to be integrated into an international joint exploration initiative mission concept for the Moon. This way offers advantages with respect to mission funding, planning and providing the service. As part of a joint mission the funding can be completely or partly acquired from space agencies' budgets. The mission planning directly allows a launch and servicing of an accompanying lunar mission. With a multi mission joint lunar program during a longer term, the relay service is more effective with respect to the single TYCHO mission cost.

The TYCHO mission is designed to include components with European heritage, available launcher candidates for utilization of European satellites and is as well compatible to the European Data Relay System, making the TYCHO mission a prime candidate for ESA and related space agencies giving them an advantage point. The relay communication service shall be available for all missions to allow a faster amortization. All negotiations about utilization of TMA-1 shall be open to every customer and shall at least include the agencies with plans for lunar missions (NASA, ESA, JAXA, RFSA, CNSA, ISRO). TYCHO is also a candidate for NASA to support their plans for TDRS applications in the libration points and TMA-1 could serve as a platform for TDRS compatible communication payloads [247].

6.1.4 TYCHO Minimum Demonstration Mission

Under consideration of the development initiation of key technology (Chapter 5.1.1) and the mission costs (Chapter 5.3.1), the possibility of a strip-down TMA-0 mission arises. It results in an alternative mission for a minimum demonstrator satellite as an in-orbit demonstration for the major critical mission point of attitude and orbit keeping in EML-4 and intensified ground tests of the communication payload.

The AOC-Subsystem as well as control strategy and the dust detection (Chapter 4.4.1.4) are subjects of in-situ measurements of the unknown influence of the EML-4 environment on the satellite. For this, it is essential to acquire real flight data and dust particle detection. The high data-rate communication of the K-band and laser channels could be conducted onboard other satellite missions or in test facilities under analogous conditions while providing adequate results.

The TYCHO minimum demonstration allows further cost and risk reduction and an even earlier launch date. It is also independent from accompanying lunar missions, but it cannot serve for the space qualification of the communication payload nor serve as a back-up relay for EDRS (Chapter 5.3.4.) or a permanent lunar communication relay (Chapter 6.1.3). In the following study this option should be analyzed according to the reduction in mass, power consumption and costs and a comparison to TMA-0 should be made. This gives a further opportunity in negotiations with agencies and organizations as possible partners in the realization of the TYCHO mission.

6.2 Mission Feasibility and Service Cost

The TYCHO mission concept is feasible with respect to technology and methods and the mission perspectives. Furthermore critical mission points and technology that need to be developed are identified (Chapter 5.1). The expected mission cost for the TMA-1 is also estimated to be in the range of 230 M€ (TMA-0, Chapter 5.3.1) when the TMA-0 development and mission results are included in the TMA-1 development due to a positive lessons learned. This mission budget outlines the overall service costs for amortization by a certain number of costumer missions during the TMA-1 mission time. For detailed figures, a further study under business economic aspects is proposed to explore the market reactions to such a relay communication mission and setting the market value and the market price. In this way, additional funding by agencies, the space industry and further public institutions can be found.

6.3 Study Summary and Perspective

The goal of the thesis was to design a concept for a demonstration mission for a communication relay satellite on the Earth-Moon-libration point EML-4 as a preparation for the operational TYCHO mission and to research the feasibility and perspective of a communication service.

For this purpose, a phase 0-A study was conducted for the demonstrator mission TMA-0 and the operational TMA-1 satellites. It defines the dual satellite relay mission objectives, the mission analysis, demonstrator mission architecture, in-orbit demonstration and the TYCHO mission perspective.

The study is based on the mission statement and the derived requirements elicitation and analysis of user lunar missions, of the TYCHO mission itself and of the satellite system. Important preliminary work for this was the analysis of possible costumer lunar missions and their high priority landing sites and mission needs, the environment of the target libration point EML-4 and possible applications as well as the definition of the demonstrator and operational missions TMA-0 and TMA-1.

During research, the mission benefits as well as the critical mission points were identified. Especially the attitude and orbital control in EML-4, the unknown EML-4 environment and communication relay performance turned out influencing and driving the mission architecture and concept design.

The mission architecture of the TMA-0 demonstrator mission sets up candidates for the launching system. The Soyuz launcher system with Kourou as the launch location was recommended as the baseline candidate due to payload performance, reliability and costs. Further launcher systems for back-up candidates were also considered. The launchers were selected to provide the GTO as the starting orbit for the mission.

The orbit design for the mission was identified as one crucial mission point. It included the transfer to EML-4, the station keeping orbit and the end-of-life transfer. Several options were compared. The weak stability transfer was selected for the transfer due to higher efficiency and thus higher satellite payload masses. The AOCS strategy for the station keeping orbit was identified for further studies because only fundamental research was found and an own control strategy could not been applied. For the end-of-life strategy the crash-landing option on the Moon was proposed. It offers a required disposal phase and requires the less delta-v compared to the alternatives. Furthermore a disposal on the Moon's surface is possible due to the Moon's category I status. The orbit design was conducted using simulations with NASA's GMAT software with analysis of all options. This was required due to the gravitational n-body effects by the Earth and the Moon, external perturbations and gravity losses. Additional verification of the results was conducted by a self-programmed trajectory software which was processed on the distributed computing platform Constellation.

A special emphasis was put on the communication architecture. The RF-band selection was challenging to fulfill the regulations by the ITU. The allocation was finally decided in the 25.5 GHz band because it allows communication from and to Earth as well as inter-satellite links. It was also selected to be compatible to EDRS and fulfill user requirements of using available ground infrastructure and it offers high-speed data rates of 400 Mbit/s. It also is an allowed band to the Moon by the IAU because it does not interfere with measurements in important bands for astronomy. As a preparation for future lunar missions, a laser communication terminal in 1064 nm with compatibility to EDRS was considered. The link budgets for RF communication showed that the data-rate of 400 Mbit/s is possible from EML-4 and that the COTS laser communication can demonstrate the required accuracy in target pointing. The analysis of the communication architecture showed that technology development should be fostered. The RF communication benefits from controllable modulators that offer flexible data-rate to serve a wide range of lunar missions. The laser development should be supported in the field of high-power diodes, bigger telescope apertures for the terminals and optical ground stations and for additional OGS locations. Also importantly, the communication architecture is already feasible.

The study then progressed towards the demonstrator satellite configuration. This was conducted to preliminary select components for the payloads and the subsystems. The configuration was also used as a basis for the mass, power and dimension budgets. The design philosophy of TYCHO was to use standard and COTS components and only initiate development when absolutely required. As far as for command and on board data handling, for electric power and for thermal control subsystems as well as for structures, existing technology and components can be used from GEO communication satellites. As dually noted, the mentioned modulators and laser terminals for the communication payloads and adequate precise reaction control thrusters and strategies for AOCS shall be researched in a further study. This AOCS study shall also evaluate the use of electric propulsion systems (like iMPD). For the chemical propulsion system, a MON/MMH bi-propellant system was chosen for the apogee-kick motor as well as for AOCS due to its efficiency and heritage. However, the continuing study shall include an option for green propellants and the effects on the mission because the new REACH regulations for the selected bi-propellant system will be enforced in 2018 which will classify MON/MMH under stricter safety and handling conditions. The study shows that the resulting budgets for mass, power and dimensions are feasible and existing launchers and component manufacturers exist. Those options are evaluated with decision making methods to find suitable candidates.

The study defines the mission schedule and the qualification tasks for the in-orbit demonstration mission. It presents an option to use an alternative platform based on the SGEO platform and evaluate technologies that need to be supported or initiated for development. The possible mission start for the operational TMA-1 is concluded for the year 2025 and based on the new and platform development phases.

For the demonstrator mission the perspective analysis included the mission cost estimation based on analogue GEO communication satellite missions. The TMA-0 mission cost is estimated in a range of 230 M€. However, the concept of a predecessor TMA-0 demonstrator mission that shall qualify the operational TMA-1 mission was argued as a plausible concept. The argumentation is based on the reduction of risks, the possibility to qualify the mission and technology and finally leading to a proven and cost efficient operational TMA-1 mission. The decision to design a demonstrator satellite that is independent from accompanying lunar mission is supported by the researched arguments. The study also presents applications beyond the demonstration as a science platform, a test-bed for technology qualification and as an operational back-up relay for EDRS.

The phase 0-A culminates in the overall TYCHO mission perspective analysis. The research presents that a communication relay satellite in EML-4 orbit is an important building block in the exploration of the Moon, the EML points and beyond. The compatibility to relay infrastructure on Earth (EDRS) and on the Moon (ILN) provides synergism between these systems and TYCHO. The TMA-1 satellite offers the opportunity not only to be a platform for further relay satellites but also for further missions to the Earth-Moon libration points due to knowledge gained from the TYCHO missions that can be transferred. The TYCHO mission is proposed as an eligible part of joint missions to the Moon with respect to partnering lunar missions as costumers, the mission planning as well as funding and costs. The cost budget calculation is advised for another study that should include a market research for evaluating the market value and the market price of the service and finding an adequate amortization rate. There is even the possibility of a minimum demonstration mission for in-orbit qualification of the AOCS and Kordylewski dust particle detection.

The phase 0-A study concludes with the mission evaluation. The TYCHO mission is plausible from today’s state-of-the-art technology methods. It is feasible with respect to a mission start in 2025 because the identified development in AOCS strategy and flexible communication data-rates are already in progress or requires modification from existing techniques. These are expected to be operational within the next three years. The remaining subsystems and components are not crucial to the mission. So following studies to progress the TYCHO mission development to phase A is advised. Permanent relay communication as an open infrastructure is assumed essential for the future of lunar exploration and thus TYCHO offers an essential part within international endeavors for un-manned and manned missions to the Moon.

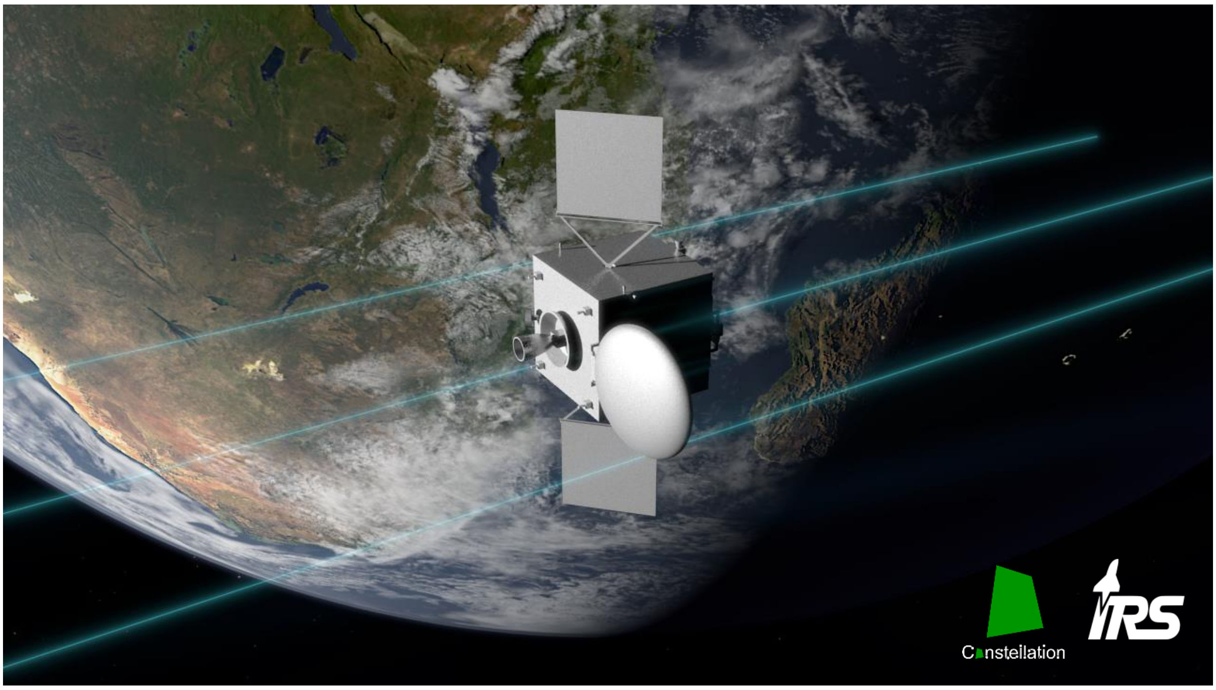

Figure 72: Artist's rendering TMA-0 satellite during GTO in Earth's vicinity.
Blender 3D animation with AIRM (Animation of Interplanetary and Reentry Missions) [248]

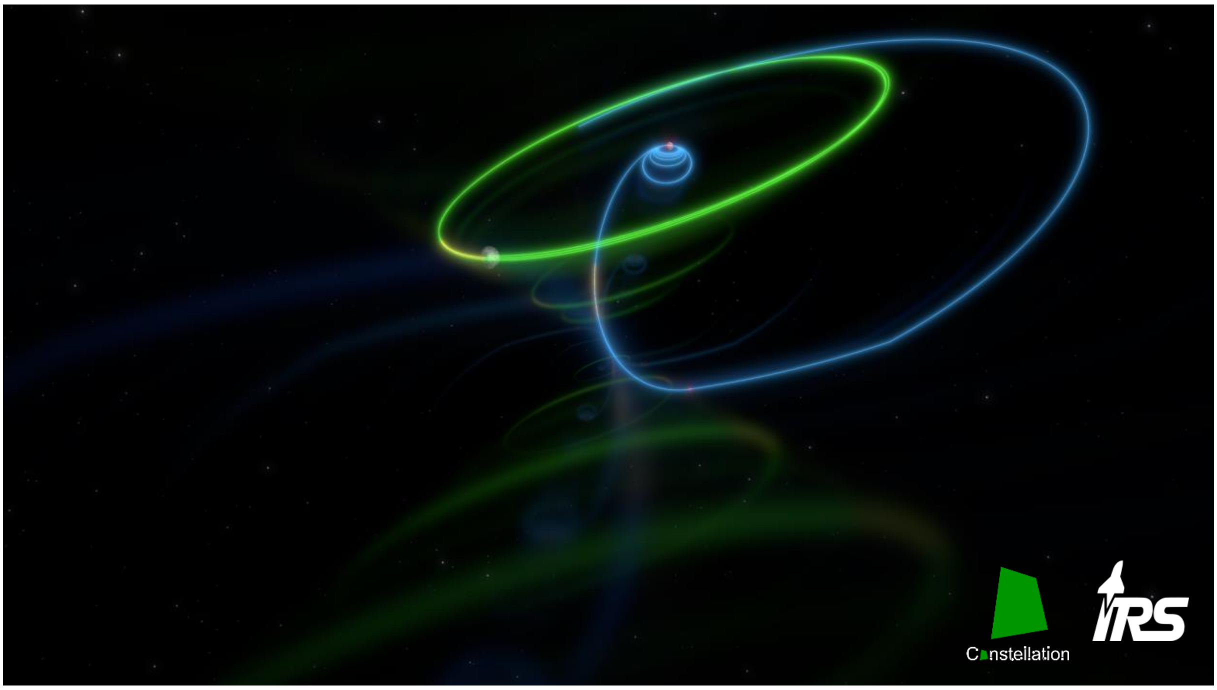

Figure 73: Artist's rendering of TMA-0 satellite during transfer to EML-4.
Blender 3D animation with AIRM (Animation of Interplanetary and Reentry Missions) [248]

List of References

[1] A. C. Clarke, "Hazards of Prophecy: The Failure of Imagination," in *Profiles of the Future: An Enquiry into the Limits of the Possible*, New York, NY, US, Harper & Row, 1962 (revised 1973), pp. 14, 21, 36..

[2] J. E. Masefield, "Sea-Fever," in *Salt-Water Ballads*, New York, USA, The Macmillan Company, 1916, p. 55.

[3] I. Newton, *Letter to Robert Hooke*, 1676.

[4] A. C. Clarke, *2001: A Space Odyssey (ISBN: 0453002692)*, New American Library (US), 1968.

[5] A. C. Clarke, ""Extra-Terrestrial Relays – Can Rocket Stations Give Worldwide Radio Coverage?"," *Wireless World*, October 1945.

[6] A. C. Clark, ""Extra-Terrestrial Relays — Can Rocket Stations Give Worldwide Radio Coverage?"," October 1945. [Online]. Available: http://www.clarkefoundation.org/docs/ClarkeWirelessWorldArticle.pdf. [Accessed 02 03 2013].

[7] R. Findley, "Telephone a Star - Communication satellites will relay messages across Earth's oceans and continents," *National Geographic*, pp. 638-651, 1962.

[8] Steg, L. & Shoemaker, E., "Libration Point Satellites," in *A Review of Space Research: The Report of the Summer Study conducted under the auspices of the Space Science Board of the National Academy of Sciences at the State University of Iowa, Iowa City, Iowa, 17 June-10 August 1962, Publication 1079, National Aca*, Iowa City, Iowa, USA, 1962, pp. 4-34 - 4-46.

[9] Apollo Operations Handbook, Lunar Module (LM 10 and Subsequent), Volume One. Subsystems Data, NASA, 1971.

[10] Schmid, P. E. (Goddard Space Flight Center), "LUNAR FAR-SIDE COMMUNICATION SATELLITES," NASA, Washington, D.C., 1968.

[11] R. W. Farquhar, The Control and Use of Libration-Point Satellites, Ph.D. Dissertation, Dept. of Aeronautics and Astronautics, Stanford University, Stanford, CA, USA, 1968.

[12] National Aeronautics and Space Administration (NASA), "PRESS KIT/JUNE 2009 - Lunar Reconnaissance Orbiter (LRO): Leading NASA’s Way Back to the Moon & Lunar Crater Observation and Sensing Satellite (LCROSS): NASA’s Mission to Search for Water on the Moon," Huntsville, AL 35812, USA, 2009.

[13] NASA, "Mars ReconnaissanceOrbiter Arrival - Press Kit," 2006.

[14] NASA, "NASA and ESA Establish a Mars Exploration Joint Initiative," [Online]. Available: http://www.nasa.gov/mission_pages/mars/news/mars-20090708.html. [Accessed 08 04 2013].

[15] ESA, "Comparative Exploration Architecture Study," 09 07 2008. [Online]. Available: http://www.esa.int/About_Us/Washington_Office/NASA_and_ESA_complete_comparative_exploration_architecture_study. [Accessed 01 04 2013].

[16] NASA, "International Lunar Network (ILN)," [Online]. Available: http://science.nasa.gov/missions/iln/. [Accessed 12 04 2013].

[17] Curtis, H., Orbital Mechanics for Engineering Students (Second Edition), Butterworth Heinemann, 2009.

[18] N. J. Cornish, "The Lagrange Points - Document Created for WMAP Education and Outreach," [Online]. Available: http://wmap.gsfc.nasa.gov/media/ContentMedia/lagrange.pdf. [Accessed 10 04 2013].

[19] Walter, U., Astronautics, Weinheim: WILEY-VCH, 2008.

[20] Marzari, F.; Tricarico, P.; Scholl, H., "Stability of Jupiter Trojans investigated using frequency map analysis: the MATROS project," [Online]. Available: http://mnras.oxfordjournals.org/content/345/4/1091.full.pdf. [Accessed 13 04 2013].

[21] NASA, "ESAS - Section 4H - Lunar Surface Outpost Communication Strategy," [Online]. Available: http://www.hq.nasa.gov/pao/FOIA/ESAS/ESAS_Appendix_4H.pdf. [Accessed 13 03 2013].

[22] K. Kordylewski, "Photographische Untersuchungen des Librationspunktes L5 im System Erde-Mond (Photographic Observations of the Libration point L5 of the Earth-Moon System)," *Acta Astronomica, Vol.11*, pp. pp.165-169, 1961.

[23] Laufer, R.; Tost, W.; Zeile, O.; Srama, R.; Roeser, H.P., "THE KORDYLEWSKY CLOUDS – AN EXAMPLE FOR ACRUISE PHASE OBSERVATION DURING THE LUNARMISSION BW1," in *11th ISU Annual International Symposium*, Strasbourg, 2007.

[24] Grün, E.; Srama, R.; et al., "Dust Detector for Phobos SRM Science Section," 2006.

[25] R. Gerzer, "Medical suggestions for lunar Habitats," in *Lunar Base Symposium (DLR, TU Kaiserslautern)*, Kaiserslautern, 2009.

[26] NASA - MSFC, "The Solar Wind," [Online]. Available: http://solarscience.msfc.nasa.gov/SolarWind.shtml. [Accessed 12 03 2013].

[27] F. J. Tipan Salazar, "DEPLOYMENT AND MAINTENANCE OF A SATELLITE FORMATION FLIGHT AROUND L4 AND L5 LAGRANGIAN POINTS IN THE EARTH-MOON SYSTEM BASED ON LOW COST STRATEGIES," 2012. [Online]. Available: http://mtc-m19.sid.inpe.br/col/sid.inpe.br/mtc-m19/2012/11.22.12.22/doc/publicacao.pdf. [Accessed 04 05 2013].

[28] E. Messerschmid and R. Bertrand, Space Stations: Systems and Utilization (ISBN: 3642084796), Springer, 2010.

[29] . H. Hagen, D. Stricker und A. Ebert, „Lebenserhaltungssysteme und technische Infrastruktur," in *Lunar Base Symposium (DLR, TU Kaiserslautern)*, Kaiserslautern, Germany, 2009.

[30] E. Belbruno, "The Dynamical Mechanism of Ballistic Lunar Capture Transfers In The Four-Body Problem From The Perspective Of Invariant Manifolds And Hill's Regions," 1994.

[31] Carpenter, J.R.; Folta, D.C.; et al., "Libration Point Navigation Concepts Supporting the Vision for Space Exploration," in *AIAA/AAS Astrodynamics Specialist Conference and Exhibit*, Providence, Rhode Island, USA, 2004.

[32] J. Miller, "Use of GPS/GNSS for Future NASA Missions," 2010. [Online]. Available: http://www.gps.gov/multimedia/presentations/2010/01/bangkok/miller.pdf. [Accessed 03 04 2013].

[33] Design Synthesis Excercise - TU Delf, "LUPOS - Lunar Positioning System - Final Report," 2009. [Online]. Available: http://www.bucksch.nl/downloads/Luposfinal.pdf. [Accessed 03 04 2013].

[34] Naval Research Laboratory, "Clementine - Lunar Image Map (licence: Public Domain)," [Online]. Available: http://solarviews.com/cap/moon/moonmap.htm. [Accessed 04 02 2013].

[35] . K. B. Bhasin, J. D. Warner and L. M. Anderson, "Lunar Communication Terminals for NASA Exploration Missions: Needs, Operations Concept and Architectures," in *26th AIAA ICSSC Conference*, San Diego, California, June 2008.

[36] NASA, "NASA's Exploration Systems Architecture Study - Final Report," 2005.

[37] AGI, "Satellite Tool Kit (STK)," [Online]. Available: http://www.agi.com/. [Accessed 08 01 2013].

[38] Mamoun, D.; et al., "Farside explorer: unique science from a mission to the farside of the moon," Springerlink.com, 2011.

[39] OHB, "Mission Architecture Definition for NEXT Lunar Lander Phase A," Bremen, 2006.

[40] Lester, D.;Thronson, H., "Low-Latency Lunar Surface Telerobotics from Earth-Moon Libration Points," in *AIAA SPACE 2011 Conference & Exposition*, Long Beach, California.

[41] ITU-T, "G.114/ SERIES G: TRANSMISSION SYSTEMS AND MEDIA, DIGITAL SYSTEMS AND NETWORKS: International telephone connections and circuits – General Recommendations on the transmission quality for an entire international telephone connection," 05 2005. [Online]. Available: http://www.itu.int/rec/T-REC-G.114-200305-I/en. [Accessed 04 04 2013].

[42] IETF Network Working Group, "IP Packet Delay Variation Metricfor IP Performance Metrics (IPPM)," [Online]. Available: www.ietf.org/rfc/rfc3393.txt. [Accessed 04 04 2013].

[43] Cecil, A.J.; Pitts, R.L.; Sparks, R.N.; Wickline, T.W.; Zoller, D.A., "Extending the International Space Station Life and Operability," [Online]. Available: www.spaceops2012.org/proceedings/documents/id1295844-paper-001.pdf. [Accessed 05 04

2013].

[44] CCDS, "Consultative Committee for Space Data Systems (ccsds.org)," [Online]. Available: http//www.ccsds.org. [Accessed 05 04 2013].

[45] IPNSIG, "InterPlanetary Networking Special Interest Group (IPNSIG)," [Online]. Available: http://ipnsig.org/. [Accessed 06 04 2013].

[46] NASA, "Disruption Tolerant Networking for Space Operations (DTN)," 03 04 2013. [Online]. Available: http://www.nasa.gov/mission_pages/station/research/experiments/730.html. [Accessed 06 04 2013].

[47] Folta, D.; Vaughn, F., "A Survey Of Earth-Moon Libration Orbits: Stationkeeping Strategies and Intra-Orbit Transfers," NASA Goddard Space Flight Center, Greenbelt, MD 20771.

[48] NASA, "GMAT - General Mission Analysis Tool," [Online]. Available: http://gmat.gsfc.nasa.gov/. [Accessed 06 04 2013].

[49] D. R. Williams, "Earth Fact Sheet (NASA)," 01 09 2004. [Online]. Available: http://nssdc.gsfc.nasa.gov/planetary/factsheet/moonfact.html. [Accessed 03 03 2013].

[50] A.R. Vasavada, D.A. Paige, and S.E. Wood, Near-Surface Temperatures on Mercury and the Moon and the Stability of Polar Ice Deposits, 1999.

[51] WMO Weather and Climate Extremes Archive. Arizona State University, "World: Lowest and Highest Temperature," [Online]. Available: http://wmo.asu.edu. [Accessed 03 03 2013].

[52] "Celestial body irradiance determination from an underfilled satellite radiometer: application to albedo and thermal emission measurements of the Moon using CERES," *Applied Optics 47*, 932008.

[53] International Telecommunication Union, "RecommendationN ITU-R SA.1625* "Feasibility of sharing between the space research service (space-to-Earth) and the fixed, inter-satellite, and mobile services in the band 25.5-27 GHz"," Geneva, 2003.

[54] Joseph A., Jr. Angelo , Spacecraft for Astronomy (Frontiers in Space)(ISBN:0816057745), Facts on File, 2007.

[55] Stefan Seel (Tesat-Spacecom, Germany); Uwe Sterr (ST2C Satellite Telecommunication Consulting, Germany); Rolf Meyer (DLR Bonn, Germany); Reinhard Czichy (Synopta); et al., "Space to Ground Bidirectional Optical Communication Link at 5.6 Gbps and EDRS Connectivity Outlook".

[56] PL Engineering Team, COLUMBUS Payloads Accomodation Handbook, Bremen, Germany, 2009.

[57] Reshetnev Company, "Loutch-5A and Loutch-5B DRSs," [Online]. Available: http://www.iss-reshetnev.com/?cid=prj_ca_loutch5a. [Accessed 09 04 2013].

[58] O. Amend and M. Berg, Interviewees, *Expected data rate for future space stations in LEO and beyond (OHB-System).* [Interview]. 05 02 2013.

[59] P. Eckart, LSC The Lunar Base Handbook: An Introduction to Lunar Base Design (GNRL USE)(2nd Edition)(ISBN: 0073294446), Learning Solutions, 2006.

[60] Saric, M.B. (Institut für Planetologie), "VL Planetologie I - Oberflächenformen und -prozesse - Vulkanismus Erde - Mars - Mond - 3," Stuttgart, 2012.

[61] Planetary Science Research Discoveries, Hawaii.edu, "A Farside Geochemical Window into the Moon," 29 04 2008. [Online]. Available: www.psrd.hawaii.edu/April08/Dewar-Th.html. [Accessed 23 05 2013].

[62] The New York Times, "Water Found on Moon, Researchers Say," 13 11 2009. [Online]. Available: http://www.nytimes.com/2009/11/14/science/14moon.html?_r=2&hp&. [Accessed 12 04 2013].

[63] Bundesnetzagentur, "Administrative Regulations for the Assignment of Frequencies for Satellite Communications (VVSatFu) (pdf)," 01 03 2010. [Online]. Available: http://www.bundesnetzagentur.de/SharedDocs/Downloads/EN/BNetzA/Areas/Telecommunications/TelecomRegulation/FrequencyManagement/FrequencyAssignment/SatelliteCommunications/VVSatFu05E100301_pdf.pdf?__blob=publicationFile. [Accessed 01 03 2013].

[64] International Academy of Astronautics, "The Next Steps in Exploring Deep Space - A Cosmic Study by the International Academy of Astronautics," 2004.

[65] skyrocket.de, "Muses A (Hiten)," [Online]. Available: http://space.skyrocket.de/doc_sdat/muses-a.htm. [Accessed 02 05 2013].

[66] M. (.-S. Wieser, Interviewee, *attitude control strategies for GEO satellites for EML-4 satellites.* [Interview]. 18 03 2013.

[67] Robutel, P.; Gabern, F., "The resonant structure of Jupiter's Trojan asteroids – I. Long-term stability and diffusion," 2006. [Online]. Available: http://mnras.oxfordjournals.org/content/372/4/1463.full.pdf. [Accessed 09 04 2013].

[68] LHOTKA, C.; ZHOU, L.Y. ; DVORAK, R., "ON THE STABILITY OF EARTH'S TROJANS," [Online]. Available: http://syrte.obspm.fr/jsr/journees2011/pdf/lhotka.pdf. [Accessed 10 04 2013].

[69] NASA, "NASA's Recommendations to Space-Faring Entities: How to Protect and Preserve the Historic and Scientific Value of U.S. Government Lunar Artifacts," 20 07 2011. [Online]. Available: http://www.collectspace.com/news/NASA-USG_lunar_historic_sites.pdf. [Accessed 11 04 2013].

[70] Bundesnetzagentur, "Frequenznutzungsplan," 08 2011. [Online]. Available: http://www.bundesnetzagentur.de/SharedDocs/Downloads/DE/BNetzA/Sachgebiete/Telekommunikation/Regulierung/Frequenzordnung/Frequenznutzungsplan/Frequenznutzungsplan2011pdf.pdf?__blob=publicationFile. [Accessed 01 03 2013].

[71] ITU, "RECOMMENDATION ITU-R RA.479-5*: Protection of frequencies for radioastronomical measurements in the shielded zone of the Moon," 2003.

[72] Arianespace, Soyuz User's Manual - Issue 2 Revision 0 - March 2012.

[73] Starsem - The Soyuz Company, Soyuz User's Manual (ST-GTD-SUM-01 - ISSUE 3 - REVISION 0), 2001.

[74] SpaceX, Falcon 9 Launch Vehicle Payload User's Guide (Rev 1), 2009.

[75] Arianespace, "Ariane 5 User's Manual (Issue 5 Revision 1 July 2011)".

[76] Indian Space Research Organisation (ISRO), "Polar Satellite Launch Vehicle User's Manual (Issue - 4)," 2005.

[77] S. Isakowitz, J. Hopkins and J. Hop, International Reference Guide to Space Launch Systems (4th Edition)(ISBN:156347591X), Library of Flight, 2004.

[78] E. Robert, Interviewee, *Launcher Performance Discussion (OHB-System).* [Interview]. 21 04 2013.

[79] K. U. Schrogl, C. Mathieu and N. Pete, Yearbook on Space Policy 2006/2007: New Impetus for Europe (ISBN: 3211999329), SpringerWienNewYork, 2010.

[80] J. McDowell, "Launch List - R-7 Family," [Online]. Available: http://planet4589.org/space/lvdb/launch/R-7. [Accessed 02 05 2013].

[81] en.Wikipedia.org, "List of Falcon 9 launches," [Online]. Available: http://en.wikipedia.org/w/index.php?title=List_of_Falcon_9_launches&oldid=553808004. [Accessed 03 05 2013].

[82] en.Wikipedia.org, "List of Satish Dhawan Space Centre launches," [Online]. Available: http://en.wikipedia.org/w/index.php?title=List_of_Satish_Dhawan_Space_Centre_launches&oldid=553601619. [Accessed 03 05 2013].

[83] en.Wikipedia.org, "List of Ariane launches (2010–2019)," [Online]. Available: http://en.wikipedia.org/w/index.php?title=List_of_Ariane_launches_%282010%E2%80%932019%29&oldid=530500172. [Accessed 03 05 2013].

[84] Seefelder, W., Lunar transfer orbits utilizing solar perturbations and ballistic capture, München: Herbert Utz Verlag GmbH, 2002.

[85] D. Quantius, J. Spurmann, E. Dekens and H. Päsler, "Weak stability boundary transfer to the Moon from GTO as a piggyback payload on Ariane 5 (DLR, AMSAT-DL)," CEAS Space J, 2012.

[86] E. Messerschmid and S. Fasoulas, Grundlagen der Raumfahrtsysteme (Skript + Übung), Universität Stuttgart, 2007.

[87] AerospaceResearch.net, Andreas HORNIG, "Constellation (distributed computing platform)," [Online]. Available: http://aerospaceresearch.net/constellation/. [Accessed 03 03 2013].

[88] University of Massachusetts Amherst - Department of Astronomy, "4th Order Runge-Kutta and Orbital Motion (Computational Physics)," 30 11 2012. [Online]. Available: http://www.astro.umass.edu/~schloerb/ph281/Lectures/4KOrbit/4KOrbit.pdf.

[89] EADS, "500 N Bipropellant European Apogee Motor (EAM)," [Online]. Available: http://cs.astrium.eads.net/sp/spacecraft-propulsion/apogee-motors/500n-apogee-motor.html. [Accessed 30 03 2013].

[90] EADS, "Satellite Propulsion Systems - AlphaBus," [Online]. Available: http://cs.astrium.eads.net/sp/spacecraft-propulsion/showcase/alphabus.html. [Accessed 30 03 2013].

[91] Aerojet, "2011-H-4232DataSheets.pdf," Redmond, WA 98052, USA, 2011.

[92] Aerojet, "Aerojet Propulsion Maneuvers Second ATV Vehicle to ISS," 23 02 2011. [Online]. Available: http://www.aerojet.com/news2.php?action=fullnews&id=267. [Accessed 30 03 2013].

[93] The Society of Japenese Aerospace Companies, "Directory of Japenese Space Products & Services 2012," 1-1-14 Akasaka, Minato-ku, Tokyo 107-0052, Japan.

[94] ASTRIUM, "400 N BI-PROPELLANT ENGINE - RELIABLE APOGE AND DEEP SPACE MANEUVERS," D 81663 Munich, Germany, 2012.

[95] ESA, "Automated Transfer Vehicle (FS003_12_ATV_updated_launch_2008.pdf)," [Online]. Available: http://esamultimedia.esa.int/docs/ATV/FS003_12_ATV_updated_launch_2008.pdf. [Accessed 31 03 2013].

[96] D. Regenbrecht, "Ariane 5 with record GTO payload mass launches tonight (DLR)," 02 08 2012. [Online]. Available: http://www.dlr.de/blogs/en/desktopdefault.aspx/tabid-7023/11643_read-587/. [Accessed 30 04 2013].

[97] F. Zazzera, F. Topputo and M. Massari, "Assessment of Mission Design Including Utilization of Libration Points and Weak Stability Boundaries," ESTEC, The Netherlands.

[98] Thales Alenia, "PROPULSION SYSTEMS," [Online]. Available: http://www.thalesgroup.com/Portfolio/Documents/Propulsion_Systems/. [Accessed 22 03 2013].

[99] EADS, "4 N Bipropellant Thruster," [Online]. Available: http://cs.astrium.eads.net/sp/spacecraft-propulsion/bipropellant-thrusters/4n-thruster.html. [Accessed 01 04 2013].

[100] EADS, "10 N Bipropellant Thruster," [Online]. Available: http://cs.astrium.eads.net/sp/spacecraft-propulsion/bipropellant-thrusters/10n-thruster.html. [Accessed 01 04 2013].

[101] EADS, "22 N Bipropellant Thruster," [Online]. Available: http://cs.astrium.eads.net/sp/spacecraft-propulsion/bipropellant-thrusters/22n-thruster.html. [Accessed 01 04 2013].

[102] EADS, "200 N Bipropellant Thrusters for ESA's ATV," [Online]. Available: http://cs.astrium.eads.net/sp/spacecraft-propulsion/bipropellant-thrusters/220n-atv-thrusters.html. [Accessed 01 04 2013].

[103] EADS, "1 N Hydrazine Thruster," [Online]. Available: http://cs.astrium.eads.net/sp/spacecraft-propulsion/hydrazine-thrusters/1n-thruster.html. [Accessed 03 04 2013].

[104] B. Wollenhaupt, Interviewee, *Mono and Bi-Propellant Thruster Data.* [Interview]. 12 04 2013.

[105] Sutton, G. P.; Biblarz, O., Rocket Propulsion Elements (Seventh Edition), Wiley-Interscience, 2001.

[106] European Cooperation for Space Standardization (ECSS), "ECSS–M–30A: Space Project Management - Project Phasing and Planning," 19 04 1996. [Online]. Available: http://www.lr.tudelft.nl/fileadmin/Faculteit/LR/Organisatie/Afdelingen_en_Leerstoelen/Afdeling_SpE/Space_Systems_Eng./Expertise_areas/Systems_engineering/References/doc/ecss-m-30a.pdf. [Accessed 12 04 2013].

[107] INTER-AGENCY SPACE DEBRIS COORDINATION COMMITTEE (IADC), "Report on the IADC Activities in particular with regard to the IADC Mitigation Guidelines," 25 03 2002. [Online]. Available: http://www.iadc-online.org/Documents/IADC_Present.2002-final.pdf. [Accessed 09 03 2013].

[108] ITU-R, FCC, "RECOMMENDATION ITU-R S.1003-1* - Environmental protection of the geostationary-satellite orbit," 2003. [Online]. Available: http://transition.fcc.gov/ib/sd/ssr/docs/ITU-R_S1003-1.pdf. [Accessed 09 03 2013].

[109] NASA, Wikipedia.org, "File:Lagrange Horseshoe Orbit.jpg," [Online]. Available: http://en.wikipedia.org/wiki/File:Lagrange_Horseshoe_Orbit.jpg. [Accessed 13 04 2013].

[110] "United Nations Treaties and Principles on the Outer Space," 1966. [Online]. Available: http://www.unoosa.org/pdf/publications/st_space_61E.pdf. [Accessed 14 04 2013].

[111] UN - COSPAR, "COSPAR PLANETARY PROTECTION POLICY," 20 10 2002. [Online]. Available: http://astro.berkeley.edu/~kalas/ethics/documents/environment/COSPAR%20Planetary%20Protection%20Policy.pdf. [Accessed 14 04 2013].

[112] ESA, "Margin Philosophy for Science Assessment Studies (SCI-PA/2007/022/)," 2007.

[113] ECSS, "Space project management - Project planning and implementation," 28 09 2007. [Online]. Available: http://www.ecss.nl/forums/ecss/dispatch.cgi/home/showFile/100434/d20070925072316/No/ecss-m-30B-Draft14%286July2007%29.pdf. [Accessed 13 04 2013].

[114] ITU, Radio Regulations Volume 1, 2008.

[115] World Radiocommunication Conference, "COMMUNICATION FROM THE COMMISSION TO THE COUNCIL, THE EUROPEAN PARLIAMENT, THE EUROPEAN ECONOMIC AND SOCIAL COMMITTEE AND THE COMMITTEE OF THE REGIONS - The World Radiocommunication Conference 2003 (WRC-03)," [Online]. Available: http://eur-lex.europa.eu/Notice.do?mode=dbl&lang=en&ihmlang=en&lng1=en,de&lng2=da,de,el,en,es,fi,fr,it,nl,pt,sv,&val=278423:cs. [Accessed 14 04 2013].

[116] ITU, RECOMMENDATION ITU-R SA.1625* - Feasibility of sharing between the space research service (space-to-Earth) and the fixed, inter-satellite, and mobile services in the band 25.5-27 GHz, Geneva, 2003.

[117] ESA, "A World First: Data Transmission Between European Satellites Using Laser Light," [Online]. Available: http://www.esa.int/Our_Activities/Telecommunications_Integrated_Applications/A_world_first_Data_transmission_between_European_satellites_using_laser_light. [Accessed 15 04 2013].

[118] Tesat, "TESAT LASER HISTORY," [Online]. Available: http://www.tesat.de/index.php?option=com_content&view=article&id=63&Itemid=59&lang=en. [Accessed 16 04 2013].

[119] Leitgeb, E.; Plank, T., et al., "Analysis and Evaluation of Optimum Wavelengthsfor Free-Space Optical Transceivers," 2010. [Online]. Available: http://nrl.northumbria.ac.uk/1065/1/Leitgeb%20E,%20Plank%20T,%20Awan%20MS,%20Brandl%20P,%20Popoola%20W,%20Ghassemlooy%20Z,%20Ozek%20F,%20Wittig%20M%20-%20Analysis%20and%20evaluation%20of%20optimum%20wavelengths...%20conference%20paper.pdf. [Accessed 16 04 2013].

[120] B. K. Levitt and J. Lesh, "Radio Frequency Interference from Near-Earth Satellites," [Online]. Available: http://tmo.jpl.nasa.gov/progress_report2/42-37/37J.PDF. [Accessed 02 04 2013].

[121] ESA & SES Astra, "SES Astra/Redu Space Services EDRS phase 0 study," 2012. [Online]. Available: http://telecom.esa.int/telecom/www/object/index.cfm?fobjectid=29510. [Accessed 17 04 2013].

[122] Witting, M.; Hauschildt, H.; Murrell, A.; et al. (ESA, DLR, TESAT, OHB), "Status of the European Data Relay Satellite System," 2012. [Online]. Available: http://icsos2012.nict.go.jp/pdf/1569603307.pdf. [Accessed 17 04 2013].

[123] ESA, "Malargüe - DSA 3," [Online]. Available: http://www.esa.int/Our_Activities/Operations/Malarguee_-_DSA_3.

[124] ESA, "Euclid - Mission Operations," [Online]. Available: http://sci.esa.int/science-e/www/object/index.cfm?fobjectid=46661.

[125] DLR, "Europe's 'data superhighway' in space sets sail," 25 06 2012. [Online]. Available: http://www.dlr.de/dlr/en/desktopdefault.aspx/tabid-10261/371_read-4006/#gallery/6391.

[126] Sans, M.; Zayer, S.I.; Zayer, I.; Daddato; R. (ESA), "Design of the ESA Optical Ground Station for Participation in LLCD," 2012. [Online]. Available: http://icsos2012.nict.go.jp/pdf/1569600363.pdf.

[127] Wertz, J. R.; Larson, W. J., Space Mission Analysis and Design, 3rd edition (ISBN:1881883108), Mcgraw-Hill, 1999.

[128] C. Nöldeke, Satellite Communications (ISBN: 3869914017), Monsenstein und Vannerdat, 2013.

[129] Heine F., Kämpfner H., Lange R., Czichy R., Meyer R., Lutzer M., "Optical Inter-Satellite Communication Operational," in *The 2010 Military Communications Conference*, 2010.

[130] ITU, "Recommendation ITU-R P.618-10 - Propagation and prediction methods required for the design of Earth-space telecommunication systems," 10 2009. [Online]. Available: https://www.itu.int/dms_pubrec/itu-r/rec/p/R-REC-P.618-10-200910-I!!PDF-E.pdf. [Accessed 17 04 2013].

[131] ITU, "RECOMMENDATION ITU-R S.1556 - Methodology to determine the epfd↓ level corresponding to the loss of synchronization in geostationary fixed satellite service networks caused by interference from non-geostationary-satellite systems," 2002. [Online]. Available: www.itu.int/dms_pubrec/itu.../R-REC-S.1556-0-200203-I!!MSW-E.doc. [Accessed 018 04 2013].

[132] U. Beyermann, Interviewee, *TeTra Modulator (Tesat)*. [Interview]. 16 04 2013.

[133] H. Hemmati, "Deep Space Optical Communications (ISBN: 0470040025)," John Wiley & Sons, 2006.

[134] A. H. B. Hashim, "MODELING INTERSATELLITE OPTICAL WIRELESS COMMUNICATION SYSTEM," UNIVERSITI TEKNOLOGI MALAYSIA, 2009.

[135] Majumdar, A. K.; Ricklin J. C., "Free-Space Laser Communications: Principles and Advances (Optical and Fiber Communications Reports)(ISBN: 0387286527)," Springer, 2008.

[136] C. Nöldeke, Interviewee, *Optical Free-space communication fundementals (Tesat, University of Stuttgart)*. [Interview]. 01 02 2013.

[137] F. Heine (Tesat Spacecom, Germany); R. Czichy (Synopta, Germany); R. Meyer (DLR Bonn, Germany); at al., "Optical Inter-Satellite Communication Operational," in *The 2010 Military Communications Conference*.

[138] Dreischer, T.; Thieme, B.; Bacher, M.; Buchheim, K.; Hyvönen, P., "OPTEL-μ: A Compact System for Optical Downlinks from LEO Satellites".

[139] OHB, "Requirements and Concepts for IOD Missions for Breakthrough Concepts and Approaches - Optical Downlink Communication IOD-Mission Outline Proposal Outline Proposal," 2013.

[140] P. G. Munuera, Interviewee, *Laser communication propagation and assumptions (OHB-System).* [Interview]. 05 02 2013.

[141] J. Thaeter, Interviewee, *RUAG laser communication terminals (OHB-System).* [Interview]. 04 04 2013.

[142] K. Buchheim, Interviewee, *Requesting data-sheet/paper about laser communication terminal.* [Interview]. 03 05 2013.

[143] Dreischer, T.; Giggenbach, D.; et al., "Enhanced Data Return from Lunar Farside using RF Optical TT&C," 2008.

[144] Thieme, B.; Dreischer, T. Buchheim, K., "SPACE TERMINAL FOR AN OPTICAL DOWNLINK SYSTEM ON SMALL SATELLITES," 2010.

[145] ESA, "ESA to catch laser beam from Moon mission," [Online]. Available: http://www.esa.int/About_Us/ESOC/ESA_to_catch_laser_beam_from_Moon_mission. [Accessed 19 04 2013].

[146] Flann, "Waveguide and Flange Data," [Online]. Available: http://www.flann.com/Products_Home/Components/FmiCat07108119.pdf. [Accessed 12 04 2013].

[147] C. D. OHB-System, Interviewee, [Interview]. 11 04 2013.

[148] RUAG, "Wide Coverage Antennas," [Online]. Available: http://www.ruag.com/de/Space/Brochures/Factsheets4upload/Wide_Coverage_Antennas.pdf. [Accessed 01 05 2013].

[149] ThalesAlenia Space, "TTC X-Band Flexible Transponder - TTC X-Band Flexible Functions," 04 2011. [Online]. Available: http://www.thalesgroup.com/Portfolio/Documents/Payload_Solutions__X_Band_Transponders/. [Accessed 19 04 2013].

[150] General Dynamics - AIS, "Small Deep-Space Transponder (SDST) - Reliable X-Band and Ka-Band Deep Space Transmission," [Online]. Available: http://www.gd-ais.com/Documents/Space%20Electronics/SDST%20DS5-212-2.pdf. [Accessed 29 04 2013].

[151] J. Taylor, "Dawn Telecommunications (JPL)," 08 2009. [Online]. Available: http://descanso.jpl.nasa.gov/DPSummary/090924dawn-FinalCorrex--update5G.pdf. [Accessed 30 04 2013].

[152] EADS - Astrium, "Antenna pointing mechanism - compact," [Online]. Available: http://www.astrium.eads.net/en/equipment/antenna-pointing-mechanism-compact.html. [Accessed 05 05 2013].

[153] EADS - Astrium, "Antenna pointing mechanism electronics (APME)," [Online]. Available: http://www.astrium.eads.net/en/equipment/antenna-pointing-mechanism-electronics-apme.html. [Accessed 02 05 2013].

[154] "AS 2100, Lockheed Martin Commercial Space Systems," [Online]. Available: http://www.astronautix.com/craft/as2100.htm. [Accessed 05 05 2013].

[155] Boieng, "BSS 702HP, Boeing," [Online]. Available: http://www.boeing.com/boeing/defense-space/space/bss/factsheets/702/702fleet.page. [Accessed 05 05 2013].

[156] Space System Loral, "1300 Series Satellite Platform," [Online]. Available: http://www.ssloral.com/html/products/1300.html. [Accessed 05 05 2013].

[157] Thales, "Spacebus 3000 Platform," [Online]. Available: http://www.thalesgroup.com/Portfolio/Space/space_product_spacebus3000/. [Accessed 05 05 2013].

[158] eoPortal Directory, "SmallGEO (Small Geostationary Satellite Platform) Initiative / HAG1 Mission," [Online]. Available: https://directory.eoportal.org/web/eoportal/satellite-missions/s/smallgeo. [Accessed 05 05 2013].

[159] EADS, "Alphabus," [Online]. Available: http://cs.astrium.eads.net/sp/spacecraft-propulsion/showcase/alphabus.html. [Accessed 05 05 2013].

[160] EADS - Astrium, "Antenna deployment mechanism (ATM)," [Online]. Available: http://www.astrium.eads.net/en/equipment/antenna-deployment-mechanism-atm.html. [Accessed 05 05 2013].

[161] EADS - Astrium, "Antenna deployment and trim mechanism (ADTM)," [Online]. Available: http://www.astrium.eads.net/en/equipment/antenna-deployment-and-trim-mechanism-adtm.html. [Accessed 05 05 2013].

[162] S. Lee, G. G. Ortiz and J. W. Alexander, "Star Tracker-Based Acquisition, Tracking, and Pointing Technology for Deep-Space Optical Communications (NASA - JPL)," 15 05 2005. [Online]. Available: http://tmo.jpl.nasa.gov/progress_report/42-161/161L.pdf. [Accessed 05 05 2013].

[163] Malin Space Science System, "ECAM-C50 - Color CMOS Camera, 5 Megapixel," [Online]. Available: http://www.msss.com/brochures/c50.pdf. [Accessed 05 05 2013].

[164] Malin Space Science Systems, "Lunar Reconnaissance Orbiter Camera (LROC)," [Online]. Available: http://www.msss.com/all_projects/lro-camera.php. [Accessed 05 05 2013].

[165] Surrey Satellite Technology LTD (SSTL), "VHRI 250 Imager," [Online]. Available: http://www.sstl.co.uk/Downloads/Datasheets/Datasheet_VHRI250_OL. [Accessed 06 05 2013].

[166] GOMspace, "NanoCam C1U - off the shelf camera subsystem," [Online]. Available: http://gomspace.com/documents/GS-DS-NANOCAM-6.1.pdf. [Accessed 06 05 2013].

[167] Malin Space Science Systems (MSSS), "ECAM Optics - Standard and Custom Options," [Online]. Available: http://www.msss.com/brochures/xfov.pdf. [Accessed 05 05 2013].

[168] H.-P. Röser, Raumfahrtanwendungen 1 + 2 (Vorlesungsskript), University of Stuttgart: IRS.

[169] N. Haala, "Digitale Bildverarbeitung (Vorlesungsskript)," 2012. [Online]. Available: http://www.ifp.uni-stuttgart.de/lehre/Vorlesungen/DigBV/index.html. [Accessed 05 05 2013].

[170] A. Hornig, "Programmierung eines optischen Horizontenfinder in Kombination mit Erdmagnetfeldvektor zum Einsatz als Lagesensor im Microsatelliten Rubin-X - Projekt: „Sun Compass“," Hochschule Bremen, 2007.

[171] C. Wood and L. Anderson, "New morphometric data for fresh lunar craters," in *Lunar and Planetary Science Conference Proceedings 9*, 1978, p. 3669–3689.

[172] R. Srama, "Priv.-Doz. Dr.-Ing. Ralf Srama (IRS, University of Stuttgart)," [Online]. Available: http://www.irs.uni-stuttgart.de/institut/mitarbeiter/srama.html. [Accessed 05 05 2013].

[173] H. Henkel, "Dust Detector for Phobos SRM Technical Section," Schwetzingen, Germany, 2006.

[174] R. Srama, "SMALL LEOPARD (DUST) (SLEO-dust-srama.pdf)," 2012.

[175] Astrium, Institut für Astrophysik Göttingen, "SODA Design Description and Development Planning (Doc. No: SNII-XX-YYY-DD-001)," 2012.

[176] European Commision, "Registration, Evaluation, Authorisation and Restriction of Chemical substances (REACH)," [Online]. Available: http://ec.europa.eu/environment/chemicals/reach/reach_intro.htm. [Accessed 29 04 2013].

[177] NASA, "NASA Goes Green: NASA Selects Green Propellant Technology Demonstration Mission," 15 08 2012. [Online]. Available: http://www.nasa-usa.de/home/hqnews/2012/aug/HQ_12-281_Green_Propellants.html. [Accessed 28 04 2013].

[178] NASA - GRC, "Chemical Equilibrium with Applications (CEA)," [Online]. Available: http://www.grc.nasa.gov/WWW/CEAWeb/. [Accessed 15 04 2013].

[179] EADS- Astrium, "Spacecraft Propellant Tank Manufacturing," [Online]. Available: http://cs.astrium.eads.net/sp/spacecraft-propulsion/propellant-tanks/manufacturing.html. [Accessed 29 03 2013].

[180] EADS - Astrium, "Surface Tension Tanks OST 01/X," [Online]. Available: http://cs.astrium.eads.net/sp/spacecraft-propulsion/propellant-tanks/235-516-litre-bipropellant-tank.html. [Accessed 05 04 2013].

[181] National Institute of Standards and Technology, "Thermophysical Properties of Fluid Systems," [Online]. Available: http://webbook.nist.gov/chemistry/fluid/. [Accessed 02 04 2013].

[182] ATK, "COPV (Composite Overwrapped Pressure Vessels) by Volume," [Online]. Available: http://www.psi-pci.com/Data_Sheet_Index_Pressurant-VOL.htm. [Accessed 06 04 2013].

[183] Lübke-Ossenbeck, Interviewee, *Momentum wheels selection for communication relay satellites in GEO and EML-4.* [Interview]. 22 04 2013.

[184] J. R. Wertz, Spacecraft Attitude Determination and Control (ISBN: 9027712042), Astrophysics

and Space Science Library, 1980.

[185] Rockwell Collins, "Satellite Stabilization Wheels," [Online]. Available: http://www.rockwellcollins.com/Products_and_Systems/Space_Components/Satellite_Stabilization_Wheels.aspx. [Accessed 02 05 2013].

[186] Honeywell, "Constellation Series Reaction Wheels," [Online]. Available: http://www51.honeywell.com/aero/common/documents/myaerospacecatalog-documents/Constellation_Reaction_Wheels.pdf. [Accessed 02 05 2013].

[187] G. Herdrich and M. Lau, Interviewees, *High precision thruster candidates for EML-4 orbit keeping. Institute of Space Systems (IRS), University of Stuttgart.* [Interview]. 14 06 2013.

[188] Jena Optronik, "ASTRO APS," [Online]. Available: http://www.jena-optronik.de/en/aocs/astro-aps.html. [Accessed 05 05 2013].

[189] Jena Optronik, "ASTRO 10," [Online]. Available: http://www.jena-optronik.de/en/aocs/astro10.html. [Accessed 05 05 2013].

[190] Selex ES, "TECHNICAL CHARATERISTICS: AA-STR, A-STR," [Online]. Available: http://selex-es.com/~/media/Files/S/Selex-Galileo/product-directory/space/A-STR.pdf. [Accessed 05 05 2013].

[191] Honeywell, "MIMU - Miniature Intertial Measurement Unit," [Online]. Available: http://www51.honeywell.com/aero/common/documents/myaerospacecatalog-documents/MIMU.pdf. [Accessed 05 05 2013].

[192] EADS - Astrium, "ASTRIX 1000 series," [Online]. Available: http://www.astrium.eads.net/media/document/astrium_gnc5_v2_2502.pdf. [Accessed 05 05 2013].

[193] EADS, "ASTRIX 200," [Online]. Available: http://www.astrium.eads.net/en/equipment/astrix-200.html. [Accessed 10 05 2013].

[194] EADS - Astrium, "Coarse Bi-Axis Sun Sensor," [Online]. Available: www.astrium.eads.net/en/equipment/bass.html. [Accessed 05 05 2013].

[195] Bradford, "Caorse Sun Sensor," [Online]. Available: http://bradford-space.com/userfiles/500-814%20Bradford%20Coarse%20Sun%20Sensor%200213.pdf. [Accessed 05 05 2013].

[196] Bradford, "Cosine Sun Sensor," [Online]. Available: http://bradford-space.com/userfiles/500-815%20Bradford%20Cosine%20Sun%20Sensor%200213.pdf. [Accessed 05 05 2013].

[197] Bradford, "Fine Sun Sensor," [Online]. Available: http://bradford-space.com/userfiles/500-813%20Bradford%20Fine%20Sun%20Sensor%200213.pdf. [Accessed 05 05 2013].

[198] Y. Kocher, Interviewee, *Sodern Earth Sensor.* [Interview]. 28 05 2013.

[199] Sodern, "STD 15 EARTHSENSOR," [Online]. Available:

http://www.sodern.com/sites/docs_wsw/RUB_52/STD15.pdf. [Accessed 03 05 2013].

[200] NEC/TOSHIBA Space Systems, "Earth Sensor Assembly," [Online]. Available: http://www.nec.com/en/global/solutions/space/satellite_communications/images/catalog_20.pdf . [Accessed 03 05 2013].

[201] ESA, Belgian Institute for Space Aeronomy, "Spenvis - Space Environment Information System," [Online]. Available: http://www.spenvis.oma.be. [Accessed 15 04 2013].

[202] G. Santin, "Radiation effects on sensors and technologies for JUICE," 9 11 2011. [Online]. Available: http://sci.esa.int/science-e/www/object/doc.cfm?fobjectid=49801. [Accessed 23 04 2013].

[203] O.-S. -. S. S. Department, Interviewee, [Interview]. 11 04 2013.

[204] Satsig.net, "List of Satellites in Geostationary Orbit," [Online]. Available: http://www.satsig.net/sslist.htm. [Accessed 01 05 2013].

[205] EADS - Astrium, "OSCAR - compact, powerful and versatile On Board Computer based on LEON3 core," [Online]. Available: http://www.astrium.eads.net/media/document/astrium_pdh2_mdef.pdf. [Accessed 05 05 2013].

[206] EADS - Astrium, [Online]. Available: http://www.astrium.eads.net/media/document/astrium_pdh3_mdef.pdf. [Accessed 05 05 2013].

[207] RUAG, "Command & Data Handling," [Online]. Available: http://www.ruag.com/de/Space/Products/Digital_Electronics_for_Satellites_Launchers/Data_Handling_Systems/command_data_handling_systems.pdf. [Accessed 05 05 2013].

[208] Defense Logistics Agency - DLA Land and MAritime, "MIL-STD-883: Test Method Standard, Microcircuits," 26 02 2010. [Online]. Available: www.landandmaritime.dla.mil/programs/milspec/ListDocs.aspx?BasicDoc=MIL-STD-883. [Accessed 08 04 2013].

[209] Space Micro, "Space Electronics Products - PROTON series," [Online]. Available: http://www.spacemicro.com/space_div/se_div.htm. [Accessed 06 05 2013].

[210] H.-P. Röser, Kleinsatellitenentwurf (Vorlesungsskript), University of Stuttgart, 2012.

[211] Azur Space, "30% Triple Junction GaAs Solar Cell," [Online]. Available: http://www.azurspace.com/images/pdfs/HNR_0003384-00-01.pdf. [Accessed 05 05 2013].

[212] Azur Space, "28% Triple Junction GaAs Solar Cell," [Online]. Available: http://www.azurspace.com/images/pdfs/HNR_0002490-00-03.pdf. [Accessed 05 05 2013].

[213] EMCORE, "ZTJ Photovoltaic Cell," [Online]. Available: http://www.emcore.com/wp-content/uploads/ZTJ_Datasheet.pdf. [Accessed 05 05 2013].

[214] EMCORE, "BTJ Photovoltaic Cell," [Online]. Available: http://www.emcore.com/wp-

content/themes/emcore/pdf/BTJ_Web.pdf. [Accessed 05 05 2013].

[215] RUAG, "SEPTA31 - Solar Array Drive Assembly," [Online]. Available: http://www.ruag.com/de/Space/Brochures/2012_Septa31.pdf. [Accessed 05 05 2013].

[216] EADS - Astrium, "Solar Array," [Online]. Available: http://www.astrium.eads.net/en/equipment/solar-array-kz8.html. [Accessed 06 05 2013].

[217] batteryuniversity.com, "What's the Best Battery?," [Online]. Available: http://batteryuniversity.com/learn/article/whats_the_best_battery. [Accessed 06 05 2013].

[218] ZVEI - Zentralverband Elektrotechnik- und Elektronikindustrie e.V., "Safe handling of lithium batteries, Guide for creating product-specific Battery Information Sheets," 05 2012. [Online]. Available: http://www.zvei.org/Verband/Fachverbaende/Batterien/Documents/Merkblaetter/02e%20Safe%20Handling%20of%20Lithiumbatteries%20201207.pdf. [Accessed 06 05 2013].

[219] NASA, "Guidelines on Lithium-ion Battery Use in Space Applications (NASA/TM-2009-215751, NESC-RP-08-75/06-069-I)," 05 2009. [Online]. Available: http://ntrs.nasa.gov/archive/nasa/casi.ntrs.nasa.gov/20090023862_2009023573.pdf. [Accessed 06 05 2013].

[220] Saft Batteries, "Saft batteries... powering outer space for half a century (data-sheet)," [Online]. Available: http://www.saftbatteries.com/doc/Documents/space/Cube710/SpaceBrochure_April2013.170bbd28-a5eb-4347-9e1b-c2fa2f483f8b.pdf. [Accessed 06 05 2013].

[221] ABSL Space, "Progress on the Space Qualification of the High Energy ABSL 18650NL Cell," 2009. [Online]. Available: https://batteryworkshop.msfc.nasa.gov/presentations/Progress_Space_Qual_High_Ener_18650NL_Cell_JNeubauer.pdf. [Accessed 06 05 2013].

[222] Quallion, "QL075KA battery," [Online]. Available: http://www.quallion.com/new-pdf/QL075KA_NEW.pdf. [Accessed 06 05 2013].

[223] D. Reulier, Interviewee, *Saft Batteries - VES and VEL series, balancing, sizing, heritage (Key Account Manager).* [Interview]. 21 05 2013.

[224] EADS - Astrium, "Medium Power PCDU," [Online]. Available: http://www.astrium.eads.net/en/equipment/medium-power-pcdu.html. [Accessed 02 05 2013].

[225] P. Fortesque, G. Swinerd and J. Stark, Spacecraft Systems Engineering, 4 edition (ISBN: 047075012X), Wiley, 2011.

[226] G. Bauer and S. O. Neumann, Thermodynamik III Wärmestrahlung - Manuskript zur Vorlesung, Stuutgart: ITLR, 2010.

[227] G. Muehlnikel, H. Kämpfner, F. Heine, H. Zech, D. Troendle, R. Meyer and S. Philipp-May, "The Alphasat GEO Laser Communication Terminal Flight Acceptance Tests," 9-12 10 2012.

[Online]. Available: http://icsos2012.nict.go.jp/pdf/1569586689.pdf. [Accessed 29 04 2013].

[228] B. G. Evans, Satellite Communication Systems, 3rd Edition (ISBN: 085296899X), London, UK: The Institution of Engineering and Technology, 2008.

[229] H. Lübberstedt, T. Miesner and A. Winkler, "Solely EP based Orbit Control System on Small GEO Satellite," 17 09 2007. [Online]. Available: http://erps.spacegrant.org/uploads/images/images/iepc_articledownload_1988-2007/2007index/IEPC-2007-274.pdf. [Accessed 06 05 2013].

[230] ESA, "Alphabus Factsheet," [Online]. Available: http://esamultimedia.esa.int/docs/telecom/Alphabus_factsheet.pdf. [Accessed 06 05 2013].

[231] MT Aerospace, "Tanks for storable media," [Online]. Available: http://www.mt-aerospace.de/en/products/space/tanks.html. [Accessed 04 05 2013].

[232] European Cooperation for Space Standardization, "ECSS-E-HB-10-02A - Space engineering verfication guidelines," 17 12 2010. [Online]. Available: http://www.ecss.nl/forums/ecss/dl.cgi/c98ca1cbf5bf9402db4151c24ab2068f/ECSS-E-HB-10-02A_17December2010_.pdf. [Accessed 20 04 2013].

[233] B. R. Elbert, The Satellite Communication Applications Handbook (ISBN: 1580534902), Artech House Print on Demand, 2003.

[234] C. D. Brown and Asselin, Spacecraft Mission Design, Second Edition (ISBN: 1563472627), AIAA, 1998.

[235] ESA, "Clean Space – Compendium of Potential Activities for 2013 & 2014," 26 03 2013. [Online]. Available: http://emits.esa.int/emits-doc/ESTEC/CleanSpace-GSTP6_E1_List_of_Activities2013&2014.pdf. [Accessed 05 05 13].

[236] O. J. Haidn, "Advanced Rocket Engines (DLR, Lampoldshausen)," Neuilly-sur-Seine, France, 2008.

[237] A. Larsson and N. Wingborg, "Green Propellants Based on Ammonium Dinitramide (ADN)," 2011. [Online]. Available: http://cdn.intechopen.com/pdfs/13473/InTech-Green_propellants_based_on_ammonium_dinitramide_adn_.pdf. [Accessed 02 05 2013].

[238] ESA, "ALPHABUS - Europe's solution for the high-power satcom market," 05 2010. [Online]. Available: http://download.esa.int/docs/telecom/Bulletin_REPRINT ALPHABUS_9.pdf. [Accessed 05 05 2013].

[239] ESA, "Small Geostationary Platform product line," [Online]. Available: http://telecom.esa.int/telecom/www/object/index.cfm?fobjectid=28211. [Accessed 05 05 2013].

[240] Thales, "Spacebus 3000 Platform," [Online]. Available: http://www.thalesgroup.com/Portfolio/Space/space_product_spacebus3000/. [Accessed 06 05 2013].

[241] ESA, "Announcement of Opportunity for hosted payload on board EDRS satellite," 27 06 2011. [Online]. Available: http://emits.esa.int/emits-doc/ESTEC/EDRShostedpayloadAO.pdf. [Accessed 05 05 2013].

[242] TU Delft, "Spacecraft cost," [Online]. Available: http://www.lr.tudelft.nl/?id=29329&L=1. [Accessed 07 05 2013].

[243] DGAP, OHB, "OHB AG: OHB System AG und Astrium GmbH unterzeichnen Vertrag über Lieferung eines Satelliten für das European Data Relay Satellite System (EDRS)," 27 05 2013. [Online]. Available: http://www.dgap.de/dgap/News/corporate/ohb-ohb-system-und-astrium-gmbh-unterzeichnen-vertrag-ueber-lieferung-eines-satelliten-fuer-das-european-data-relay-satellite-system-edrs/?newsID=757495. [Accessed 12 05 2013].

[244] EUTELSAT|IGO, "Histrocial Background - From 1977 to 2001," [Online]. Available: http://www.eutelsatigo.int/en/eutelsat.php?menu=1. [Accessed 07 05 2013].

[245] Federal Aviation Administration, "The Economic Impact of Commercial Space Transportation on the U.S. Economy in 2009," 09 2010. [Online]. Available: http://www.faa.gov/news/updates/media/Economic%20Impact%20Study%20September%202010_20101026_PS.pdf. [Accessed 29 05 2013].

[246] Engineering Systems Learning Center (ESLC), Engineering Systems Learning Center (ESLC), "MIT Industry Systems Study - Communications Satellite Constellations," 14 10 2003. [Online]. Available: http://ardent.mit.edu/real_options/de%20Weck%20System%20Study/unit1_summary.pdf. [Accessed 05 05 2013].

[247] NASA - Group Projects: Human Exploration , "Space Communication: Lunar Support," 2004. [Online]. Available: http://trajectory.grc.nasa.gov/projects/lunar.shtml. [Accessed 09 05 2013].

[248] B. Olberts, B. Bonev, A. Heckmann, F. Herzog, S. T. Latzko, M. Schneider and E. Messerschmid, "AIRM - THE LINK BETWEEN MISSION ANALYST AND THE GENERAL PUBLIC," in *IAC 12*, Neapel, 2012.

[249] eoPortal Directory, "SMART-1 (Small Mission for Advanced Research in Technology)," [Online]. Available: https://directory.eoportal.org/web/eoportal/satellite-missions/s/smart-1. [Accessed 20 04 2013].

[250] Cosgrove, d.; Frey, S.; Marchese, J.; Owens, B.; Bester, M., "ARTEMIS Operations from Earth-Moon Libration Orbits to Stable Lunar Orbits," University of California, Berkeley, CA, 94720.

[251] eoPortal Directory, "Chang'e - 1 (Lunar-1 Mission of China)," [Online]. Available: https://directory.eoportal.org/web/eoportal/satellite-missions/c-missions/chang-e-1. [Accessed 20 04 2013].

[252] Haruyama, J.; Matsunaga, T.; Ohtake, M.; et al., "Global lunar-surface mapping experiment using the Lunar Imager/Spectrometer on SELENE," in *Earth Planets Space, 60*, 2008, p. 243–255.

[253] Krishna, A.; Gopinath, N.S.; Hegde, N.S.; Malik, N.K., "Imaging and power generation strategies for Chandrayaan-1," Bangalore 560 017, India.

[254] eoPortal Directory, "Chang'e-2 (Lunar-2 Mission of China) / CE-2," [Online]. Available: https://directory.eoportal.org/web/eoportal/satellite-missions/c-missions/chang-e-2. [Accessed 20 04 2013].

[255] eoPortal Directory, "GRAIL (Gravity Recovery and Interior Laboratory)," [Online]. Available: https://directory.eoportal.org/web/eoportal/satellite-missions/g/grail. [Accessed 20 04 2013].

[256] Boroson, D. M.; Scozzafava, J. J.; Robinson, B. S.; et al., "The Lunar Laser Communications Demonstration (LLCD)," in *Third IEEE International Conference on Space Mission Challenges for Information Technology*, 2009.

[257] R. Laufer, Lunar Mission BW1: Scientific Objectives and Small Satellite Concept, Stuttgart, 2010.

[258] M. Lachenmann, Missionsanalyse und Nutzlastauswahl des Kleinsatelliten Lunar Mission BW1, Stuttgart, 2012.

[259] ESMO, "ESMO COMMS, Derived Requirements COMMS-B2-05 - FINAL," 2011.

[260] Cohen, B. A.; Bassler, J. A.; Harris, D. W.; Hill, L.; Hammond, M. S.; McDougal, J. M, "The International Lunar Network (ILN) and the US Anchor Nodes mission," NLSI Lunar Science Forum, 2009.

[261] ILOA.org, "SPACEDEV ILO PHASE SIX EXECUTIVE SUMMARY: "ILO PRELIMINARY PAYLOAD DEFINITION" (2008)," [Online]. Available: http://www.iloa.org/spdv_study6.html. [Accessed 20 04 2013].

[262] Paul, M.V.; Spencer, D.B., "THE PENN STATE LUNAR LION: A UNIVERSITY MISSION TO EXPLORE THE MOON (IAC-12. B4.8.5)," in *63rd International Astronautical Congress*, Naples, Italy, 2012.

[263] M. Lavagna and e. al., "ITALY AS A COMPETITOR FOR THE GOOGLE LUNAR X PRIZE: THE AMALIA MISSION (GLEX-2012.02.2.1x12303)," in *GLEX*.

[264] M. Safyan, "Preliminary Mission Analysis for the Barcelona Moon Team Rover," International Space University, 2010.

[265] Tristancho, J.; Barruccoy, M.; Weedz, R.; et al., "A lunar explorer self-contained PicoRover," in *38th COSPAR Scientific Assembly*, Bremen, Germany, 2010.

[266] Team Synergy Moon, "Bilan de liaison radio pour GLXP_GB," 2013.

[267] Part Time Scientists, " lander concept documentation," 2013.

[268] OHB-System AG, "Mission Architecture Definition for NEXT Lunar Lander Phase A," Bremen, 2009.

[269] European Space Agency (ESA), "European Lunar Lander - CALL FOR DECLARATIONS OF INTEREST - Experiment Interface Definition Document: Part A (EID-A)," 2012.

[270] SpaceX, "Dragonlab Datasheet," [Online]. Available: http://www.spacex.com/downloads/dragonlab-datasheet.pdf. [Accessed 20 04 2013].

[271] S. presenter, Interviewee, *Concept study for Dragon capsule moon mission.* [Interview]. 05 10 2011.

[272] T. L. Saaty, Decision making for leaders : the analytic hierarchy process for decisions in a complex world (0-9620317-8-X), Pittsburgh, PA: RWS Publ., 2008.

[273] MediaGlobe study, SpaceTech 1989-1999, TopTech studies, TU-Delft, "Spacecraft (SC) preliminary mass estimation & allocation," [Online]. Available: http://www.lr.tudelft.nl/?id=29336&L=1. [Accessed 12 03 2013].

[274] TU Delft, "Spacecraft (SC) preliminary power estimation & allocation (an example)," [Online]. Available: http://www.lr.tudelft.nl/?id=29319&L=1. [Accessed 19 03 2013].

Appendix

A User Requirements

Table 99: Past and future space observatory missions with their average downlink data-rates

Past and Future Space Observatories				
#	Observatory	Objective	Year	Data-Rate [Mbit/s]
1	HEAO-1	X-ray	1977	0.128
2	HEAO-2	X-ray	1978	0.128
3	EXOSAT	X-ray	1983	0.008
4	HIPPARCOS	Visible (precision astronomy)	1989	0.024
5	Hubble	Near ultraviolet, visible, near infrared	1990	0.2
6	SOHO	Solar Observation	1995	0.2
7	HETE	Gamma-ray, X-ray	1996	0.25
8	FUSE	Ultraviolet	1999	1.0
9	WMAP	Microwave	2001	0.667
10	RHESSI	Gamma-ray, X-ray	2002	4.0
11	GALEX	Ultraviolet	2003	0.34
12	Spitzer	Infrared	2003	0.085
13	SWIFT	Gamma-ray	2003	2.25
14	SOLAR-B	X-ray, ultraviolet, visible	2006	4.0
15	Fermi	Gamma-ray	2008	1.2
16	IBEX	High-energetic particle science	2008	0.32
17	Herschel	Far infrared, sub-millimeter	2009	1.5
18	Kepler	Visible, infrared (Exoplanets)	2009	0.55
19	Planck	Infrared, microwave	2009	1.5
20	SDO	Solar observation	2010	130
21	AMS-2 (ISS)	Cosmic rays	2011	0.3
22	Spektr-R	Radio	2011	144
23	GAIA	Visible, infrared (precision astronomy)	2013	1.0
24	IRIS	Solar observation	2013	0.7
25	Spektr-RH	Radio	2014	0.512
26	WSO	Ultraviolet	2016	1.5
27	James Webb	Infrared	2018	28
28	Euclid	Visible, near infrared	2020	59

Table 100: Lunar missions between 2004 and 2026 and their data-rates

Mission	Organisation	Type	Year	Data-Rate [Mbit/s]
SMART-1	DLR	LO	2004	0.5
Artemis P1 & P2	NASA	LO	2007	0.004
Chang'e-1	CNSA	LO	2007	3.0
Selene-1	JAXA	LO	2007	10.0
Chandrayaan-1	ISRO	LO	2008	8.4
LRO	NASA	LO	2009	5.3*
Chang'e-2	CNSA	LO	2010	12.0
GRAIL	NASA	LO	2011	0.128
LADEE	NASA	LO	2013	622.0
BW-1	Institute of Space Systems, University of Stuttgart	LO	2014	5.0
ESMO	ESA Student Mission	LO	2014	0.008
ILN Node 1-4	NASA	LL	2015	0.003
ILO	ILOA	LL	2015	1.0
Lunar Lion	GLXP: Pen State University	LL	2015	0.1
Amalia	GLXP: Team Italia	LR	2015	1.0
BMT Lunar Rover	GLXP: Barcelona Team	LR	2015	1.0
PicoRover	GLXP: Team FREDNET	LR	2015	0.6
Tesla	GLXP: Team Synergy Moon	LL-LR	2015	1.4
Asimov Sr. & Jules	GLXP: Part Time Scientists	LL-LR	2015	10.0
NEXT Lunar Lander	ESA, OHB	LL	2018	1.0
Lunar Lander	ESA, Astrium	LL	2018	1.0
Dragon	SpaceX	MOM	>2022	300.0
Farside	Student Mission	LL-LO	2026	0.034

LO lunar orbiter, LL lunar lander, LR lunar rover, MOM manned orbiting module

[249] [250] [251] [252] [253] [12] [254] [255] [256] [257] [258] [259] [260] [261] [262] [263] [264] [265] [266] [267] [268] [269] [270] [271] [38]

B Orbit Design

B.1 2D-Simulation with TYCHO application on Constellation

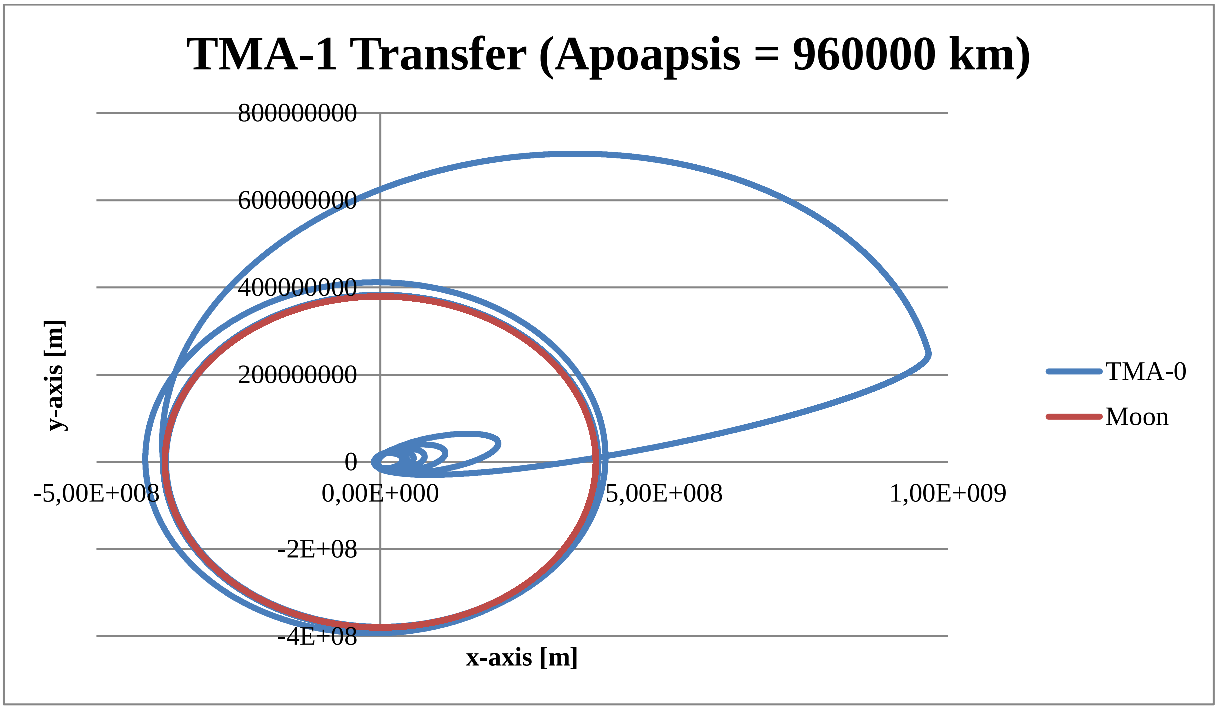

Figure 74: 2D-Sim: transfer trajectory (#33)

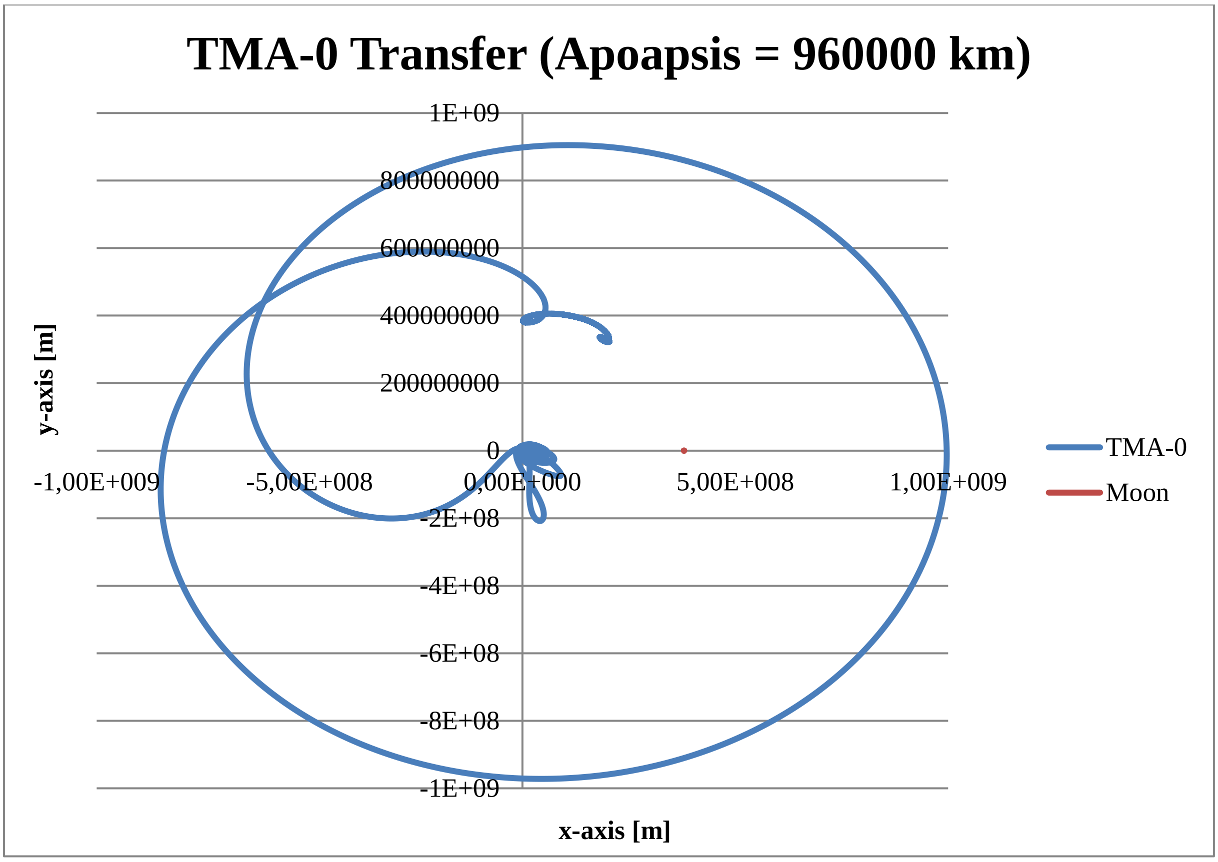

Figure 75: 2D-Sim: transfer trajectory in co-rotating frame (#33)

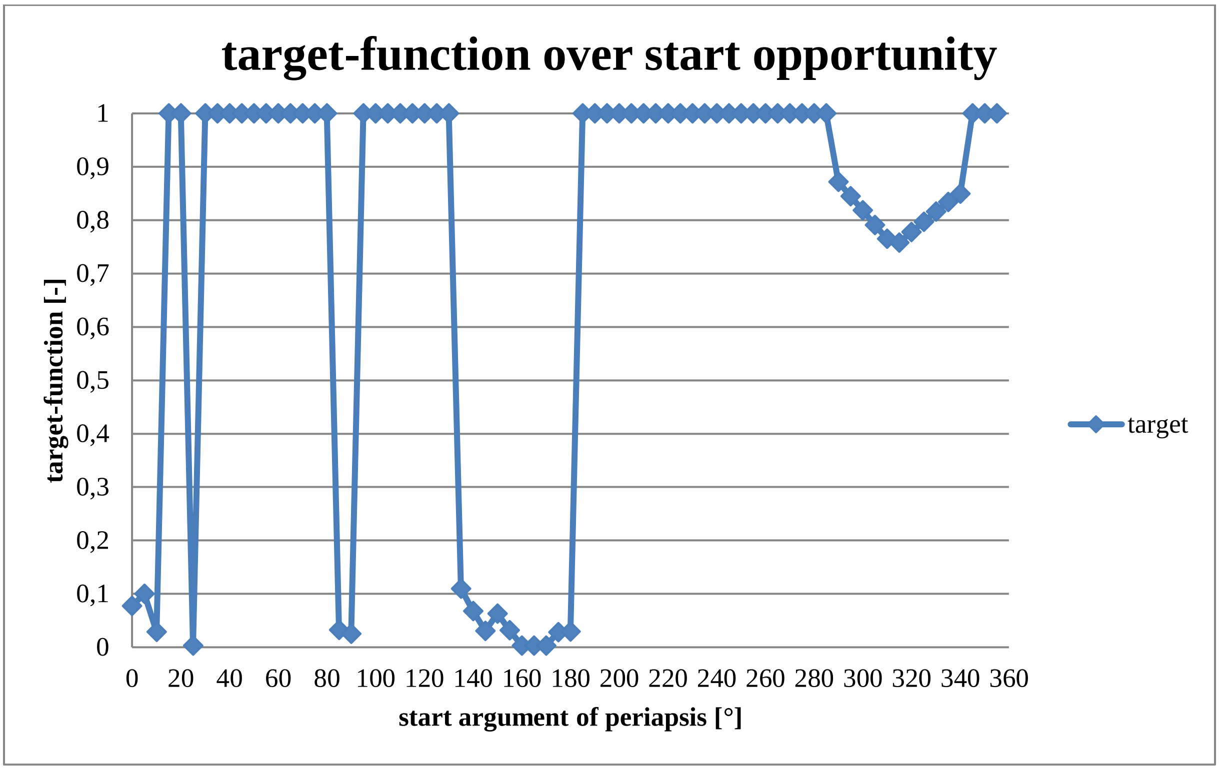

Figure 76: 2D-Sim: target function over start opportunity (smaller is better)

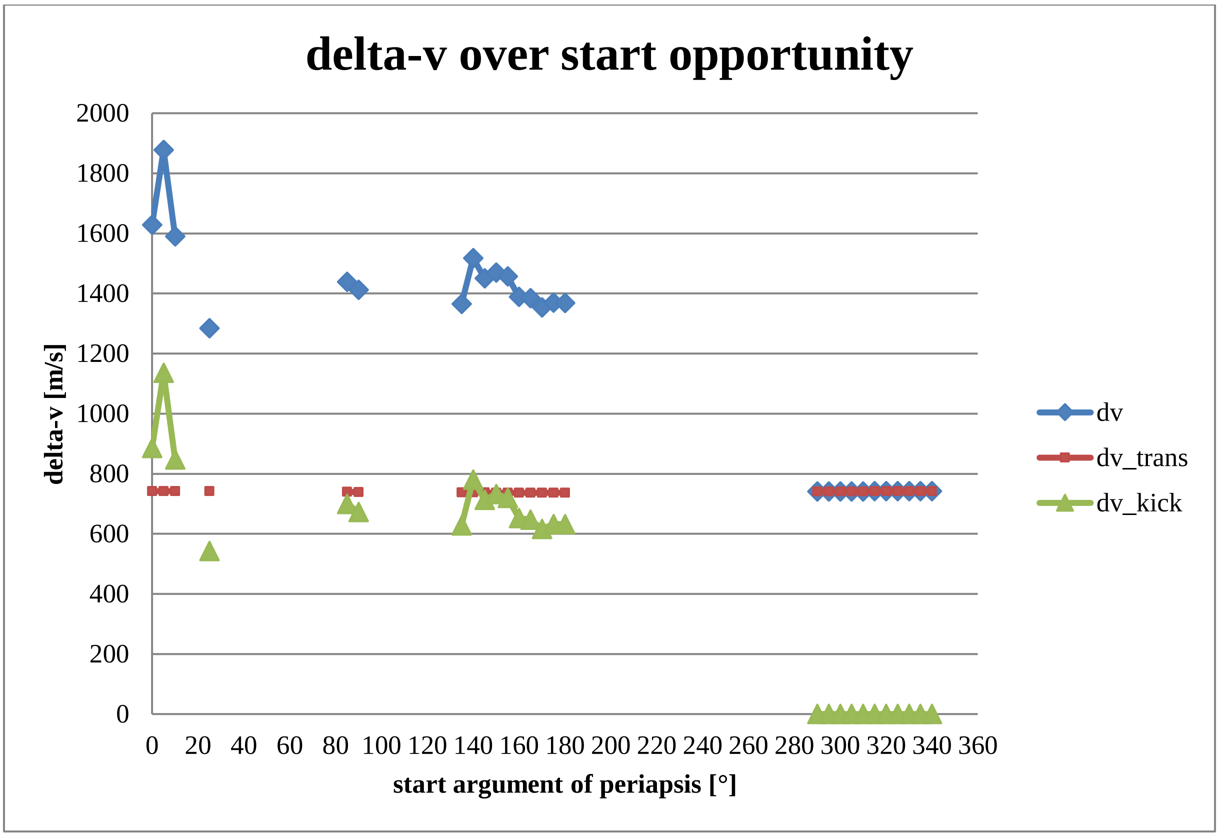

Figure 77: 2D-Sim: delta-v over start opportunity

B.2 3D-Simulation with NASA GMAT

Table 101: Satellite masses after station keeping of three years of two thrusters (full, best & worst)

		ISP			
		229 s		**290 s**	
		29 [m/(s*a)]	**57 [m/(s*a)]**	**29 [m/(s*a)]**	**57 [m/(s*a)]**
#	**Mass1 [kg]**	**Mass2-1 best [kg]**	**Mass2-1 worst [kg]**	**Mass2-2 best [kg]**	**Mass2-2 worst [kg]**
1	802	771	742	777	754
2	1239	1191	1147	1201	754
3	1657	1594	1535	1607	1560
4	813	782	753	788	765
5	1268	1219	1175	1229	1194
6	1697	1632	1572	1645	1598
7	811	780	751.	786	763
8	1313	1263	1216	1273	1236
9	1684	1620	1560	1633	1585
10	819	787	758	794	771
11	1260	1212	1167	1222	1186
12	1709	1644	1583	1657	1609
13	826	794	765	801	777
14	1272	1223	1178	1233	1197
15	1716	1650	1590	1664	1615
16	828	796	767	803	779
17	1276	1227	1182	1237	1201
18	1722	1656	1595	1670	1621
19	933	897	864	904	878
20	1436	1381	1331	1393	1352
21	1938	1864	1796	1880	1825
22	939	903	***870***	910	884
23	1446	1391	***1340***	1402	1361
24	1953	1878	***1809***	1894	1839
25	940	904	871	911	885
26	1454	1398	1347	1410	1369
27	1955	1880	1811	1896	1840

C Demonstrator Satellite Configuration

C.1 Communication Payload

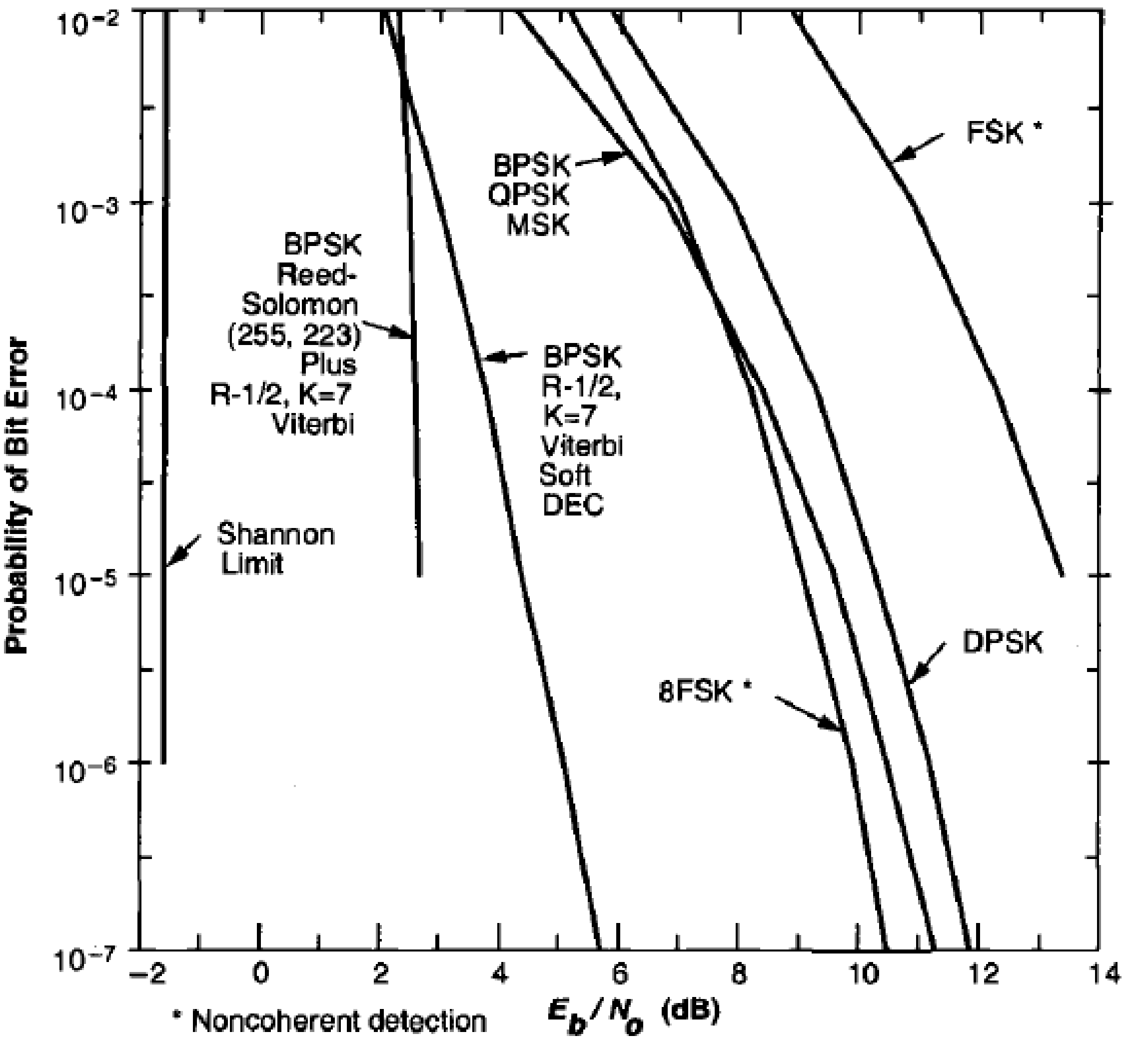

Figure 78: Bit error probability as a function of Eb/No. The theoretical performance limit can be approached by use of error correction coding. [127]

Noise Temperature	Frequency (GHz)					
	Downlink			Crosslink	Uplink	
	0.2	2–12	20	60	0.2–20	40
Antenna Noise (K)	150	25	100	20	290	290
Line Loss (dB)	0.5	0.5	0.5	0.5	0.5	0.5
Line Loss Noise (K)	35	35	35	35	35	35
Receiver Noise Figure (dB)	0.5	1.0	3.0	5.0	3.0	4.0
Receiver Noise (K)	36	75	289	627	289	438
System Noise (K)	221	135	424	682	614	763
System Noise (dB-K)	23.4	21.3	26.3	28.3	27.9	28.8

Figure 79: System noise temperatures in satellite communication links in clear weather. The temperatures are referred to the antenna terminal

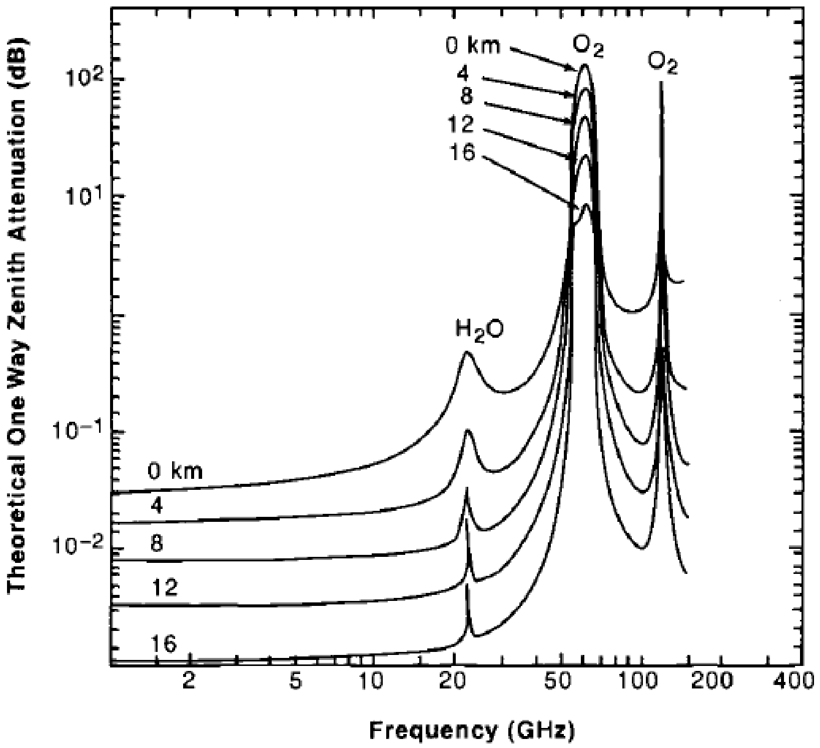

Figure 80: Theoretical vertical one-way attenuation from specified height to the top of the atmosphere. Plot assumes 7.5 g/m³ of water vapor at the surface, and does not include effect of rain or cloud attenuation

Attitude and Orbital Control

```
%----------------------------------------
%---------- Mission Sequence
%----------------------------------------

BeginMissionSequence;
While DefaultSC.ElapsedDays < 100
   BeginScript
      GMAT ElapsedSecs_b4 = DefaultSC.ElapsedSecs;

      GMAT EML4_x = DefaultSC.EML4_rev.X;
      GMAT EML4_y = DefaultSC.EML4_rev.Y;
      GMAT EML4_z = DefaultSC.EML4_rev.Z;
      GMAT EML4_distance_b4 = (EML4_x^2+EML4_y^2+EML4_z^2)^0.5;
   EndScript;
   Propagate DefaultProp(DefaultSC);
   BeginScript
      GMAT dt = DefaultSC.ElapsedSecs-ElapsedSecs_b4;

      GMAT EML4_x = DefaultSC.EML4_rev.X;
      GMAT EML4_y = DefaultSC.EML4_rev.Y;
      GMAT EML4_z = DefaultSC.EML4_rev.Z;
      GMAT EML4_distance = (EML4_x^2+EML4_y^2+EML4_z^2)^0.5;
      GMAT r = EML4_distance;
   EndScript;
   If DefaultSC.ElapsedDays > 0
      If r < box_r_max & dr_dot > box_r_dot_max | r > box_r_max
         BeginScript
            GMAT DefaultSC.EML4_rev.VX = DefaultSC.EML4_rev.VX
                - DefaultSC.EML4_rev.X/(DefaultSC.EML4_rev.X^2+DefaultSC.EML4_rev.Y^2)^0.5*pulse;
            GMAT DefaultSC.EML4_rev.VY = DefaultSC.EML4_rev.VY
                - DefaultSC.EML4_rev.Y/(DefaultSC.EML4_rev.X^2+DefaultSC.EML4_rev.Y^2)^0.5*pulse;
         EndScript;
      EndIf;
   Else
   EndIf;
   BeginScript
      GMAT dr = EML4_distance - EML4_distance_b4;
      GMAT dr_dot = dr/dt;
   EndScript;
EndWhile;
```

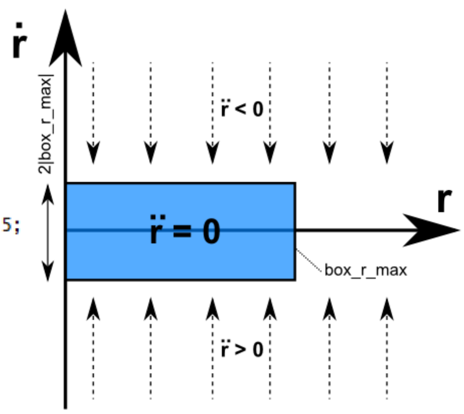

Figure 81: GMAT code for phase-space control

Propulsion type:	pulsed plasma thruster (PPT or somtimes refered to as iMPD)							
Single thruster parameter			*Masses*			*Misc.*		
Capacity	20-80	µF	Thruster	2,5-7	kg	Sat m0 target orbit	1454	kg
Max. Utw	1300	V	PPU	1-2	kg	Operation time	15	a
Isp	25000	m/s	Sensors	0,5-1	kg			
Ibit	100-1400	µNs	Structure	0,5-2	kg	Cost estimation	2,5	Mio€
Fmax @ 2 Hz	200-2800	µN	Housing	0,5-2	kg	Recurring	2	Mio€
Ptw	40-130	W	SYSTEM	5-14	kg	(per thruster)		
MIBIT	10-50	µg / Puls				Volume estimation	30x30x30	cm³
Estimated propellant consumption (exemplary for single thruster)								
DeltaV 15a	435	m/s						
mPropellant 15a	25,1	kg						
Number of Pulses @ 50 µg	501615291							
TRL	5-6							
Solid propellant, no tank structures required								

Figure 82: iMPD ADD SIMP-LEX thruster at IRS as possible high precision AOCS thruster [187]

C.2 Electrical Power Subsystem

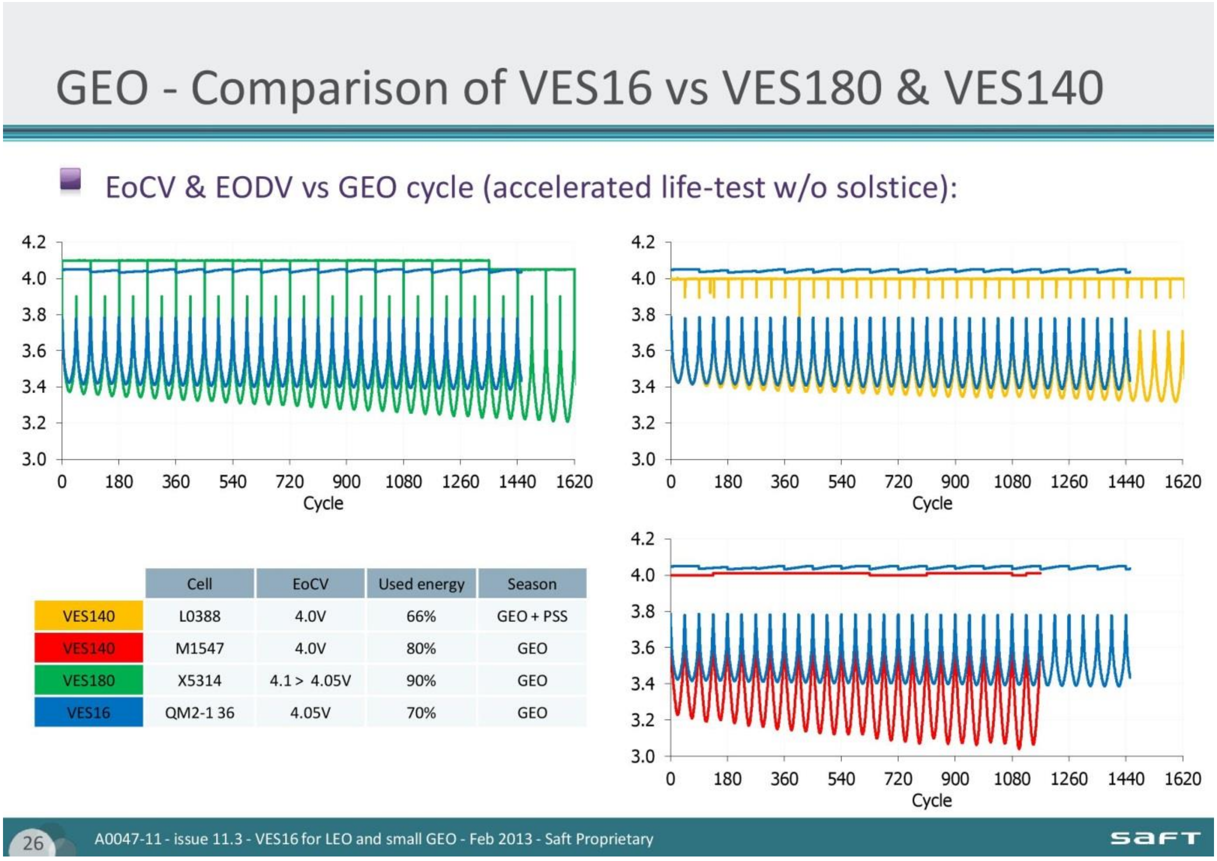

Figure 83: Battery capacity over GEO cycle (VES16, VES180, VES140) [223]

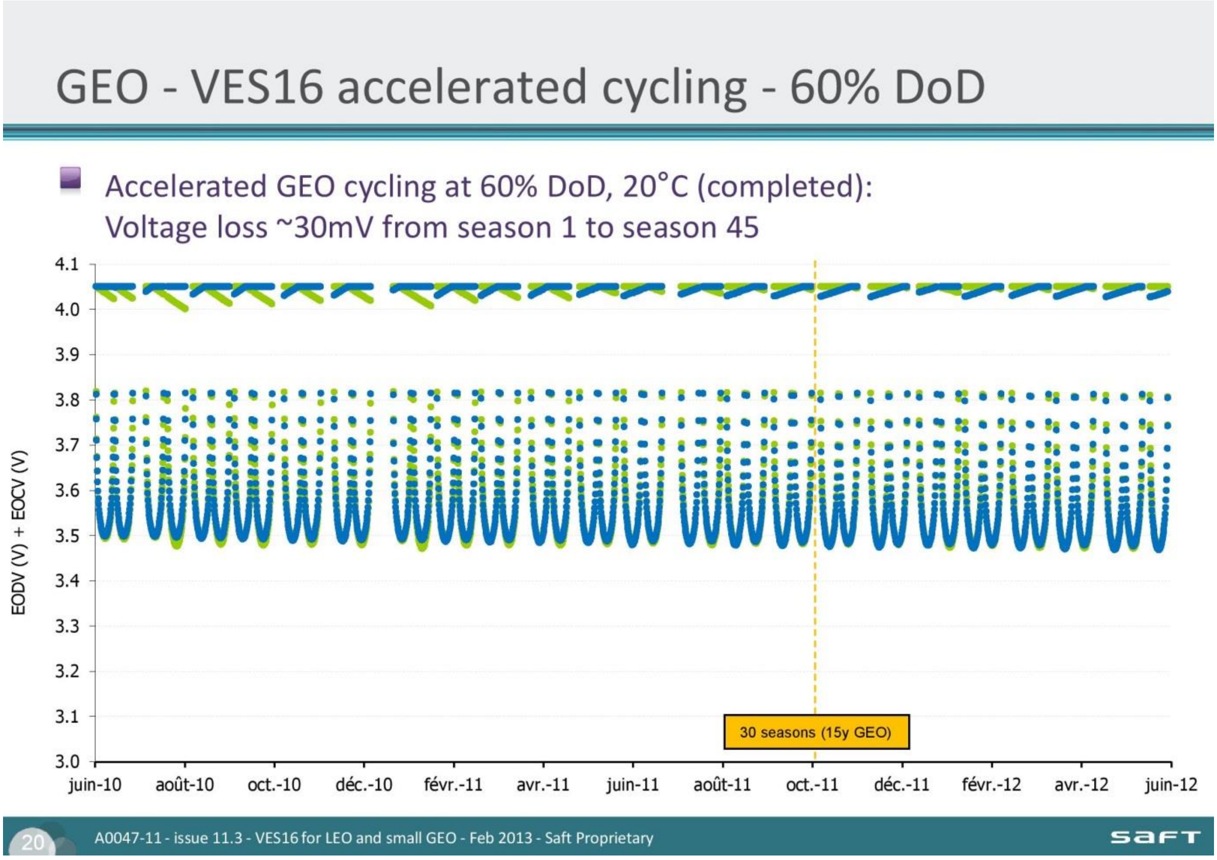

Figure 84: Battery capacity over GEO cycle (VES16, 60% DOD) [223]

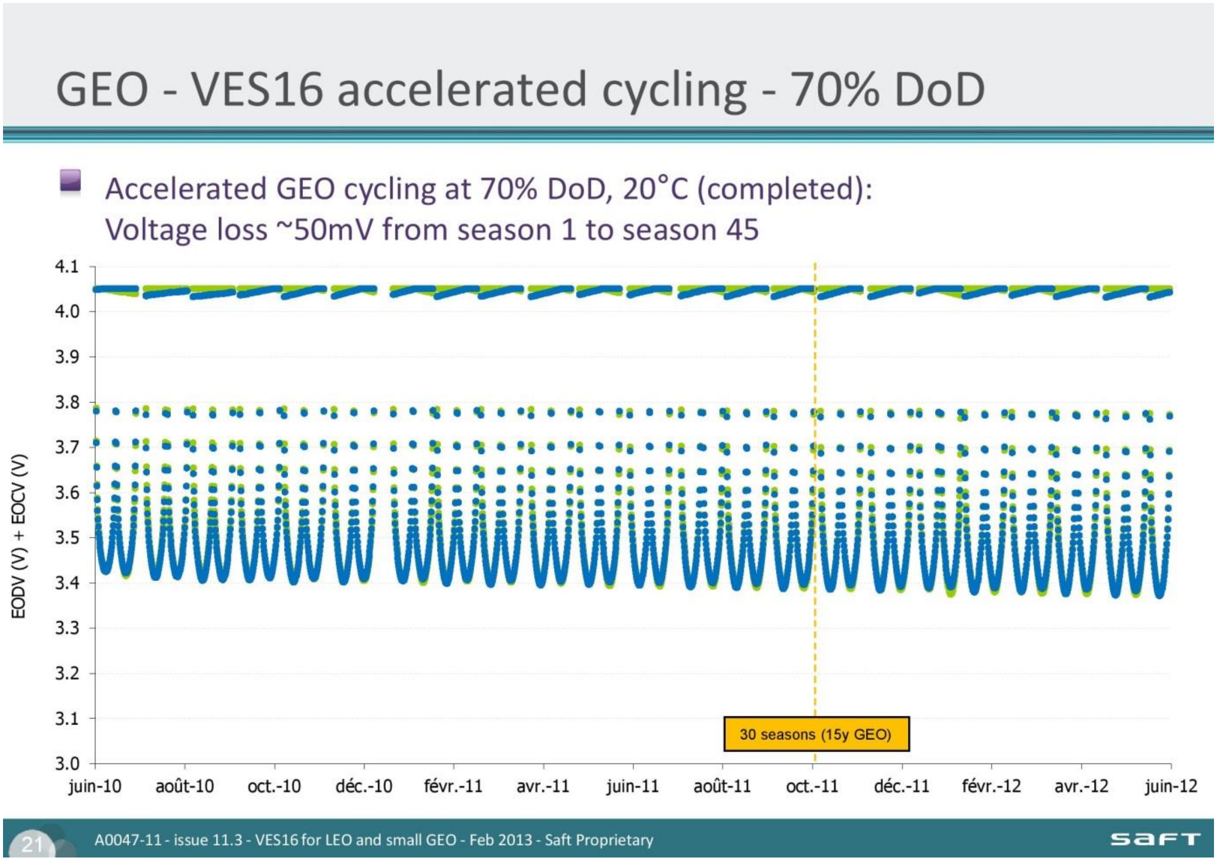

Figure 85: Battery capacity over GEO cycle (VES16, 70% DOD) [223]

C.3 Decision Matrices

The following decision matrices are structured according to the analytic hierarchy process (AHP) technique developed by Thomas L. Saaty in the 1970s [272]. It is applied to find the best decision that suits the goal. The criteria elements are structured in hierarchy and can be related to any aspect of the decision problem.

Table 102: Decision matrix: AOCS - Reaction wheels

	RDR 57-0	RDR 68-3	RSI 45 75/60	HR14	HR16
Angular Momentum [Nms]	57	68	45	50	50
ranking	0.211	0.252	0.167	0.185	0.185
factor	0.375				
Motor Torque [mNm]	90	75	75	100	100
ranking	0.192	0.231	0.231	0.173	0.173
factor	0.25				
Power [W]	90	90	90	105	105
ranking	0.212	0.212	0.212	0.182	0.182
factor	0.250				
Mass [kg]	7.6	7.6	7.7	8.5	9
ranking	0.212	0.212	0.209	0.189	0.182
factor	0.125				
Decision Rank	**0.207**	**0.232**	**0.199**	**0.182**	**0.181**

Table 103: Decision matrix: AOCS - Inertial measurement units

	MIMU	Astrix 1090	Astrix 1120	Astrix 200
BIAS [°/hr]	0.005	0.01	0.003	0.0005
ranking	0.076	0.038	0.127	0.759
factor	0.25			
Noise [°/rt-hr]	0.005	0.005	0.002	0.0002
ranking	0.034	0.034	0.085	0.847
factor	0.25			
Power [W]	22	12	12	18
ranking	0.17	0.311	0.311	0.1
factor	0.125			
Mass [kg]	4.7	4.2	4.2	13
ranking	0.278	0.311	0.311	0.1
factor	0.125			
TRL	9	8	8	9
ranking	0.265	0.235	0.235	0.265
factor	0.25			
Decision Rank	**0.15**	**0.155**	**0.189**	**0.506**

Table 104: Decision matrix: AOCS - Star trackers

	Astro APS	Astro 10	A-STR	AA-STR
Time [s]	10	8	6	9
ranking	0.199	0.249	0.331	0.221
factor	0.143			
Accuracy xy	1 arcsec	1.5 arcsec	3.6 arcsec	3.3 arcsec
ranking	0.445	0.297	0.124	0.135
factor	0.286			
Accuracy z	5	12	21	15.6
ranking	0.506	0.211	0.121	0.162
factor	0.286			
Power [W]	10	11	13.5	12.6
ranking	0.29	0.264	0.215	0.230
factor	0.143			
Mass [kg]	1.98	3.37	3.55	2.6
ranking	0.344	0.202	0.192	0.262
factor	0.143			
Decision Rank	**0.391**	**0.247**	**0.175**	**0.187**

Table 105: Decision matrix: EPS - Solar Cells

	Azur 3G30C	Azur 3G28C	Emcore ZTJ	Emcore BTJ
Power max / cell	1.18	1.1	1.03	1.0
ranking	0.274	0.255	0.239	0.232
factor	0.33			
Avg. efficiency η	28.6	26.6	28.1	27.1
ranking	0.259	0.241	0.255	0.245
factor	0.5			
Mass [g]	2.595	2.595	2.234	2.234
ranking	0.269	0.269	0.231	0.231
factor	0.167			
Decision Rank	**0.266**	**0.25**	**0.245**	**0.239**

Table 106: Decision matrix: EPS - Batteries

	VES 180	VL 48E	VES 16	18650NL	QL075KA
Energy Capacity [Wh]	17280	16320	16128	16776	16640
ranking	0.208	0.196	0.194	0.202	0.2
factor	0.4				
TRL	9	9	8	9	9
ranking	0.205	0.205	0.182	0.205	0.205
factor	0.4				
Mass [kg]	107	109	156	108	116
ranking	0.218	0.214	0.15	0.216	0.201
factor	0.2				
Decision Rank	**0.211**	**0.205**	**0.14**	**0.208**	**0.202**

C.4 TMA-0 Mission and System Budgets

Table 107: Dry mass distribution of selected large GEO telecommunication satellites [273]

Spacecraft		Percentage of Spacecraft Dry Mass by Subsystem							Dry Mass
Name		Payload	Structure	Thermal	EPS	TT&C	AOCS	Propulsion	[kg]
1	ANIK E	27.6%	22.8%	4.7%	28.7%	2.9%	3.9%	9.4%	1270.0
2	ARABSAT (not 2)	21.4%	15.8%	5.3%	30.9%	5.1%	11.6%	10.0%	573.1
3	ASTRA 1B	30.0%	16.2%	4.5%	30.7%	2.3%	6.2%	10.2%	1178.6
4	DFS Kopernikus	24.1%	18.4%	4.1%	30.8%	4.4%	7.2%	11.0%	656.0
5	Fordsat	28.9%	19.5%	5.0%	33.2%	0.9%	7.4%	5.1%	1094.0
6	HS 601	49.8%	12.2%	3.1%	19.3%	4.7%	4.4%	6.5%	1459.0
7	Intelsat VII	30.8%	17.3%	6.7%	25.8%	1.0%	10.1%	7.6%	1450.0
8	Intelsat VIIA	28.8%	15.4%	6.9%	27.4%	0.9%	9.1%	7.5%	1823.0
9	OLYMPUS	28.5%	21.6%	5.2%	27.4%	3.0%	5.2%	9.2%	1158.0
10	SATCOM K3	19.0%	17.6%	4.4%	35.6%	3.5%	6.7%	13.2%	1017.7
11	TELSTAR 4	24.1%	10.9%	5.6%	35.0%	4.8%	4.4%	6.2%	1621.0
	Average	28.4%	17.1%	5.0%	29.5%	3.1%	6.9%	8.7%	1209.1
	Standard Deviation	8.0%	3.6%	1.1%	4.6%	1.6%	2.5%	2.4%	378.8

Table 108: Power distribution of GEO communication satellites by subsystems [274]

Spacecraft		Power Distribution of GEO Communication Satellites by Subsystem							
Name		Payload	TT&C	AOCS	Thermal	EP Management and Distribution	Charging	Propulsion	Total Power
1	ANIK E	3000.0	42.0	28.0	100.0	25.0	287.0	?	3482.0
2	ARABSAT (not 2)	990.5	38.3	125.1	90.5	18.2	99.2	?	1361.8
3	ASTRA 1B	2136.0	43.0	28.0	105.0	68.0	410.0	?	2790.0
4	DFS Kopernikus	896.0	28.0	39.0	235.0	46.0	168.0	?	1412.0
5	Fordsat	2461.0	51.3	130.1	92.0	41.0	335.8	?	3109.8
6	HS 601	2660.0	80.0	70.0	280.0	30.0	230.0	?	3350.0
7	Intelsat VII	2580.0	38.0	226.0	263.0	83.0	373.0	6.0	3569.0
8	Intelsat VIIA	3612.0	28.0	226.0	222.0	53.0	420.0	6.0	4567.0
9	OLYMPUS	2150.0	46.1	116.6	287.0	32.5	200.0	?	2832.2
10	SATCOM K3	2570.7	42.6	28.3	95.0	51.4	362.0	?	3150.0
11	TELSTAR 4	4816.5	98.0	76.0	137.0	38.0	507.4	?	5672.9

<TMA-0>
Configuration <2013/05/05>

System	Subsystem	Component	Supplier	Model	No. of units	Unit mass [kg]	Maturity margin [%]	Subtotal [kg]
						Mass Budget		
Satellite								
	Payload(s)							
	Repeater Subsystem				0	**0,0**	**#DIV/0!**	**0,0**
		included in Payload, PDH & TT&C						0,0
	Antenna Subsystem				5	**17,1**	**5%**	**18,0**
		Parabolic HG Antenna (2m) + Feeder Horn			1	6,00	5%	6,3
		Pointing Mechanism Electronics	EADS	APME	1	2,00	5%	2,1
		Pointing Mechanism	EADS	APM-10	1	8,10	5%	8,5
		Omnidirectional LG Antenna			2	0,50	5%	1,1
	Payload				18	**80,6**	**7%**	**86,2**
		High Data-Rate (RF channel 1)						0,0
		Modulators (TeTra)	Tesat	TeTra	2	2,1	20%	5,0
		Wave Guide Switches			2	0,2	5%	0,4
		Microwave Power Module			2	3,0	5%	6,3
		Pol. Filter			1	1,0	5%	1,1
		High Data-Rate (RF channel 2)						0,0
		Modulators (TeTra)	Tesat	TeTra	2	2,1	20%	5,0
		Wave Guide Switches			2	0,2	5%	0,4
		Microwave Power Module			2	3,0	5%	6,3
		Pol. Filter			1	1,0	5%	1,1
		High Data-Rate (Laser)						0,0
		Laser Communication Terminal	Tesat	LCT-2	1	50,0	5%	52,5
		Pointing Measurmenet System	MSSS	ECM-C50 &	1	0,4	10%	0,4
		Space Weather Detectors						
		Dust Detector 1		SLEO	1	4,3	10%	4,7
		Dust Detector 2		SODA	1	2,7	10%	3,0
	Payload total					97,7	7%	104,2
	Platform subsystems							
	Electrical Power Subsystem				7	**213,9**	**5%**	**224,6**
		Battery (modular) incl. Charge Control			1	160,5	5%	168,5
		PCDU (incl 5% power level as losses)			1	22,0	5%	23,1
		Solar Cells			1	6,0	5%	6,3
		Solar Pannel			2	10,0	5%	21,0
		Solar Array Drive Mechanism	RUAG	SEPTA31	2	2,7	5%	5,7
	Onboard Data Handling Subsystem				6	**40,0**	**5%**	**42,0**
		Command and Datahandling	RUAG		2	16,0	5%	33,6
		Mass Memory Unit			4	2,0	5%	8,4
	Payload Data Handling				2	**20,0**	**5%**	**21,0**
		Payload Datahandling Unit	Space Micro	PROTON 200K	2	10,0	5%	21,0
	TT&C Subsystem				3	**6,2**	**5%**	**6,5**
		Transceiver (TTC (incl. 2W SSPA)			2	3,00	5%	6,3
		- Transmitter			1	70%	5%	
		- Receiver			1	30%	5%	
		3dB Hybrid Coupler			1	0,20	5%	0,2
	Attitude and Orbit Control Subsystem				26	**60,3**	**5%**	**63,3**
		Sun Sensor	Bradford	Coars	8	0,2	5%	1,8
		Sun Sensor		Fine	8	0,4	5%	3,2
		IMU	Honeywell	MIMU	2	4,7	5%	9,9
		Star Trackers	Jena Optronik	Astro APS	2	2,0	5%	4,2
		Earth Sensor	Sodern	STD 15	2	3,4	5%	7,1
		Reaction Wheels	Rockwell Collins	RDR 68-3	4	8,9	5%	37,2
	Electric Propulsion Subsystem				0	**0,0**	**#DIV/0!**	**0,0**
		tbc						0,0
	Chemical Propulsion Subsystem				22	**95,0**	**5%**	**99,8**
		Helium Pressure Tank	ATK	Selene	1	10,2	5%	10,7
		Helium (gas)			1	2,4	5%	2,5
		Propellant Tanks	EADS	OST 01/X	2	29,0	5%	60,9
		Reaction Thrusters	EADS	22 N BiProp	16	0,7	5%	10,9
		Apogee Kick Motor	EADS	EAM 500 N	1	5,0	5%	5,3
		Feedlines and System (10%)			1	9,0	5%	9,5
	Thermal Control Subsystem				7	**24,9**	**20%**	**29,9**
		Heater (Ka-Band)			1	0,1	20%	0,1
		Heater (Satellite)			1	2,0	20%	2,4
		MLI			1	6,0	20%	7,2
		Radiator (Satellite)			2	5,0	20%	12,0
		Radiator (LCT)			1	5,0	20%	6,0
		Thermal Miscellaneous (10% TCS)			1	1,8	20%	2,2
	Harness				4	**46,2**	**20%**	**55,4**
		EPS Harness			1	11,7	20%	14,0
		TT&C Harness (10% PL)			1	8,6	20%	10,3
		PL Harness (20% PL)	Tesat		1	17,2	20%	20,7
		DataHarness (10% PL)			1	8,6	20%	10,3
	Structure				1	**129,3**	**20%**	**155,2**
		Structure (20% Satellite)			1	129,3	20%	155,2
	Platform total					635,8	9,7%	697,7
Total dry						733,5	9,3%	801,8
System margin							20,0%	160,4
Total dry with margin								962,2
Propellant mass		(margin already included)			1	1058	0%	1058,0
Total wet mass								2020,2
Launcher capability								3200,0
	Launcher mass margin							1179,8

Figure 86: Detailed mass budget on components level

<TMA-0>
Configuration <2013/05/05>

System	Subsystem	Component	Redundancy concept				Units' power modes definition: Power per Unit [W] Maximum	Power per Unit [W] Standby	Margin	"On" Consumption	"Standby" Consumption
Satellite											
	Payload(s)										
	Repeater Subsystem									0,0	0,0
		included in Payload, PDH & TT&C									
	Antenna Subsystem									15,8	2,3
		Parabolic HG Antenna (2m) + Feeder Horn									
		Pointing Mechanism Electronics	1	of	1		15,0	2,2	5%	15,8	2,3
		Pointing Mechanism									
		Omnidirectional LG Antenna									
	Payload									525,4	58,0
		High Data-Rate (RF channel 1)									
		Modulators (TeTra)	1	of	2	Cold	25,0	5,0	20%	30,0	6,0
		Wave Guide Switches									
		Microwave Power Module	1	of	2	Cold	130,0	5,0	5%	136,5	5,3
		Pol. Filter									
		High Data-Rate (RF channel 2)									
		Modulators (TeTra)	1	of	2	Cold	25,0	5,0	20%	30,0	6,0
		Wave Guide Switches									
		Microwave Power Module	1	of	2	Cold	130,0	5,0	5%	136,5	5,3
		Pol. Filter									
		High Data-Rate (Laser)									
		Laser Communication Terminal	1	of	1		160,0	30,0	5%	168,0	31,5
		Pointing Measurmenet System	1	of	1		2,5	1,8	5%	2,6	1,8
		Space Weather Detectors									
		Dust Detector 1	1	of	1		10,0	1,0	10%	11,0	1,1
		Dust Detector 2	1	of	1		9,8	1,0	10%	10,8	1,1
	Payload total									541,2	60,3
	Platform subsystems										
	Electrical Power Subsystem									72,5	7,0
		Battery (modular) incl. Charge Control	1	of	1		1,0	1,0	5%	1,1	1,1
		PCDU (incl 5% power level as losses)	1	of	1		54,0	1,0	5%	56,7	1,1
		Solar Cells									
		Solar Pannel									
		Solar Array Drive Mechanism	2	of	2		7,0	2,3	5%	14,7	4,9
	Onboard Data Handling Subsystem									84,0	46,2
		Command and Datahandling	1	of	2	Cold	60,0	40,0	5%	63,0	42,0
		Mass Memory Unit	4	of	4		5,0	1,0	5%	21,0	4,2
	Payload Data Handling									21,0	2,1
		Payload Datahandling Unit	2	of	2		10,0	1,0	5%	21,0	2,1
	TT&C Subsystem									54,7	27,4
		Transceiver (TTC (incl. 2W SSPA)	2	of	2	Hot	2,0	1,0	12,7	54,7	27,4
		- Transmitter	1	of	1	Hot	17,0	3,0	5%	17,9	3,2
		- Receiver	1	of	1	Hot	10,0	2,0	5%	10,5	2,1
		3dB Hybrid Coupler	1	of	1					0,0	0,0
	Attitude and Orbit Control Subsystem									479,9	81,9
		Sun Sensor	8	of	8		0,0	0,0	5%	0,0	0,0
		Sun Sensor	8	of	8		0,0	0,0	5%	0,0	0,0
		IMU	2	of	2		32,0	22,0	5%	67,2	46,2
		Star Trackers	2	of	2		10,0	6,0	5%	21,0	12,6
		Earth Sensor	2	of	2		6,5	1,0	5%	13,7	2,1
		Reaction Wheels	4	of	4		90,0	5,0	5%	378,0	21,0
	Electric Propulsion Subsystem									0,0	0,0
		tbc									
	Chemical Propulsion Subsystem									10,5	1,1
		Helium Pressure Tank									
		Helium (gas)									
		Propellant Tanks									
		Reaction Thrusters									
		Apogee Kick Motor									
		Feedlines and System (10%)	1	of	1		10,0	1,0	5%	10,5	1,1
	Thermal Control Subsystem									145,2	0,0
		Heater (Ka-Band)	1	of	1		10,0	0,0	20%	12,0	0,0
		Heater (Satellite)	1	of	1		100,0	0,0	20%	120,0	0,0
		MLI									
		Radiator (Satellite)									
		Radiator (LCT)									
		Thermal Miscellaneous (10% TCS)	1	of	1		11,0	0,0	20%	13,2	0,0
	Harness										
		EPS Harness									
		TT&C Harness (10% PL)									
		PL Harness (20% PL)									
		DataHarness (10% PL)									
	Structure										
		Structure (20% Satellite)									
	Platform total									857,2	164,6
Total dry										1398,4	224,9
System margin									20,0%	279,7	45,0
Total dry with margin										1678,0	269,9

Figure 87: TMA-0 Power budget for “on” and “standby” consumption

<TMA-0>
Configuration <2013/05/05>

System	Subsystem	Component	[ALL]	GTO	Safe mode, eclipse	Transfer	Idle	Science	Operating, RF	Operating, RF & Laser	Duty Cycle [%/Orbit]	Average consumption
			Duty Cycle Input [Min]	5760,0	1598,4	129600,0	7200,0	7200,0	716400,0	716400,0	Period [Min] 1584158,4	
			Duty Cycle Input [%/Orbit]								Total 0%	
			Duty Cycle [%/Orbit]	0%	0%	8%	0%	0%	45%	45%	Total 100%	Switch Minutes
			Modes									
Satellite												
	Payload(s)											
	Repeater Subsystem		Off	0,0	0,0	0,0	0,0	0,0	0,0	0,0		0,0
		included in Payload, PDH & TT&C										
	Antenna Subsystem		Off	0,0	0,0	0,0	2,3	2,3	15,8	15,8		14,3
		Parabolic HG Antenna (2m) + Feeder Horn										
		Pointing Mechanism Electronics	Off	Off	Off	Off	Standby	Standby	On	On	90%	14,3
		Pointing Mechanism										
		Omnidirectional LG Antenna										
	Payload		Off	0,0	0,0	21,8	77,6	78,4	388,9	525,4		416,3
		High Data-Rate (RF channel 1)										
		Modulators (TeTra)	Off	Off	Off	Off	Standby	Standby	On	On	90%	27,2
		Wave Guide Switches										
		Microwave Power Module	Off	Off	Off	Off	Standby	Standby	On	On	90%	123,5
		Pol. Filter										
		High Data-Rate (RF channel 2)										
		Modulators (TeTra)	Off	Off	Off	Off	Standby	Standby	On	On	90%	27,2
		Wave Guide Switches										
		Microwave Power Module	Off	Off	Off	Off	Standby	Standby	On	On	90%	123,5
		Pol. Filter										
		High Data-Rate (Laser)										
		Laser Communication Terminal	Off	Off	Off	Off	Standby	Standby	Standby	On	45%	90,6
		Pointing Measurmenet System	Off	Off	Off	Off	Standby	On	On	On	91%	2,4
		Space Weather Detectors										
		Dust Detector 1	Off	Off	Off	On	On	On	On	On	100%	11,0
		Dust Detector 2	Off	Off	Off	On	On	On	On	On	100%	10,8
	Payload total			0,0	0,0	21,8	79,9	80,7	404,7	541,2		430,6
	Platform subsystems											
	Electrical Power Subsystem		Off	72,5	72,5	72,5	72,5	72,5	72,5	72,5		72,5
		Battery (modular) incl. Charge Control	Off	On	On	On	On	On	On	On	100%	1,1
		PCDU (incl 5% power level as losses)	Off	On	On	On	On	On	On	On	100%	56,7
		Solar Cells										
		Solar Pannel										
		Solar Array Drive Mechanism	On	On	On	On	On	On	On	On	100%	14,7
	Onboard Data Handling Subsystem		Off	67,2	63,0	67,2	67,2	84,0	84,0	84,0		82,5
		Command and Datahandling	Off	On	Off	On	On	On	On	On	100%	63,0
		Mass Memory Unit	Off	Standby	Off	Standby	Standby	On	On	On	91%	19,5
	Payload Data Handling		Off	0,0	0,0	2,1	2,1	2,1	21,0	21,0		19,2
		Payload Datahandling Unit	Off	Off	Off	Standby	Standby	Standby	On	On	90%	19,2
	TT&C Subsystem		Off	56,7	56,7	56,7	56,7	56,7	56,7	56,7		56,7
		Transceiver (TTC (incl. 2W SSPA)		On	On	On	On	On	On	On	100%	56,7
		- Transmitter	Off	On	On	On	On	On	On	On	100%	17,9
		- Receiver	Off	On	On	On	On	On	On	On	100%	10,5
		3dB Hybrid Coupler	Off	Off	Off	Off	Off	Off	Off	Off	0%	0,0
	Attitude and Orbit Control Subsystem		Off	177,5	177,5	177,5	177,5	177,5	177,5	177,5		177,5
		Sun Sensor	Off	On	On	On	On	On	On	On	100%	0,0
		Sun Sensor	Off	On	On	On	On	On	On	On	100%	0,0
		IMU	Off	On	On	On	On	On	On	On	100%	67,2
		Star Trackers	Off	On	On	On	On	On	On	On	100%	21,0
		Earth Sensor	Off	On	On	On	On	On	On	On	100%	13,7
		Reaction Wheels	Off	On	On	On	On	On	On	On	100%	75,6
	Electric Propulsion Subsystem		Off	0,0	0,0	0,0	0,0	0,0	0,0	0,0		0,0
		tbc										
	Chemical Propulsion Subsystem		Off	1,1	10,5	10,5	10,5	10,5	10,5	10,5		10,5
		Helium Pressure Tank										
		Helium (gas)										
		Propellant Tanks										
		Reaction Thrusters										
		Apogee Kick Motor										
		Feedlines and System (10%)	Off	Standby	On	On	On	On	On	On	100%	10,5
	Thermal Control Subsystem		Off	0,0	133,2	37,2	37,2	37,2	37,2	37,2		37,2
		Heater (Ka-Band)	Off	Off	Off	Off	Standby	Standby	Standby	Standby	0%	0,0
		Heater (Satellite)	Off	Standby	On	On	On	On	On	On	100%	24,0
		MLI										
		Radiator (Satellite)										
		Radiator (LCT)										
		Thermal Miscellaneous (10% TCS)	Off	Standby	On	On	On	On	On	On	100%	13,2
	Harness											
		EPS Harness										
		TT&C Harness (10% PL)										
		PL Harness (20% PL)										
		DataHarness (10% PL)										
	Structure											
		Structure (20% Satellite)										
	Platform total											455,9
Total dry												886,5
System margin												177,3
Total dry with margin												1063,8

Figure 88: TMA-0 power modes

Table 109: Lunar missions from the year 2000 up to 2030

Launch Year	Mission Name (Operator)	Lunar Target	Status
2003	SMART-1 (ESA)	Orbit	completed
2007	Artemis (NASA)	Orbit	completed
	Chang'e-1 (CNSA)	Orbit	completed
	Selene-1 (JAXA)	Orbit	completed
2008	Chandrayaan-1 (ISRO)	Orbit	completed
2009	LRO (NASA)	Orbit	in orbit
	LCROSS (NASA)	Landing	completed
2010	Chang'e-2 (CNSA)	Orbit	completed
2011	Grail (NASA)	Orbit	completed
2013	LADEE (NASA)	Orbit	planned
	Chang'e-3 (CNSA)	Orbit	planned
2014	BW1 (IRS, Univ. Stuttgart)	Orbit	planned
	ESMO (ESA, Students)	Orbit	proposed
	MoonLite (UK Space Agency)	Orbit	proposed
	MoonRaker (UK Space Agency)	Orbit	proposed
2015	Chandrayaan-2 (ISRO)	Orbit	planned
	Chandrayaan-2 (ISRO)	Landing	planned
	Luna-Glob 1 (RFSA)	Orbit	planned
	Chang'e-4 (CNSA)	Orbit	planned
	ILN Node 1 (NASA)	Landing	planned
	ILN Node 2 (NASA)	Landing	planned
	Moon Express (GLXP)	Landing	proposed
	Team Italia (GLXP)	Landing	proposed
	Barcelona Team (GLXP)	Landing	proposed
	Team Frednet (GLXP)	Landing	proposed
	Part-Time Scientists (GLXP)	Landing	proposed
	Synergy Moon (GLXP)	Landing	proposed
	PenState Lunar Lion (GLXP)	Landing	proposed
	ILO (ILOA)	Landing	proposed
	(Astrobotic Technology)	Landing	proposed
	DSE-Alpha (Space Adventures)	Orbit/manned	proposed
2016	(Shackleton Energy Company)	Landing	proposed
	Luna-Resurs (RFSA)	Landing	proposed
	ILN Node 3 (NASA)	Landing	proposed
2017	ILN Node 4 (NASA)	Landing	proposed
2018	Chang'e-5 (CNSA)	Orbit	planned
	European Lunar Lander (ESA)	Landing	proposed
2020	Moon Orbiter (KARI)	Orbit	proposed
	(ISRO)	Landing/manned	proposed
	(JAXA)	Landing/manned	proposed
	(Golden Spike)	Landing/manned	proposed
2021	Lunar-Grunt (RFSA)	Orbit	proposed
	Lunar-Grunt (RFSA)	Landing	proposed
2022	Dragon (SpaceX)	Orbit/manned	proposed
2024	Aurora Programme (ESA)	Landing/manned	proposed
2025	Moon Lander (KARI)	Landing	planned
	CLEP Mission (CNSA)	Landing/manned	proposed
2026	Farside (ESA, Students)	Orbit	proposed
	Farside (ESA, Students)	Landing	proposed
2027	(RFSA)	Landing/manned	proposed